Biologie

Dissertationsthema

Translational control of virulence-associated traits of *Yersinia pseudotuberculosis*

Inaugural-Dissertation
zur Erlangung des Doktorgrades
der Naturwissenschaften im Fachbereich Biologie
der Mathematisch-Naturwissenschaftlichen Fakultät
der Westfälischen Wilhelms-Universität Münster

vorgelegt von

Marcel Volk

aus Lingen (Ems)

- 2021 -

Dekanin/Dekan:	Prof. Dr. Susanne Fetzner .....
Erste Gutachterin/Erster Gutachter:	Prof. Dr. Petra Dersch .....
Zweite Gutachterin/Zweiter Gutachter:	Prof. Dr. Eva Liebau .....
Tag der mündlichen Prüfung(en):	21.05.2021 .....
Tag der Promotion:	28.05.2021 .....

Tabel of contents

Abbreviations

%	per cent
Δ	deletion
° C	degree Celsius
A	adenine
Amp	ampicillin
APS	ammonium persulfate
aSD	anti-Shine-Dalgarno
ATP	adenosine triphosphate
Axx	absorption
BCIP	5-Brom-4-chlor-3-indoxylphosphat
BLAST	basic local alignment search tool
BHI	brain-heart-infusion
bp	base pairs
BSA	bovine serum albumin
Ca^{2+}	calcium ion
cAMP	cyclic adenosine monophosphate
Cb	carbeniciliin
cDNA	complementary DNA
CDS	coding sequence
CIP	calf intestinal phosphatase
Cm	chloramphenicol
cm	centi meter
Csr	carbon storage regulatore
Ct	cylcle threshold
Da	dalton
DIG	digoxygenin
DNA	desoxyribonucleic acid
DNase	desoxyribonuclease
dNTP	desoxyribonucleosid-triphosphate
dsDNA	double-stranded DNA
DYT	double yeast trypotone
ECF	extracytoplasmatic σ-factor
EDTA	ethylenediaminetetraacetic acid
EF	elongation factor
e.g.	exempli gratia (lat.)
EMSA	electrophoretic mobility shift assay
et al.	et alit (lat.)
EtBr	ethidium bromide
EtOH	ethanol
exp.	exponential
f	femto (1×10^{-15})
FC	fold change
fig.	figure
g	gram
G	guanine
g	gravitational force
GMAK	Next generation sequencing platform
h	hour(s)
HF	high fidelity
HCl	hydrochloric acid
His	histidine
HZI	Helmholtz centre for infection research
IF	initiation factor
IM	inner membrane
Inv	invasin
IPTG	isopropyl-β-D-1-thiogalacto-pyranoside
K	lysine
Kan	kanamycin
kb	kilobase

kDa	kilo Dalton
KEGG	Kyoto Encyclopedia of genes and genomes
l	liter
L	leucin
lacZ	reporter gene encoding for β-galactosidase
LB	Luria-Bertani medium
lcr	low calcium response protein
LPS	lipopolysaccharide
LRR	leucin-rich-repeats
µ	micro (1 x 10^{-6})
m	milli (1 x 10^{-3}) or meter
M	methionine
M	molar (mol/L)
mA	millampere
MAPK	mitogen activated protein kinase
M-cell	microfold-cell
min	minutes
mM	millimolar
MNase	Micrococcus nuclease
mol	amount of substance (6.022 × 10^{23} [Avogadro constant])
MOPS	3-(N-morpholino)propanesulfonic acid
mRNA	messenger RNA
µg	microgram
µl	microliter
N	any nucleotide
n	nano (1 x 10^{-9})
ncRNA	non-coding RNA
NEB	New England Biolabs
ng	nanogram
Ni-NTA	nickel-nitrilotriacetic acid
nm	nanometer
nM	nanomolar
ns	not significant
nt	nucleotide
OD	optical density
OM	outer membrane
ORF	open reading frame
ori	origin of replication
p	pico (1 x 10^{-12})
PAA	polyacrylamide
PAGE	polyacrylamide gel electrophoresis
PCR	polymerase chain reaction
pH	negative logarithm of H+ ions
phoA	reporter gene encoding for alkaline phosphatase
PNK	T4 polynucleotide kinase
pNPP	*para*-Nitrophenylphosphate
Psp	phage shock protein
PTC	peptidyl transferase center
PVDF	polyvinylidene fluoride
qRT-PCR	quantitative real-time PCR
^{R}	resistance
RBS	ribosomal binding site
RF	release factor
Ribo-Seq	high-throughput RNA sequencing of ribosomal footprints
RNA	ribonucleic acid
RNase	ribonuclease
RNAP	RNA polymarase
RNA-seq	high-throughput RNA sequencing
RPF	ribosome protected footprints
RPKM	reads per kilobase million
rpm	rotations per minute
RRF	ribosome recycling factor

rRNA	ribosomal RNA
RT	room temperature
RT-PCR	reverse transcribed polymerase chain reaction
S	Svedberg
SD	Shine-Dalgarno
SDS	sodiumdodecyl sulfate
sec	second
sRNA	short regulatory RNA
ssDNA	single-stranded DNA
stat	stationary
t	time
T3S	type three secretion
T3SS	type three secretion system
TAE	tric-acetate buffer
Taq	DNA polymerase of Thermus aquaticus
TBE	tris-borate-EDTA
TCA	trichloroacetic acid
TCA	tricarboxylic acid cycle
TCS	two-component system
TEMED	tetramethylethylenediamine
TE	translational efficiency
Tris	Tris-(hydroxymethyl)-aminoethane
tRNA	transfer RNA
TSS	transcriptional start site
U	units
U	uridine
UP-element	upstream-element
USA	united states of america
UTR	untranslated region
UV	ultra violett
V	volume
vir	virulence regulon transcriptional activator
(v/v)	volume per volume
(w/v)	weight per volume
wt	wild type
Yop	*Yersinia* outer protein

List of Figures

List of Tables

Abstract

A high number of gastrointestinal infections in humans are caused by enteric pathogens such as *Yersinia pseudotuberculosis* which causes a self-limiting gastrointestinal disease called Yersiniosis, characterized by abdominal pain and diarrhea. In the process of infection, *Y. pseudotuberculosis* is confronted with the host immune system, after the bacteria were taken up by the microfold (M) cells which allow transmigration of the bacteria into underlying lymphatic tissue called Peyer´s patches. In order to fight against the host immune system, *Yersinia* synthesizes a special set of virulence plasmid-encoded virulence factors: a type 3 secretion system (T3SS), the secreted Yop (*Yersinia* outer protein) effector proteins, and the adhesin YadA. Upon contact with innate immune cells such as macrophages, *Y. pseudotuberculosis* uses its T3SS to translocate the Yop proteins into the target cell to preventing phagocytosis. Due to the high energy cost of this bacterial defense system (including T3SS, Yops, and YadA) and its transcriptional activator LcrF, it is strictly regulated to be only expressed under appropriate conditions. In fact, several post-transcriptional control factors including the translocon pore protein YopD, the regulator protein CsrA and different RNases have been found to regulate LcrF and the T3SS, Yop, and YadA system. Besides the already known regulations of these factors on the post-transcriptional level, it was hypothesized that translation could also be regulated in addition. Therefore, this study analyzed whether also translation is influenced to control the expression and synthesis of the T3SS, Yops, and YadA proteins.

For this purpose, the Ribo-Seq technology was established for *Y. pseudotuberculosis* to analyze the translation of the T3SS, Yops, and YadA proteins. The results demonstrated that the translation of the T3SS, *yop*, and *yadA* transcripts is mainly affected immediately prior to host cell contact, when the T3SS, *yop*, and *yadA* genes are expressed on a low level. This low expression is due to the function of the temperature-inducible expression of LcrF. In the absence of target cells, translation of the T3SS, *yop*, and *yadA* transcripts is repressed by the presence of the translocator and RNA-binding protein YopD. Immediately upon host cell contact, YopD is translocated and depleted from the bacterial cytoplasm which leads to a strong upregulation of the translation of the few present T3SS, *yop*, *yadA,* and *lcrF* transcripts. This initiates the second activation step in which high expression of the T3SS components mainly occurs through upregulation of the T3SS, *yop*, and *yadA* gene transcription, followed by a highly efficient translation process of the *yop* transcripts.

To allow this highly efficient translation process, the *yop* transcripts were found to be optimized. The *yop* transcripts were shown to encode short, AU-rich 5’ UTRs which also harbor prolonged optimal RBS sequences which facilitate translation initiation. It was further shown that this type of 5’ UTRs is sufficient to allow a very efficient translation of the *yop* transcripts, especially under secretion conditions. Furthermore, it was observed that the *yop* and *yadA* transcripts encode several rare codons, which are decoded by low abundant tRNAs. In an analysis of certain tRNAs important for the decoding of these rare codons, it was observed, that several of these tRNAs are strongly upregulated under the conditions where the T3SS, *yop,* and *yadA* transcripts are translated. This increase in tRNAs is thought to contribute to an increased translation elongation which further supports the highly efficient translation of these transcripts.

In conclusion, it was shown that the T3SS, *yop,* and *yadA* transcripts are optimized for a highly efficient translation, especially in the case of the *yop* and *yadA* transcripts, and that the translational regulation is somehow facilitated by YopD.

1 Introduction

All living cells need to express their genetic information and respond to internal and external signals by adapting their gene expression (Crick 1970). Therefore, the cells need to activate genes that provide the cells with the benefit of a necessary product and, on the other hand, silence gene expression of unrequired genes. This activation and deactivation usually appear on different levels, like transcriptional or post-transcriptional. In pathogenic bacteria, the expression of virulence-associated genes is tightly controlled. Hence, these genes are regulated at several levels when not required, like outside of the host. After host entry, the virulence-associated genes need to respond fast to achieve a powerful anti-host defense, which can be accomplished by regulation at the transcriptional or post-transcriptional level (Chakravarty and Massé 2019; Thomas and Wigneshweraraj 2014; Volk *et al.* 2019). The entire regulation and the strong expression of virulence-associated genes are not fully understood because new components, as well as new regulatory mechanisms, are constantly being discovered. This study will focus on the control of translation of virulence-associated genes in *Yersinia pseudotuberculosis*, necessary to defend the bacteria from the host immune system and its role within the regulatory network of *Yersinia* virulence.

1.1 Transcription and translation in bacteria

The expression of genes occurs in two main steps, consisting of the transcription and the translation. During transcription, the genetic information stored in DNA is transcribed into a messenger RNA (mRNA) (Lee *et al.* 2012). Ribosomes afterwards decode the mRNA into a protein in the process of translation (Rodnina 2018). By these steps, the genetic information can be transferred from DNA into a functional protein. The transcription, as well as the translation, are facilitated by multiprotein, multiprotein-DNA, and multiprotein-RNA complexes. Furthermore, many protein factors are required in the process of transcription and translation, and also regulatory features inside the DNA or mRNA sequence contribute to the function of both processes (Lee *et al.* 2012; Rodnina 2018). While the overall mechanisms of transcription and translation are the same for bacteria and eukaryotes, the specialized complexes involved, as well as some steps in the processes, differ between the two.

1.1.1 The transcription machinery in bacteria

The first step in gene expression is the transcription of the genetic code into an mRNA. This process is carried out by the RNA-polymerase (RNAP), a multiprotein complex that is able to synthesize an RNA copy based on the DNA template. The RNAP consists of five proteins, two α subunits, one β, and one β’ subunit, and an ω subunit (Burgess 1969; Murakami 2002). The ω subunit is often observed as part of the RNAP *in vitro* studies, while it is not often found to be part of the RNAP core *in vivo*. It is hypothesized, that the ω subunit has a chaperone function in forming the core (Gentry and Burgess 1993; Ghosh *et al.* 2001; Weiss *et al.* 2017). The β and β’ subunits form the biggest part of the RNAP with the catalytic center and the ability to unravel the DNA (Severinov *et al.* 1997). Both α subunits assist in the assembly of the different subunits and form the first interaction in the emerging RNAP complex (Hayward *et al.* 1991) (see Figure 1.1). It is also known that the α subunits interact with the DNA in its upstream (UP)-elements, located upstream of the -35 region of the promoter. The UP-elements consist

of AT-rich sequences, which allow binding of the C-terminal domain of the α subunits to the DNA. This binding positively affects the transcription initiation by RNAP (Ebright and Busby 1995; Estrem *et al.* 1998, 1999; Ross *et al.* 1993).

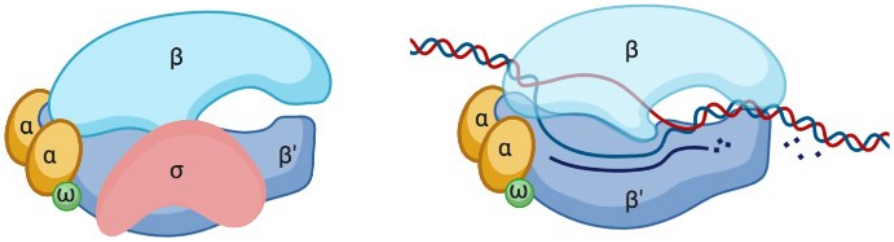

Figure 1.1) Schematic of an RNA-Polymerase in complex with a σ factor and in the process of transcription.
The transcription in all living beings is carried out by RNA-polymerase (RNAP). In bacteria, the RNAP core is made up of five proteins with an additional dissociable sixth factor. The core consists of two α, a β and a β', and an ω subunit. The dissociable protein is a σ-factor. The σ-factor is needed for recruiting the RNAP to the DNA and is released upon transcription initiation (left). The β and β' subunits facilitate the catalytic function of transcribing the DNA sequence (light blue line) into mRNA (dark blue line underneath the DNA). The mRNA is formed by incorporation of different nucleoside triphosphates (dark blue dots) (right) (Lee *et al.* 2012)[1]. Created with BioRender.com

Besides the RNAP core, a dissociable factor is part of the RNAP. This is the σ-factor, which is only part of the RNAP in prokaryotes. The σ-factor interacts with the free RNAP to form the holoenzyme (Burgess *et al.* 1969). Within the complex, the σ-factor can detect the initiation sequence of the promoter, located on the DNA. After recruiting the RNAP to a DNA sequence to be transcribed, the σ-factor leaves the complex. The free σ-factor can now bind a new RNAP core. With the σ-factor, the RNAP can easily be led to any promoter upstream of transcriptional start sites (TSSs) in the genome (Feklístov *et al.* 2014; Khesin *et al.* 1969).

Important for the detection of a TSS specific for a certain σ-factor is the promoter region upstream of the TSS, especially the regions ten base pairs upstream (-10 element) and 35 base pairs upstream (-35 element) of the TSS. These regions contain conserved DNA sequences with which the σ-factor can interact. The -10 element is the more important area for detection in this context (Pribnow 1975). After detection of the -10 and -35 elements by the σ-factor, transcription is initiated, upon which the σ-factor leaves the complex (Lamond and Travers 1983; Moran *et al.* 1982).

Based on the fact that transcription initiation is mainly dependent on the σ-factor, it allows a subgrouping of transcription by using different σ-factors. Consequently, bacteria can rapidly adapt their gene expression to certain environmental conditions. For a variety of genes, the housekeeping σ-factor RpoD (σ^{70}) is used. It detects most of the TSSs and is permanently present in the cell (Gross *et al.* 1998; Paget and Helmann 2003; Pasternak *et al.* 1996). Besides, special σ-factors for stress-dependent genes can be found, known as alternative σ-factors. These can be present in the cell in an inactive form or are only expressed under certain stress conditions. Some well-characterized alternative σ-factors are RpoS, RpoE, RpoH, FliA, and SpoIIAC (Abril *et al.* 2020; Gruber and Gross 2003; Kazmierczak *et al.* 2005; Shimada *et al.* 2017; Wösten 1998). The set of genes activated by alternative σ-factors is referred to as regulons. RpoS is an alternative σ-factor that is only expressed during stationary growth. The regulon of RpoS consists of genes for different stress resistances to overcome the stress (Lange and Hengge-

[1] Adapted from (Lee *et al.* 2012) by permission of Annual Reviews under the turmes of the Copyright Clearance Center: Activating Transcription in Bacteria; Lee, Stephen, and Busby, Copyright ©2012.

Aronis 1991; Liu *et al.* 2018). The alternative σ-factor RpoE is one example out of the group of extracytoplasmic (ECF) σ-factors (Lonetto *et al.* 2019; Pinto *et al.* 2019). RpoE is present within the bacteria in an inactive form and is activated upon membrane stress. Active RpoE activates genes for cell envelope stress response, mainly small regulatory RNAs (sRNAs), but also other stress-related genes as well as other alternative σ-factors (Erickson and Gross 1989; Hayden and Ades 2008; Hews *et al.* 2019; Palonen *et al.* 2013). RpoH is part of the RpoE regulon. It is important for heat-stress resistance and is thereby referred to as the heat-stress σ-factor. RpoH activates the transcription of chaperones and other compounds for heat-stress survival (Emetz and Klug 1998; Grossman *et al.* 1987). For all bacteria with flagella-mediated motility, the alternative σ-factor FliA is present. This σ-factor activates transcription of flagellar genes and controls the process of flagellum assembly (Ohnishi *et al.* 1990; Starnbach and Lory 1992). The last alternative σ-factor to be mentioned here is SpoIIAC, which is present in *Bacillus* species and other spore-forming bacteria and is important in the formation of spores (Sun *et al.* 1991; Wösten 1998).

For further regulation of transcription, several activators and repressors are present within the cell. These can block the transcription by interfering with the binding of the RNAP-σ-factor-complex to the DNA or by promoting the recruitment of RNAP-σ-factor-complexes to a specific location. For both functions, an extensive set of regulatory proteins and protein families is known. Some of these work in a general way on different genes, while others affect only a few genes. One of the best known transcriptional repressors is the histone-like nucleoid-structuring protein (H-NS) (Cukier-Kahn *et al.* 1972; Grainger 2016). Similar to the histones in eukaryotes, H-NS binds to the DNA and condenses it. Therefore, the RNAP cannot bind to the initiation site and start the transcription of the respective gene. H-NS operates on a variety of different transcripts, by binding to the DNA in the region upstream of the promoter (Dole *et al.* 2004; Winardhi *et al.* 2015).

For the activators, several different classes are known, depending on the target. One of the best-analyzed activators is AraC. AraC is continuously synthesized. In the presence of arabinose in the cell, arabinose binds to AraC, allowing AraC to recruit RNAP and work as an activator for gene expression (Johnson and Schleif 1995; Lee *et al.* 1974; Schleif 2010). The mechanism of recruiting the RNAP is common in all transcriptional activators. However, they differ in the binding site of the RNAP as well as in the ability to bind additional factors. Some other activators are only expressed if needed and can directly recruit RNAP.

Taken together, transcription in general is regulated by the presence of specific σ-factors as well as by transcriptional activators and repressors. The so-transcribed mRNA can directly be used for translation.

1.1.2 The components of the translational machinery

The translation machinery consists of a core complex, the ribosome, and several additional factors. The ribosome itself is a large multiprotein complex that consists of RNA and ribosomal proteins. In total, the bacterial ribosome is composed out of 3 ribosomal RNAs (rRNAs), which are sorted according to their size in sedimentation and called 23S rRNA, 16S rRNA, and 5S rRNA. In addition to these, around 54 ribosomal proteins are also part of the ribosome (see Figure 1.2) (Clemons *et al.* 1999; Nanninga 1967; Yusupov *et al.* 2001). In contrast to most known enzymes, the rRNA builds the biggest part of the

ribosome and has some main catalytic functions. Therefore, the ribosome is also called a ribozyme (Lilley 2001). The ribosome core particle, which is also called the 70S particle, is made out of two subunits. These subunits have different functions in the translation process. The small subunit, also known as the 30S particle, is formed by the 16S rRNA and 21 ribosomal proteins. Its function is to recognize the ribosome binding site (RBS) of mRNAs and position their codons in the proper location within the 70S ribosome particle (Simonetti *et al.* 2008; Wimberly *et al.* 2000). The codons represent a sequence of three nucleotides located in the mRNA that is assigned to an amino acid (Taylor and Coates 1989; Wong 1975). The large subunit, also called the 50S particle, is formed by the 23S and the 5S rRNA and 33 ribosomal proteins (see Figure 1.2) (Sander *et al.* 1975). Its function is to position the transfer RNA (tRNA) and facilitated the peptidyl transferase activity inside the peptidyl transferase center (PTC). Both subunits together form the platform for codon detection and decoding, as well as the peptidyl transferase activity to form an amino acid chain from single amino acids. In the fully assembled 70S ribosome, three positions for tRNAs are formed. These sites are referred to as the A-site for the aminoacyl-tRNA site, the P-site for poly-peptide chain tRNA, and the E-site for the empty tRNA that exits the complex (Ramakrishnan 2002; Schmeing and Ramakrishnan 2009).

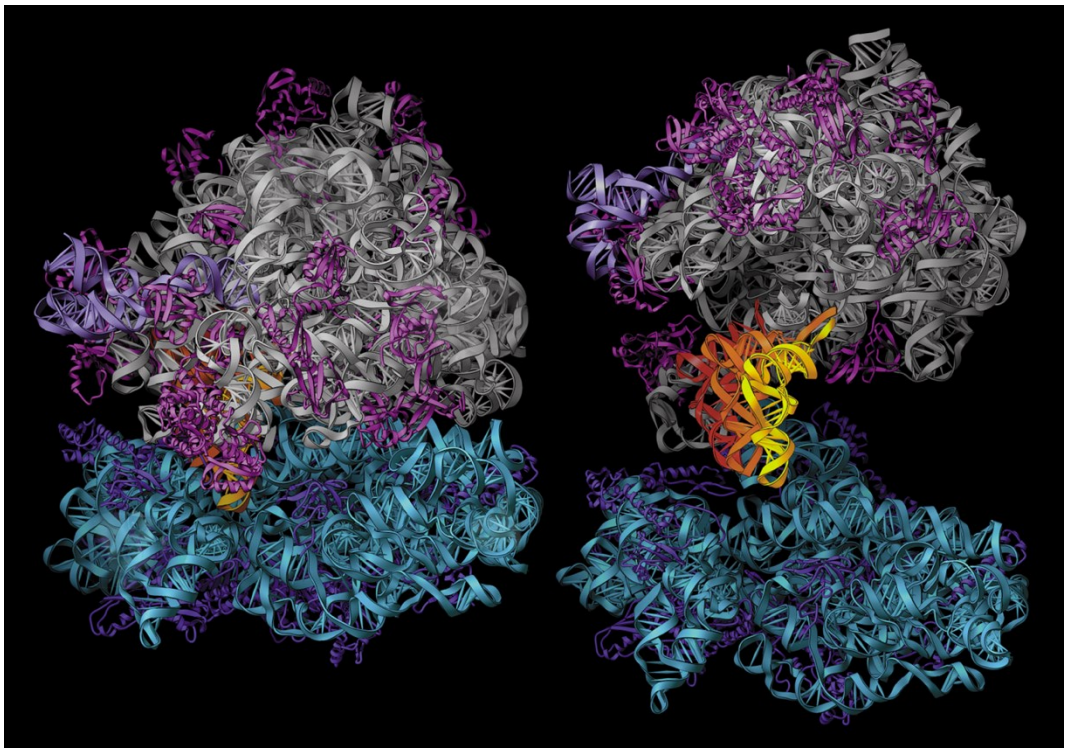

Figure 1.2) Structure of the 50S and 30S particles of *T. thermophilus*.

The ribosome represents the complex for translation in all living cells. It is formed out of ribosomal RNA rRNA) and ribosomal proteins, whereby the rRNA represents the major part of the ribosome. The ribosome in bacteria forms the 70S particle, which consists of the two sub-particles, 50S and 30S. The 50S particle, also called the large subunit, functions in tRNA positioning and peptidyl transferase. The 50S particle consists out of the 23S rRNA (light gray), the 5S rRNA (light purple), and 33 ribosomal proteins (purple structures). Despite this, the 30S particle has the function of mRNA and RBS detection. It is made by the 16S rRNA (light blue) and 21 ribosomal proteins (dark purple structures). The 70S particle is able to bind three tRNA in different positions located in the insight of the particle (yellow, orange, and red structures). On the left side, the ribosome is shown in the closed 70S particle form. On the right side, both subunits are opened, showing the location of the bound tRNAs ((Yusupov *et al.* 2001)[2], figure from the Noller Lab homepage: http://rna.ucsc.edu/rnacenter/ribosome_images.html, download date 09.11.2020).

[2] Adapted from (Yusupov *et al.* 2001) by permission of American Association for the Advancement of Science (AAAS)/ Science under the turmes of the Copyright Clearance Center: Crystal Structure of the Ribosome at 5.5 Å Resolution; Yusupov, Yusupova, Baucom, Lieberman, Earnest, Cate, Noller, Copyright ©2001

The amino acids required for translation are provided by another type of specialized RNA that can carry an amino acid and, on the other hand, can basepair with the appropriate codon. These RNAs are the tRNAs. They form a special secondary structure known as the cloverleaf structure with three hairpin loops. The second hairpin loop harbors the anticodon, which can basepair with the codon in the triplet code, located on the mRNA. At the 3' end of every tRNA, also called acceptor stem, the matching amino acid for this codon is bound to the tRNA (Hoaglanf *et al.* 1958; Zamecnik 2005). The loading of tRNAs is carried out by aminoacyl tRNA synthetase, which binds a free tRNA with the matching anticodon and the amino acid. Under ATP hydrolysis the tRNA is loaded with the amino acid. For every amino acid, a special aminoacyl tRNA synthetase is needed (Ibba and Söll 2000). Loaded aminoacyl-tRNAs can then be used by the ribosome for translation. The levels of total tRNAs and tRNA genes differ from organism to organism. Furthermore, not all codons need to have a perfect fitting tRNA (Silva *et al.* 2006). This is based on the fact that the first two nucleotides of the codon are sufficient for tRNA recognition. The third position is thereby negligible. This results in the ability to use tRNAs that only bind perfectly within the first two nucleotides and binds the third position in a non-canonical base pairing (non-Watson-Crick base-pairing) (Leontis and Westhof 2001; Watson and Crick 1953).

The mRNA, as the blueprint for translation, not only contains the coding sequence (CDS) but also regulatory elements. The element that is first recognized by the ribosome is the RBS. This is a region around 10 nucleotides upstream of the coding region where the ribosome initially binds the mRNA. The RBS, also known as the Shine-Dalgarno sequence (consensus sequence from *E. coli* AGGAGGU (Scherer *et al.* 1980)), interacts with the homologous anti-Shine-Dalgarno (aSD) sequence located within the 3' end of the 16S rRNA (small subunit) (Shine and Dalgarno 1975). Through the interaction of both sequences, the mRNA is positioned within the small subunit. The next feature is the coding region which is decoded by the ribosome and the tRNAs. The last feature is the stop codon. This codon is not recognized by a tRNA, but detected by a special protein factor that releases the amino acid chain from the ribosome, disassembles the mRNA and the big and small subunit of the ribosome. This allows the two subunits to initiate translation on a new mRNA (Rodnina 2018; Steitz 2008).

The last set of translational factors are proteins that interact with the ribosome, tRNAs and the mRNA at different steps in the process of translation. These factors are specific for certain steps in translation or provide the energy for the movement of the ribosome along the mRNA. In total nine factors contribute to the translation with three initiation factors (IFs in detail IF1, IF2, and IF3) (Gualerzi *et al.* 1977; Kay and Grunberg-Manago 1972; Milon *et al.* 2010), two elongation factors (EFs) called EF-Tu and EF-G (Jaskunas *et al.* 1975; Miller 1972), three release factors (RFs detail RF1, RF2, and RF3) (Craigen *et al.* 1985; Craigen and Caskey 1987; Grentzmann *et al.* 1994) and one ribosome recycling factor (RRF) (Hirashima and Kaji 1972).

All these parts together form the translational apparatus, which is capable of translating the genomic information, provided by the mRNA, into a protein sequence.

1.1.2.1 Steps in the translation of mRNA to protein

The ribosome, the tRNAs, the mRNA and all additional factors interact to perform translation, which is organized in four phases (see Figure 1.3). These phases are the initiation of the translation, the

elongation and finally the termination and recycling. The steps in translation are best analyzed in the *in vitro* model where a free RBS harboring mRNA is targeted by a ribosome. This model is referred to as the pioneering ribosome model. While transcription and translation often occur simultaneously in bacteria, the mechanism will be different, in the case of initiation, but hardly any detail is known about this mechanism (Agirrezabala and Frank 2010; Rodnina 2018).

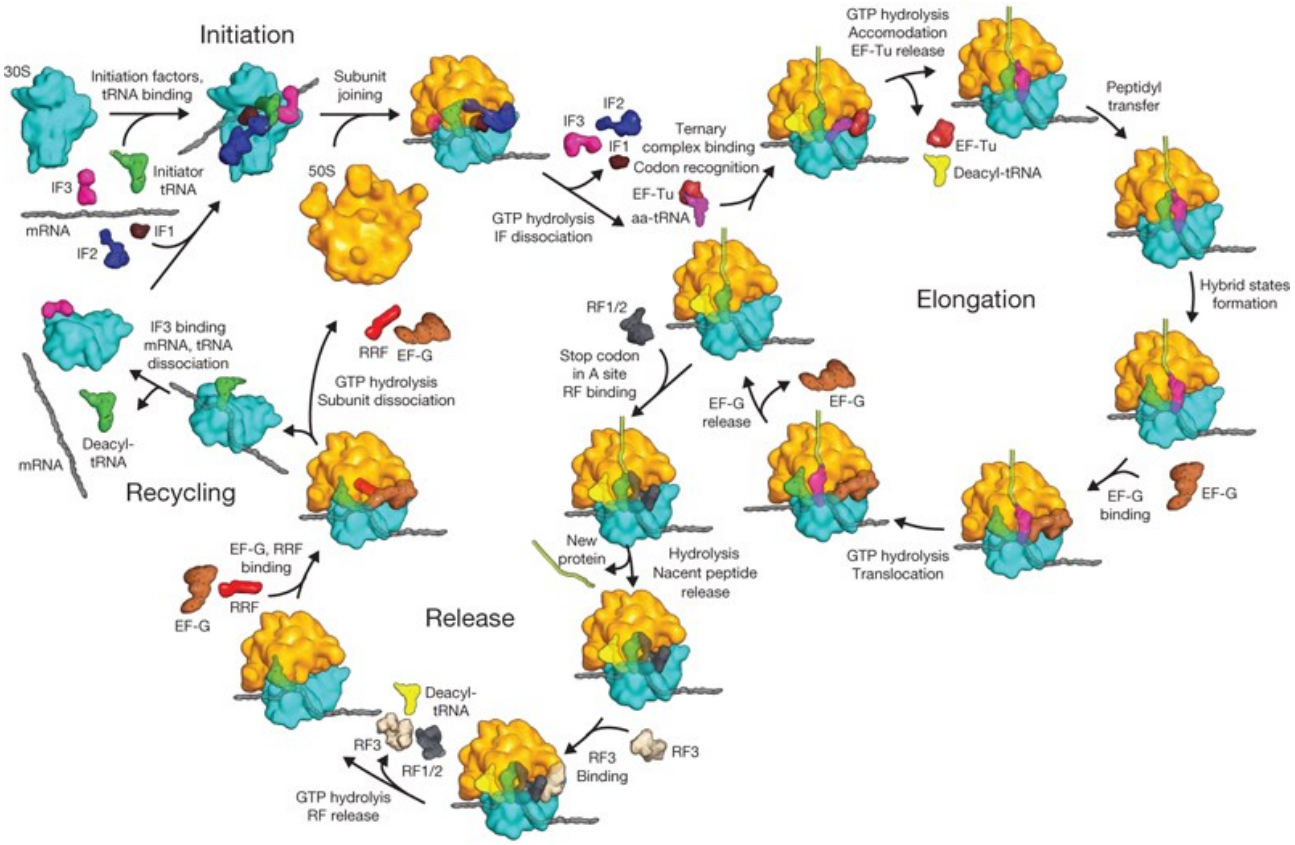

Figure 1.3) Steps of bacterial translation by the pioneering mechanism.

In bacteria as well as in eukaryotic cells the translation occurs in 4 steps. The steps are initiation (top left part), elongation (right part), release or termination (middle bottom) and recycling (left). In the case of bacterial translation, the 30S particle interacts with IF1, IF2, and IF3 as well as with the fMet-tRNA and the mRNA for initiation. Afterward, the 50S particle is recruited to complete the 70S particle. After initiation IF1, IF2 and IF3 are released and amino aminoacyl-tRNA (aa-tRNA) bound to EF-Tu provides the tRNA for translation. By the new tRNA, the ribosome performs a peptidyl transfer of the polypeptide to the new amino acid. In the next step, the whole ribosome is moved by one codon. This movement is facilitated by EF-G by the hydrolysis of GTP. In a circular process, the next tRNA is recruited as mentioned and the polypeptide is elongated. Upon reaching the stop-codon the termination is reached. Depending on the stop-codon RF1 or 2 binds and releases the polypeptide chain from the bound tRNA. With the help of RF3, RF1/2 as well as the tRNA in the exit position of the ribosome is released. To detach the 70S particle itself from the mRNA, the step of recycling is needed. In this final step RRF together with EF-G interact with the ribosome and by GTP hydrolysis disassemble the 70S particle into the 30S and 50S particle and release the mRNA. All components can be used for a new cycle of translation, as shown in the schematic (Schmeing and Ramakrishnan 2009)[3].

In the pioneering ribosome model, the first phase is represented by translation initiation. For this step, the small subunit interacts with free mRNA and binds to the RBS. Additionally, IF1, IF2, and IF3 interact with the small subunit of the ribosome, while IF2 and IF3 specifically assist in recruiting a fMet-tRNA (Gualerzi *et al.* 1977; Milon *et al.* 2010; Sette *et al.* 1997). Thereby, the fMet-tRNA with the start codon

[3] Used from (Schmeing and Ramakrishnan 2009) by permission of Springer Nature Ltd.: under the turmes of the Copyright Clearance Center: What recent ribosome structures have revealed about the mechanism of translation; Schmeing and Ramakrishnan, Copyright ©2009

(AUG) needs to be located on the P-site of the ribosome. After this, the large subunit enters the complex, forming the translational-active 70S particle and release the IFs.

To start the phase of elongation, EF-Tu-tRNAs randomly enter the ribosome at the A-site (Jaskunas *et al.* 1975; Richman and Bodley 1972). Every EF-Tu-tRNA that enters the ribosome is checked for proper base pairing between the codon and the anti-codon and non-fitting tRNAs are released again. A matching tRNA is stabilized in the A-site by the hydrolysis of GTP in the EF-Tu, leading to the releases of EF-Tu-GDP from the ribosome and exposes the amino acid bound to the tRNA. Next, the ribosome forms an ester-bond between both the amino acids in the A- and P-site of the ribosome. This transfers the polypeptide chain to the tRNA in the A-site, leaving an empty tRNA in the P-site. After the transfer of the polypeptide chain, EF-G interacts with the ribosome. By hydrolysis of the bound GTP, the ribosome is moved forward by one codon (Acharya *et al.* 1973; Miller 1972; Richman and Bodley 1972). In this confirmation, the ribosome can decode the next codon in the same manner as before.

At the end of the translation, when the ribosome reaches the stop codon, the phase of translation termination starts. During this step, RF1 or RF2, depending on the stop-codon, enters the ribosome as the tRNAs before. After RF1 or RF2 is positioned, it triggers the release of the polypeptide chain from the tRNA and from the ribosome itself. In the following step, RF3 interacts with RF1 or RF2 within the ribosome and thereby sets RF1 or RF2 and RF3 free (Craigen *et al.* 1985; Craigen and Caskey 1987; Grentzmann *et al.* 1994; Mikuni *et al.* 1994). Finally, after RF1, RF2, and RF3 left the ribosome, the remaining mRNA-ribosome complex needs to be disassembled, to allow the ribosome to perform a new round of translation. This last phase is thereby called the recycling phase. To disassemble the complex, RRF together with EF-G interacts with the ribosome (Hirashima and Kaji 1970, 1972; Janosi *et al.* 1996). After the interaction, EF-G hydrolyses the bound GTP, splitting apart the large and small subunit. This reaction frees both subunits as well as the mRNA and the remaining empty tRNA. After this phase, all components can start a new translation on the same mRNA or on another mRNA following the same procedure (Figure 1.3) (Melnikov *et al.* 2012; Rodnina 2018; Schmeing and Ramakrishnan 2009; Steitz 2008).

The pioneering ribosome model is the best-known way how translation occurs but it only explains the mechanism for free mRNA. Furthermore, the mechanism only works on mRNAs containing a leader sequence and a RBS. For mRNAs, without a RBS or leaderless mRNAs, the translation itself might happen in the same way only the initial phase is different. For both non-RBS containing transcripts, the start-codon seems to be important for ribosome recruitment and initiation.

1.1.3 Regulation of translation in bacteria

The first step of translational regulation is achieved by leadercontaining and leaderless mRNAs. This type of regulation was first discovered in persistent *E. coli* cells after encountering stress. The translation of certain essential mRNAs, while the majority of mRNAs is silenced, is guaranted by the toxin-antitoxin system MazEF (Vesper *et al.* 2011). Upon activation, MazF functions as an RNase cleaving the leader of specific mRNA molecules to generate leaderless mRNAs. Furthermore, MazF cleaving the last 43 nucleotides from the 3' end of the 16S rRNA including the aSD sequence, leading to preferential translation of leaderless mRNAs (Sauert *et al.* 2016; Vesper *et al.* 2011). This process can be reversed

in case of the 16S rRNA by the RNA ligase RtcB, resulting in a normal leader containing mRNA translation (Temmel *et al.* 2017).

Translation can also be controlled by the composition of the ribosomal proteins incorporated into the ribosome. In a study with immunoprecipitated ribosomes in eukaryotic cells, it was shown that the absence of the ribosomal proteins RPS25/eS25 or RPL10A/uL1 changes the translation of mRNAs important for cell metabolism, proliferation, and survival (Shi *et al.* 2017). The presence of the ribosomal proteins can enhance the translation of these mRNAs while on the other hand, it can lead to depletion of other mRNAs (Shi *et al.* 2017). For bacteria, ribosome heterogeneity is also reported but only for the ribosomal proteins L31 encoded by *rpmE* and L36 encoded by *rpmJ* (Lilleorg *et al.* 2019). Each of these proteins are encoded by two genes, resulting in two versions of the same protein. The proteins encoded by *rpmE* and *rpmJ* are incorporated into the ribosome under exponential growth conditions. At stationary growth, both proteins are exchanged with the alternative version encoded by the genes *ykgM/rpmE2* and *ykgO/rpmJ2*, respectively, resulting in higher fitness by an improved translation of mRNAs contributing to growth under stationary conditions (Lilleorg *et al.* 2019). Moreover, the exchange of L31 encoded from *rpmE* to the version encoded by *ykgM/rpmE2* also grants higher fitness to *E. coli* when growing at lower temperatures (Lilleorg *et al.* 2020).

Apart from translational regulation by modification of the ribosome, translation can also be regulated by sRNAs or thermo-sensitive RNA elements (Kortmann and Narberhaus 2012; Nuss *et al.* 2015; Chelsea *et al.* 2014). Both are most likely known to block the RBS for initiating ribosomes and thereby inhibiting translation or affecting the mRNA stability. While the thermo-sensitive RNA elements, so-called RNA thermometers, are part of the mRNA itself, the sRNA is transcribed independent of the target mRNA and can regulate different target mRNAs (Kortmann and Narberhaus 2012; Nitzan *et al.* 2017). Upon expression, sRNAs, are capable to rapidly regulate the translatiom of target mRNAs by base-pairing (Nitzan *et al.* 2017). In contrast. the thermo-sensitive RNA elements form a secondary RNA structure which changes in response to temperature. An increase of temperature promotes melting of the structure allowing translation initiation (Kortmann and Narberhaus 2012). Global approchaes identifiying sRNAs and thermo-sensitive RNA elements leaved several sRNAs as well as thermo-sensitive RNA elements that contribute in the regulation of virulence-associated genes in the human pathogen *Yersinia,* which have been analyzed in further detail (Böhme *et al.* 2012; Knittel *et al.* 2018; Righetti *et al.* 2016; Chelsea *et al.* 2014).

1.2 The genus *Yersinia*

The genus *Yersinia* is formed by 19 known species (Savin *et al.* 2019) of Gram-negative, rod-shaped bacteria, that belong to the γ-proteobacteria. All strains are facultative anaerobe, and present in soil, water, on plants and also on or in animals. The bacteria can grow within a wide variety of temperatures from 4°C up to 42°C with optimal growth at 25°C. Most of the 19 species are non-pathogenic, however, some of the strains are animal pathogens such as *Y. ruckeri* (Ross *et al.* 1966) that infects salmonids or *Y. entomophaga* (Hurst *et al.* 2011), which might infect insects (Chen *et al.* 2010; McNally *et al.* 2016; Reuter *et al.* 2014; Savin *et al.* 2019). Out of the 19, three species are known to be human pathogens namely *Y. pestis*, *Y. pseudotuberculosis* and *Y. enterocolitica*. All of these strains contain a virulence

plasmid of around 70 kilobases (kb) that encodes for virulence factors. This plasmid is called pCD1 in *Y. pestis* and pIB1 or pYV in *Y. pseudotuberculosis* and *Y. enterocolitica*. The virulence plasmids are highly conserved between all three strains whereby the plasmids from *Y. pestis* and *Y. pseudotuberculosis* are more similar to each other than the one from *Y. enterocolitica* (Bölin *et al.* 1988; Cornelis *et al.* 1998; Goguen *et al.* 1984; Portnoy *et al.* 1984; Snellings *et al.* 2001). Therefore, it is hypothesized that the plasmids were obtained independently by horizontal gene transfer.

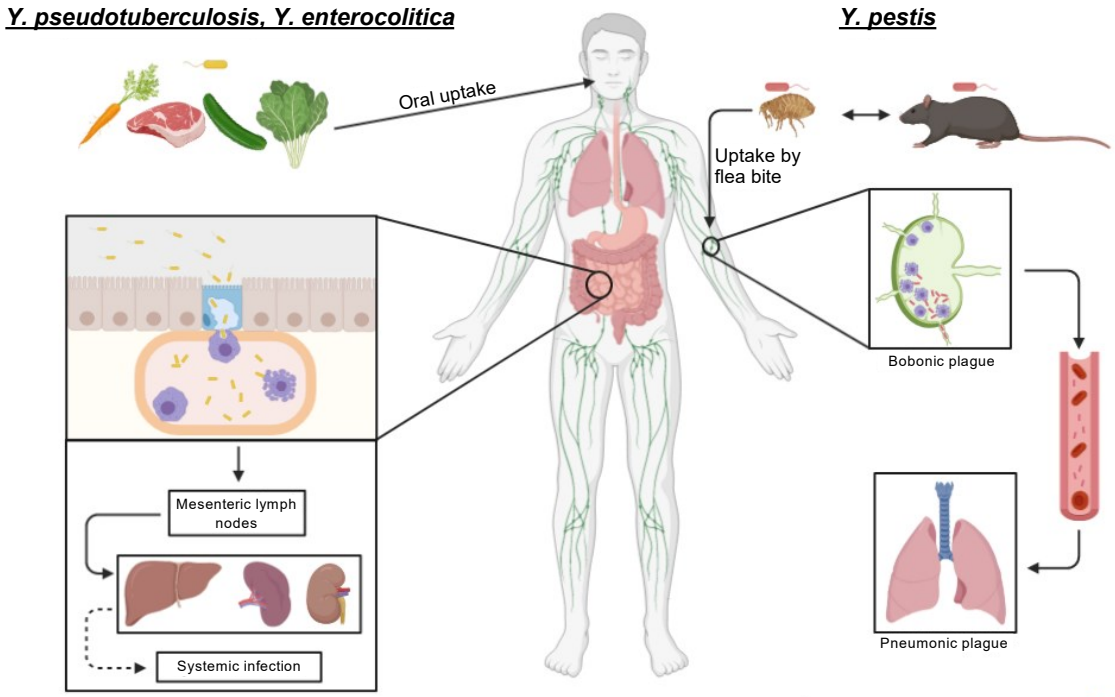

Figure 1.4) Routes of enteropathogenic *Yersinia* infection in contrast to *Y. pestis* infection.

Pathogenic *Yersinia* infects the human in two different ways based on the type of pathogen. *Y. pestis,* the causative agent of the plague, infects humans via the bite of an infected flea, which gets infected by rodents. Infection with *Y. pestis* can lead to bubonic plague or pneumonic plague. In contrast, the enteropathogenic *Y. pseudotuberculosis* and *Y. enterocolitica* species infect humans by contaminated food or water. After uptake, both pathogens enter the body via M-cells in the ileum. Underneath the M-cells they colonize the lymphatic tissue known as Peyer's patches. Afterwards, they can spread further to the mesenteric lymph nodes as well as to the liver, spleen and kidney. In rare cases, they can also spread systemically (Heroven and Dersch 2014)[4]. Created with BioRender.com.

Out of the three human pathogens, *Y. pestis* is the most prominent one. It is the causative agent of the plague. The plague was a severe disease in the middle ages referred to as the "Black Death". Nevertheless, the plague is still present today, for example in Madagascar but also in parts of the United States (USA) with several cases each year (Bertherat 2019). The plague is spread by fleas, where *Y. pestis* is colonizing the foregut (Sebbane *et al.* 2006). In contrast to *Y. pseudotuberculosis* and *Y. enterocolitica*, *Y. pestis* carries two additional virulence-associated plasmids. These plasmids are referred to as pMT1 and pPCP1 (Hu *et al.* 1998; Lindler *et al.* 1998; Pilsl *et al.* 1996). Both plasmids enable *Y. pestis* to infect deeper tissues and they provide benefits for the survival within the flea. After injection of *Y. pestis* into the host by a flea bite, *Y. pestis* disseminates into the lymph nodes to replicate. In the lymph nodes, it encounters the host immune system (Crowell 1919; Guinet *et al.* 2008). To prevent phagocytosis and inhibit an immune response, *Y. pestis* uses a type 3 secretion system (T3SS) to

[4] (Heroven and Dersch 2014) is licensed under the terms of the Creative Commons Attribution License. Copyright © Heroven and Dersch

translocate effector proteins into the cytosol of the immune cells. This leads to the death of the immune cells and thereby to the formation of the black swellings, so-called buboes, which represents one form of the infection and gave the disease its name, bubonic plague (Demeure *et al.* 2019; Pha and Navarro 2016). At later stages, *Y. pestis* spreads further to other organs, e. g. the lung. After infecting the lung, *Y. pestis* can spread from human to human by droplet coughing. This stage is called the pneumonic plague (Cleri *et al.* 1997; Pechous *et al.* 2016). Untreated infections can rapidly lead to death by a septic shock after *Y. pestis* spread systemically and infect the blood (Figure 1.4) (Achtman *et al.* 1999; Demeure *et al.* 2019; Erhardt and Dersch 2015; Perry and Fetherston 1997).

Y. pseudotuberculosis and *Y. enterocolitica* cause a self-limiting gastrointestinal disease called Yersiniosis (Bölin *et al.* 1982; Chlebicz and Śliżewska 2018). The symptoms of this disease are abdominal pain and diarrhea. In rare cases, systemic infections are possible, leading to autoimmune diseases like erythema nodosum or reactive arthritis (Jalava *et al.* 2006; Kaasch *et al.* 2012; Vasala *et al.* 2014). In contrast to *Y. pestis*, *Y. pseudotuberculosis* and *Y. enterocolitica* are taken up by contaminated food or water (Schiemann 1987). During the passage of the gastrointestinal tract, the bacteria interact with specialized cells in the epithelium of the ileum called microfold-cells (M-cells). M-cells show a reduced amount of microvilli on their apical surface (Autenrieth and Firsching 1996; Hamzaoui *et al.* 2004). They have the function of taking up material from the lumen of the small intestine and present it to immune cells at the basolateral side. The bacteria enter the M-cells and migrate to the underlying tissues (Kanaya *et al.* 2020; Wang *et al.* 2014). After trans-migration, the *Yersiniae* are released by an unknown mechanism and reach the Peyer's patches, a special area at the basal side of the epithelium that belongs to the mucosa-associated lymphoid tissue. This tissue is composed of different immune cells and plays an important role in the immune response and infection control of the small intestine (Kobayashi *et al.* 2019). Hence to ensure survival, *Yersinia* needs to counteract the host immune system, in particular macrophages and neutrophils. Both types of immune cells are present in the Peyer's patches and are additionally recruited to the side of infection. These are immune cells of the innate immune system and represent the first line of defense against pathogens, preferentially bacteria. To clear bacterial infections, immune cells phagocytize the bacteria and subsequently digest them (Chaplin 2010; Thaiss *et al.* 2016). To counteract the immune cells, enteropathogenic *Yersinia* also use a T3SS to translocate effector proteins into the immune cells. These effector proteins function as inhibitors of phagocytosis and can lead to immune cell apoptosis (Erfurth *et al.* 2004; Rosqvist *et al.* 1988; Ruckdeschel *et al.* 1997). After defeating the host immune system, the bacteria can disseminate further, first to the mesenteric lymph nodes and afterward to the liver, spleen, and kidney. Finally, *Y. pseudotuberculosis* and *Y. enterocolitica* can also spread systemically (Figure 1.4) (Erhardt and Dersch 2015; Heroven and Dersch 2014; Sansonetti 2004; Wren 2003).

Although *Y. pestis* and *Y. pseudotuberculosis* seem to be significantly different, especially by looking at the virulence phenotype, they are closely related to each other. In phylogenetic studies, it was shown that *Y. pestis* emerged from *Y. pseudotuberculosis* between 2,000 to 10,000 years ago (Achtman *et al.* 1999; Demeure *et al.* 2019; Reuter *et al.* 2014). The difference in pathogenicity is thought to originate from mutations in the chromosome, as well as the two additional plasmids *Y. pestis* acquired (Demeure *et al.* 2019).

1.2.1 Pathogenesis of enteropathogenic *Yersinia* species

The pathogenicity of the two enteropathogenic strains, *Y. pseudotuberculosis* and *Y. enterocolitica,* can be separated into two infection phases. Both phases are characterized by unique virulence factors which provide benefits in the respective situations. In the first, initial phase of the infection, the bacteria are taken up by the host into the intestinal lumen. After migration through the M-cells, the bacteria enter the acute or ongoing infection phase, where they encounter the host immune system. In this phase, the overall gene expression changes from the colonization to the defense mode. This allows the bacteria to escape the attacks of the host immune mechanisms and to replicate in the lymphoid tissue (Figure 1.5) (Chen *et al.* 2016; Cossart and Sansonetti 2004; Erhardt and Dersch 2015).

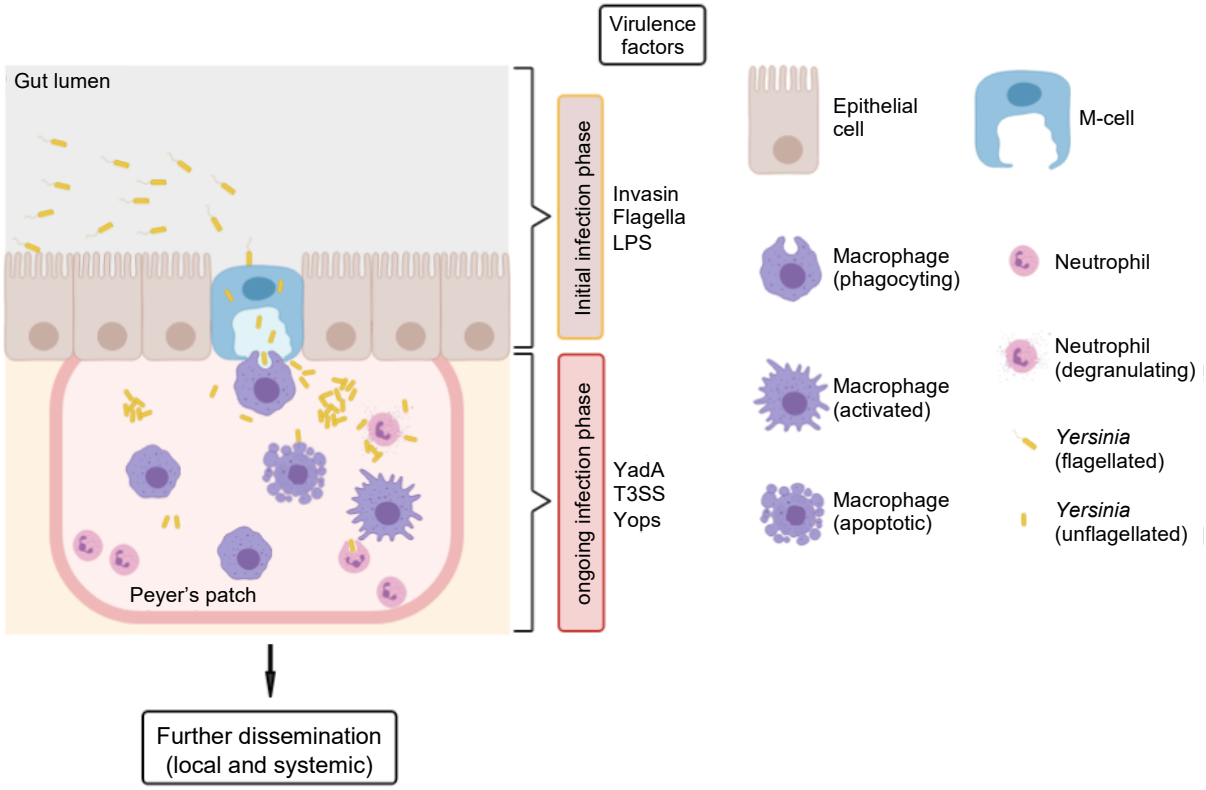

Figure 1.5) The infection phases of *Y. pseudotuberculosis* in the small intestine (ileum).

The infection of enteropathogenic *Yersiniae* can be divided into the initial infection and the ongoing infection. In the initial infection phase, the bacteria colonize the small intestine and compete for niches in the gut. In addition, they express adhesions and invasins to be taken up by the M-cells. After uptake by the M-cells and release into the lymphatic tissue (Peyer's patches), *Yersiniae* change to the ongoing infection phase. Here, they encounter the host immune system, and express the type 3 secretion system (T3SS), effector proteins (Yops) and the adhesin YadA to prevent phagocytosis. These components that are expressed during the ongoing infection phase are encoded on the *Yersinia* virulence plasmid ((Sansonetti 2004)[5] modified from (Stephanie Christine Seekircher 2014; Vollmer 2020)). Created with BioRender.com.

1.2.1.1 Initial infection phase

In the initial infection phase, the bacteria are taken up via contaminated food or water. First, the *Yersinia* enter the stomach, where they need to survive the acidic pH. Afterwards, the bacteria reach the ileum where they interact with the M-cells in which they enter and are passaged across the intestinal epithelium. To achieve this, the bacteria express specific virulence factors including flagella and the

[5] Adapted from (Sansonetti 2004) by permission of Springer Nature Ltd. under the turmes of the Copyright Clearance Center: War and peace at mucosal surfaces; Sansonetti, Copyright ©2004

adhesion molecule invasin (Inv) (Erhardt and Dersch 2015; Kapatral *et al.* 1996; Leo and Skurnik 2011; Mikula *et al.* 2013; Sadana *et al.* 2017, 2018; Simonet and Falkow 1992). The flagella are needed for the bacteria to move through the lumen of the small intestine and reach the intestinal epithelium. Upon reaching the M-cells, invasin is needed to interact with receptors on the M-cells surface to facilitate *Yersinia* uptake and subsequent migration through the M-cells (Isberg 1989).

1.2.1.2 Ongoing infection phase

After release of *Yersinia* from the M-cells into the subepithelial lymphoid tissue, the bacteria adjust their gene expression from motility and invasion to defense against attacking phagocytic immune cells. This is achieved by the repression of the early phase virulence genes and the induction of genes required for T3SS-mediated host defense. These genes are encoded on the *Yersinia* virulence plasmids pIB1/pYV (Bölin *et al.* 1982; Portnoy *et al.* 1984). The virulence plasmid pIB1/pYV encodes the T3SS itself, different effector proteins, that prevent phagocytosis, and the adhesion molecule YadA to stabilize the interaction between the bacteria and the host cells for T3SS activation. Their expression is tightly regulated by temperature and host cell contact to ensure maximal system activation only under the conditions where immune cell attack (Volk *et al.* 2019). Upon activation, the system responds strongly to counteract the phagocytosis by immune cells, in particular by professional phagocytic cells like macrophages and neutrophils (Cornelis *et al.* 1998; Fällman *et al.* 2002; Trosky *et al.* 2008). Additionally, the bacteria increase the copy-number of the virulence plasmid from one copy per cell at ambient non-pathogenic conditions to around four to five copies per cell in the ongoing infection phase (Erhardt and Dersch 2015; Nuss *et al.* 2017; Wang *et al.* 2016).

1.3 The Ysc-Yop virulence

The T3SS and the effector proteins are encoded by the *ysc-yop* genes located on the virulence plasmid (Bölin *et al.* 1982). The *ysc* genes comprise 25 genes that encode the proteins that make up the T3SS. The effector proteins and the proteins forming the translocon pore are part of the *yop* genes. As these gene products are translocated to the host cell, *yop* stands for *Yersinia outer protein*. The adhesinYadA is also crucial for Ysc-Yop-mediated virulence but is not part of either group. Together, the *ysc-yop* and *yadA* genes, represent the armory of *Yersinia* to counteract the immune response during the ongoing infection phase (Fällman *et al.* 2002; Heroven and Dersch 2014; Sansonetti 2004).

1.3.1 The multiprotein complex of the T3SS

For the translocation of effector proteins into host cells, *Yersinia* uses the T3SS multiprotein complex. This complex acts like a molecular syringe that transports unfolded proteins through the bacterial cell membranes and through the host cell membrane into the host cytosol (Dewoody *et al.* 2013).

The T3SS can be divided into three main parts, the basal body located in the bacterial cell envelope, the needle spanning the space between bacteria and host cells forming a tunnel and the pore complex in the host membrane (Dewoody *et al.* 2013). Upon expression of the T3SS genes, the basal body is assembled first in a hierarchical manner. Assembly starts by oligomerization of YscC in the outer membrane reaching into the periplasm forming the C-ring. The periplasmic part of the YscC ring recruits YscD that span further into the inner membrane. YscD interacts with YscJ in the inner membrane leading

to the assembly of the so-called MS-ring (Diepold *et al.* 2010; Gamez *et al.* 2012; Goodin *et al.* 2005; Kowal *et al.* 2013; Silva-Herzog *et al.* 2008). After assembly of this frame structure, the ATPase complex is formed at the cytoplasmic side of the inner membrane. The ATPase complex consists of YscN, YscL and YscK (Blaylock *et al.* 2006; Diepold *et al.* 2010; Woestyn *et al.* 1994). It is hypothesized that YscK interacts with YscJ to localize the ATPase complex in the membrane-spanning frame structure (Diepold *et al.* 2010). Assembly of the ATPase complex into the basal body facilitates the formation of a C-ring structure by oligomerization of YscQ at the intracellular side of the MS-ring via interaction with YscJ (Bzymek *et al.* 2012; Diepold *et al.* 2015). In parallel, the export apparatus is assembled in the inner membrane, consisting of the proteins YscRSTUV. The export apparatus forms the substrate translocation channel and functions in conferring substrate specificity (Diepold *et al.* 2011). The oligomerization of YscV triggers the interaction of the assembled export apparatus with the basal body complex, forming the functional basal body (Diepold *et al.* 2011). Upon basal body assembly, the formation of the needle structure is induced. Here, a tunnel is formed by YscI spanning the periplasmic space. YscI is thought to interact with the export apparatus as well as with the C-ring formed by YscC. Afterwards, the needle protein YscF is exported from the needle structure to the extracellular side of the YscC C-ring (Cao *et al.* 2017; Deng *et al.* 2017; Dewoody *et al.* 2013; Souza *et al.* 2018).

In addition to the needle protein YscF, YscP also plays a role in this step. It works as a molecular ruler controlling the length of the needle structure. After reaching the appropriate length, YscP is thought to mediate a substrate switch on YscU to the later substrates like the low calcium response protein V (LcrV), YopB and YopD to form the translocon pore (Agrain *et al.* 2005; Payne and Straley 1999; Wood *et al.* 2008). While the basal body and needle are assembled directly, the pore complex only assembles upon host cell contact. Without cell contact, the T3SS is present in an inactive state in which LcrV seals the needle as a tip protein (Broz *et al.* 2007; Chaudhury *et al.* 2013). Upon cell contact, YopB and YopD are exported into the membrane of the target cell by interaction with LcrV to form the translocon pore, resulting in a tunnel connecting both cells (Sarker *et al.* 1998). With the assembly of the pore complex, the T3SS is active and able to translocate effectors into the target cell (Figure 1.6) (Cornelis 2000; Deng *et al.* 2017; Dewoody *et al.* 2013; Diepold and Wagner 2014; Mecsas 1996).

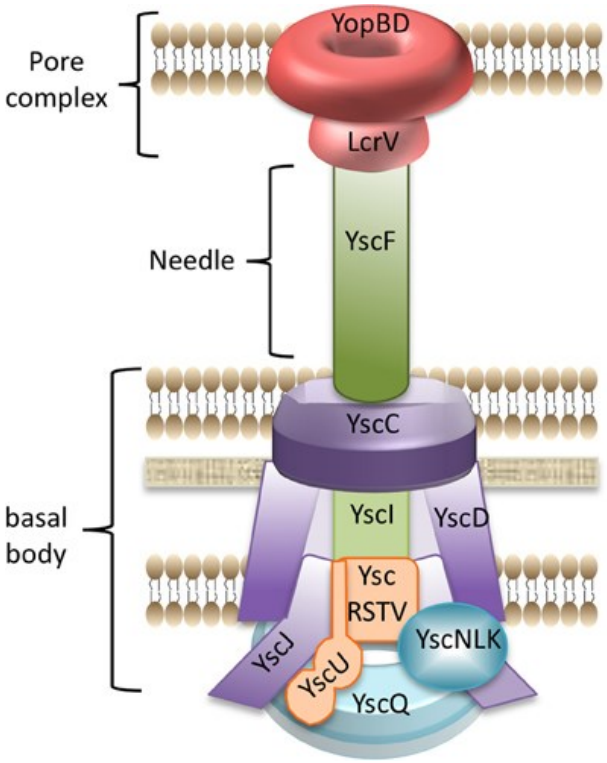

Figure 1.6) The type 3 secretion system (T3SS) of *Yersinia* as a schematic model.

The T3SS complex consists of the basal body, the needle, and the translocation pore. The basal body forms a C-ring in the outer membrane by YscC and prolongation to the inner membrane by YscD (purple). In the cytoplasm, YscJ forms the MS-ring (purple). YscQ (light blue) forms a second C-ring in the cytoplasm attached to YscJ. The ATPase complex of YscNLK (blue) is attached to YscJ in the basal body as well as to the export apparatus formed by YscRSTUV (orange). The space between the export apparatus and the C-ring of YscC is spaced by YscI (light green). The needle is formed by YscF (green), which polymerizes extracellularly. On top of the needle, the translocon pore complex is formed within the target cell membrane. The pore complex is built by YopBD (red) and the needle tip by LcrV (light red) (Dewoody *et al.* 2013)[6].

In the case of *Yersinia,* a second signal that triggers the activation of the T3SS and translocation of effector proteins is known. It was observed that growing *Yersinia* at 37°C in the absence of calcium results in T3SS activation and secretion of effectors into the growth media. So far, it is still under investigation how calcium (Ca^{2+}) depletion activates the T3SS (Straley *et al.* 1993). This process of secretion mimic host cell contact *in* vitro and is referred to as *"secretion conditions"*. This is an artificial but well-established model to analyze the regulation of *ysc-yop* virulence in *Y. pseudotuberculosis* under controlled culture conditions (Wiley *et al.* 2007)

1.3.2 The *Yersinia* outer proteins (Yops)

The second group of proteins in the Ysc-Yop virulence group are the effector proteins (Bölin *et al.* 1985). The effector proteins are translocated into the target cell upon cell contact in a T3SS-dependent manner (Trosky *et al.* 2008). In addition to the effector proteins, the translocon pore proteins are also part of the Yops. To ensure proper expression of the *yop* genes, they are regulated in a temperature- and LcrF-dependent manner with a fine-tuned regulation by additional factors. In this context, LcrF is the transcriptional activator of the *ysc-yop* genes and is encoded on the virulence plasmid. The expression of LcrF is temperature regulated and tightly controlled (Schwiesow *et al.* 2015). In addition to the

[6] (R. S. Dewoody et al. 2013) is licensed under the terms of the Creative Commons Attribution License. Copyright © Dewoody, Merrit and Marketon.

expression itself, the hierarchy of translocation is tightly controlled to ensure high efficiency of Yop delivery in the host cell (Fahlgren *et al.* 2009; Viboud and Bliska 2005).

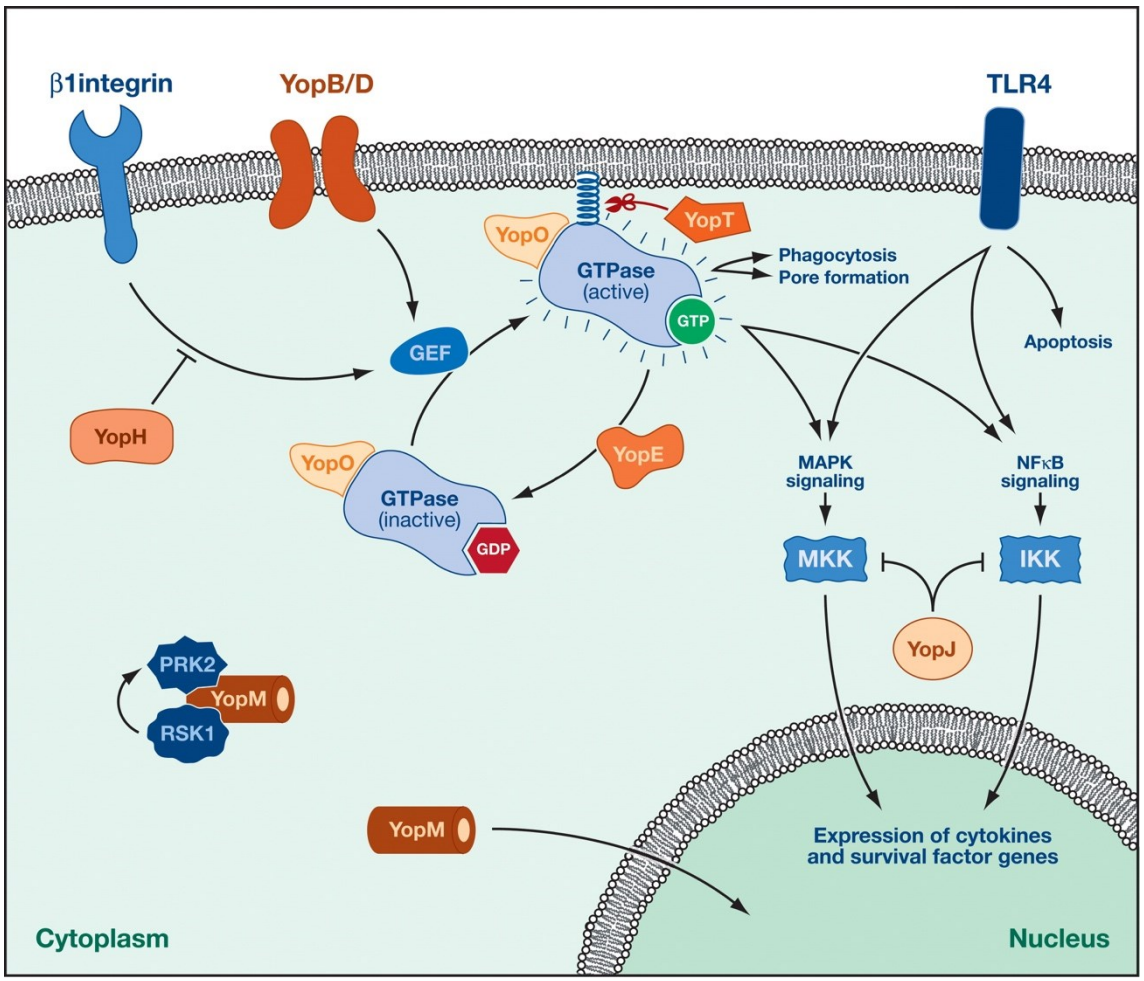

Figure 1.7) Function of the Yops after translocation into the host cell.

The Yop effector proteins trigger different functions in phagocytic immune cells to prevent phagocytosis. YopH phosphorylates a great variety of proteins, associating with β1-integrins, to block the activation of phagocytosis (left side). The effectors YpkA/YopO, YopT and YopE interfere with the activation of small Rho GTPases, which trigger phagocytosis (center). Also, YopE can lead to actin depolymerization. To prevent cell signaling, YopP/YopJ inhibits MAPK and NF-κB signaling to block the recruitment of immune cells (right). Besides this, it can lead to apoptosis. YopM itself has no catalytic function but interacts with RSK1 and PRK2 from the immune cell and thereby inhibiting the inflammasome (bottom) (Viboud and Bliska 2005)[7].

The first proteins transported by the T3SS are **YopB** (~42 kDa) and **YopD** (~33 kDa), which form the translocon pore within the target cell membrane, producing a channel for Yop translocation (Montagner *et al.* 2011). Under conditions where the T3SS is inactive (non-cell-contact or non-secretion conditions), YopB and YopD remain in the bacterial cytosol (Håkansson *et al.* 1993, 1996). To stabilize both proteins and prevent their degradation, they interact with the chaperone LcrH. In addition to its function in stabilization, LcrH inhibits aggregation of YopB and YopD as well as preventing pore-formation within the inner membrane of the bacteria (Figure 1.7) (Costa *et al.* 2010; Edqvist *et al.* 2007; Viboud and Bliska 2005).

Once YopB and YopD form the translocon pore, the effector proteins are exported. The core set of effectors in all pathogenic *Yersinia* consist of YopE, YopH, YopM, YopK/YopQ, YopJ/YopP and

[7] Used from (Viboud and Bliska 2005) by permission of Annual Reviews under the turmes of the Copyright Clearance Center: *YERSINIA* OUTER PROTEINS: Role in Modulation of Host Cell Signaling Responses and Pathogenesis; Viboud and Bliska, Copyright ©2005.

YpkA/YopO. *Y. pestis* and *Y. enterocolitica* encode an additional Yop called YopT (Forsberg *et al.* 1994). In most strains of *Y. pseudotuberculosis*, *yopT* and the associated chaperone *sycT* are deleted. Loss of YopT in *Y. pseudotuberculosis* might be compensated by the presence of YopE, which has the same target protein suggesting that both effectors facilitate a similar function in host defense (Viboud *et al.* 2006). Furthermore, YopT, YopE and YopH belong to the group of chaperone-requiring Yops, while YopM, YopK/YopQ, YopJ/YopP and YpkA/YopO lack a chaperon (Wattiau *et al.* 1994; Wattiau *et al.* 1996; Woestyn *et al.* 1996). While it is known that the chaperones play a role in protein stability within the bacteria, the Yop chaperones assist in the regulation of the translocation hierarchy (Trosky *et al.* 2008; Viboud and Bliska 2005).

The first translocated Yop is **YopH**, a ~51 kDa protein, which functions as a tyrosine phosphatase (Black 1997; Bölin and Wolf-Watz 1988). The translocation hierarchy is thought to be due to a high affinity of the YopH specific chaperone SycH to the export apparatus of the T3SS. In the absence of cell-contact or non-secretion conditions, YopH-SycH is present within the bacterial cell (Woestyn *et al.* 1996). After T3SS activation, SycH is recruited to the sorting platform of the export apparatus and thereby translocates YopH as the first effector (Wulff-Strobel *et al.* 2002). In the eukaryotic cell, YopH acts on different signaling pathways such as p130Cas and Fys in macrophages or SCAP2 in macrophages, which contribute in recruitment of immune cells. YopH dephosphorylates these signaling molecules, thereby inhibiting the respective signaling cascade (Bliska *et al.* 1991; Hamid *et al.* 1999; de la Puerta *et al.* 2009; Shaban *et al.* 2020). Upon immune cell contact, β1-integrins are activated by the interaction of YadA via a fibronectin bridge. The function of YopH as phosphatase counteracts this activation by blocking the activation of the signaling pathway (Shaban *et al.* 2020; Thinwa *et al.* 2014). Additionally, YopH also interferes with other signaling pathways, for example inhibiting degranulation of neutrophils as well as blocking immune cell signaling of macrophages, T-cells, and B-cells (Figure 1.7) (Andersson *et al.* 1999; Hamid *et al.* 1999; Rolán *et al.* 2013; Shaban *et al.* 2020).

After the translocation of YopH, a greater variety of Yops is translocated. Yops that are translocated in this step, all belong to the group of chaperone-lacking Yops. This includes YpkA/YopO, YopM, YopJ/YopP and YopK/YopQ. These Yops target different proteins within the host cell and further facilitate inhibition of phagocytosis, inhibition of immune cell signaling and can lead to apoptosis (Grosdent *et al.* 2002; Trosky *et al.* 2008; Visser *et al.* 1995). **YpkA** (~82 kDa) of *Y. pestis* and *Y. pseudotuberculosis* or **YopO** of *Y. enterocolitica* targets RhoA and inhibits phagocytosis, e. g. by phosphorylating substrates like actin-modulating proteins (Lee *et al.* 2017; Pha *et al.* 2014). **YopM** (~46 kDa; pIB1) unlike the other Yops is lacking enzymatic activity but contains two protein-binding domains. As a characteristic, YopM contains a long stretch of leucine-rich-repeats (LRRs) (Kobe 2001; Vieux and Barrick 2011). After entering the cell, YopM binds the two eukaryotic proteins RSK1 (ribosomal S6 kinase 1) and PRK2 (protein kinase C related kinases 2) decreasing the production of several proinflammatory cytokines. Moreover, the RSK1-YopM-PRK2 complex inhibits caspase-1 activity. This prevents caspase 1-mediated activation of the inflammasome leading to inflammation or pyroptosis (LaRock and Cookson 2012). Taken together, YopM interferes with the recruitment of more immune cells (Boland *et al.* 1998; Chung *et al.* 2016; Höfling *et al.* 2015; Malik and Bliska 2020; Rüter *et al.* 2014). **YopJ** (~32 kDa) of *Y. pestis* and *Y. pseudotuberculosis* or **YopP** of *Y. enterocolitica* inactivates members of the MAPK (mitogen-activated protein kinase) kinase (MKK) family and IKK (IκB kinase) to

repress the NF-κB pathway, inhibiting proinflammatory responses and cell survival mechanisms (Bliska 2006). This inhibits the recruitment of additional immune cells and causes apoptosis in the available immune cell pool (Monack *et al.* 1997; Orth 2002; Palmer *et al.* 1999; Schoberle *et al.* 2016; Sweet *et al.* 2007). The last Yop out of this intermediate group is **YopK** (*Y. pestis* and *Y. pseudotuberculosis*)/**YopQ** (*Y. enterocolitica*) which has a more regulatory function, compared to the other Yops. YopK is the smallest protein of the family with ~21 kDa and is known to interact with YopB and YopD in the cytosol of the host cell. Thereby, it regulates the delivery of Yops into the host cell. YopK/YopQ also interacts with RACK1 and is hypothesized to inhibit caspase-1 activity together with YopM (Dewoody *et al.* 2011; R. Dewoody *et al.* 2013; Thorslund *et al.* 2013). Together YpkA/YopO, YopM, YopJ/YopP, and YopK/YopQ mainly inhibit the recruitment of immune cells to the place of infection and assist in the inhibition of phagocytosis. Lastly, they can force the cell into apoptosis (Figure 1.7) (Cornelis 2002; Trosky *et al.* 2008; Viboud and Bliska 2005).

The Yops that are translocated last are **YopT** (~36 kDa) and **YopE** (~23 kDa), with YopE being the final one. YopT, as well as YopE, are bound to their cognate chaperones SycT and SycE, respectively. Unbound YopT and YopE are rapidly degraded within the bacteria cell (Forsberg and Wolf-Watz 1990; Wattiau and Cornells 1993). As for YopH-SycH, the chaperone is thought to facilitate the hierarchy of translocation. After translocation, both proteins target small Rho GTPases like RhoA, Rac-1, and Cdc42 and inhibit their function leading to actin depolymerization and rounding of cells (Aepfelbacher *et al.* 2003; Aili *et al.* 2003, 2008; Viboud *et al.* 2006). This supports inhibition of phagocytosis (Von Pawel-Rammingen *et al.* 2002). Besides its function as an effector protein, YopE was also shown to regulate protein translocation. Upon translocation, YopE blocks the translocation pore by forming a plug. This plugging is sensed by the bacteria and stops translocation of additional Yops (Trosky *et al.* 2008; Viboud and Bliska 2001). Subsequently, this process leads to the detachment of the bacteria from the targeted host cell. The plugging also seals the translocon pore that remains in the host cell membrane after detachment, inhibiting the release of cytosolic material and thereby the recruitment of immune cells (Figure 1.7) (Bliska *et al.* 1993; Cornelis 2002; Trosky *et al.* 2008; Viboud and Bliska 2005).

1.4 The adhesion molecule YadA

The adhesin YadA does not belong to the Ysc or Yop proteins but it is a crucial part of the T3SS-Yop promoted virulence. Similar to invasins that are necessary for uptake by M-cells, the adhesin YadA is essential for cell-cell interaction (Eitel *et al.* 2002; Heise and Dersch 2006). YadA is needed to stabilize the interaction between the bacteria and their target cells in the contact region of the T3SS for proper translocation activity. YadA is activated in a temperature-dependent manner controlled by the transcriptional activator LcrF (Skurnik and Toivanen 1992). In contrast to other adhesins, YadA is the only adhesin encoded on the virulence plasmid. In addition to temperature, media composition was also reported to affect YadA expression (Skurnik and Toivanen 1992). The *yadA* gene encodes a ~45 kDa protein that forms a homotrimeric complex anchored within the outer membrane by the C-terminus. The homotrimeric shape is referred to as "*lollipop*"-shape (Schütz *et al.* 2010; Skurnik and Wolf-Watz 1989; El Tahir and Skurnik 2001), which contains a host cell interaction domain in the N-terminus. This region promotes binding to fibronectin bound to β1-integrins (Eitel *et al.* 2002; Heise and Dersch 2006). YadA also has additional functions in addition to mediating cell-cell interaction. It facilitates serum resistance

by inhibiting complement-induced lysis and allows autoagglutination of *Yersiniae* (Ackermann *et al.* 2008; Mikula *et al.* 2013; Mühlenkamp *et al.* 2015; Pilz *et al.* 1992; Schindler *et al.* 2012).

1.5 Regulation of the Type III secretion system

Different types of regulatory proteins are known to regulate Ysc-Yop-mediated virulence. The regulators range from global regulators like CsrA, encoded on the chromosome, to *ysc-yop* genes special regulators encoded on the virulence plasmid. Some regulators are able to act bifunctionally as they contain a T3SS or effector function as well as a regulatory function. One of the most prominent regulators is the "*low calcium response protein F*" (LcrF) or "*virulence regulon transcriptional activator F*" (VirF) from *Y. pseudotuberculosis* or *Y. enterocolitica*, respectively. LcrF is the transcriptional activator of many T3SS- and Yop-related genes. LcrF itself is also tightly regulated (Böhme *et al.* 2012; Hoe and Goguen 1993; Schwiesow *et al.* 2015). YopD together with LcrH, LcrQ/YscM, and TyeA-YopN-SycN are additional regulators of the *ysc-yop* genes (Bamyaci *et al.* 2018; Cambronne and Schneewind 2002; Kusmierek *et al.* 2019).

1.5.1 The virulence master regulator LcrF

The LcrF/VirF protein is so far the only confirmed transcriptional activator of Ysc-Yop-mediated virulence in *Yersinia* and was first identified in *Y. pestis* as a regulator for T3SS-associated genes (Yother *et al.* 1986). It is encoded on the virulence plasmid and located between two operons encoding T3SS structural components. The *lcrF* gene itself forms a bicistronic operon with *yscW* (Böhme *et al.* 2012).

The *lcrF* gene encodes for a ~31 kDa protein of the AraC-like transcriptional activator family, which is expressed at elevated temperatures. LcrF functions by forming a homodimer which binds upstream of the RNAP binding site of the majority of *ysc-yop* genes and operons and *yadA* (Schwiesow *et al.* 2015). As shown for other AraC-like transcriptional activators, it interacts with σ-factors to recruit the RNAP to initiate transcription of these virulence-associated genes (G. Cornelis *et al.* 1989; G. R. Cornelis *et al.* 1989; Schwiesow *et al.* 2015; Skurnik and Toivanen 1992; Yang *et al.* 2011). LcrF expression is controlled by a variety of different factors to ensure it only occurs under appropriate conditions. To guarantee efficient repression under T3SS-inactive conditions (non-cell-contact and non-secretion) or non-T3SS-inducing (environmental) conditions, LcrF is regulated at the transcriptional level as well as at the post-transcriptional level (Böhme *et al.* 2012; Kusmierek *et al.* 2019; Steinmann and Dersch 2013; Straley *et al.* 1993).

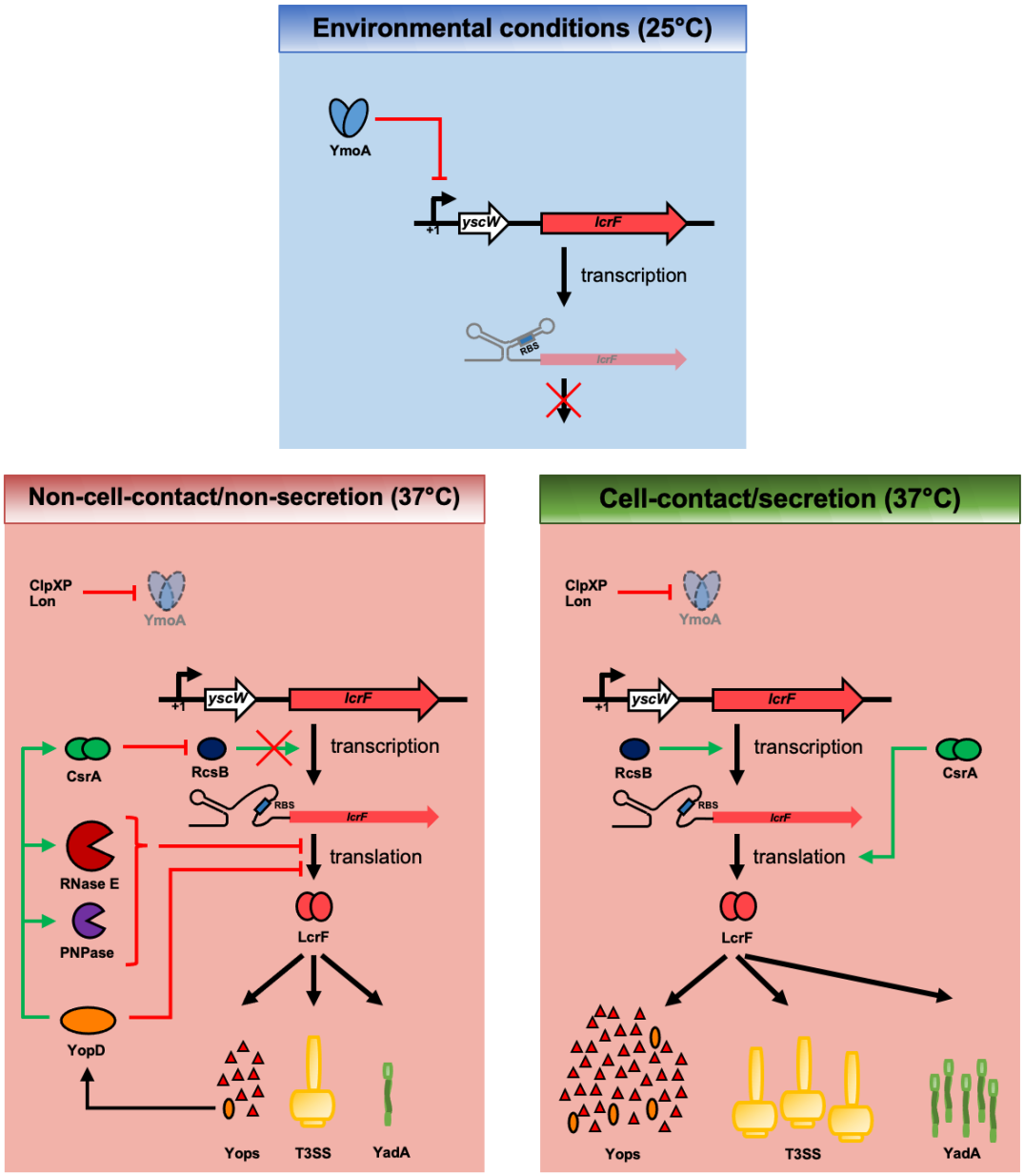

Figure 1.8) Regulation of *ysc-yop* genes and *yadA* by the master regulator LcrF.

The regulation of the master regulator LcrF changes depending on the conditions. At 25°C, *lcrF* expression is blocked by YmoA. Under these conditions, only low amounts of the *yscW-lcrF* mRNA are transcribed which are not efficiently translated due to a thermo-sensitive loop in the RBS region of *lcrF* (top panel). At elevated temperatures, without a cell-contact or secretion signal, the repression of YmoA is released by proteolytic degradation. In addition, the thermo-sensitive loop is melting, allowing LcrF synthesis. In a feedback mechanism, CsrA and YopD repress LcrF production. Besides CsrA and YopD, RNases and RcsB are also part of the regulation which are also controlled by CsrA and YopD (bottom left panel). Under cell-contact/secretion conditions at 37°C, the repressive effect of YopD is eliminated, and CsrA facilitates translation of LcrF. This leads to strong activation of LcrF, triggering the synthesis of the T3SS, the Yops and YadA under these conditions (bottom left panel) (modified from (Kusmierek *et al.* 2019))[8].

At moderate temperatures (25°C), the transcription of the *yscW-lcrF* operon is blocked by the nucleoid-associated protein YmoA. YmoA achieves this repression by interacting with the DNA downstream of the TSS, of the *yscW-lcrF* operon (Böhme *et al.* 2012). To further ensure inhibition, a thermo-sensitive stem-loop structure is located in the intergenic region between *yscW* and *lcrF* (Böhme *et al.* 2012). The formation of the hairpin structure in the mRNA depends on the temperature (Kortmann and Narberhaus

[8] (Kusmierek *et al.* 2019) is licensed under the terms of the Creative Commons Attribution License. Copyright ©. Kusmierek, Hoßmann, Witte, Opitz, Vollmer, Volk, Heroven, Wolf-Watz, Dersch.

2012) and is also called "*RNA thermometer*" (Righetti *et al.* 2016). In the case of *lcrF*, the hairpin structure is formed to mask the RBS of *lcrF* to inhibit translation of the *lcrF* coding region. Under these conditions, the RBS interacts with a repetition of four uracils, called a four-U element, by imperfect base pairing. Through this, a nearly inhibition of protein expression is ensured for the *yscW-lcrF* operon (see Figure 1.8) (Hoßmann 2017; Kusmierek 2018; Loh *et al.* 2019; Steinmann and Dersch 2013; Volk *et al.* 2019).

When *Yersinia* encounters elevated temperatures, the expression of virulence-associated genes needs to be activated. When human pathogenic *Yersinia* infects the human, the body temperature is sensed by the bacteria. Accordingly, the repressive effect of YmoA is released by proteolytic degradation facilitated by the proteases ClpXP and Lon (Jackson *et al.* 2004). With YmoA degraded, transcription of *yscW-lcrF* is activated (Cornelis 1993; Miller *et al.* 2014). Additionally, the thermo-sensitive loop of the *lcrF* mRNA melts and exposes the RBS, allowing translation of *lcrF* (Böhme *et al.* 2012; Kusmierek *et al.* 2019; Loh *et al.* 2019; Righetti *et al.* 2016). Newly synthesized LcrF activates the expression of the *ysc* and *yop* genes as well as *yadA* to establish the anti-phagocytosis system. However, in the absence of immune cell contact, the expression of LcrF needs to be maintained on a lower level, even at host body temperature, to not further express the energy-consuming Ysc-Yop and YadA proteins. To achieve this, different factors interfere with the expression of *lcrF* (Kusmierek *et al.* 2019). A strong effect is promoted by the translocon pore protein YopD. Besides its translocon forming ability, YopD acts as an RNA-binding protein (Kusmierek *et al.* 2019; Williams and Straley 1998). YopD binds the *yscW-lcrF* mRNA, and inhibit its translation. Furthermore, YopD has a positive effect on RNases, including RNase E and PNPase that are part of the degradosome, an RNA degradation complex (Kusmierek 2018; Kusmierek *et al.* 2019; Steinmann 2013). Due to the activating effect on RNases, the degradation of the *yscW-lcrF* mRNA is increased to downregulate LcrF expression. YopD also has a positive effect on CsrA, the RNA-binding protein of the carbon storage regulator (Csr) system. CsrA mostly regulates the translation of mRNAs by interfering with the binding of the ribosome to the RBS (Heroven *et al.* 2008; Hoßmann 2017; Romeo *et al.* 1993). In the LcrF regulation network, CsrA represses RcsB expression. RcsB is a transcriptional activator of *yscW-lcrF* that is activated by different external divalent cations (Li *et al.* 2015). The effect of CsrA on *yscW-lcrF* transcription is therefore indirect. Together, YopD, the RNases, and CsrA control *lcrF* at the transcriptional and post-transcriptional level, with YopD having the most significant impact (Fowler *et al.* 2009; Jessen *et al.* 2014). The repression of *lcrF* under non-cell-contact and non-secretion conditions ensures low levels of the T3SS, Yops, and YadA that are sufficient to prepare the cells for a cell-contact but on the other hand, reduce the metabolic burden (Hoe and Goguen 1993; Steinmann and Dersch 2013; Volk *et al.* 2019).

Upon cell-contact or calcium depletion from the growth medium at 37°C (secretion conditions), the regulatory network adapts to achieve a high expression of LcrF. This subsequently leads to increased production of the T3SS, YadA, and the Yops. To form the translocon pore in the membrane of the target cell, YopD is translocated by the T3SS, which reduces YopD-mediated repression of *lcrF* (Steinmann 2013; Steinmann and Dersch 2013). By exporting YopD, the negative effect of the RNase is also reduced, which leads to a stabilization of the *yscW-lcrF* transcript (Kusmierek *et al.* 2019). Additionally, CsrA facilitates a positive effect on the translation of *lcrF* by promoting an open thermo-sensitive hairpin structure. This ensures better interaction of the ribosome at the RBS of *lcrF* (Hoßmann 2017; Kusmierek

2018). These changes strongly activate the synthesis of LcrF and thereby lead to even higher levels of the T3SS, YadA, and especially of the Yops (Böhme *et al.* 2012; Cornelis 1993; Hoe and Goguen 1993; Volk *et al.* 2019).

The expression of the T3SS, Yops, and YadA can be tightly controlled by this complex regulatory mechanism of LcrF in response to different environmental conditions. It also enables *Yersinia* to mount a fast counterattack upon detection of immune cells. Unfortunately, the signal sensed to trigger the synthesis of LcrF and its downstream genes is yet unknown. Furthermore, additional factors might contribute to the regulation of *lcrF* like the recently identified influence of RNase III on the secretion of *Yersinia* effectors. Similar to a *yopD* mutant, an *rnc* mutant secretes Yops even under non-T3SS-inducing conditions (non-secretion conditions) and results in higher LcrF levels (Vollmer 2020). So far, YopD and RNase III work independently of each other. Research on the effect of RNase III on *lcrF* and the *ysc-yop* regulation is still in process.

1.5.1.1 The Carbon storage regulator system in *Yersinia*

The "*carbon storage regulator*" (Csr) system plays an essential role in the control of virulence and the expression of LcrF and the T3SS and Yops. This is supported by the fact that a *csrA* deletion strain is avirulent. The regulon of the Csr system shows a wide variety of direct and indirect targets, of which virulence traits are only one part. The Csr system consists of the RNA-binding protein CsrA (~9 kDa) that binds the sequence motive GGA in the loop region of hairpin structures (Gutiérrez *et al.* 2005; Liu and Romeo 1997; Romeo *et al.* 1993). A CsrA homodimer binds two consecutive GGA motifs, which can cause a positive or negative effect on the target RNA stability (Dubey *et al.* 2005). In addition, the GGA motives can overlap with the RBS of an mRNA and lead to activation or repression of target mRNA translation (Dubey *et al.* 2005). The two other genes of the Csr system *csrB* and *csrC* encode for sRNAs. Both sRNAs form a unique secondary structure with many GGA motif-containing hairpins (Liu *et al.* 1997). Thereby, CsrB and CsrC can sequester free CsrA from the cytosol and inactivate it. This process can be reversed by the degradation of CsrB and/or CsrC by RNases, releasing CsrA (Suzuki 2006; Weilbacher *et al.* 2003). By modulating the amount of free CsrA in the cell, the rate of CsrA-dependent gene expression can be regulated (Nuss *et al.* 2017; Romeo and Babitzke 2019; Romeo *et al.* 2013; Timmermans and Van Melderen 2010; Romeo *et al.* 2012).

1.5.2 Yop-dependent regulation of the *ysc-yop* mRNAs

In addition to the transcriptional activator LcrF and CsrA, additional regulators control the expression of the system. These regulators can function on single targets (proteins or mRNAs) or multiple targets, facilitating a more general effect.

One of the most important factors is, **YopD**. Besides the regulation of LcrF, YopD also plays a crucial role in the regulation of the T3SS and especially the Yops, which appears to occur at the post-transcriptional level by binding the respective mRNAs (Olsson *et al.* 2004). This interaction occurs mostly in the 5' UTR of the mRNAs and leads to translational inhibition (Anderson *et al.* 2002). YopD further supports the degradation of the target mRNAs by RNases. For *Y. enterocolitica,* it was shown that YopD, by interaction with **LcrH**, can directly recruit mRNAs to the degradosome (Francis *et al.*

2001). This effect is promoted by YopD-LcrH complex binding to a specific motive (AUAAA) on the target mRNAs in close proximity to the RBS (Anderson *et al.* 2002; Cambronne and Schneewind 2002; Wattiau *et al.* 1994). Upon binding, the complex recruits YscM/LcrQ, which tethers to LcrH in the complex. Afterwards, YscM/LcrQ promotes the transfer of the mRNA-YopD-LcrH-YscM/LcrQ complex to the degradosome (Francis *et al.* 2001). Based on the observation that LcrQ from *Y. pseudotuberculosis* can complement an *yscM* deletion in *Y. enterocolitica,* similar functions in regulation can be assumed for LcrQ in *Y. pseudotuberculosis*. Therefore, YopD represses many virulence factors and acts at a more global scale (Chen and Anderson 2011; Lee, Mazmanian, and Schneewind 2001).

The previously mentioned **YscM1/LcrQ** also affects the chaperone-requiring Yops. In the case of *Y. pseudotuberculosis*, it strongly affects YopE. The YscM/LcrQ protein has a size of ~13 kDa and the respective monocistronic gene is located downstream of one of the T3SS operons, with its own promoter (Rimpiläinen *et al.* 1992; Stainier *et al.* 1997). It belongs to the *ysc* genes, although it is not part of the T3SS. The protein has two binding domains to allow the interaction with two distinct proteins (Li *et al.* 2014). As for YopD-LcrH, it is also capable of binding YopE-SycE as long as YopE is not translocated/secreted by the bacterial cell. Binding of YscM/LcrQ to YopE-SycE leads to proteolytic degradation of YopE by the protease ClpXP (Sorg *et al.* 2005; Wulff-Strobel *et al.* 2002). Due to this degradation, the intracellular level of YopE is decreased. Furthermore, the low levels of YopE in the cell under non-cell-contact/non-secretion conditions are thought to support the hierarchy of translocation, which results in latest translocation of YopE upon immune cell contact (Cambronne *et al.* 2000; Cambronne and Schneewind 2002; Sorg *et al.* 2005; Thomas and Brett Finlay 2003).

The last complex that is known to control the translocation/secretion of Yops is the **SycN-YopN-TyeA** complex. This complex binds to the sorting platform and thereby inhibiting the binding of Yops or chaperones to the sorting platform themselves. Under non-secretion or non-cell contact conditions when the T3SS is in an inactive state. Upon cell contact or secretion the complex is released, and YopN is translocated/secreted by the T3SS (Amer *et al.* 2016; Bamyaci *et al.* 2018; Cheng *et al.* 2001; Day and Plano 1998; Joseph and Plano 2013). The release of YopN allows binding of other Yops to the export apparatus resulting in their translocation. Hence, SycN-YopN-TyeA ensures inactivation of the T3SS under non-induced conditions and prevents leakage through the T3SS (Ferracci *et al.* 2005).

In summary, these additional regulators can efficiently repress the expression and activation of the T3SS under T3SS inactive conditions even in the presence of LcrF. Also, the activation of the T3SS under cell-contact or secretion conditions can be achieved rapidly, as two of the repressors are also secreted, removing the repressive plug and allowing LcrF to further activate the system.

1.6 Aim of the study

For *Y. pseudotuberculosis* to survive in the host and to establish an acute infection, an efficient counterattack of immune cell-mediated phagocytosis is essential. To do so, the synthesis of T3SS components, YadA and especially the Yop effectors is highly regulated. To mimicked host cell contact *in vitro,* calcium was depleted from the growth medium at 37°C, to achieve "*secretion conditions*". This model was used in the analysis of *Y. pseudotuberculosis* under guarantee controlled culture conditions (Wiley *et al.* 2007). The expression of virulence genes under these conditions is rapidly induced and extremely high and is associated with a immediate growth arrest of the bacteria.

These observations raised the question, how the bacteria manage this immediate strong production of the Yops and the T3SS components. Previous analysis indicated that also control of translation and preferred translation of *ysc-yop* mRNAs are responsible for this high production of virulence proteins. To address this hypothesis, Ribo-Seq (Ingolia *et al.* 2009; Oh *et al.* 2011) should be applied on *Yersinia* to analyze the efficiency of translation using a high-throughput RNA sequencing approach. This technique not only allows the analysis of the translation efficiency on a genomic scale and provides information about the location of translated sequences from the start- to stop-codons and it also provides infromations about the speed of translation. To reveal whether translation efficiency of the *ysc-yop* genes is increased under secretion conditions a comparison of Ribo-Seq analysis obtained from *Y. pseudotuberculosis* grown a non-secretion and secretion conditions was intended. In addition, a comparison of the wildtype strain of *Y. pseudotuberculosis* and a *csrA* and a *yopD* mutant should be analyzed, based on their known function to control the regulation of LcrF as well as the T3SS, YadA, and the Yops on the post-transcriptional level. Candidate genes identified by the Ribo-Seq analyses which reveal a translational regulation should be further analyzed. A particular focus should be given to mRNA regions upstream of the coding sequence as well as in the RBS of these genes. In addition, the control of the expression of tRNAs, as part of the translational apparatus, should be analyzed, due to their effect on translation elongation efficiency/speed and their impact on the codon usage of genes.

The results of this work will contribute to our understanding of the regulatory networks associated with the T3SS-mediated virulence of *Y. pseudotuberculosis*. Furthermore, they will clarify whether the secretion system is mainly regulated at the transcriptional/post-transcriptional level or more on the translational level. These results could pave the way to better adjust treatments of *Y. pseudotuberculosis* infections, and they might also improve the treatment of *Y. pestis* infections as many functions of T3SS regulation are easily transferable to this strain.

2 Material and Methods

2.1 Material

2.1.1 Strains, oligonucleotides, and plasmids

The *Y. pseudotuberculosis* and *E. coli* strains used in this study are listed in Table 2.1.

Table 2.1) Bacterial strains

Strain	Description	Reference
E. coli		
S17-1λpir	*recA, thi, pro, hsdR*–M1^{+}(RP4--2Tc::Mu--Km::Tn7), *λpir*	(Simon *et al.* 1983)
CC118λpir	F^{-} Δ(*ara-leu*)7697 Δ(*lacZ*)74 Δ(*phoA*)20 *araD139, galE, galK, thi, rpsE, rpoB, arfE^{am}*, *recA1*, *λpir*	(Manoil and Beckwith 1986)
Y. pseudotuberculosis		
YPIII	pIB1, wild type	(Bölin *et al.* 1982a)
YP53	YPIII, Δ*csrA,* Kan^{R}	(Heroven *et al.* 2008)
YP91	YPIII, Δ*yopD*	(Kusmierek *et al.* 2019)
YP93	YPIII, Δ*lcrQ*	(Geyer 2014)
YP145	YP53, Δ*csrA, ΔyopD,* Kan^{R}	(Kusmierek *et al.* 2019)
YP427	YPIII, Δ*lcrF*$_{(bp\ 1\text{-}802\ of\ CDS)}$	(Geyer 2014)
YP189	YPIII, Δ*yadA,* Kan^{R}	(Geyer 2014)
YP275	YPIII, Δ*yopE,* Kan^{R}	(Schweer *et al.* 2013)
YP393	YPIII, Δ*yopH,* Kan^{R}	This study
YP394	YPIII, Δ*yopM,* Kan^{R}	This study
YP395	YPIII, Δ*yopP/J,* Kan^{R}	This study
YP396	YPIII, Δ*yopK/Q,* Kan^{R}	This study
YP397	YP91, Δ*yopD*, Δ*yopE,* Kan^{R}	This study
YP398	YP91, Δ*yopD*, Δ*yopH,* Kan^{R}	This study
YP399	YP91, Δ*yopD*, Δ*yopM,* Kan^{R}	This study
YP400	YP91, Δ*yopD*, Δ*yopP/J,* Kan^{R}	This study
YP401	YP91, Δ*yopD*, Δ*yopK/Q,* Kan^{R}	This study
YP402	YP91, Δ*yopD*, Δ*yadA,* Kan^{R}	This study
YP430	YPIII, Δ(*rpoE-rseABC*), Kan^{R}	This study
YP431	YP427, Δ*lcrF*$_{(bp\ 1\text{-}802\ of\ CDS)}$, Δ(*rpoE-rseABC*), Kan^{R}	This study

The oligonucleotide primers for molecular cloning were purchased from Metabion or Eurofins and are listed in Table 2.2. Corresponding restriction sites and other modifications are highlighted. Underlining highlights restriction sites, bold shows T7 promoters, and italics highlights terminators.

Table 2.2) Oligonucleotides for DNA amplification

Oligo-nucleotide	Sequence (5'→3')	Restric-tion site	Description
I305	CAGTCATAGCCGAATAGCCT		Amplification of Kan^{R} from pKD4_forward
I306	CGGTGCCCTGAATGAACTGC		Amplification of Kan^{R} from pKD4_reverse
I661	GTGTAGGCTGGAGCTGCTTC		Mutagenesis test with Kan^{R}_reverse

I662	CATATGAATATCCTCCTTAGTTCC		Mutagenesis test with Kan^R_forward
III981	TGAACGGCAGGTATATGTG		pAKH3 sequencing_forward
III982	CACTTAACGGCTGACATGG		pAKH3 sequencing_reverse
V557	CACCGGTCGCAGGATCAA		Mutagenesis test with *yopE*_forward
V558	TCTGTTGAGCATTCCACACT		Mutagenesis test with *yopE*_reverse
VIII910	GCGGCGGGTACCTTTTGTAGTGGGCTGACTCC	*Kpn*I	YadA-FLAG cloning_forward
VIII911	GCGGCGAAGCTT*TTA*CTTATCGTCGTCATCCTTGTAATC*CTCGAG*CCACTCGATATTAAATGATGCG	*Hind*III	YadA-FLAG cloning_reverse
VIII912	GCGGCGGGTACCGTTTTAATAGCCAAGGTAATAAAT	*Kpn*I	YopE-FLAG cloning_forward
VIII913	GCGGCGAAGCTT*TTA*CTTATCGTCGTCATCCTTGTAATC*CTCGAG*CATCAATGACAGTAATTTCTGC	*Hind*III	YopE-FLAG cloning_reverse
VIII914	GCGGCGGAGCTCCGTGTATTTAATTAAGGAGGG	*Sac*I	YopH-FLAG cloning_forward
VIII915	GCGGCGAAGCTT*TTA*CTTATCGTCGTCATCCTTGTAATC*CTCGAG*GCTATTTAATAATGGTCGCC	*Hind*III	YopH-FLAG cloning_reverse
VIII916	GCGGCGGGTACCTTATATAAATAAGAGCAACGTCAC	*Kpn*I	YopK/YopQ-FLAG cloning_forward
VIII917	GCGGCGAAGCTT*TTA*CTTATCGTCGTCATCCTTGTAATC*CTCGAG*TCCCATAATACATTCTTGATCG	*Hind*III	YopK/YopQ-FLAG cloning_reverse
VIII918	GCGGCGGGTACCTGCAGTGAAAAACTCGATAA	*Kpn*I	YopM-FLAG cloning_forward
VIII919	GCGGCGAAGCTT*TTA*CTTATCGTCGTCATCCTTGTAATC*CTCGAG*CTCAAATACATCATCTTCAAGTTT	*Hind*III	YopM-FLAG cloning_reverse
VIII920	GCGGCGGGTACCTTCATACCGCTGTTAATTCC	*Kpn*I	YopJ/YopP-FLAG cloning_forward
VIII921	GCGGCGAAGCTT*TTA*CTTATCGTCGTCATCCTTGTAATC*CTCGAG*TACTTTGAGAAGTGTTTTATATTCAG	*Hind*III	YopJ/YopP-FLAG cloning_reverse
VIII922	GCGGCGGAGCTCCAAGAACTGGTTGTTCGCAG	*Sac*I	*yopH* mutagenesis cloning up fragment_forward
VIII923	*GAAGCAGCTCCAGCCTACAC*GCTTCCCTCCTTAATTAAATACAC		*yopH* mutagenesis cloning up fragment_reverse
VIII924	*GGAACTAAGGAGGATATTCATATG*CCTATGAGTAAATAAAATTACTAAGAG		*yopH* mutagenesis cloning down fragment_forward
VIII925	GCGGCGGAGCTCCAATACCTTCTTCGGCTATCC	*Sac*I	*yopH* mutagenesis cloning down fragment_reverse
VIII926	GTTTCGAACGTAGATTGAGAC		Mutagenesis test with *yopH*_forward
VIII927	AACTGGATGGAGATCCTCAC		Mutagenesis test with *yopH*_reverse
VIII928	GCGGCGGAGCTCGCCATTATTTTGCTATACCG	*Sac*I	*yopK/yopQ* mutagenesis cloning up fragment_forward
VIII929	*GAAGCAGCTCCAGCCTACAC*AGTTACTACTCCCAAATTTACTT		*yopK/yopQ* mutagenesis cloning up fragment_reverse

VIII930	*GGAACTAAGGAGGATATTCATATG*GCTATA TTAAAGAGTTTGGGATATGG		*yopK/yopQ* mutagenesis cloning down fragment_forward
VIII931	GCGGCGGAGCTCCACAATGCGATCCAGTA CTC	*Sac*I	*yopK/yopQ* mutagenesis cloning down fragment_reverse
VIII932	GGCAGAATAATTCGATAGTTG		Mutagenesis test with *yopK/yopQ*_forward
VIII933	GCTATTAACTTCATGTTTTTCTTC		Mutagenesis test with *yopK/yopQ*_reverse
VIII934	GCGGCGGAGCTCCGTCAGCAGTAATACAT TG	*Sac*I	*yopM* mutagenesis cloning up fragment_forward
VIII935	*GAAGCAGCTCCAGCCTACAC*ATTGAATGC CTTTCTGAAAATATT		*yopM* mutagenesis cloning up fragment_reverse
VIII936	*GGAACTAAGGAGGATATTCATATG*ACGCAA GAGCGTTCATAATT		*yopM* mutagenesis cloning down fragment_forward
VIII937	GCGGCGGAGCTCTACCAATTTTTTGATGG GGGC	*Sac*I	*yopM* mutagenesis cloning down fragment_reverse
VIII938	GACGGTTTCAAAAGGGGTAC		Mutagenesis test with *yopM*_forward
VIII939	CAAATCCCTGAAGCGTTGAC		Mutagenesis test with *yopM*_reverse
VIII940	GCGGCGGAGCTCCTTGGACGAAGCAGTTT AAT	*Sac*I	*yopJ/yopP* mutagenesis cloning up fragment_forward
VIII941	*GAAGCAGCTCCAGCCTACAC*TATTTATCCT TATTCAGGGAATTAACAG		*yopJ/yopP* mutagenesis cloning up fragment_reverse
VIII942	*GGAACTAAGGAGGATATTCATATG*TGTATT TTGGAAATCTTGCTCC		*yopJ/yopP* mutagenesis cloning down fragment_forward
VIII943	GCGGCGGAGCTCGCATAACTCAGTCCGGT TGT	*Sac*I	*yopJ/yopP* mutagenesis cloning down fragment_reverse
VIII944	ACAGGAGGTATCGGAGTTTA		Mutagenesis test with *yopJ/yopP*_forward
VIII945	TTTGTCTGCTGTTTTATGGAC		Mutagenesis test with *yopJ/yopP*_reverse
IX043	GATCTGGTGTTCAGTGAATC		Mutagenesis test with *yadA*_forward
IX044	GAGTGACAAGGGTTTTCGCG		Mutagenesis test with *yadA*_reverse
IX121	GCGGCGGAGCTCCGGCTTCTTTGTCACAA AGC	*Sac*I	*(rpoE-rseABC)* mutagenesis cloning up fragment_forward
IX125	CTTGATCAATGAGCCACTGC		Mutagenesis test with *(rpoE-rseABC)* _forward
IX133	*GAAGCAGCTCCAGCCTACAC*CCGAGGTGA ACTCTCCCGAA		*(rpoE-rseABC)* mutagenesis cloning up fragment_reverse
IX134	*GGAACTAAGGAGGATATTCATAT*GCCAACG GCTATGCGTATTCA		*(rpoE-rseABC)* mutagenesis cloning down fragment_forward

IX135	GCGGCGGAGCTCGGCATTTCGCACATCTA AATC	*Sac*I	*(rpoE-rseABC)* mutagenesis cloning down fragment_reverse
IX136	CACAGGAATAAACCCCAACG		Mutagenesis test with *(rpoE-rseABC)* _reverse
pBAD-for (Seqlab)	ATGCCATAGCATTTTTATCC		pBAD sequencing_forward
pBAD-rev (Seqlab)	GATTTAATCTGTATCAGG		pBAD sequencing_reverse

underlined: restriction site, **bold**: FLAG-Tag, *italic*: overlap with Kanamycin-cassette

The plasmids that were used in this study are listed in Table 2.3. All plasmids constructed for this study were sequenced with the barcodes sequencing service of *Microsynth Seqlab*.

Table 2.3) Plasmids

Plasmid	Description	Reference
pAKH3	mutagenesis vector, ori pR6K, *sacB*$^+$, Amp^R	(Heroven, Sest, et al. 2012)
pBAD30	cloning vector, ori p15A, P_{araC}, *araO2*, *araC,* Amp^R	(Guzman et al. 1995)
pKD4	mutagenesis vector, ori pR6K, Kan^R, Amp^R	(Datsenko and Wanner 2000)
pRG10	pAKH3, ori pR6K, *yadA*::Kan^R, *sacB*$^+$, Amp^R	(Geyer 2014)
pJNS13	pAKH3, ori pR6K, *yopE*::Kan^R, *sacB*$^+$, Amp^R	(Schweer et al. 2013)
pMV30	pBAD30, ori p15A, *yadA*$_{(-242\ till\ +1302)}$[1]-FLAG, Amp^R	This study
pMV31	pBAD30, ori p15A, *yopE*$_{(-28\ till\ +657)}$[1]-FLAG, Amp^R	This study
pMV32	pBAD30, ori p15A, *yopH*$_{(-25\ till\ +1404)}$[1]-FLAG, Amp^R	This study
pMV33	pBAD30, ori p15A, *yopK/Q*$_{(-117\ till\ +546)}$[1]-FLAG, Amp^R	This study
pMV34	pBAD30, ori p15A, *yopM*$_{(-48\ till\ +1227)}$[1]-FLAG, Amp^R	This study
pMV35	pBAD30, ori p15A, *yopP/J*$_{(-38\ till\ +864)}$[1]-FLAG, Amp^R	This study
pMV36	pAKH3, ori pR6K, *yopH*::Kan^R, *sacB*+, Amp^R	This study
pMV37	pAKH3, ori pR6K, *yopM*::Kan^R, *sacB*+, Amp^R	This study
pMV38	pAKH3, ori pR6K, *yopP/J*::Kan^R, *sacB*+, Amp^R	This study
pMV39	pAKH3, ori pR6K, *yopK/Q*::Kan^R, *sacB*+, Amp^R	This study
pMV43	pAKH3, ori pR6K, *(rpoE-rseABC)*::Kan^R, *sacB*+, Amp^R	This study

[1] relative to the translational start of the gene

2.1.2 Media, supplements, and buffer

Liquid media were prepared according to the company information or lab protocol (see Table 2.4) with Milli Q H_2O. For solid media, 15g/l of Difco® Agar Nobel (BD Biosciences) were added prior to the liquid media. To cultivate *Yersinia*, $CaCl_2$ was added to the liquid media to a final concentration of 1 mM. For selective media supplements (antibiotics) were added according to Table 2.5

Table 2.4) Media

Media	Composition
LB (Luria-Bertani) medium / Lennox	5 g Bacto yeast extract, 10 g Bacto Tryptone, 5 g NaCl
BHI (Brain Heart Infusion) medium	37 g/l BHI (BD Biosciences)
DYT (Double Yeast Tryptone) medium	10 g/l yeast extract, 5 g/l NaCl, 16 g/l tryptone

Table 2.5) Media supplements

Supplements	Stock solution	Final concentration
$CaCl_2$	1 M in H_2O	1 mM
Carbenicillin	100 mg/ml in H_2O	100 µg/ml
Chloramphenicol (for Ribo-Seq)	50 mg/ml in 70% ethanol	
Ciprofloxacin (for Ribo-Seq)	10 µg/ml in H_2O	0.4 µg/ml
Kanamycin	50 mg/ml in H_2O	50 µg/ml
Triclosan	20 mg/ml in 70% ethanol	20 µg/ml

All buffers used in this study are listed in Table 2.6. Buffers were prepared according to the company manuals or lab protocols. All chemicals, if not specified otherwise, were obtained from the following companies: AppliChem, BD Biosciences, BioRad, Carl Roth. LI-COR biosciences, Macherey and Nagel, NEB, Omnilab, PEQLAB, Roche, Serva, Sigma-Merck, Thermo Scientific, and VWR International.

Table 2.6) Buffers and other solutions

Buffer/solution	Composition
CDP* detection buffer	100 mM Tris; 100 mM NaCl; pH 9.5
CDP* maleic acid buffer	100 mM maleic acid; 150 mM NaCl; pH 7.0
CDP* wash buffer	100 mM maleic acid; 150 mM NaCl; 0.3% (v/v) Tween-20; pH 7.0
CDP* blocking reagent (10x)	10% (w/v) blocking reagent (Roche) in CDP* maleic acid buffer
Church buffer (moderate)	10 mg/ml BSA; 500 mM sodium phosphate buffer; 15% (v/v) formamide; 1 mM EDTA; 7% (w/v) SDS
Formamid-Urea (FU)-Mix (2x)	6 M urea; 80% (v/v) formamide; 10% (v/v) TBE buffer (10x)
Hybridisation buffer (agarose northern blot)	50% (v/v) formamide; 5x SSC; 2 x CDP* blocking reagent; 0.1% (w/v) N-Laurylsarcosin; 0.02% (w/v) SDS
Lysis buffer (RNA)	2% (w/v) SDS; 10 mM sodium acetate, pH 4.5
Lysozyme-TE-buffer	50 mg/ml lysozyme in TE buffer
MOPS buffer (20x)	200 mM MOPS; 50 mM sodium acetate; 10 mM EDTA
Resuspension buffer (RNA)	300 mM sucrose; 10 mM sodium acetate, pH 4.5
Polysome digestion buffer (10x)	150 mM $CaCl_2$; 1 U/µl SUPERase•In™ RNase Inhibitor
Ribo-Seq pre-lysis buffer (10x)	100 mM $MgCl_2$; 1 M NH_4Cl; 200 mM Tris-HCl; pH 8.0; in Milli Q H_2O
Ribo-Seq lysis buffer (1x)	10 mM $MgCl_2$; 100 mM NH_4Cl; 20 mM Tris-HCl; pH 8.0; 0.4% (v/v) Trition X-100; 10 U/ml DNase I; 20 U/ml Superase-in; 0.325 mg/ml Chloramphenicol; in Milli Q H_2O
RNA loading buffer (5x)	31% (v/v) formamide; 2.7% formaldehyde; 0.1 mg/ml EtBr; 4 mM EDTA, pH 8.0; 0.03% (w/v) bromphenol blue; 20% (v/v) glycerol in 1x MOPS buffer
RNA washing buffer I	2x SSC; 0.1% (w/v) SDS
RNA washing buffer II	0.1x SSC; 0.1% (w/v) SDS
SDS running buffer (10x)	330 mM Tris-HCl, pH 8.3; 1.92 M glycine; 1% (w/v) SDS
SDS sample buffer (2x)	62 mM Tris; 20 % (v/v) glycerol; 3 % (w/v) SDS; 8% (v/v) 2-mercaptoethanol; 0.02% (w/v) bromphenol blue
SDS separating buffer (4x)	1.5 M Tris-HCl, pH 8.8; 4% (w/v) SDS
SDS stacking buffer (4x)	500 mM Tris-HCl, pH 6.8; 4% (w/v) SDS
Sodium phosphate buffer (1M)	500 mM Na_2HPO_4; 0.34% (w/v) H_3PO_4; pH 7.2
SSC (20x)	3 M NaCl; 300 mM sodium citrate; pH 7.0
Stripping buffer (acrylamide NB)	0.1% SDS

10% sucrose gradient buffer	10 mM $MgCl_2$; 100 mM NH_4Cl; 20 mM Tris-HCl; pH 8.0; 10% (w/v) sucrose, in Milli Q H_2O
50% sucrose gradient buffer	10 mM $MgCl_2$; 100 mM NH_4Cl; 20 mM Tris-HCl; pH 8.0; 50% (w/v) sucrose, in Milli Q H_2O
TAE buffer (50x)	2 M Tris; 1 M acetic acid; 100 mM EDTA
TBE buffer (10x)	890 mM Tris; 890 mM boric acid; 25 mM EDTA
TBS buffer (10x)	200 mM Tris-HCl, pH 7.5; 1.5 M NaCl
TBSM buffer	5% (w/v) powdered milk in TBS (1x)
TBST buffer (10x)	200 mM Tris-HCl, pH 7.5; 1.5 M NaCl; 0.1% (v/v) Tween-20
TBST buffer (1x)	20 mM Tris-HCl, pH 7.5; 150 mM NaCl; 0.01% (v/v) Tween-20
TBSTM buffer	5% (w/v) powdered milk in TBST (1x)
TE buffer	100 mM Tris; 1 mM EDTA; pH 7.5
TES buffer	10 mM Tris; 1 mM EDTA; 150 mM NaCl
Transblot buffer	25 mM Tris; 192 mM glycine; 20% (v/v) methanol
Transformation buffer	272 mM sucrose; 15% (v/v) glycerol; pH 7.0

2.1.3 Antibodies, enzymes, kits and size standards

All antibodies, enzymes, commercial kits, commercial kits for RNA- and Ribo-Seq and molecular size standards are listed in the Table 2.7 to Table 2.10.

Table 2.7) Antibodies

Antibody	Dilution	Buffer	Source	Manufacturer
Primary antibodies				
Polyclonal Anti-YadA	1:6,666	1x TBSTM	Rabbit	Davids Biotechnology
Polyclonal Anti-all Yops	1:13,333	1x TBSTM	Rabbit	Davids Biotechnology
Polyclonal Anti-LcrF	1:2,000	1x TBSTM	Rabbit	Greg Plano
Polyclonal Anti-H-NS	1:100,000	1x TBSTM	Rabbit	Davids Biotechnology
Monoclonal Anti-FLAG® M2	1:10,000	1x TBSTM	Mouse	Sigma-Aldrich
Anti-digoxygenin alkaline phosphatase	1:7,500	1x Blocking-solution	Sheep	Roche
Secondary antibodies				
IRDye® 800CW Goat anti-Rabbit IgG	1:10,000	1x TBST	Goat	LI-COR, Inc.
IRDye® 800CW Goat anti-Mouse IgG	1:10,000	1x TBST	Goat	LI-COR, Inc.
IRDye® 680RD Goat anti-Rabbit IgG	1:10,000	1x TBST	Goat	LI-COR, Inc.

Table 2.8) Enzymes

Enzyme	Manufacturer
Alkaline phosphatase, calf intestinal (CIP)	NEB
Antarctic phosphatase	NEB
DNase I – RNase free	Thermo Scientific
TURBO™ DNase (2 U/µL)	Invitrogen
Lysozyme	Sigma
Micrococcal Nuclease (MNase)	NEB
Phusion® High-fidelity DNA polymerase	NEB
Restriction enzymes	NEB

RiboLock RNase inhibitor	Thermo Scientific
SUPERase• In™ RNase Inhibitor	Thermo Scientific
T4 DNA ligase	Promega

Table 2.9) Commercial kits

Kit	Manufacturer
Standard Kit	
Dig-luminescent detection	Roche
DreamTaq Green PCR Master Mix	Thermo Scientific
Luna® Universal One-Step RT-qPCR Kit	NEB
NucleoSpin® Gel and PCR Clean-up	Macherey-Nagel
NucleoSpin® Plasmid	Macherey-Nagel
QIAquick™ Plasmid Midiprep	Qiagen
SV Total RNA Isolation	Promega
RNA- and Ribo-Seq Kit	
MinElute PCR Purification	Qiagen
MICROBExpress™ Bacterial mRNA Enrichment Kit	Thermo Scientific/ Invitrogen
NEBNext® Multiplex Small RNA Library Prep Set for Illumina® (Set 1)	NEB

Table 2.10) Molecular size standards

Size standard	Manufacturer
DNA Ladder	
GeneRuler DNA Ladder mix	Thermo Scientific
Ultra-Low Range (ULR) DNA Ladder	Thermo Scientific
RNA Ladder	
RNA Molecular Weight Marker I, Dig-labeled	Roche
Protein Ladder	
PageRuler Prestained Protein Ladder	Thermo Scientific

2.1.4 Software

For data analysis, visualization and publication the following software was used: ApE (A plasmid Editor) and SnapGene Viewer (SnapGene software (from GSL Biotech; available at snapgene.com) for planning, visualization, and documentation of DNA sequences; LightCycler® 96 System software (Roche) for the qPCR cycler; Image Lab 2.0.1 (BioRad) to visualize gel images and Image Studio 5.2 (LI-COR Inc.) to visualize blots and analyze them; for advanced RNA quality control, the QIAxcel System was used with the QIAxcel ScreenGel software 1.6.0 (Qiagen); GraphPad Prism 8 for data processing; Integrated Genome Browser (IGB) (Freese *et al.* 2016) was used as a genome viewer for visualizing the mapping results of the Ribo-Seq data; Qlucore Omics Explorer 3.6.27 was used to analyze the Ribo-Seq data; and Microsoft Office for Mac (version 16.29 [2019]) including Excel, PowerPoint, and Word was used for all-day purposes such as general data analysis and documentation.

As databases NCBI (National Centre for Biotechnology Information) and KEGG (Kyoto Encyclopedia of Genes and Genomes) were used.

2.1.5 Equipment

The technical equipment used in this study was manufactured by the following companies: Analytic Jena, Beckman Coulter, BioComp, BioRad, BMG Labtech, Brand, Eppendorf, G. Heinemann, GFL, InforsHT, KNF, LiCor, Millipore, Mettler Toledo, Qiagen, Scientific Industries, Vacuubrand, VWR, Witeg.

The lab material in this study was manufactured by Abena, BioRad, Biozym, Braun, Carl-Roth, Covaris, Eppendorf, G. Kisker, Greiner Bio-One, Roche, Sarstedt, Sigma/Merck, Starlab, Süd Laborbedarf, Thermo Fisher Scientific.

2.2 Microbiological Methods

2.2.1 Sterilization methods

Liquid and solid media were heat sterilized for 20 minutes at 121°C and 1 bar overpressure in an autoclave. Non-autoclavable solutions (e.g. antibiotics or sucrose) were filtered using sterile filters with a pore diameter of 0.2 µm.

Glass equipment such as pipettes or flasks were heat sterilized for 20 minutes at 121°C and a vacuum of less than 100 mbar in an autoclave.

Lab benches and lab equipment were sterilized with 70% ethanol or 1% Incidin™. Non-autoclavable labware and glass pipets were sterilized with 2% Sekusept™.

2.2.2 Cultivation and storage of bacteria

Bacteria were grown on solid media or in liquid media depending on the experiment. *E. coli* strains (see Table 2.1) on solid LB media were grown at 37°C overnight. Cultures of *E. coli* were grown in defined liquid LB media overnight in a shaker at 37°C and 200 rpm. The cultures were inoculated with a single colony of *E. coli* from solid LB media plates. If needed, the appropriate antibiotics were added to the LB media plates as well as to the liquid media for selection.

Solid LB media for cultivating *Yersinia* strains (see Table 2.1) were grown at 25°C for 2 days. For liquid overnight cultures a certain amount of liquid LB media, supplemented with 1 mM $CaCl_2$, was inoculated with a single *Yersinia* colony and incubated at 25°C with 200 rpm in a shaker. As for *E. coli,* the required antibiotics were added to the media for selection. Cultures for *ysc-yop* and T3SS (non-secretion/secretion) conditions were grown over the day. Therefore cultures were prepared from overnight cultures in fresh liquid LB media in flasks that are filled to a maximum of 20% of total volume. Afterward, cultures were incubated for 2 hours at 25°C with 200 rpm. For 25°C conditions, cultures were grown for additional 4 hours at 25°C with 200 rpm, for non-secretion conditions (37°C) cultures were shifted to 37°C and incubated for 4 hours with 200 rpm. To induce secretion conditions up on Ca^{2+} depletion (-Ca^{2+}) 20 mM of $MgCl_2$ and 20 mM of Na-oxalate were added to the culture to sequester Ca^{2+} and it was incubated for 4 hours at 37°C with 200 rpm.

For short term storage, not longer than 14 days, bacteria were stored at 4°C on solid media. Long term storage was carried out in glycerol stocks at -80°C. Therefore 1.25 ml of the overnight culture was mixed with 750 µl 80% glycerol (final concentration 30% glycerol), inverted, and then directly stored at -80°C.

2.2.3 Bacterial growth curves

To control the growth of the constructed mutants, growth curves were performed. Therefore overnight cultures for the corresponding mutants were prepared. From these overnight cultures over day cultures with 30 ml and a start OD_{600} of 0.1 were inoculated. The cultures were then grown at 25°C or 37°C as mentioned above for 8 to 10 hours. At specific time points within the growth, the OD_{600} was measured.

2.2.4 Cultivation of bacteria harboring a pBAD based expression plasmid

Similar to the normal cultivation the bacterial cells were inoculated and grown for 2 hours at 25°C with 200 rpm. Thereafter, the P^{BAD} promoter was induced by the addition of finally 0.1% arabinose and the cultures were cultured at the three different conditions as mentioned in section 2.2.2.

2.2.5 Determination of bacterial cell density

The optical density of bacterial cultures was measured spectrophotometrically using UV-micro cuvettes. The optical density was measured at 600 nm using 1 ml bacterial culture, measured against sterile LB medium as reference. High-density cultures with an OD_{600} greater than 1 were diluted 1:10 in LB medium before measuring.

2.3 Molecular biological methods for DNA analysis

2.3.1 Isolation of genomic DNA

Genomic DNA of *Y. pseudotuberculosis* was isolated by using the phenol:chloroform:isoamyl alcohol purification method. For this purpose, 300 µl of an overnight culture were mixed with 300 µl phenol:chloroform:isoamyl alcohol (25:24:1). Samples were then centrifuged at 15,800 g for 5 minutes. After centrifugation, the aquarius layer was transferred to a new reaction tube and mixed with 300 µl chloroform:isoamyl alcohol (24:1) to remove remaining phenol. After mixing samples were again centrifuged at 15,800 g for 3 minutes. The aquarius layer was again transferred to a fresh tube and mixed with three volumes of pure ethanol. Genomic DNA was then precipitated for one hour at 4°C. Precipitated genomic DNA was collected at 15,800 g for 30 minutes at 4°C. Thereafter the supernatant was discarded and the pellet was washed two times with 70% ethanol. Finally, the genomic DNA was resuspended in H_2O_{dest} and diluted to a concentration of 100 ng/µl.

2.3.2 DNA amplification by polymerase chain reaction (PCR) and DNA gel electrophoresis

For specific amplification of DNA fragments, the polymerase chain reaction (PCR) was used (Saiki et al. 1988). The reaction was performed as mentioned in the manufacturer's protocols for the different polymerases.

Mainly two DNA polymerases were used in this study. To amplify DNA fragments for molecular cloning the *Phusion® High-fidelity DNA polymerase* was used in a reaction volume of 100 µl. For amplification of DNA fragments for testing positive clones, the *DreamTaq Green Mix* with the DreamTaq polymerase was used with reaction volumes of 20 µl.

DNA fragments of every PCR were separated by agarose gel electrophoresis and visualized with ethidium bromide.

2.3.3 DNA purification from agarose gels

To isolate a DNA fragment with a special size out of a mixture of fragments, DNA fragments were separated by agarose gel electrophoresis and stained. Thereafter the DNA fragments of interest were cut out using a scalpel. Purification was performed with the *NucleoSpin® Gel and PCR Clean-up* column-based kit according to the manufacturer's protocol. DNA was eluted from the column with 30 µl nuclease-free H_2O_{dest} and stored at -20°C.

2.3.4 DNA purification

For purification of PCR amplified DNA fragments, the *NucleoSpin® Gel and PCR Clean-up* kit was used according to the manufacturer's protocol. DNA was eluted with 30 µl nuclease-free H_2O_{dest} and stored at -20°C.

2.3.5 Isolation of plasmid DNA

For the isolation of plasmids from bacteria cells two different kits were used. Plasmids constructed by molecular cloning were isolated using the *NucleoSpin® Plasmid* kit according to the manufacturer's protocol. For this, an overnight culture of bacteria harboring the plasmid of interest were grown in LB media containing the required antibiotic. DNA was eluted in 50 µl nuclease-free H_2O_{dest}.

Plasmids for stocks were isolated using the *QIAquick™ Plasmid Midiprep* kit according to the manufacturer's protocol. Therefore an overnight culture similar to the *NucleoSpin® Plasmid* kit was inoculated in DYT media containing the required antibiotic. Finally, DNA was eluted in 100 µl nuclease-free H_2O_{dest}.

2.3.6 Determination of DNA concentration

The nucleic acid concentration was determined by measuring the absorbance with a NanoDrop photo spectrometer. The concentration in µg/ml was then calculated by the machine using the following function.

$$DNA\ concentration\ \mu g/ml = A_{260} \times 50\ \mu g/ml$$

The purity of the DNA was controlled by measuring the ratio of A_{260}/A_{280}. The ratio for clean DNA should be from 1.8 to 1.9.

2.4 Molecular cloning

2.4.1 Cloning by DNA restriction digestion

For molecular cloning DNA fragments need to be inserted into the desired vector. Therefore inserts and vectors have to be digested, with the same restriction enzymes for ligation later on. Restriction sites for the DNA fragments were added within the PCR by adding the restriction sites to the 5' end of the primers. For the vectors, the restriction sites located in the multiple cloning site were used. In this study restriction enzymes with *high-fidelity* were used as mentioned in the manufacturer's protocol in a suitable buffer. A standard restriction digestion was incubated at 37°C for one to two hours in a final volume of 50 µl.

After restriction digestion samples were purified using the *NucleoSpin® Gel and PCR Clean-up* kit (section 2.3.4). To prevent self-religation of the vector, the vector was dephosphorylated after the restriction digest. The dephosphorylation reaction was performed in a final volume of 50 µl for 1.5 hours at 37°C as mentioned in the manufacturer's protocol.

After dephosphorylation, the samples were purified with the *NucleoSpin® Gel* and *PCR Clean-up* kit (section 2.3.4).

2.4.2 Ligation of DNA fragments

For introducing the inserts into the appropriate vectors both parts were fused by ligation. The ligation reaction was achieved by the T4 DNA ligase. Any ligation was incubated overnight at 16°C in a final volume of 10 µl as mentioned in the manufacturer's protocol.

As a control, to check the rate of re-ligation, a reaction without an insert was performed. To prepare the samples for electro transformation they were dialyzed by using a 0.025 µm filter (VSWP) on H_2O_{dest}. The dialysis was incubated for 15 minutes and afterward directly used for electrotransformation.

2.4.3 Plasmid construction

For the construction of all plasmids used in this study, different primers to amplify the inserted fragments were used. They are listed in the following tables. In addition to the primers, the restriction enzymes, the vectors, and the part introduced by the insert are documented (Table 2.11) Plasmid constructionand Table 2.12).

Table 2.11) Plasmid construction

Plasmid	Primer	Restriction sites	Backbone	Gene of interest
pMV30	VIII910 VIII911	*Kpn*I, *Hind*III	pBAD30	*yadA*-1xFLAG
pMV31	VIII912 VIII913	*Kpn*I, *Hind*III	pBAD30	*yopE*-1xFLAG
pMV32	VIII914 VIII915	*Sac*I, *Hind*III	pBAD30	*yopH*-1xFLAG
pMV33	VIII916 VIII917	*Kpn*I, *Hind*III	pBAD30	*yopK/Q*-1xFLAG
pMV34	VIII918 VIII919	*Kpn*I, *Hind*III	pBAD30	*yopM*-1xFLAG
pMV35	VIII920 VIII921	*Kpn*I, *Hind*III	pBAD30	*yopP/J*-1xFLAG

For the controlled expression of the different Yop proteins and YadA harboring a C-terminal 1xFLAG-tag, plasmids **pMV30** to **pMV35** were constructed. The fragments were produced by PCR using the primers given in Table 2.11. Thereafter fragments were digested with *Kpn*I and *Hind*III. For **pMV32**, different from the other plasmids, the digestion was done with *Sac*I and *Hind*III. The fragments encode the 5' UTR, the coding sequence, and a fused C-terminal 1xFLAG-tag. After digestion, the fragments were ligated into the vector pBAD30 harboring an arabinose inducible P_{BAD} promoter.

Table 2.12) Mutagenesis plasmid construction

Plasmid	Primer up fragment	Primer down fragment	mutated gene
pMV36	VIII922 VIII923	VIII924 VIII925	*yopH*::Kan^R
pMV37	VIII934 VIII935	VIII936 VIII937	*yopM*::Kan^R
pMV38	VIII940 VIII941	VIII942 VIII943	*yopP/J*::Kan^R
pMV39	VIII928 VIII929	VIII930 VIII931	*yopK/Q*::Kan^R
pMV43	IX121 Ix133	IX134 IX135	*(rpoE-rseABC)*:: Kan^R

To construct the plasmids for *Yersinia* knock-out mutagenesis (**pMV36** to **pMV39** and **pMV43**), an up and a down fragment was generated by using the mentioned primers (Table 2.12). The up and down fragments are between 450 bp to 600 bp in length and are located upstream and downstream of the coding sequence to be knocked-out. The amplified fragments are needed for the homologous

recombination of the mutated DNA fragment with the equivalent region in the genome. The primers next to the coding sequence to be mutated harboring an overlap to the kanamycin resistance cassette. The kanamycin resistance cassette was amplified with the primers I661 and I662 from the template pKD4. In a third PCR reaction, the up and down fragments together with the kanamycin resistance cassette were combined and amplified by PCR with the forward primer of the up fragment and the reverse primer of the down fragment. The fused fragments, as well as the suicide vector pAKH3, were digested with *Sac*I and ligated.

Cloning of all the different plasmids was accomplished as described in sections 2.4.1 to 2.4.2.

2.4.4 DNA sequencing

DNA sequencing of the constructed plasmids was performed by Microsynth Seqlab (Germany), according to the conditions required by Microsynth Seqlab.

2.4.5 Bacterial transformation

Transformation is the introduction of DNA, in this case, plasmids, into a recipient strain. DNA can be introduced by different transformation processes. In this study, the transformation was performed by electroporation.

2.4.5.1 Preparation of electrocompetent bacteria

The lab strains of *E. coli,* as well as *Y. pseudotuberculosis,* needed special treatment for increased competence. The preparation of electrocompetent *E. coli* and *Y. pseudotuberculosis* differ from each other.

To prepare electrocompetent *E. coli*, a culture with 100 ml DYT media was inoculated 1:100 with an overnight culture of the required strain. The culture was then grown at 37°C (see chapter 2.2.2) to an OD_{600} of 0.6 to 0.8. Afterwards, the culture was cooled on ice for at least 10 minutes. The cooled culture was harvested by centrifugation in the following step with 3,700 g for 5 minutes at 4°C. After discarding the supernatant the cell pellet was washed two times with 20 ml of cold sterile water and centrifuge with 3,700 g for 10 minutes at 4°C. The supernatant was discarded after each washing step. Thereafter, the pellet was washed once with 20 ml cold 10% (v/v) glycerol in water and centrifuge with 3,700 g for 10 minutes at 4°C. Again, the supernatant was discarded and the pellet was resuspended in 5 ml cold 10% (v/v) glycerol in water. The cell suspension was then divided into aliquots of 50 µl and stored at -20°C. One aliquot was used per transformation.

In contrast, competent *Yersinia* were prepared freshly for every transformation. For the preparation, 20 ml BHI media were inoculated with an overnight culture of the required *Yersinia* strain, according to the inoculations dilution (wildtype 1:50, *ΔcsrA* 1:20, *ΔyopD* 1:40). The cells were cultured for 3 hours at 25°C (see chapter 2.2.2). Cells were harvested by centrifugation at 3,700 g for 5 minutes at 4°C. The supernatant was discarded and the pellets were washed two times with 10 ml cold transformation buffer. After each centrifugation at 3,700 g for 7 minutes at 4°C, the supernatant was discarded. In the end, the pellets were resuspended in 1 ml cold transformation buffer. The resuspended cells were used directly afterward for transformation.

2.4.5.2 Transformation by electroporation

For the transformation of *E. coli* as well as *Y. pseudotuberculosis*, 45 µl of cells were mixed with 1 µl of purified plasmid DNA or the whole dialyzed ligation reaction. To keep the cells competent, the whole procedure was carried out on ice. Afterward, the cell-DNA mix was transferred to an electroporation cuvette with a gap of 2 mm. Next, the mixture was pulsed with 2.5 kV for at least 5 ms. This loosens in the cell envelope and allowed the bacterial cells to take up the plasmid DNA.

Directly after electroporation, cells were mixed with 1 ml of the respective media (BHI media for *Y. pseudotuberculosis,* and DYT media for *E. coli*). *Y. pseudotuberculosis* transformants were grown for 2 hours at 25°C, while *E. coli* was grown for 1 hour at 37°C. Finally, the cells were pelleted at 5,400 g for 2 minutes. The supernatant was discarded and the pellet was resuspended in 100 µl of media. This suspension was afterward plated on LB media plates with the appropriate antibiotic for selection.

2.5 Mutagenesis of *Y. pseudotuberculosis*

For the construction of the mutant strains, mutagenesis plasmids were constructed as mentioned in chapter 2.4.3 based on the pAKH3 suicide plasmid. In the process of mutagenesis, the wildtype gene was exchanged by a kanamycin resistance cassette. The suicide plasmid carrying the mutated gene fragment was introduced into the desired *Yersinia* strain. The exchange of the wildtype gene with the kanamycin resistance cassette was promoted by homologous recombination.

2.5.1 Bacterial conjugation

For introducing the desired suicide plasmid into *Yersinia*, *E. coli* S17-*1 λpir* was transformed with the suicide plasmid. This *E. coli* strain can build pili for conjugation and thereby transfer plasmid DNA to other bacteria (Sana, Laubier, and Bleves 2014). Besides, this *E. coli* strain harbors the *pir* gene that is needed to replicate the suicide plasmid. Strains without the *pir* gene, like the *Yersinia* strains, are not able to replicate the suicide plasmid.

For the conjugation, one culture of *E. coli* S17-*1 λpir* with the desired suicide plasmid and one with the recipient *Yersinia* strain is needed. The culture for *Yersinia* is inoculated in BHI media with the appropriate dilution (wildtype 1:50, Δ*yopD* 1:40). The volume was adjusted to the number of conjugations, with 4 ml of *Yersinia* culture per conjugation. Every *E. coli* strain was inoculated 1:100 from an overnight culture in BHI media supplemented with antibiotics. As for the *Yersinia*, the culture volume was adjusted to the number of conjugations in which 1 ml culture was needed per conjugation. The *Yersinia* strains were grown for 3.5 hours at 25°C and the *E. coli* strains were grown for 3 hours at 37°C. Afterwards, the *E. coli* strains were further incubated for 0,5 hours at 37°C without shaking. This step allowed the *E. coli* strains to build up the pili. For conjugation, 1 ml of *E. coli* was added to a filter paper with a pore size of 0.22 µm (GSWP), that was placed in a filtration setting attached to a pump. The cells were washed with 2 ml of BHI media to wash away the antibiotic. After that, 4 ml of *Yersinia* were added to the filter. Thereafter, the filter was taken from the filtration setting and placed on an LB plate, which was incubated for 4 to 5 h at 25°C. After incubation, the cells were washed off the filter with 1 ml LB media. The received cell suspension was collected in a 1.5 ml tube. 100 µl of the suspension were directly plated on an LB plate with triclosan, carbenicillin, and kanamycin (concentrations see Table

2.5). The triclosan was used to select for *Yersinia*, due to the natural resistance against triclosan, while the *E. coli* S17-*1 λpir* is triclosan-sensitive. Carbenicillin was added to select for *Yersiniae* harboring the suicide plasmid. Furthermore, kanamycin was added to select for the mutation. The remaining suspension was centrifuged at 5,400 g for 2 minutes and the pellet was resuspended in 100 µl of LB media. This was plated on a second LB plate. Afterwards, both plates were incubated at 25°C for two days.

2.5.2 Mutant selection and validation

To select strains with an integrated suicide plasmid after the conjugation, overnight cultures of 5 colonies for every conjugation were prepared. The overnight cultures were prepared with triclosan (see Table 2.5), to again check for *Yersinia,* and with kanamycin (see Table 2.5), because the mutated gene was exchanged with a kanamycin cassette. From every overnight culture, 50 µl were directly plated on LB plates supplemented with 10% sucrose and kanamycin. The plating on sucrose selects for *Yersinia* that have lost the suicide plasmid whereas the kanamycin selects for the resistance received by the mutant version of the targeted gene. The selection by sucrose works through the *sacB* gene located on the suicide plasmid. Sucrose induces the expression of the *sacB* gene which encodes for a protein converting sucrose to the toxic substance levan (Gay *et al.* 1985). Clones that were grown on the sucrose plates were subsequently patched to plates supplemented with carbenicillin and kanamycin or only kanamycin. Clones that grow on plates with kanamycin but not on carbenicillin and kanamycin were finally tested by PCR for the exchange of the original gene with the kanamycin resistance cassette. All identified mutants were then validated by northern blot to confirm absence of the equivalent mRNA.

2.6 Molecular biological methods for RNA analysis

2.6.1 RNA purification

For the analysis of cellular total RNA, the RNA needs to be isolated from the cells. The isolation is important due to the unstable nature of RNA and furthermore to make it accessible for different RNA techniques
(e. g. sequencing). Depending on the RNA analysis technique, two different methods for RNA isolation were used. The first method was the isolation by a column-based kit. This method was used when RNA longer than 250 nucleotides was used for the experiments. If RNAs smaller than 250 nt were analyzed, the method of hot phenol isolation was performed.

2.6.1.1 Column-based RNA purification

To isolate total RNA, cultures of *Y. pseudotuberculosis* were grown under the conditions mentioned (see chapter 2.2.2). After that 4 ml of every culture were standardly transferred to a 2 ml reaction tubes. Cells were harvested by centrifugation at 15,800 g for 1 minute and the supernatant was discarded. The pellets were directly frozen with liquid nitrogen to stop every cellular activity. The frozen cell pellets were stored at -20°C for short term or the RNA isolation was carried out directly.

The first step in RNA isolation was the lysis of the bacterial cells. Therefore the cell pellets were resuspended in 200 µl of a lysozyme-TE buffer (see Table 2.6) with a concentration of 50 mg lysozyme

per ml buffer. The suspension was incubated at room temperature for 10 minutes to allow the lysozyme to lyse the bacteria cells. The isolation of the RNA from the lysed cells was carried out with the SV total RNA isolation kit from Promega according to the manual. After the isolation, the isolated total RNA was eluted in 50 - 100 µl of nuclease-free water and stored at -20°C.

2.6.1.2 RNA purification using hot phenol

The isolation with hot phenol is based on the protein denaturing effect of phenol. Molecules, denatured by phenol form a phase with the phenol whereas undenatured molecules like RNA resolve in the aquarius phase on top. By this separation, the RNA can be isolated from the cells. For the purification 2 ml of culture were harvested in a 2 ml reaction tube and centrifuged by 15,800 g for 1 minute. The pelleted bacterial cells were frozen in liquid nitrogen and stored at -20°C for short term.

For the isolation, the pellets were resuspended in 200 µl of resuspension buffer (see Table 2.6). In the following, 200 µl of lysis buffer (see Table 2.6) were added and mixed by pipetting. For lysis, the cells were incubated at 65°C for 1.5 minutes. Afterwards, 400 µl of prewarmed (65°C) aqua phenol (pH 4.5) was added to the lysed cell suspension and mixed vigorously. This mixture was incubated at 65°C for 3 minutes followed by freezing on liquid nitrogen for 1 minutes. For separation of the phase, the samples were centrifuged for 10 minutes at 15,800 g. The aquarius phase was afterward transferred to a fresh 1.5 ml reaction tube. The phenol step was repeated two times. To eliminate residual phenol, which would interfere with subsequent applications, the aquarius phase was mixed with chloroform:isoamyl alcohol (24:1) and centrifuged for 3 minutes at 15,800 g. The upper phase was transferred to a fresh 1.5 ml tube and mixed with 1/10 sample volume of 3 M sodium acetate pH 4.5 and 2.5 sample volumes of pure ethanol and inverted several times to precipitate the RNA. For RNA concentration, the samples were stored at -80°C for 1 h or at -20°C overnight. After the precipitation, the RNA was pelleted by centrifugation at 15,800 g for 45 minutes and 4°C. The RNA pellet was washed with 800 µl 70% ethanol for 10 minutes at 15,800 g at 4°C, air-dried and resuspended in 50 – 100 µl of nuclease-free water and stored at -20°C.

2.6.2 Determination of RNA concentration and purity

To determine the nucleic acid concentration the sample was measured at 260 nm using the NanoDrop photometer (Thermo Fisher Scientific). The concentration in µg/ml is then calculated by the machine using the following function.

$$RNA\ concentration\ \mu g/ml = A_{260} \times 40\ \mu g/ml$$

The purity of the RNA was controlled by measuring the ratio of A_{260}/A_{280}. The ratio should be about 2.0. To exclude phenol contamination in the sample, the ration of A_{260}/A_{230} was measured. This ratio should be higher than the ratio of A_{260}/A_{280}.

2.6.3 Northern blot analysis of mRNA transcripts by agarose northern blot

To analyze the abundance of a specific RNA molecule under different conditions and in different strains, a northern blot analysis was performed. This method was used for long RNA molecule like mRNA with 300 nucleotides or longer. To detect these RNAs, total RNA was separated on an agarose gel and

transferred to a membrane. A specific DNA probe, which was complementary to the target RNA, was added to the membrane. Finally, the probe was detected by an antibody-based DIG-labeling and detection kit (Roche).

2.6.3.1 DNA amplification (PCR) for northern blot probes

The first step was to synthesis a DNA probe for the agarose-based northern blot analysis. The primers used for a probe PCR are mention in the following table (Table 2.13)

Table 2.13) Oligonucleotides for Northern Blot probes (agarose Northern blot)

Oligonucleotide	Sequence (5'→3')	Function
VIII798	CAGTGCCATCTTAAACACGC	*yopE* (fw)
VIII799	GTAATTTCTGCATCTGTTGCG	*yopE* (rev)
VIII806	GGGAAAAAAGACAGTGAAGG	*yopK/Q* (fw)
VIII807	AATACATTCTTGATCGCAGGA	*yopK/Q* (rev)
VIII810	GTACCTGAATTGCCGCAAAA	*yopM* (fw)
VIII811	CTTCAAGTTTGTCTGTAGTCTC	*yopM* (rev)
VIII818	GCGCAATGTGCATGAATGATA	*yopH* (fw)
VIII819	TAATAATGGTCGCCCTTGTC	*yopH* (rev)
VIII956	AAACTTTACTGCAGGTGTCG	*yadA* (fw)
VIII957	AAATGATGCGTTGTACATGAC	*yadA* (rev)
VIII920	GCGGCGGGTACCTTCATACCGCTGTTAATTCC	*yopJ/P* (fw)
VIII921	GCGGCGAAGCTTTTACTTATCGTCGTCATCCTTGTA ATCCTCGAGTACTTTGAGAAGTGTTTTATATTCAG	*yopJ/P* (rev)

For PCRs of the probe a standard Taq polymerase was used together with the DIG-DNA labeling mix (Roche). The DIG-DNA labeling mix contains dUTP which is linked with digoxigenin (DIG). This digoxigenin can later be detected by antibodies. The PCR was carried out according to the manufactory protocol with the addition of 2.5 mM $MgCl_2$.

The PCR was controlled by agarose gel electrophoresis (see chapter 2.3.2). A PCR clean-up can be performed but was not mandatory (see chapter 2.3.4). Probes were stored at -20°C

2.6.3.2 Detection of mRNA signals by agarose northern blot analysis

The RNA samples for the northern blot were mixed with water to a certain RNA amount of 3 µg per sample for high abundant target RNAs to 40 µg of total RNA for low abundant target RNAs. The prepared samples were mixed with 5x RNA loading buffer (see Table 2.6) and denatured at 70°C for 10 minutes and subsequently loaded onto the gel. Therefore, a 1.2% (w/v) agarose gel in 1x MOPS buffer (see Table 2.6) v was prepared. The gel runs for 75 minutes at 120 V in 1x MOPS buffer as running buffer. The 16S rRNA and 23S rRNA were detected as a loading control. This was possible, due to the ethidium bromide within the 5x RNA loading buffer. Both signals were visualized with UV-light (226 nm) and documented using a GelDoc system (BioRad).

Subsequently, total RNA, separated by the gel, was transferred to a membrane by a vacuum blot. In this study, the RNA was transferred onto a Nytran N membrane which is a (weakly) positively charged nylon membrane. The transfer was carryout at 50 mbar vacuum for 1.5 hours in 10x SSC buffer (see

Table 2.6). In the following step, the RNA was covalently bound to the membrane by UV light using an auto-crosslinker (Stratagene). All downstream steps were carryout as mentioned in the DIG Luminescent Detection Kit (Roche). As a substrate for the chemiluminescence reaction the CDP-Star (Roche) was used and the signals were documented by X-ray films.

For analysis of the results, the signals for the loading control as well as the signals from the probe detection were quantified using ImageJ (LI-COR Biosciences). For this all loading controls were calculated to one reference sample. The same procedure was done for the probe signals. Then the ratio of probe signal/loading control was calculated to normalize the data. This calculation then results in a fold-change of the different conditions to the reference sample, in which the reference sample had a fold-change of 1.

2.6.4 Northern blot analysis of short RNA transcripts by polyacrylamide northern blot

For the analysis of RNAs smaller than 250 nucleotides, a polyacrylamide based northern blot analysis was used. The difference between the agarose-based and acrylamide-based northern blot is the gel system, the transfer onto a membrane, and the detection method. For the detection of tRNAs, an 8% polyacrylamide gel with urea was used. Urea was added to denature the RNA to prevent the formation of secondary structures within the gel matrix. To prepare an 8% polyacrylamide-urea gel (20 cm x 20 cm), the following recipe was used.

	8% polyacrylamide-urea gel
Urea	16.8 g (7 M final concentration)
10x TBE buffer	4 ml
40% acrylamide (19:1)	8 ml
H_2O_{dest}	add up to 40 ml

The gel solution was incubated at room temperature until the complete urea was dissolved. Thereafter, 120 µl of 10% APS and 20 µl of TEMED were added to the solution and the gel was poured into the prepared gel chamber. The gel polymerized after pouring for at least 1 hour.

The RNA samples for the experiment were prepared with a final amount of 5 µg total RNA per lane and mixed one to one with formamide urea (FU)-mix (see Table 2.6). The samples were then boiled for 10 minutes at 70°C. In the following step, the samples were loaded onto the gel and were separated for 2.5 hours at 300 V. Afterwards, the RNA was transferred onto a positively charged nylon membrane by semidry electroblotting (VWR Peqlab). The transfer was carried out at 250 mA for 2.5 hours. To fix the RNA on the membrane, the membrane was UV-crosslinked (Stratagene) as for the agarose-based northern blot membrane. For the detection of target RNAs, DNA oligonucleotides linked with two different types of fluorophore were used, which were detected at 700 nm or 800 nm with the LiCor Odyssey Fc system (LI-COR Biosciences). The oligonucleotide primers for northern blot probes were purchased from Integrated DNA Technologies (IDT) and are listed in table 2.14.

Table 2.14) Oligonucleotides for Northern Blot probes (polyacrylamide Northern blots)

Oligonucleotide	Sequence (5'→3')
YPK_R0071, tRNA-Lys	5'IRD800 - GCGACCAATTGATTAAGAGTCAACTGCTCT
YPK_R0062, tRNA-Lys	5'IRD800 - TGCGACCAATTGATTAAAAGTCAACTGCTC
YPK_R0004, tRNA-Ala	5'IDR700 - CGCTGACCTCCTGCGTGCAAGGCAGGCGCT
YPK_R0013, tRNA-Asp	5'IDR700 - CCGCGACCCCCTGCGTGACAGGCAGGTATT
YPK_R0009, tRNA-Glu	5'IDR700 - TGTTACAGCCGTGAAAGGGCAGTGTCCTAG
YPK_R0074, tRNA-Leu	5'IDR700 - CATAAGCCGAGGGATTTTAAATCCCTTGTGTC
YPK_R0024, tRNA-Asn	5'IDR700 - GTGACATACGGATTAACAGTCCGCCGTTCT
YPK_R0068, tRNA-Ser	5'IDR700 - TACAGTCGACGGTTTTCAAGACCGTTGCCT
5S rRNA	5'IRD800 - CTCTCGCATGGGGAGACCCCACACTACCATC

To detect the target RNAs, the oligonucleotides were incubated with the membrane. Therefore the crosslinked membrane was hybridized with 20 ml of Church moderate buffer (see Table 2.6) and 15 nM of the oligonucleotide for detection of tRNAs or 5 nM to detect 5S rRNA as the loading control. Hybridization was performed at 42°C under slow rotation for at least 6 h in a hybridization oven. The order of the oligonucleotides was arranged so that the 5S rRNA loading control was used as the last probe. After hybridization, the membrane was washed 5 minutes at room temperature with RNA washing buffer I (see Table 2.6). Thereafter, the membrane was rinsed two times with H_2O_{dest} to eliminate residual SDS which would interfere with the detection. The detection was done with the LiCor Odyssey Fc system (LI-COR Biosciences) in the corresponding channels with a detection time of 0.5 minutes. After detection, the membrane was stripped in stripping buffer (see Table 2.6) for 10 minutes at 90°C. To confirm stripping, the membrane was again analyzed with the same detection conditions. The stripping was successful when the signal was completely eliminated or reduced to an intensity equal to the background. Successful stripping allowed hybridization with the next probe.

To analyze the results, the signals for the loading control and the probes were quantified using ImageStudio (LI-COR Biosciences). The calculation of the fold-change was afterward done as for the agarose northern blots (see chapter 2.6.3.2).

2.6.5 Quantitative real-time PCR analysis

To detect changes of specific target RNAs a quantitative real-time PCR (qRT-PCR) analysis, including reverse transcription, was performed. In this experiment, specific primer pairs target the RNA of interest. In the following step, this RNA is reversely transcribed into complementary DNA (cDNA) which is then used for a quantitative PCR. The quantification is achieved by SYBR Green I. This dye binds to the DNA and its fluorescence can be monitored.

After the isolation of total RNA (see chapter 2.6.1) the samples need to be treated with DNase, to remove contaminating genomic DNA which would interfere with the analysis. For a standard DNase digestion, 20 µg of total RNA was digested as following.

Example of a DNase digestion:

RNA [20 µg]	variable
10x DNase buffer	24 µl
Ribo-lock	0,5 µl
Turbo-DNase	3 µl
H_2O_{dest}	add up to 240 µl

The reaction was incubated for 1 hour at 37°C. After digestion 160 µl of H_2O_{dest} were added to every sample. The removal of the enzyme from the RNA was achieved by a phenol:chloroform extraction. Therefore 400 µl of phenol:chloroform:isoamyl alcohol (25:24:1) was added to the samples and mixed vigorously. For phase separation, the samples were centrifuged at 15,800 g for 5 minutes. The upper aquarius phase was transferred to a fresh 1.5 ml reaction tube, mixed with 400 µl chloroform:isoamyl alcohol (24:1), and centrifuged again at 15,800 g for 3 minutes. Finally, the RNA was precipitated as described earlier (see chapter 2.6.1.2). The RNA pellet was resuspended in 50 - 100 µl of nuclease-free water. Finally, the RNA was diluted to a final concentration of 20 ng/µl.

The qRT-PCR was performed by using the Luna® Universal One-Step RT-qPCR Kit (NEB) in a LightCyler 96 (Roche). The qRT-PCR was performed in a final volume of 10 µl according to the manufacturer's protocol with an RNA amount of 20 ng. For every primer pair, a master mix was prepared that was aliquoted for every reaction including a technical duplicate. For the quantification, the primers listed in Table 2.15 were used for the referred mRNAs. The *sopB* mRNA was used as a reference in all experiments.

Table 2.15) Oligonucleotides used for qRT-PCR

Oligonucleotide	Sequence (5'→3')	Function
III393	CCGACGTAAAGCCGCGATAC	*sopB* (fw)
III394	CCTCGTTCATAAGCACTCGTC	*sopB* (rev)
III44	GAGACAACTCCACACCCAAAC	*lcrF* (fw)
III45	GCAAAAGCAGTAATTCCTCAATAC	*lcrF* (rev)
VIII798	CAGTGCCATCTTAAACACGC	*yopE* (fw)
VIII799	GTAATTTCTGCATCTGTTGCG	*yopE* (rev)
VIII810	GTACCTGAATTGCCGCAAAA	*yopM* (fw)
VIII811	CTTCAAGTTTGTCTGTAGTCTC	*yopM* (rev)
VIII818	GCGCAATGTGCATGAATGATA	*yopH* (fw)
VIII819	TAATAATGGTCGCCCTTGTC	*yopH* (rev)

For every primer pair and sample combination, a non-target control with water instead of RNA as well as a non-reverse transcription control were performed. In the non-reverse transcription control, the reverse transcriptase was replaced by water. The first step in all reactions was the reverse transcription of the RNA into cDNA, followed by a 3-step PCR with 45 cycles. Fluorescence was measured after every elongation step. After the PCR, a melting curve was performed from 55°C to 95°C.

Step	Temperature	Time	
1. Reverse transcription			
Reverse transcription	55°C	10 min	
2. Quantitative PCR			
Denaturation (initial)	95°C	5 min	
Denaturing	95°C	10 s	] 45 cycles
Annealing	55°C	20 s	
Elongation	72°C	10 s	
Elongation (final)	72°C	5 min	
3. Melt curve			
Denaturing	95°C	10 s	
Annealing	55°C	1 min	
Melt curve	55°C to 95°C		
4. Cooling			
Sample cooling	37°C		

To analyze the data of the qRT-PCR the Cq (quantification cycle) value was calculated using the Roche software (version 1.1). The Cq value is the calculated cycle when the signal increases exponentially over the threshold and was automatically calculated by the software. With the given Cq values, the relative expression was calculated by the following formula. The primer efficiency was calculated as described in 2.6.5.1.

$$relative\ expression = \frac{primer\ efficiency^{\Delta Cq}gene\ of\ inerest}{primer\ efficiency^{\Delta Cq}reference\ gene}$$

Using the relative expression, the log_2 fold-change was calculated with the following formula:

$$log_2\ fold\ change = log_2\ relative\ expression$$

2.6.5.1 Determination of primer efficiency

To determine the primer efficiency for all used primer pairs, a standard qPCR reaction was used. Instead of RNA, genomic DNA with 3 different concentrations (20 ng/µl, 10 ng/µl, and 5 ng/µl) was used. With the Cq values, the primer efficiency was calculated using the following formula:

$$primer\ efficiency = 10^{(\frac{-1}{slope})}$$

Primer efficiencies rank between 1.8 and 2.

2.6.6 Ribo-Seq

The method of Ribo-Seq, based on ribosome profiling, is a next-generation sequencing approach to analyze the translatome of cells. The method is based on the work of Nicholas Ingolia from the group of Jonathan Weissman. They established a method of sequencing ribosome-protected mRNA fragments to get a translatome in *Saccharomyces cerevisiae* (Ingolia *et al.* 2009). Two years later the method was also established for *E. coli* by Eugene Oh and Annemarie Becker from the groups of Jonathan Weissman and Bernd Bukau (Oh *et al.* 2011).

The concept behind is to isolate mRNA from a cell in association with translating ribosomes. This would represent the pool of actively translated mRNAs. After isolation, the total RNA is digested with an RNase that can digest every single- and double-stranded RNA but not the mRNA part that is covered by the translating ribosome. This so-called ribosome footprint, which is around 30 nucleotides in length, can be isolated from the sample and sequenced. The sequencing result represents the position of 70S ribosome complexes on the mRNA (Ingolia *et al.* 2009; Oh *et al.* 2011).

Ribo-Seq consists of special steps including cell harvest, cell lysis, and handling to stabilize the ribosomes on the mRNA as well as to prepare the footprints from the samples to generate the translatome samples. In addition, the Ribo-seq also includes the preparation of transcriptome samples to finally compare the translatome with the transcriptome. This provides the ability to analyze the translational efficiency, which is a comparison if the translation is driven by the amount of transcript or by translation.

All main steps from cell harvest and cell lysis to the preparation of the ribosome footprints and the fragmented mRNA, as well as the preparation of the libraries and the sequencing are shown in the graphical workflow (Figure 2.1).

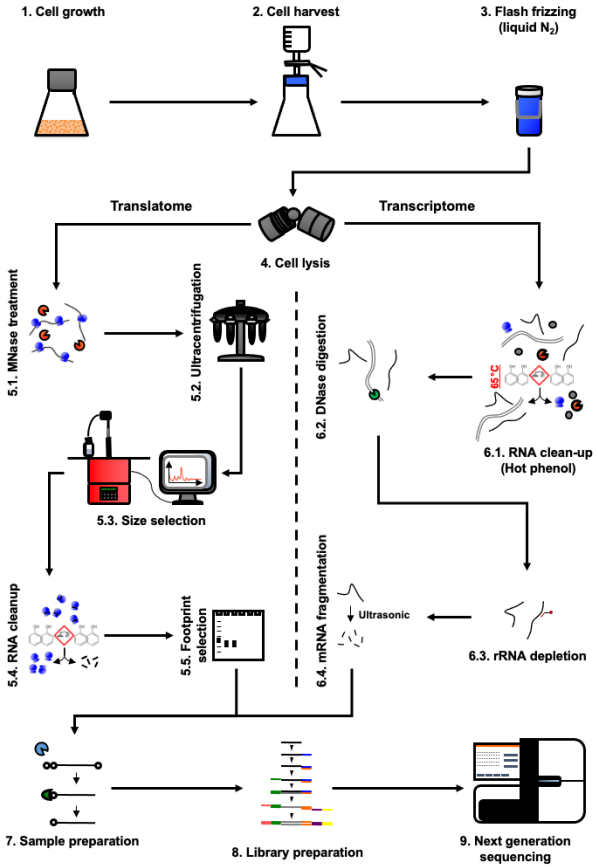

Figure 2.1) Ribo-Seq work-flow.

The work-flow shows the different steps of the Ribo-Seq approach including cell growth, harvest, and cell lysis, followed by the splitting of the samples for ribosome footprint generation as well as for mRNA isolation. After these different steps, all samples were prepared for library preparation and afterwards, paired-end libraries were generated. Finally, libraries were sequenced using the next-generation sequencing technique of Illumina.

2.6.6.1 Cell growth and harvest

For the experiments a greater amount of culture was needed compared to the other experiments in this study, so 100 ml of culture were cultivated at 25°C, 37°C and -Ca2+ conditions as mentioned in section 2.2.2. After the growth, the cells were rapidly harvested by filtration, to avoid release of ribosomes from the mRNA. The filtration was performed with a standard glass filtration equipment with a filter of 90 mm in diameter, that was attached to a pump. To collect the bacteria a nitrocellulose membrane with a pore size of 0.2 µm was placed in the filtration setup. When all the liquid was sucked through the filter the cells were scraped with a cell culture scraper and directly frozen in liquid nitrogen and stored at -80°C.

2.6.6.2 Cell lysing and sample clean-up

To lyse the bacterial cells without disrupting ribosome-mRNA integrity, the lysis was performed using the cryo mixer milling approach. Thereby, the cell pellets were lysed with 800 µl of Ribo-Seq lysis buffer (see Table 2.6) in grinding jars chilled in liquid nitrogen. The buffer contains magnesium and ammonium salts to stabilize the ribosomes on the mRNA as well as Tris for buffering and keeping the pH at 8.0. As a detergent Triton X-100 is part of the buffer. DNase I is added to the lysis buffer to digest the genomic DNA so that the ribosome-mRNA complexes were not trapped in the genomic DNA that is removed as cell debris later on. To avoid RNA digestion by RNases the RNase inhibitor Superase●in was added to the lysis buffer. To further stabiles the ribosome complexes chloramphenicol was added to the buffer. The antibiotic chloramphenicol interacts with the ribosome and stabilizes the interaction of both subunits. Addition of ciprofloxacin was used to neutralize all bacteria, to enable wot in a biosafety level 1 lab later on.

Lysing was carried out by a Tissue Lyser II (Qiagen) with a mixing frequency of 15 Hz for 2 minutes for 4 times. Between every repetition, the grinding jars were chilled again in liquid nitrogen. After lysing, the samples were thawed at room temperature for 15 minutes and then transferred to 1.5 ml reaction tubes.

To clarify the samples from cell debris, they were centrifuged for 10 minutes with 15,000 g at 4°C and the supernatants were transferred to fresh 1.5 ml reaction tubes. Thereafter the samples were frozen in liquid nitrogen and stored at -80°C to keep ribosome-mRNA complex integrity intact.

2.6.6.3 Determination of the RNA density

For the footprint preparation, the A_{260} of the lysates was measured to guarantee the same amount of RNA per reaction. To determine the A_{260} of every sample, a part of the sample was diluted 1:200 in 1x Ribo-seq pre-lysis buffer (see Table 2.6). Then the A_{260} was measured using quartz cuvettes in a standard UV-Vis photometer. As reference 1x Ribo-Seq pre-lysis buffer was used. By using the following formula the volume of the sample was calculated needed per footprint preparation.

$$\frac{A_{260}\ for\ digestion}{A_{260}\quad of\ sample} = volume\ sample\ [ml]$$

The absorption was adjusted to 7.7 (A_{260} of 7.7) for each mRNA-ribosome sample. After calculation, the required volume was transferred to two fresh 1.5 ml tubes and stored at -80°C. One of the samples was for footprint preparation the other one was used as undigested control to ensure that the polysomes

were intact. Additional, 50 µl of each sample were transferred to another fresh 1.5 ml reaction tube to isolate the total RNA for the transcriptome. These samples were also stored at -80°C.

2.6.6.4 Footprint preparation

The preparation of the footprints was done by RNase digestion. To do so, the RNase MNase (NEB) was used. This RNase digest single- and double-stranded RNA, but not RNA that is covered by the ribosome. This results in short RNA fragments of around 28 nucleotides that were protected by the ribosome. For the digestion, the samples of the cell lysates, that were adjusted to an A_{260} of 7.7, were mixed as:

Example of polysome digestion:

Cell lysate [A_{260} 7.7]	variable
10x polysome digestion buffer	11 µl
Micrococcal Nuclease (2,000 U/µl)	1.54 µl (≙ 400 U/A_{260})
H_2O_{dest}	add up to 110 µl

The undigested control was treated the same without the addition of the MNase. In this reaction, the MNase was replaced by water. The digestion reaction was carried out at 25°C for 1 hour. In the end, the reaction was stopped by the addition of EGTA pH 8.0 with a final concentration of 10 mM. Afterwards, the samples were placed on ice and loaded on ultracentrifugation gradients.

2.6.6.5 Ultracentrifugation of footprints

The sucrose gradients needed for the separation of ribosomes were prepared using the gradient station from Biocomp. Therefore two sucrose solutions were prepared. One with 10% sucrose in 1x Ribo-Seq pre-lysis buffer (see Table 2.6) and the second with 50% sucrose in 1x Ribo-Seq pre-lysis buffer (see Table 2.6). To stack the gradients the centrifugation tubes were marked according to the marker block provided by the gradient station. The ultracentrifugation tubes were filled with 10% sucrose in 1x Ribo-Seq pre-lysis buffer (see Table 2.6) till the mark. Subsequently, the 50% sucrose in 1x Ribo-Seq pre-lysis buffer (see Table 2.6) was sub-layered and the tubes were closed with the short caps. The formation of continuous gradients was achieved by using the following program.

Program for gradient forming:

Lids	short
Gradient type	suc (sucrose)
Density	10% - 50%
Rotor	SW 41 Ti
Steps	14

The prepared gradients were placed in the rotor buckets of the SW 41 Ti ultracentrifugation rotor and chilled on ice. 100 µl of footprint digestion or control was loaded on a gradient. The separation was then performed by ultracentrifugation at 200,000 g for 3 hours at 4°C in a Beckman ultracentrifuge (Optima L-80 XP Ultracentrifuge).

After the ultracentrifugation, fractions of every gradient were collected and the profile was measured at 260 nm (A_{260}) and 280 nm (A_{280}). The A_{260} represents the nucleic acids in this case mainly RNA and the A_{280} represents proteins. As ribosomes consist of RNA and proteins, so both profiles should follow a similar pattern, while the A_{260} value should be higher because the ribosome mainly consists of RNA.

From the digested sample, the generated peak representing the 70S ribosome particle was collected in a 1.5 ml tube and stored at -80°C.

2.6.6.6 Isolation of footprints

To efficiently isolate the whole RNA of the footprints, the collected fractions including the 70S ribosome particles were split into four samples of 200 µl into 1.5 ml tubes. These samples were mixed with nuclease-free water to a final volume of 400 µl. To every sample, 400 µl of prewarmed (65°C) acid phenol (125:24:1; pH 4.5) was added and mixed vigorously. Samples were then incubated at 65°C for 5 minutes with 1,400 rpm in a thermomixer (Eppendorf). Thereafter samples were chilled on ice for 5 minutes. To separate the phases, the samples were centrifuged for 5 minutes at 15,800 g. The upper aquarius phase was transferred to a new 1.5 ml tube. Thereafter, 400 µl of room temperature acid phenol (125:24:1) was added to the sample and again mixed vigorously. The samples were then incubated at room temperature for 5 minutes. For separation, the samples were centrifuged 5 minutes at 15.800 g and the upper aquarius phase was transferred to a new 1.5 ml tube. To eliminate residual phenol, a chloroform:isoamyl alcohol extraction was performed. Therefore 400 µl of chloroform:isoamyl alcohol (24:1) was added to the sample and mixed vigorously, followed by centrifugation at 15,800 g for 3 minutes to separate the phases. The upper aquarius phase was then transferred to a 2.0 ml *DNA LoBind* tube (Eppendorf) and the RNA was precipitated by the addition of 1/10 sample volume of 3 M sodium acetate pH 4.5, 2 µl of glycogen, and 2.5 sample volumes of pure ethanol. To ensure efficient precipitation the samples were inverted several times and precipitated at -80°C for 1 hour.

After precipitation, the RNA was pelleted by centrifugation at 15,800 g for 45 minutes and 4°C. The RNA pellet was washed with 700 µl 70% ethanol for 15 minutes at 4°C with 15,800 g. After discarding the supernatant the pellet was air-dried and resuspended in 15 µl of nuclease-free water. The same samples were pooled and stored at -20°C.

For isolation of the footprints from the 70S ribosome particle RNA, a gel extraction was performed using a 15% polyacrylamide-urea gel (20 cm x 20 cm) according to the following recipe:

	15% polyacrylamide-urea gel
Urea	16.8 g (7 M final concentration)
10x TBE buffer	4 ml
40% acrylamide (19:1)	15 ml
H_2O_{dest}	add up to 40 ml

The gel solution was incubated at room temperature until the urea was completely dissolved. Afterwards, 120 µl of 10% APS and 20 µl of TEMED were added to the solution and the gel was poured into the prepared gel chamber. The gel polymerized after pouring for at least 1 hour.

Before the samples were loaded onto the gel, it was installed and pre run for 20 minutes at 150 V. The isolated footprint RNA samples were mixed 1:1 with FU-mix (see table 2.6). As marker, three oligonucleotides with 20 nucleotides, 30 nucleotides, and 40 nucleotides were used (see table 2.16). They were mixed in 5 µl with a final amount of 100 ng per oligonucleotides and as well mixed with the FU-mix (see Table 2.6) 1:1. All samples and the marker were boiled at 65°C for 10 minutes, chilled on ice and loaded onto the gel. Gel run was performed for 3 hours at 300 V.

Table 2.16) Oligonucleotides used as a marker

Oligonucleotide	Sequence (5'→3')
VIII309	GTTACCAGTCAGGCATTTGAGAAGCACACGGTCACACTGC
VIII310	GTTACCAGTCAGGCATTTGAGAAGCACACG
VIII311	GTTACCAGTCAGGCATTTGA

To visualize the RNA the gel was stained with SYBR® Gold (Thermo Fisher Scientific) in TBE buffer for 20 minutes at room temperature. After intercalation of the SYBR® Gold into the RNA molecules, it was visualized with UV-light (300 nm) and documented using a GelDoc system (BioRad).

For every sample lane, the area between the 20 nucleotides and the 40 nucleotides marker band was cut and transferred to a 2.0 ml *DNA LoBind* tube (Eppendorf). In the tube, the gel was crushed using a tip. Afterwards, 400 µl of TE buffer (see Table 2.6) was added to every tube and the samples were incubated overnight at 4°C on a rotating wheel. This allows the RNA to migrate from the gel into the buffer.

On the next day, the gel was removed from the buffer using a Spin-X® centrifuge filter tube (Corning). By centrifugation at 15,800 g for 3 minutes the polyacrylamide gel pieces were pelleted. The liquid was then transferred onto a Spin-X® centrifuge filter tube (Corning) which was placed in a 1.5 ml *DNA LoBind* tube (Eppendorf). The samples were centrifuged at 2,000 g for 1 minute and afterwards cleaned using the phenol:chloroform extraction method as described in chapter 2.6.5. The aquarius phase was than transferred to a 1.5 ml *DNA LoBind* tube (Eppendorf) and precipitated by adding 1/10 sample volume of 3 M sodium acetate pH 4.5, 1 µl of GlycoBlue (Thermo Fisher Scientific), and 2.5 sample volumes of pure ethanol at -80°C for 1 hour.

The RNA was pelleted by centrifugation at 15,800 g for 45 minutes and 4°C. The pellet was washed with 700 µl 70% ethanol for 15 minutes at 15,800 g at 4°C. After discarding the supernatant the pellet was air-dried and finally resuspended in 20 µl of nuclease-free water. The resuspended samples were stored at -20°C.

With this step, the samples were ready for the pre-library sample preparation (see chapter 2.6.6.11).

2.6.6.7 Isolation of total RNA

To isolate total RNA for the transcriptome part of the Ribo-Seq 40 µl of lysate from chapter 2.6.6.2 were taken. Every sample was mixed with 160 µl of resuspension buffer (see Table 2.6). The isolation was performed as described in chapter 2.6.1.2 using the hot phenol method. In the end, the samples were washed two times with chloroform:isoamyl alcohol (24:1) and precipitated by adding 1/10 sample volume of 3 M sodium acetate pH 4.5, 2 µl of glycogen, and 2.5 sample volumes of pure ethanol at -80°C for 1 hour.

The precipitated total RNA was pelleted as described earlier (see chapter 2.6.6.6). The pellets were resuspended in 40 µl of nuclease-free water and the concentration was measured (see chapter 2.6.2).

2.6.6.8 DNase digestion of total RNA

As for the qRT-PCR the remaining DNA needs to be removed. For this purpose, a DNase digestion was performed as disccribed in chapter 2.6.5. In contrast to chapter 2.6.5 more total RNA (30 µg) was used for one reaction as mentioned in the following example:

Example of a DNase digestion:

total RNA [30 µg]	variable
10x DNase buffer	24 µl
Ribo-lock	0.5 µl
Turbo-DNase	3 µl
H_2O_{dest}	add up to 240 µl

After DNase digestion, the samples were cleaned up using the phenol:chloroform extraction method (see section 2.6.5) with the specifications described in chapter 2.6.6.6. After precipitation, centrifugation, and drying of the RNA pellet, the RNA was resuspended in 20 µl of nuclease-free water and the concentration was measured (see chapter 2.6.2).

2.6.6.9 rRNA depletion of digested total RNA

In the next step, the ribosomal RNA (rRNA) was depleted. For rRNA depletion, the MICROB*Express*™ bacterial mRNA enrichment kit (Thermo Fisher Scientific) was used according to the manufacturer's protocol. As input 8 µg of total RNA was used for every sample. The depletion works by hybridization of the 16S and 23S rRNA to complementary sequences bound to magnetic beats which were removed by a magnetic setting later on. The sample was finally precipitated in a 1.5 ml *DNA LoBind* tube (Eppendorf) and resuspended in 20 µl of nuclease-free water. The rRNA depletion was controlled by a Bioanalyzer analysis. The quality control was performed by the Helmholtz Centre for Infection Research (HZI) in-house sequencing facility (GEMK) using a nano- or pico-Chip for the Agilent 2100 Bioanalyzer system (Agilent). Samples with less than 5 - 10% of rRNA were used for downstream applications.

2.6.6.10 mRNA fragmentation

After rRNA depletion, the enriched mRNA was fragmented for library preparation. The fragmentation was carried out by a mechanical shearing using the *Covaris* focused-ultrasonicator (Covaris) and microTUBE Snap-Cap AFA Fiber tubes. Every fragmentation contained 300 ng of enriched mRNA. The fragmentation to fragments of 200 nt length was performed by the HZI in-house sequencing facility (GEMK) using the following protocol.

Program for mRNA fragmentation:

Processing time	150 s
Fragment size range	200 nt
Intensity	5
Duty cycle	10%

After fragmentation, the mRNA was precipitated, centrifuged, and resuspended as described in chapter 2.6.6.6. The fragmented mRNA was resuspended in 10 µl of nuclease-free water and the fragmentation was quality controlled by Bioanalyzer analysis (Agilent) performed by the HZI in-house sequencing facility (GEMK) using the appropriate chip.

Samples were now ready for pre-library sample preparation (see chapter 2.6.6.11).

2.6.6.11 Pre-library sample preparation of footprints and mRNA

First, the ribosome footprints and the fragmented mRNA need to be dephosphorylated. This step was important because the MNase produces 3’ phosphate ends, which would interfere with the library preparation. The fragmented mRNA needs to be dephosphorylated, due to the mechanical shearing which produces different phosphorylated RNA ends.

The dephosphorylation was performed with the Calf Intestinal Phosphatase (NEB). As input 1 µg of fragmented mRNA was used for each transcriptome sample and the entire ribosome footprints sample was used. The reactions were prepared using the following protocol:

Example of a dephosphorylation digestion:

RNA [1 µg]	variable
10x reaction buffer	5 µl
Calf Intestinal Phosphatase (CIP)	4 µl
H_2O_{dest}	add up to 50 µl

The dephosphorylation reactions were performed at 37°C for 30 minutes with 800 rpm in a thermomixer (Eppendorf). The incubation was followed by a phenol:chloroform extraction (see chapter 2.6.5 and 2.6.6.6). After precipitation, centrifugation, and drying of the RNA pellet, the RNA was resuspended in 20 µl of nuclease-free water.

After the dephosphorylation, all RNAs were re-phosphorylated with a 5’ monophosphate. The 5’ monophosphate was necessary for the following library preparation. After dephosphorylation the entire sample (20 µl) was used for 5’ re-phosphorylated. The reactions were setup as described in the following protocol:

Example of a 5’ phosphorylation digestion:

RNA	20 µl
10x PNK buffer A	5 µl
10 mM ATP	20 µl
T4 Polynucleotide Kinase (10 U/µL)	1 µl
H_2O_{dest}	add up to 50 µl

The reactions were incubated at 37°C for 30 minutes with 800 rpm in a thermomixer (Eppendorf) and cleaned as described above for the dephosphorylation. The samples were resuspended in 10 µl of nuclease-free water and the concentration was measured (see chapter 2.6.2).

2.6.6.12 Library preparation and sequencing

In the final step, all samples were used for library preparation. The libraries were prepared with the NEBNext® Multiplex Small RNA Library Prep Set for Illumina® (Set 1) (NEB) according to the manufactory protocol with some adjustments. For the Ribo-Seq libraries, 5 µl of samples were directly used for the preparation. For transcriptome libraries, 200 ng of fragmented mRNA were used. Due to the low RNA amount in all samples, the amount of the adaptors was reduced. For the 3' SR adaptor, a 1:5 dilution and for the 5' adaptor a 1:2 dilution was used. For the PCR amplification, the primers listed in Table 2.17 were used in suitable combinations. The primers were designed based on the NEB

multiplex primers for the Illumina Nova-Seq system, because they were not available for the NEBNext® Multiplex Small RNA Library Prep Set for Illumina® (Set 1) (NEB). The PCR amplification was performed as mentioned with 18 cycles. The number of cycles was determined by test libraries to not overamplify the final libraries.

Table 2.17) Oligonucleotides used for Nova-Seq sequencing

Oligonucleotide	Sequence (5'→3')	Index-sequence
NEBNext i501 Primer_modified	AATGATACGGCGACCACCGAGATCTACACTATAGCCTACA CTCTTTCCCGTTCAGAGTTCTACAGTCCG*A	TATAGCCT
NEBNext i502 Primer_modified	AATGATACGGCGACCACCGAGATCTACACATAGAGGCAC ACTCTTTCCCGTTCAGAGTTCTACAGTCCG*A	ATAGAGGC
NEBNext i503 Primer_modified	AATGATACGGCGACCACCGAGATCTACACCCTATCCTACA CTCTTTCCCGTTCAGAGTTCTACAGTCCG*A	CCTATCCT
NEBNext i504 Primer_modified	AATGATACGGCGACCACCGAGATCTACACGGCTCTGAAC ACTCTTTCCCGTTCAGAGTTCTACAGTCCG*A	GGCTCTGA
NEBNext i505 Primer_modified	AATGATACGGCGACCACCGAGATCTACACAGGCGAAGAC ACTCTTTCCCGTTCAGAGTTCTACAGTCCG*A	AGGCGAAG
NEBNext i506 Primer_modified	AATGATACGGCGACCACCGAGATCTACACTAATCTTAACA CTCTTTCCCGTTCAGAGTTCTACAGTCCG*A	TAATCTTA
NEBNext i507 Primer_modified	AATGATACGGCGACCACCGAGATCTACACCAGGACGTAC ACTCTTTCCCGTTCAGAGTTCTACAGTCCG*A	CAGGACGT
NEBNext i508 Primer_modified	AATGATACGGCGACCACCGAGATCTACACGTACTGACACA CTCTTTCCCGTTCAGAGTTCTACAGTCCG*A	GTACTGAC
NEBNext i701 Primer_modified	CAAGCAGAAGACGGCATACGAGATCGAGTAATGTGACTG GAGTTCAGACGTGTGCTCTTCCGATC*T	ATTACTCG
NEBNext i702 Primer_modified	CAAGCAGAAGACGGCATACGAGATTCTCCGGAGTGACTG GAGTTCAGACGTGTGCTCTTCCGATC*T	TCCGGAGA
NEBNext i703 Primer_modified	CAAGCAGAAGACGGCATACGAGATAATGAGCGGTGACTG GAGTTCAGACGTGTGCTCTTCCGATC*T	CGCTCATT
NEBNext i704 Primer_modified	CAAGCAGAAGACGGCATACGAGATGGAATCTCGTGACTG GAGTTCAGACGTGTGCTCTTCCGATC*T	GAGATTCC
NEBNext i705 Primer_modified	CAAGCAGAAGACGGCATACGAGATTTCTGAATGTGACTGG AGTTCAGACGTGTGCTCTTCCGATC*T	ATTCAGAA
NEBNext i706 Primer_modified	CAAGCAGAAGACGGCATACGAGATACGAATTCGTGACTG GAGTTCAGACGTGTGCTCTTCCGATC*T	GAATTCGT
NEBNext i707 Primer_modified	CAAGCAGAAGACGGCATACGAGATAGCTTCAGGTGACTG GAGTTCAGACGTGTGCTCTTCCGATC*T	CTGAAGCT
NEBNext i708 Primer_modified	CAAGCAGAAGACGGCATACGAGATGCGCATTAGTGACTG GAGTTCAGACGTGTGCTCTTCCGATC*T	TAATGCGC
NEBNext i709 Primer_modified	CAAGCAGAAGACGGCATACGAGATCATAGCCGGTGACTG GAGTTCAGACGTGTGCTCTTCCGATC*T	CGGCTATG
NEBNext i710 Primer_modified	CAAGCAGAAGACGGCATACGAGATTTCGCGGAGTGACTG GAGTTCAGACGTGTGCTCTTCCGATC*T	TCCGCGAA
NEBNext i711 Primer_modified	CAAGCAGAAGACGGCATACGAGATGCGCGAGAGTGACTG GAGTTCAGACGTGTGCTCTTCCGATC*T	TCTCGCGC
NEBNext i712 Primer_modified	CAAGCAGAAGACGGCATACGAGATCTATCGCTGTGACTG GAGTTCAGACGTGTGCTCTTCCGATC*T	AGCGATAG

*: Phosphorothioate (PTO) bound

The final cDNA libraries were afterward cleaned using the MinElute PCR Purification kit (Qiagen) according to the manufacturer's protocol. The libraries were eluted in 10 µl of nuclease-free water. The

cleaned cDNA libraries were delivered to the HZI in-house sequencing facility (GEMK) for a final purification step by BluePippin (Sage Science), whereby the sample was separated by size, and all libraries with >150 bp were used for sequencing. The purified and size-selected cDNA libraries were quality controlled by Bioanalyzer (Agilent) using a *High Sensitivity DNA Chip* and the concentration was finally measured by *Qubit* (Thermo Fisher Scientific) quantification.

The sequencing was performed by the HZI in-house sequencing facility (GEMK) using the NovaSeq 6000 sequencing system from Illumina (S1 flow cell) with the standard program for paired-end reads with 100 cycles (PE50, 2x50 bp reads). The samples were introduced with a goal of 10 million reads per library.

2.6.6.13 Bioinformatic analysis

The fastq files produced by the sequencing were used in a downstream bioinformatics approach to detect open-reading frames (ORFs), analyze the expression of genes in the transcriptome and translatome, and calculate translational efficiencies (TE) (Gelhausen *et al.* 2020). This will gain information if expression of particular *Yersinia* genes is driven by transcription or translation. The bioinformatics analysis was performed in cooperation by the group of Rolf Backofen from the Institute of Bioinformatics (Freiburg).

Data were trimmed to exclude adaptors by the tool cutadapt(2.1) (Martin 2011) Afterwards, the reads were mapped to the *Y. pseudotuberculosis* genome (NC_010465.1) and the *pIB1* virulence plasmid (NZ_CP032567) by the tool segemehl (version 0.3.4) (Otto *et al.* 2014) and rRNA and multi-mapped reads were removed by SAMtools(1.9) (Li *et al.* 2009). Next, the ORFs were predicted by the REPARATION tool and the Ribo-TISH tool (Ndah *et al.* 2017; Zhang *et al.* 2017) All steps were controlled by MultiQC quality control (Ewels *et al.* 2016). Differential translations were calculated from the data using xtail (Xiao *et al.* 2016). Analyzed data were provided in a tabularized form included e. g. translational efficiency, RPKM normalized read counts, codon counts, nucleotide and amino acid sequences. The mapped reads were provided as coverage files for a genome browser, and some additional information, e. g. potential start/stop codon and ribosome binding sites (Gelhausen *et al.* 2020). The data were provide as GFF files for a genome browser.

2.7 Biochemical methods

2.7.1 Preparation of bacterial whole-cell extracts

To detect and compare protein levels in bacteria cells, an equal volume of bacteria (OD_{600} = 1) was transferred to a 2 ml reaction tube. The cells were harvested by centrifugation for 1 minute at 15,800g. Afterwards, the supernatants were discarded and the pellets were resuspended in 50 µl 2x SDS-sample buffer (see Table 2.6). The resuspended samples were boiled for 10 minutes at 95°C for denaturing of the proteins. After denaturing the samples were centrifuged shortly and 2.5 µl to 10 µl of samples were used for SDS-polyacrylamide gel electrophoresis (SDS-PAGE) and western blot.

2.7.2 Preparation of direct culture samples

In addition to the analysis of whole-cell proteins inside of bacteria cells, also intracellular proteins together with secreted proteins were analyzed. Therefore 100 µl of culture was directly transferred to a 1.5 ml reaction tube and mixt with 100 µl 2x SDS-sample buffer (see Table 2.6). The samples were boiled for 10 minutes at 95°C for denaturing of the proteins and cell debris was pelleted. Top adjust the cell numbers, the OD_{600} was measured for every sample and the sample volume was calculated so that 10 µl of the sample was equal to an OD_{600} of 1. The samples were separated by SDS-PAGE. This allowed detection of proteins of interest inside of cells and in the supernatant, and to use a loading control.

2.7.3 SDS-polyacrylamide gel electrophoresis (SDS-PAGE)

The SDS-PAGE is a method to separate proteins by their size in an electric field. The sodium dodecyl sulfate (SDS) thereby denatures the proteins and giving them a negative charge based on the length of the amino acid chain. This charge allows the denatured proteins to migrate into a polyacrylamide gel.

In contrast to the polyacrylamide-urea gel for separating RNAs, the SDS-PAGE consists out of two gel parts, an upper gel part, and a lower gel part. The upper gel part has the function of focusing (stacking) the sample while the second gel part is for the separation of the sample by size, equal to the polyacrylamide-urea gel.

In this study, two different acrylamide concentrations were used in the separation gels. For the analysis of proteins between 70 kDa and 20 kDa, a 12% SDS separation gel was used. For proteins smaller than 20 kDa a 15% SDS separation gel was used. The used recipes are mentioned below.

	SDS separation gel	
	12%	**15%**
Lower gel buffer (see Table 2.6)	1.25 ml	1.25 ml
30% acrylamide (37.5:1)	2 ml	2,5 ml
H_2O_{dest}	1.75 ml	1.25 ml
10% APS	25 µl	25 µl
TEMED	10 µl	10 µl
	SDS stacking gel	
Upper gel buffer (see Table 2.6)	1.25 ml	
30% acrylamide (37.5:1)	0.55 ml	
H_2O_{dest}	3.25 ml	
10% APS	40 µl	
TEMED	20 µl	

For every gel, an appropriate volume of PageRuler™ Prestained Protein Ladder (Thermo Fisher Scientific) was loaded to monitor the migration. Protein samples were separated by SDS-PAGE at 30 mA until sufficient separation was achieved, which was normally 45 minutes. Afterwards, the gels were further used for western blot.

2.7.4 Western blot analysis

Western blotting was used to detect the proteins of interest, separated on an SDS-PAGE. The separated samples were transferred to a membrane. Afterwards, the protein of interest was detected by specific antibodies as well as the loading control. The transfer of the proteins onto a polyvinylidene difluoride (PVDF) membrane (Sigma-Merck) was performed by wet/tank blot for 1 hour at 100 V.

After the transfer, the membrane was dried to immobilize the proteins on the membrane. Then, the membrane was blocked for 1 hour at room temperature on a shaker in TBS-M buffer (see Table 2.6). Afterwards, the membrane was incubated with the primary antibody, against the protein/s of interest, at 4°C overnight with shaking in TBST-M buffer (see Table 2.6). On the next day, the membrane was washed three times for 5 minutes with TBST (see Table 2.6). This washing step removes unbound antibody. In the next step, the secondary antibody was incubated with the membrane for 1 hour at room temperature and shaking in TBST buffer (see Table 2.6). The secondary antibody was directed against the primary antibody and was labeled with a fluorophore for detection. To wash away unbound antibody the membrane was washed three times with TBST (see Table 2.6) for 5 minutes. To remove residual Tween, the membrane was rinsed with TBS (see Table 2.6) because Tween can interfere in the fluorescence detection. Finally, the signals were detected using the LiCor Odyssey Fc system with fluorophore detection.

To analyze the results, the signals for the histone-like nucleoid structuring protein (H-NS) were used as loading control. The signals for H-NS and the protein of interest were quantified using ImageStudio (LI-COR Biosciences). The calculation of the fold-change was done as described for the northern blot approaches (see chapter 2.6.3).

3 Results

The T3SS as well as the effector proteins (Yops) and the adhesin YadA of *Y. pseudotuberculosis* are highly expressed genes upon innate immune cell-contact situation to counteract the phagocytosis of the bacterium. It is already reported, that the level of the respective mRNAs is strongly upregulated under these conditions (Kusmierek *et al.* 2019). This upregulation is promoted by LcrF, the transcriptional activator of the *ysc-yop* virulence system. In a non-cell-contact setup, the expression of LcrF, the T3SS, the Yops, and YadA can be modeled by Ca^{2+}- depletion in an *in vitro* situation at 37°C (in this study abbreviated with -Ca^{2+}). Under these conditions, *Y. pseudotuberculosis* secrete effector Yops into the culture medium in a T3SS-dependent manner. While secreting the Yops, the bacteria encounter a growth arrest. In contrast to this, *Y. pseudotuberculosis* cultured at 37°C in the presence of Ca^{2+} *in vitro* does not secret effector Yops into the medium and expresses the same genes at a significantly lower level. In addition, the bacteria show no growth arrest and divide normally (Bölin and Wolf-Watz 1988; Straley and Bowmer 1986) (Figure 3.1).

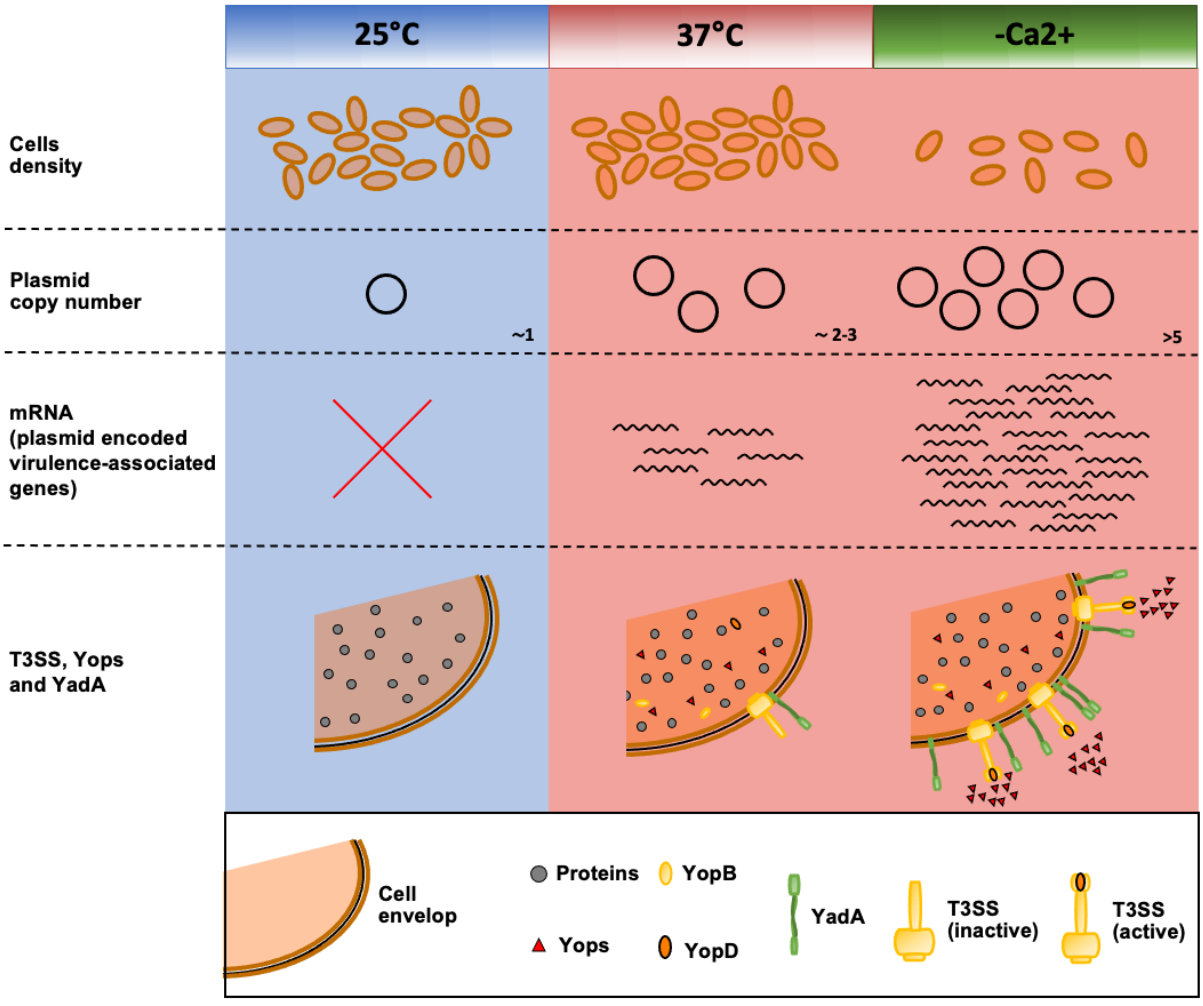

Figure 3.1) Overview of *Y. pseudotuberculosis* behavior under lab conditions at 25°C, 37°C, and -Ca^{2+} conditions.
Schematic of the bacterial cell density, plasmid copy number, mRNA level of virulence-associated mRNAs and of the plasmid and T3SS-, Yops- and YadA- synthesis of *Y. pseudotuberculosis* in an *in vitro* culture at 25°C ("*environmental*"), 37°C (non-secretion), and at 37°C in the absence of Ca^{2+} (secretion/-Ca^{2+}) (Bölin and Wolf-Watz 1988; Kusmierek *et al.* 2019; Wang *et al.* 2016).

Based on the observation of the bacterial growth arrest under -Ca^{2+}-conditions combined with the observed strong secretion of Yops into the culture medium, it was hypothesized that the expression of

yop genes might not only be regulated at the level of transcription but also at the translational level. To answer this question, the translation efficiency (TE) of the *ysc*, *yops,* and *yadA* mRNAs was determined. For this purpose, a high-throughput sequencing technique called Ribo-Seq was established to determine translation rates at the different conditions (25°C, 37°C, -Ca^{2+}). This technique allows the determination of the translatome as well as the transcriptome of the bacteria in the same sample (Ingolia et al. 2009). The results enabled us to analyze the efficiency of translation for every gene.

3.1 Differential translation of *Yersinia* virulence genes under secretion conditions identified by Ribo-Seq

The technique of the Ribo-Seq is based on the protective effect of the ribosomal-bound mRNA against RNases (Ingolia *et al.* 2009). By sequencing these protected mRNA fragments obtained from *Y. pseudotuberculosis*, referred to as ribosome protected footprints (RPF), the translatome can be determined. For this approach, the bacterial cells need to be harvested and lysed in a way that the mRNA-ribosome complexes are not damaged or affected. After gentle lysis, an aliquot of the sample was used to determine the translatome and another to determine the transcriptome (mRNA) of *Y. pseudotuberculosis*. This allows direct genome-wide correlation of the transcriptome and the translatome of *Y. pseudotuberculosis* to calculate the translational efficiency (TE) later on and to identify if a gene is regulated at the transcriptional or translational level.

For the analysis of the translatome, lysed cells were treated with MNase (Micrococcal nuclease) from *Staphylococcus aureus*, an RNase that digests single- and double-stranded RNA (Cuatrecasas *et al.* 1967). Through the action of this enzyme, all mRNA regions that are not protected by a ribosome were degraded. The protected regions consisted of fragments of ~28 nucleotides (the RPF) that could be isolated by gradient ultracentrifugation of the digested samples and subsequent fragmentation of the transcripts to receive the 70S ribosomal particle covering the RPF (see supplement Figure 5.1). Later on, the RPFs were used for library preparation and Illumina-based deep sequencing. This sample then represented the translatome part of the Ribo-Seq. The samples for the transcriptome were rRNA depleted, mechanically fragmented, and finally also used for library preparation and Illumina-based deep sequencing. These samples represent the transcriptome data (mRNA) of the Ribo-Seq. Due to those two sample sets, the Ribo-Seq experiment represented a transcriptome (mRNA) and a translatome (RPF) analysis in one approach. The obtained data were then bioinformatically analyzed and the TE was calculated from the data to identify effects at the level of translation (detailed procedure see chapter 2.6.6). So far, this study is the first approach where Ribo-Seq was establishing and used in a pathogenic bacterium under virulence-related conditions to directly compare translatome and transcriptome changes.

3.1.1 Establishing Ribo-Seq for *Y. pseudotuberculosis*

The method of Ribo-Seq for *Y. pseudotuberculosis* differs in several steps from methods established for other organisms. Optimal isolation and protection of ribosomal-bound mRNA complexes often depends on the characteristic properties of the individual bacterium and efforts adaptation of the harvesting and lysing method. The cell harvest, cell lysis, and sample preparation for the transcriptome

and translatome and the preparation of the final cDNA libraries for Illumina-based deep sequencing used for *Y. pseudotuberculosis* are illustrated in Figure 3.2.

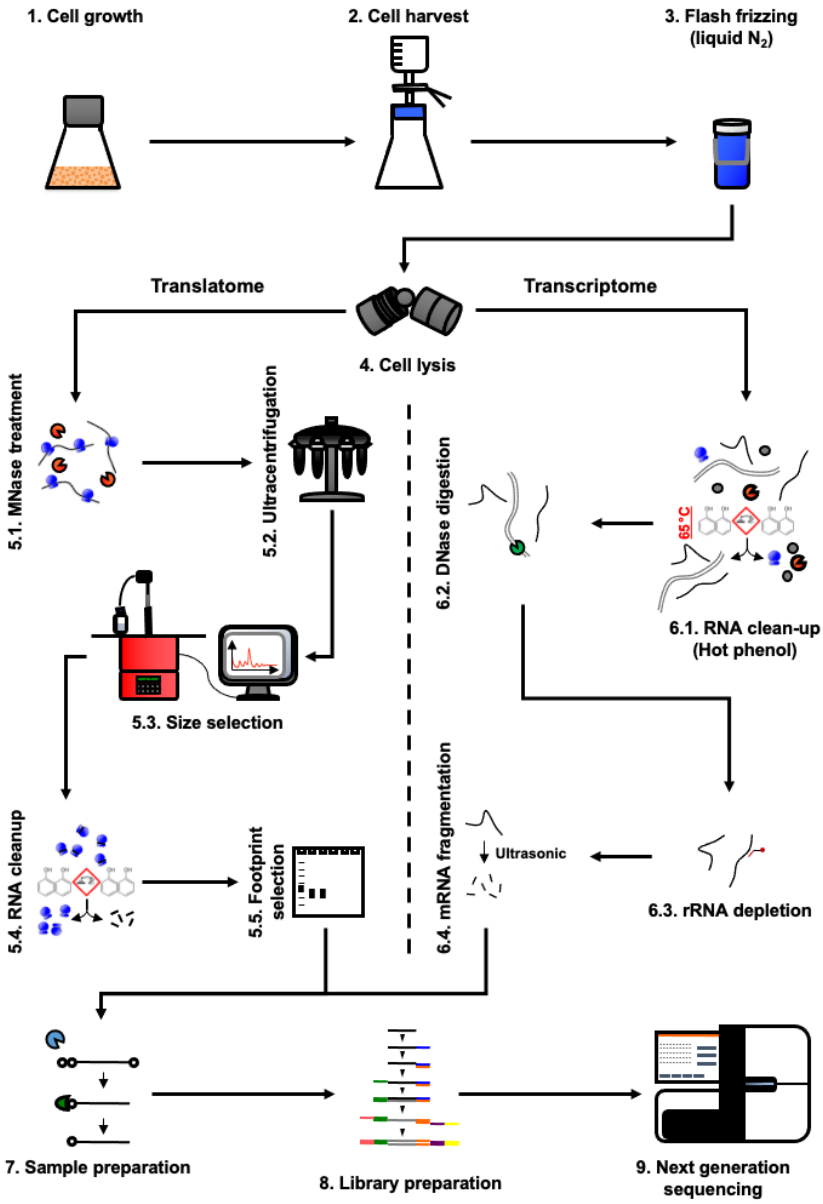

Figure 3.2) Ribo-Seq work-flow.
The work-flow shows the different steps of the Ribo-Seq approach including cell growth, harvest, and cell lysis, followed by the splitting of the samples for ribosome footprint generation as well as for mRNA isolation. After these different steps, all samples were prepared for library preparation and afterwards, paired-end libraries were generated. Finally, libraries were sequenced using the next-generation sequencing technique of Illumina.

In contrast to commonly used lysis methods, the bacteria cells were not harvested by centrifugation, instead, they were harvested by rapid filtration. This step is crucial to reduce cell stress which will lead to the dissociation of ribosomes from the mRNA. Subsequently, the harvested bacteria cells were frozen in liquid nitrogen to fix the ribosomal-bound mRNA complexes in the bacteria cells. Therefore, it was also necessary to lyse the cells in the liquid nitrogen frozen state by cryo-lysing (Becker *et al.* 2013; Brar and Weissman 2015; Ingolia *et al.* 2009). After lysing, the sample was split into two separate fractions one for ribosomal footprint generation (translatome) and one for transcriptome generation.

To generate the ribosomal footprint, the bacterial lysed was digested with an RNase which cleaves all RNA molecules that were not protected by the 70S ribosomal particle. For Ribo-Seq of eukaryotic cells,

RNase I was established to generate the ribosomal footprint with a size of 30 nucleotides. When Ribo-Seq was established for bacteria, it was observed that RNase I was not as efficient and precise as in eukaryotes. Therefore, the MNase (Micrococcal nuclease) treatment was established for bacteria. In contrast to RNase I, the MNase generates a ribosomal footprint of around 28 nucleotides but with a bigger variety ranking from 40 nucleotides down to 20 nucleotides (Becker *et al.* 2013). The amount of MNase, therefore, needed to be adjusted due to the fact that MNase digests every type of RNA, including the rRNA of the ribosome, resulting in an enrichment of non-translational reads in the Illumina-based deep sequencing. Moreover, exceedingly high amounts of MNase would increase the unintended digestion of rRNA, while too low amounts of MNase would result in incomplete digestion of the polysomes. In parallel to the digestion, a control sample was treated without MNase to see whether the harvest and lysis haven't affected the ribosomal-bound mRNA complexes. After digestion, the different ribosomal particles, including free transcripts, 30S ribosomal particles (small subunit), 50S ribosomal particles (large subunit), 70S ribosomal particles, and polysomes, were separated by a sucrose based gradient ultracentrifugation. Next, the adsorption at 260 nm was detected throughout the whole gradient of the digested and undigested sample to generate a ribosome profile, representing the different ribosomal particles mentioned.

A typical ribosome profile represents four main peaks and a polysome tail with several peaks. The first peak with the lowest migration (0 to 10 mm from tube top) represents the free transcripts including sRNAs, tRNAs, free rRNAs (not incorporated in a ribosome particle), and mRNAs. The second peak at around 12.5 mm from the tube top represents the 30S ribosomal particles (small subunit), which were free in the bacteria cell to initiate translation. Next to this peak, at 20 mm from the tube top, the peak representing the 50S ribosomal particles (large subunit) was located, which was also free for newly initiated translations. At around 25 mm from the tube top, a big peak represents one 70S ribosomal particle bound to a transcript for translation was identified. After this peak, the polysomes were visualized, in which every peak represents the addition of one 70S ribosomal particle to a transcript (Becker *et al.* 2013; Ingolia *et al.* 2012) (see Figure 3.3AB). To confirm that harvest and lysing did no affected the ribosomal-bound mRNA complexes, the polysomes needed to be present with defined peaks, while the peaks representing the isolated 30S ribosomal particles (small subunit) and 50S ribosomal particles (large subunit) needed to be rather small (see Figure 3.3A). In contrast, the digested sample should show a significant reduction of the polysomes and an increase of the peak representing isolated 70S ribosomal particles, due to the shift of the digested polysomes to the 70S ribosomal particles (monosomes). For the translatome, this peak was isolated from the gradient.

It occurs that the peak representing disomes (first peak after the 70S peak, representing two 70S ribosomal particles on one transcript) is often not fully digested. This is in agreement with previous studies which also show, that a significant reduction of this peak is sufficient, due to the problems with a stronger digestion. The close proximity of two 70S ribosomal particles on one transcript might block the activity of the MNase between both particles, resulting in no cleavage (Becker *et al.* 2013; Ingolia *et al.* 2012). The peaks representing the 30S ribosomal particles (small subunit) and 50S ribosomal particles (large subunit) should only be slightly affected by the digestion (see Figure 3.3A) (Becker *et al.* 2013; Ingolia *et al.* 2012).

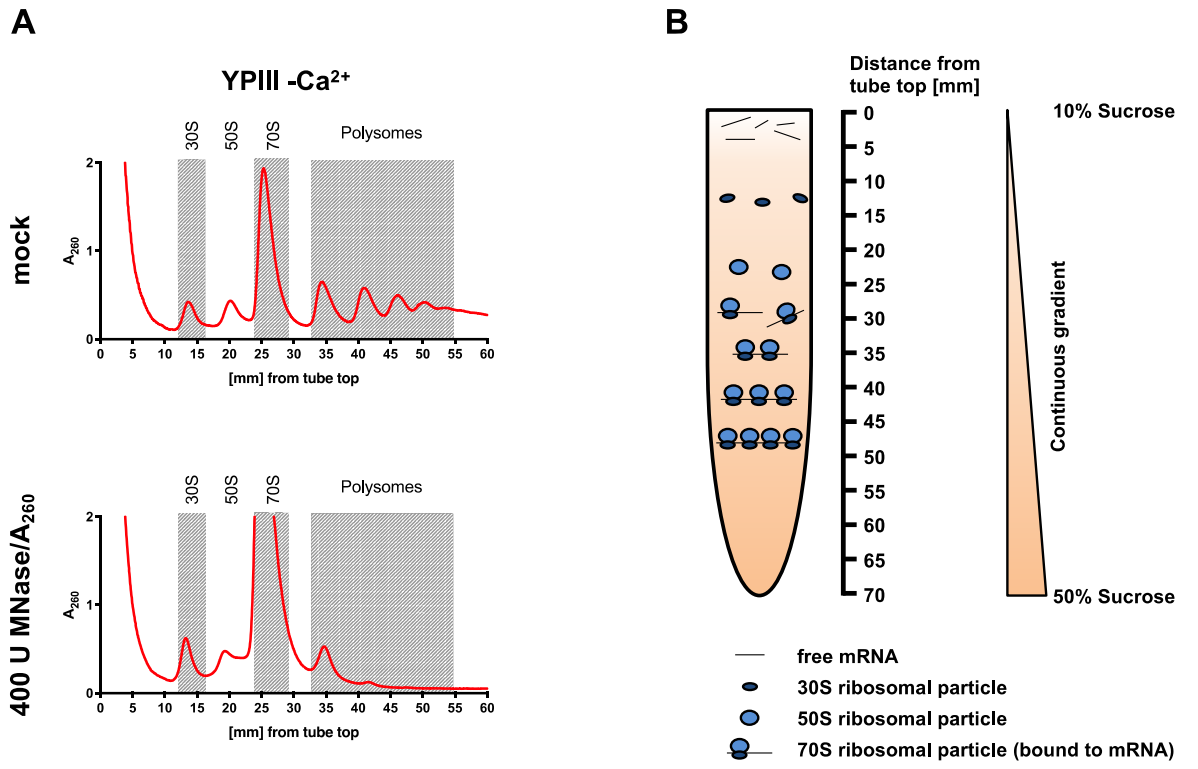

Figure 3.3) Ribosome profile of *Y. pseudotuberculosis* under secretion (-Ca^{2+}) conditions after gradient ultracentrifugation with and without MNase digestion.

(**A**) Ribosome profile obtained by sucrose-based gradient ultracentrifugation and detection of the absorption at 260 nm throughout the whole gradient from top to bottom as indicated by the x-axis. The representing samples were generated from *Y. pseudotuberculosis* YPIII under secretion (-Ca^{2+}) conditions. The different ribosome fractions are indicated on top of every graphic, while the top graphic shows an undigested sample and the bottom graph shows an MNase treated sample. Representative graphics for the wildtype, Δ*csrA,* and Δ*yopD* mutants at 25°C, 37°C and secretion (-Ca^{2+}) conditions are visible in Figure 5.1. (**B**) Graphical overview of the migration of the different ribosomal particles throughout a schematic gradient.

For the *Y. pseudotuberculosis* wildtype (YPIII) as well as the Δ*csrA* and Δ*yopD* mutants grown at 25°C, 37°C, and under secretion (-Ca^{2+}) conditions, the ribosome profiles show the expected pattern as mentioned above for undigested samples (see Figure 7.1). Furthermore, the digestion with MNase leads to a reduction of the polysomes with the related increase in the 70S ribosomal particle representing peak in all tested samples and conditions (see Figure 7.1). This indicates successful preservation of the ribosomal-bound mRNA complexes as well as efficient digestion towards 70S ribosomal particle in all tested strains and conditions.

After 70S ribosomal particle (monosome) isolation, the RNA was isolated from these samples by a specific acid phenol isolation procedure based on a special phenol. This type of acid phenol represents a mixture of phenol, chloroform, and isoamyl alcohol (125:24:1) with a higher amount of phenol compared to phenol:chloroform:isoamyl alcohol (25:24:1) commonly used for RNA isolation. The higher amount of phenol increases its isolation abilities, while on the other hand reduces the problems with the sucrose-based viscous samples obtained by the gradients (Ingolia *et al*. 2009). The RNA isolated from the gradients was subsequently loaded onto a denaturing urea-based polyacrylamide gel to isolate the generated ribosome footprints by gel extraction. Due to the mentioned fact, that the MNase is not as precise as the RNase I, all RNA fragments with a size between 40 nucleotides and 20 nucleotides were isolated.

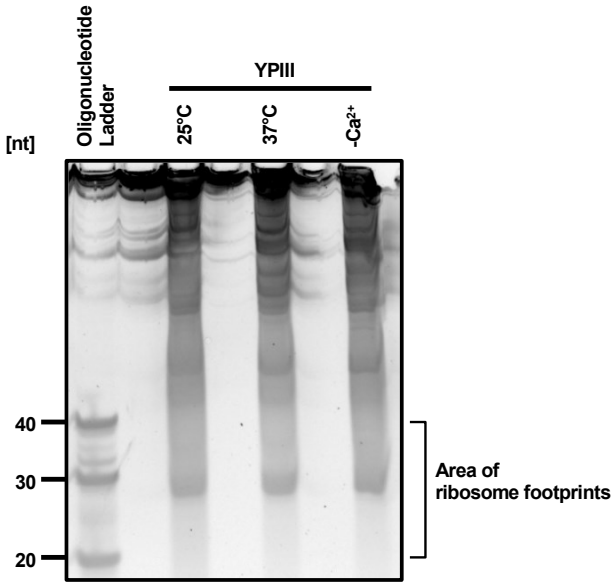

Figure 3.4) Ribosome footprint isolation by polyacrylamide gel electrophoreses.

Representative gel for ribosome footprint isolation from *Y. pseudotuberculosis* grown at 25°C, 37°C and under secretion (-Ca^{2+}) conditions. Marker was prepared from three oligonucleotides with the size of 20, 30, and 40 nucleotides. The area which was cut per lane is highlighted on the right side of the gel image.

The gel images for the ribosome footprint isolation for the *Y. pseudotuberculosis* wildtype, Δ*csrA,* and Δ*yopD* mutants show a very similar pattern under all growth conditions (25°C, 37°C and -Ca^{2+}). It is notable for all gel images, that a more defined band is observable at around 28 nucleotides as expected from the MNase digestion. The higher molecular size bands (smear) of various sizes represent RNA molecules of different length produced by the MNase. The bands at the top of the gel represent rRNA molecules. As this pattern was expected and is similar to other published figures the samples were used for pre-library preparation (Becker *et al.* 2013; Ingolia *et al.* 2009, 2012).

In parallel to the ribosome footprint preparation and isolation, the transcriptome samples were generated. After the bacteria cell lysis, an aliquot of the lysate was used for the analysis of the transcriptome. Therefore, the total RNA was isolated from the sample and DNase treated. After that, the rRNA was depleted from the sample to increase the reads obtained from mRNA molecules. To deplete the rRNA molecules, an oligonucleotide hybridization with magnetic beads was used (MICROBExpress™ Bacterial mRNA Enrichment Kit, Thermo Scientific (Morrissey and Collins 1989)). Due to the oligonucleotide, only the 16S and 23S rRNA but not the 5S rRNA were depleted from the sample. To control whether the depletion was successful the sample was afterwards quality controlled by *Bioanalyzer* analysis. When the amount of 16S and 23S rRNA was less than 10% the sample was classified as rRNA “free”. The rRNA “free” transcriptome samples were then ready for RNA fragmentation (see Figure 3.5A).

After rRNA depletion, all samples for the *Y. pseudotuberculosis* wildtype and the Δ*csrA* and Δ*yopD* mutant under the three growth conditions (25°C, 37°C and -Ca^{2+}), maintained an rRNA contamination of less than 10%. Most of the samples represent an even lower contamination of less than 5% (see Figure 3.5A). These results qualified the samples for further treatment in the pre-library preparation.

After rRNA depletion, the transcriptome samples were mechanically fragmented by ultrasonic (Covaris system) to generate fragments of around 200 nucleotides in size. Due to the physics of mechanical

fragmentation, the generated fragments will represent a wide variety of sizes from around 100 nucleotides up to 500 nucleotides, with an average size of 200 nucleotides. The fragmentation was essential to finally allow library preparation. Furthermore, the fragmentation allows sequencing of larger parts of the same transcript due to the multiple fragments generated from one transcript. After fragmentation, the transcriptome samples were also ready for pre-library preparation.

In the pre-library preparation, two main problems caused by the MNase digestion as well as transcript fragmentation were addressed. The first problem was the multiple 5'- and 3'-end phosphorylation states generated by the MNase digestion or mechanical fragmentation. For library preparation, a 5' monophosphate was needed to allow ligation of the different adaptor molecules (see NEBNext® Small RNA Library Prep Set for Illumina®). To overcome the problem, all samples for translatome and transcriptome were dephosphorylated to remove every type of phosphorylation. Afterwards, the samples were phosphorylated with a 5' monophosphate to allow usage of the *NEBNext® Small RNA Library Prep Set for Illumina®* (by NEB) for library preparation. After dephosphorylation and 5' monophosphate phosphorylation all translatome and transcriptome samples of the *Y. pseudotuberculosis* wildtype, Δ*csrA,* and Δ*yopD* mutant grown at 25°C, 37°C and under secretion (-Ca^{2+}) conditions were controlled by a *Bioanalyzer* analysis. The translatome samples should represent the main peak at around 30 nucleotides in the *Bioanalyzer* analysis due to the ribosome footprint size, while the transcriptome samples should have a main peak at 100 nucleotides with a constant decreasing signal by increasing sizes, due to the mechanical fragmentation.

All translatome samples represent one main peak as expected, but with a somewhat greater size than 30 nucleotides (see Figure 3.5B). This different fragment size can be explained by the weaker separation ability for smaller fragments of the used *Bioanalyzer* pico chip for quality control, which was used due to the low RNA concentration. Based on this information, all samples for the translatome passed the quality control. The samples for the transcriptome also encounter the problem of weaker separation of the smaller fragments. In addition, the main peak represents the remaining 5S rRNA and tRNAs of the sample which were not able to be depleted (see Figure 3.5C). Based on the *Bioanalyzer* quality control all transcriptome samples qualified for the library preparation.

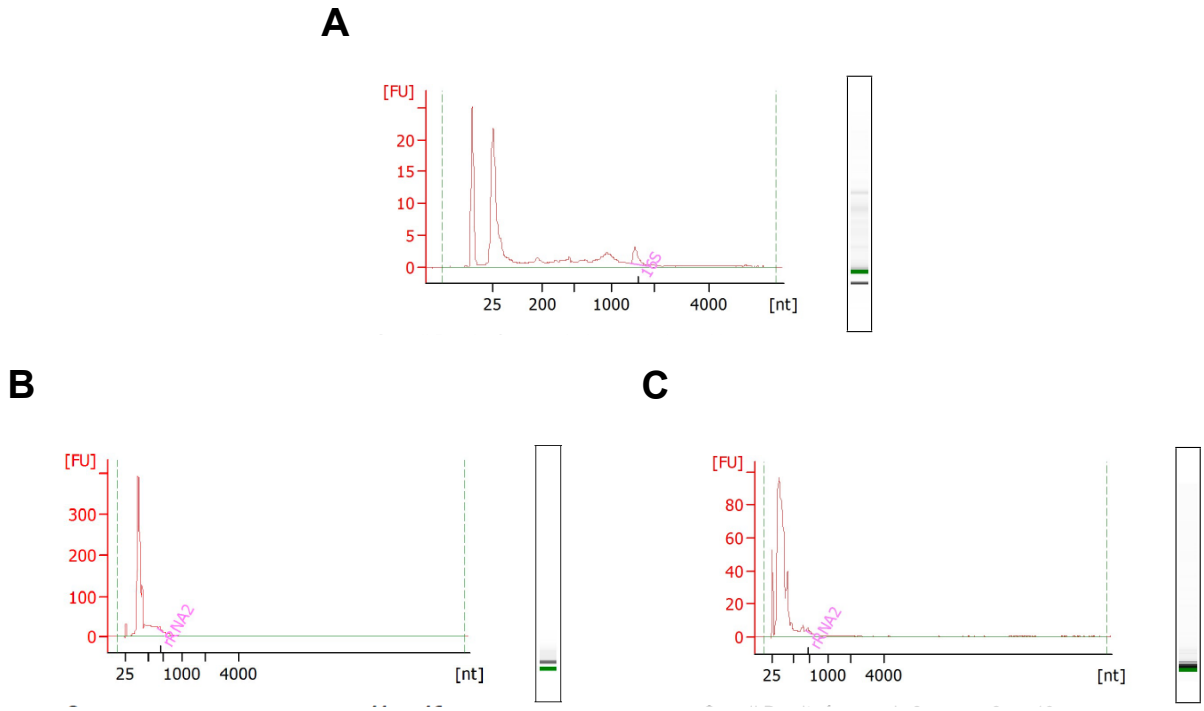

Figure 3.5) *Bioanalyzer* quality control profiles at different steps in the process of sample preparation prior to library preparation.

The graphics represent different quality control steps within the sample preparation of the translatome and transcriptome samples of *Y. pseudotuberculosis* YPIII and the Δ*csrA* and Δ*yopD* mutants grown at 25°C, 37°C and under secretion (-Ca^{2+}) conditions. (**A**) *Bioanalyzer* profile of a representative transcriptome sample after rRNA depletion achieved with an RNA nano chip. Representative *Bioanalyzer* profile after pre-library preparation of a (**B**) translatome sample and a (**C**) transcriptome sample achieved with an RNA pico chip.

After successful pre-library preparation, confirmed by *Bioanalyzer* quality control, the translatome and transcriptome samples were used for library preparation under use of the *NEBNext® Small RNA Library Prep Set for Illumina®* (by NEB). The kit used the RNA as a template to add adaptors to the 5'-and 3'-ends. These adapters were later in the process used to work as binding platforms for special sequencing primers. These primers introduce a special index sequence to both ends of the RNA molecule. This allows the identification of the strand later on and also facilitates strand-specific of the sequencing. Besides the index, the primer also adds the anchor sequences to the ends of the RNAs. This anchor immobilizes the library later on in the flow cell of the Illumina sequencer. Finally, the constructed RNA library was amplified by PCR into a double-stranded complementary DNA (cDNA) molecule for sequencing. In the PCR process, the primers can build primer-dimers which contained now transcriptome or translatome read. To exclude the primer-dimers, the cDNA libraries were size-selected by *BluePippin* (Sage Science). The *BluePippin* system is based on a size separation on an agarose-based gel system with real-time imaging and selection of certain DNA fragments by size (see *BluePippin* system, Sage Science). Primer-dimers had sizes of 70 base pairs for primer-dimers of identical primers and 130 base pairs for primer-dimers of forward and reverse primers, while the libraries had sizes of 160 base pairs and longer. Therefore, the threshold for size selection was set to 160 base pairs to collect all fragments with a size of 160 base pairs and longer and thereby eliminate the primer-dimer contaminations. After *BluePippin*, the quality and size selection was controlled by a *Bioanalyzer* quality control, for DNA. For the translatome, the *Bioanalyzer* analysis result should reveal a main peak at 160 to 170 base pairs, due to the size of the ribosome footprints (30 nucleotides) together with the primers on both sides. For the transcriptome samples, the highest peak should include 160 base pairs, due to

the threshold setting of the size selection. The peak should decrease constantly towards larger fragments which is due to the mechanical fragmentation of the transcriptome samples.

For all translatome and transcriptome samples of *Y. pseudotuberculosis* wildtype and Δ*csrA,* and Δ*yopD* mutant grown at 25°C, 37°C, and under secretion (-Ca^{2+}) conditions, expected patterns were observed (see Figure 3.6AB). In case of the translatome samples, smaller peaks were detected which represent libraries with a larger size. These libraries on the one hand represent ribosome footprints with more than 30 nucleotides (for libraries with up to 200 base pairs), while on the other hand, they represent libraries where ribosomal rRNA is incorporated (libraries with >200 base pairs) (see Figure 3.6A). The incorporation of rRNA occurs through the MNase treatment which also digests rRNA (see footprint preparation earlier), which is not depleted in the process of translatome sample preparation. The amount of rRNA-contaminated libraries compared to the libraries with the right size is very small whereby the libraries are classified as qualified. After positive final quality control, all libraries were used for Illumina-based deep sequencing.

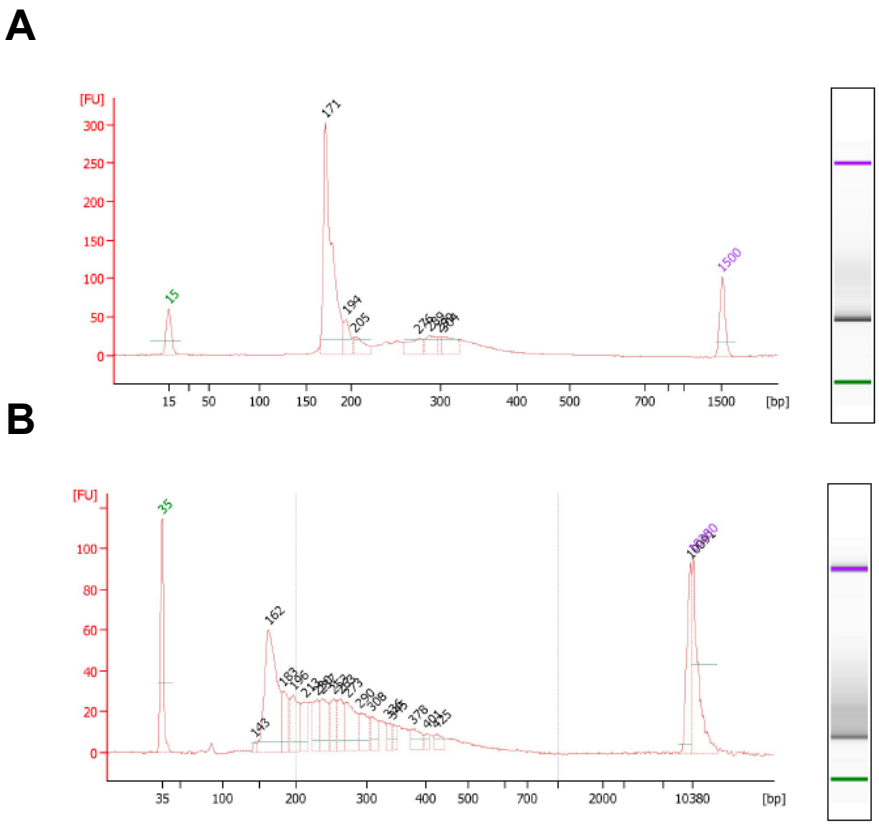

Figure 3.6) *Bioanalyzer* quality control profiles of final cDNA libraries after *BluePippin* selection prior to Illumina-based deep sequencing.

The graphics represent the final quality control of the cDNA libraries after size selection by *BluePippin*. Both graphics show a representative example of the cDNA libraries from *Y. pseudotuberculosis* YPIII and the Δ*csrA* and Δ*yopD* mutants grown at 25°C, 37°C and under secretion (-Ca^{2+}) conditions for the (**A**) translatome and (**B**) transcriptome.

After passing the final *Bioanalyzer* quality control, the different samples were sequenced by an Illumina-based deep sequencing with paired-end reads. The obtained reads were bioinformatically analyzed to identify changes in the translatome and transcriptome and to finally calculate the translation efficiency (TE).

3.1.2 Global analysis of translation in *Y. pseudotuberculosis*

The Ribo-Seq was established for the wildtype (YPIII) as well as two mutant strains, Δ*csrA,* and Δ*yopD,* grown under 25°C, non-secretion (37°C) and secretion (-Ca^{2+}) conditions (see chapter 2.14.6). Both mutants were used, due to their striking effect on the expression of the virulence regulator *lcrF*, and thereby also on the T3SS, Yops, and YadA (Kusmierek *et al.* 2019). For the RNA-binding protein CsrA, it was already shown that it is able to inhibit ribosome initiation by binding to the RBS, but there are rare cases where it supports translation initiation (Leistra *et al.* 2018). YopD, in its function as an RNA-binding protein, might inhibit binding of other factors. For YopD it was shown, that it has a strong repressive effect on LcrF synthesis whereby loss of YopD leads to uncontrolled Yop secretion at 37°C even without a secretion signal (Ca^{2+} depletion) (Fowler *et al.* 2009; Kusmierek *et al.* 2019). To confirm appropriate quality of the sequencing results as well as of the RNA samples (mRNA and RPF), the sample-to-sample distances were calculated using the Spearman correlation. Therefore the reads for the chromosome (NC_010465.1) and the plasmid pIB1 (NZ_CP032567) were analyzed together. In the calculation, all libraries of one strain were analyzed in relation to each other, but not between the strains.

A first, more general observation in all strain backgrounds (YPIII, Δ*csrA*, Δ*yopD*) shows that in all correlations, the libraries for the transcriptome (mRNA) form cluster apart from the translatome (RPF) cluster under the same growth conditions. This was assumed, due to the differences in sample preparations for the transcriptome and the translatome data (see chapter 2.6.6). Furthermore, the clusters of samples from 25°C (mRNA and RPF) always show a high similarity while they always form clusters apart from the 37°C as well as -Ca^{2+} samples. This difference between 25°C and 37°C as well as -Ca^{2+} in all backgrounds (YPIII, Δ*csrA*, Δ*yopD*) is, on the one hand, possible by the expression of the *ysc-yop, yadA, and lcrF* genes encoded on the virulence plasmid pIB1 which are expressed with increased temperature and especially under secretion conditions (-Ca^{2+}). On the other hand, also the expression of chromosomally encoded genes changes with increased temperature, such as (i) repression of genes for flagella-mediated motility, (ii) changes in the expression of metabolic pathways (e. g. upregulation of genes encoding components of the TCA cycle at 37°C), and (iii) changes of chromosomally encoded virulence factors (Heroven *et al.* 2012; Kusmierek 2018; Nuss *et al.* 2015; Nuss *et al.* 2017) (see Figure 3.6, 3.7, 3.8).

Besides the general observations mentioned earlier, the data for the wildtype (YPIII) show a more pronounced clustering of the different growth conditions (25°C, 37°C, and -Ca^{2+}). The 37°C sample and -Ca^{2+} samples also form distinct clusters as expected by the activation and strong expression of the virulence plasmid pIB1 encoded genes under -Ca^{2+} conditions compared to 37°C (Kusmierek 2018; Kusmierek *et al.* 2019). Thereby is to mention for the 37°C and -Ca2+ samples, that the samples prepared by the same method are slightly closer to each other than the samples of the same condition. This difference in clustering can be explained by the preparation of the samples for transcriptome (mRNA) and translatome (RPF). While the transcriptome (mRNA) samples contain every transcribed RNA type including 5' UTRs, 3' UTRs, sRNAs, and tRNAs as well as CDS the translatome (RPF) samples only contain the CDS of an mRNA (Ingolia et al. 2012). The clustering gives a first hint, that the method worked successfully because the libraries are grouped as expected from the growth conditions at different temperatures and T3SS-expression behavior that was previously shown (see Figure 3.6).

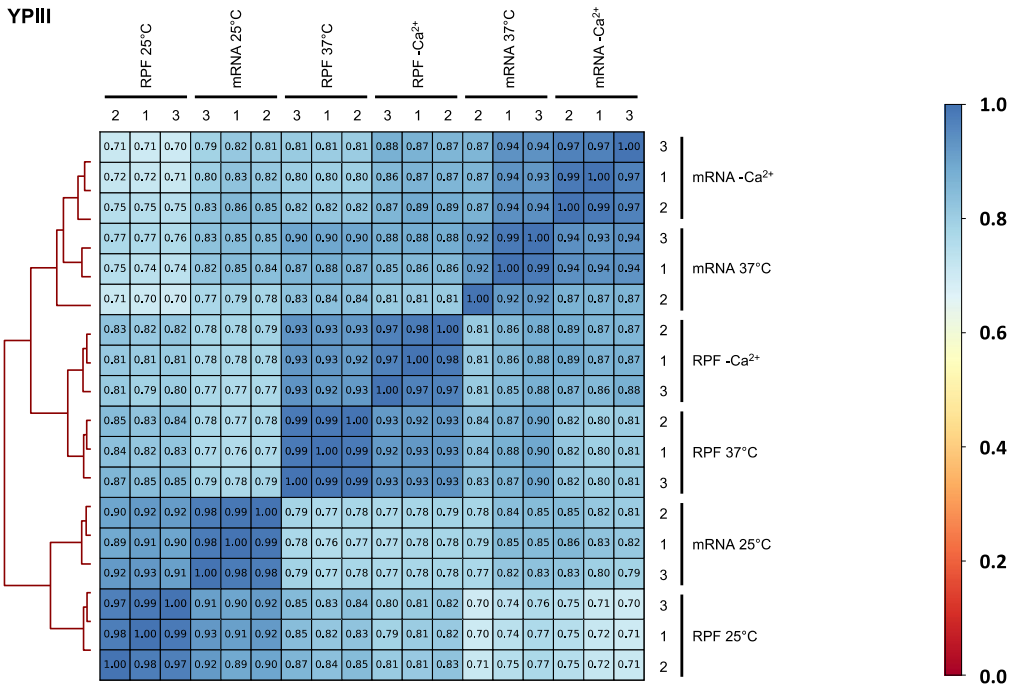

Figure 3.7) Global transcriptome and translatome read distribution of *Y. pseudotuberculosis* wildtype (YPIII) by Ribo-Seq.

Wildtype bacteria of *Y. pseudotuberculosis* YPIII were first incubated at 25°C for 2 hours for every condition later on. Thereafter, one culture per wildtype was further incubated at 25°C for 4 hours (25°C). A second culture was shifted to 37°C for 4 hours for uninduced T3SS conditions (37°C) and a last culture was calcium-depleted and incubated for 4 hours at 37°C for T3SS induced conditions (-Ca^{2+}). For every strain and condition, a biological triplicate was generated. After incubation, the bacteria were harvested by rapid filtration and frozen in liquid nitrogen. Lysis was performed by cryo mixer milling. Every sample was then split into two sub-samples, of which one was used for the transcriptome (mRNA) and the second was used for the translatome (RPF) analysis. For the transcriptome, samples were purified by the hot phenol method followed by the digestion of contaminating DNA and rRNA depletion. The samples for the translatome analysis were digested with MNase and afterwards separated by ultracentrifugation. The fractions containing the 70S ribosome were isolated and purified by the acid-phenol method. With both sample sets, complementary DNA (cDNA) libraries were generated and sequenced by Illumina deep sequencing. Reads obtained by the sequencing were trimmed, cleaned, and finally mapped to the genomic sequence of *Y. pseudotuberculosis* YPIII (NC_010465.1) and the virulence plasmid pIB1 (NZ_CP032567). The data were analyzed using the xtail method of differential gene expression with the correlation of the transcriptome and the translatome by calculating the translation efficiency. Spearman correlation for sample-to-sample distances was calculated for the single replicates for quality control.

The sample-to-sample correlation of the transcriptome (mRNA) and translatome (RPF) in the Δ*csrA* mutant shows a slightly different outcome, compared to the wildtype. The samples at 37°C and -Ca^{2+} cluster together indicating that there is more or less no difference between the samples. This combined clustering of the 37°C and -Ca^{2+} samples in both methods can be explained by the observation that the activation of the T3SS is somehow impaired while the synthesis of LcrF is repressed in this mutant (Kusmierek *et al.* 2019). However, the differences in the methods are more pronounced than the different growth conditions. This high similarity can be explained by the global function of the CsrA protein in transcript regulation. Deletion of CsrA leads to a deregulation of many transcripts at the level of transcript stability and translational initiation, resulting in a loss of adaptation to different conditions (Heroven *et al.* 2012; Romeo and Babitzke 2019) (see Figure 3.8).

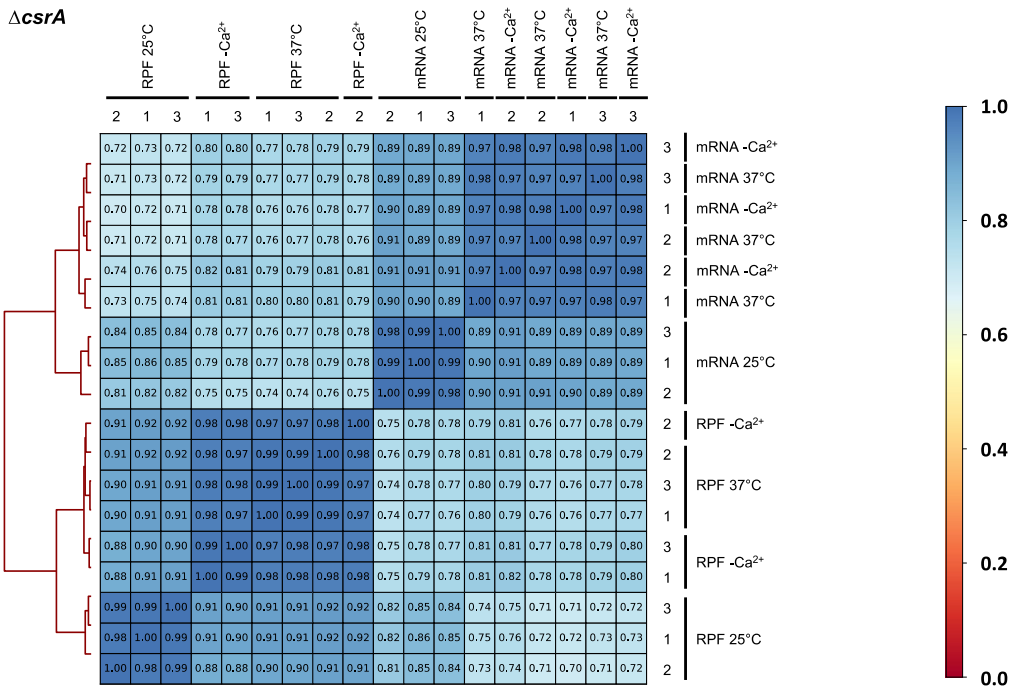

Figure 3.8) Global transcriptome and translatome read distribution of *Y. pseudotuberculosis* Δ*csrA* mutant by Ribo-Seq. Spearman correlation for sample-to-sample distances was calculated for the single replicates obtained by Ribo-Seq. The analyses were performed and the data were analyzed as mentioned in Chapter 2.6.6

In the case of the *yopD* mutant, the clustering is more similar to the wildtype, with one major difference. While the 37°C and -Ca^{2+} samples form slightly distinct clusters both conditions show still a high degree of similarity. This means that the differences under both conditions are not as prominent as in the wildtype. This similarity is due to the deletion of the translocon pore protein YopD. Besides the function as a translocon pore protein, YopD is also a regulator protein of the *ysc-yop* and *yadA* genes (Kusmierek *et al.* 2019; Olsson *et al.* 2004). Deletion of *yopD* leads to T3SS activation already at 37°C, resulting in the secretion of effector proteins into the growth media. Moreover, this activates the *ysc-yop* and *yadA* genes already at 37°C in a similar way as in bacteria grown at -Ca^{2+} condition (Kusmierek *et al.* 2019) (see Figure 3.9).

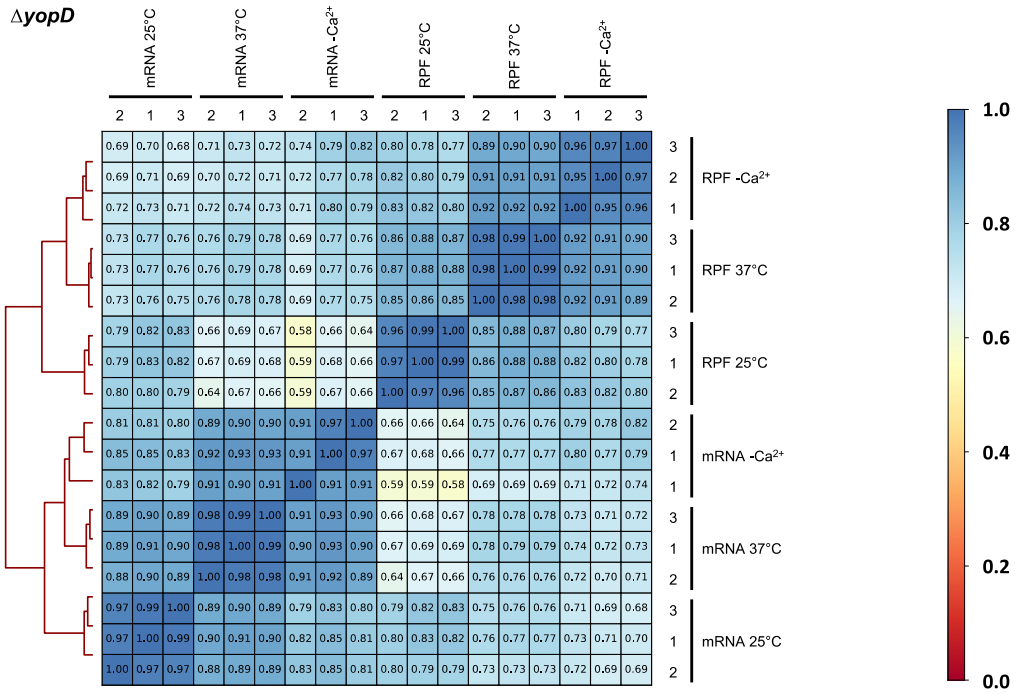

Figure 3.9) Global transcriptome and translatome read distribution of *Y. pseudotuberculosis* Δ*yopD* mutant by Ribo-Seq. Spearman correlation for sample-to-sample distances was calculated for the single replicates obtained by Ribo-Seq. The analyses were performed and the data were analyzed as mentioned in Chapter 2.6.6

In the following approach, the read distribution between the chromosome and the pIB1 virulence plasmid was analyzed. Therefore, the total reads for every library were divided into the reads mapped to the chromosome as well as to the pIB1 plasmid. Subsequently, a relative read distribution was calculated for the chromosome and the virulence plasmid pIB1 based on the total numbers of reads. The relative distribution was calculated because the size of the libraries differed between samples. As for the Spearman correlation, the libraries were compared within a strain but not between strains.

The relative read distribution in the wildtype shows that more or less 100% of the reads map to the chromosome while less than 1% map to the virulence plasmid pIB1 in both, the transcriptome (mRNA) and translatome (RPF) analysis. Upon the shift from 25°C to 37°C around 2,5% of the total reads map to the plasmid. Again, the amount is equal for the transcriptome (mRNA) and translatome (RPF) analysis. Under secretion conditions (-Ca^{2+}), 30% of the total reads map to pIB1 at the transcriptome (mRNA) analysis, and slightly more (32%) map to it in the translatome (RPF) analysis. This indicates that the transcriptome (mRNA) and translatome (RPF) shift significantly from the chromosome to the virulence plasmid pIB1 with increased temperature and in the presence of the secretion signal (see Figure 3.10A). This indicates that the induction of the virulence plasmid pIB1 encoded genes occurs predominantly through the upregulation of transcription (see Figure 3.10A).

Notably, this read distribution differs in the Δ*csrA* and Δ*yopD* mutant strains. While the Δ*csrA* mutant strain still shows a strong increase of virulence plasmid pIB1 encoded transcripts, with an even higher read count of 10% at 37°C, the percentage of reads in the translatome (RPF) stays under 5% for every condition (see Figure 3.10B). This result strongly suggests that the changes of the pIB1 transcripts (mRNA) are not affected compared to the wildtype but the translation of these transcripts is strongly impaired. This observation might explain the low synthesis of T3SS and Yop proteins and the avirulent phenotype of the Δ*csrA* mutant strain (Kusmierek *et al.* 2019; Nuss *et al.* 2017). The Δ*yopD* mutant

strain shows a read distribution which is also different from the wildtype and Δ*csrA* mutant. At 25°C the read counts for the translatome (RPF) on the virulence plasmid pIB1 is under 1% as in the wildtype and the Δ*csrA* mutant strain. In contrast to both stains, the read counts of the transcriptome (mRNA) are already at around 4% in the Δ*yopD* mutant strain. Strikingly, the shift from 25°C to 37°C is sufficient to increase the read counts of the transcriptome (mRNA) of pIB1 to approximately 45% of the total transcriptome. In addition, also the translatome (RPF) of pIB1 increases with temperature shift to 20% of the total translatome (RPF). For the transcriptome (mRNA), this change of read counts is even stronger than for the wildtype under secretion (-Ca^{2+}) conditions. A comparison at 37°C and -Ca^{2+} reviled, that in the Δ*yopD* mutant the read distribution remains unchanged (see Figure 3.10C). This shows that the induction of the virulence plasmid encoded genes in the Δ*yopD* mutant occurs at elevated temperature independent of a secretion signal.

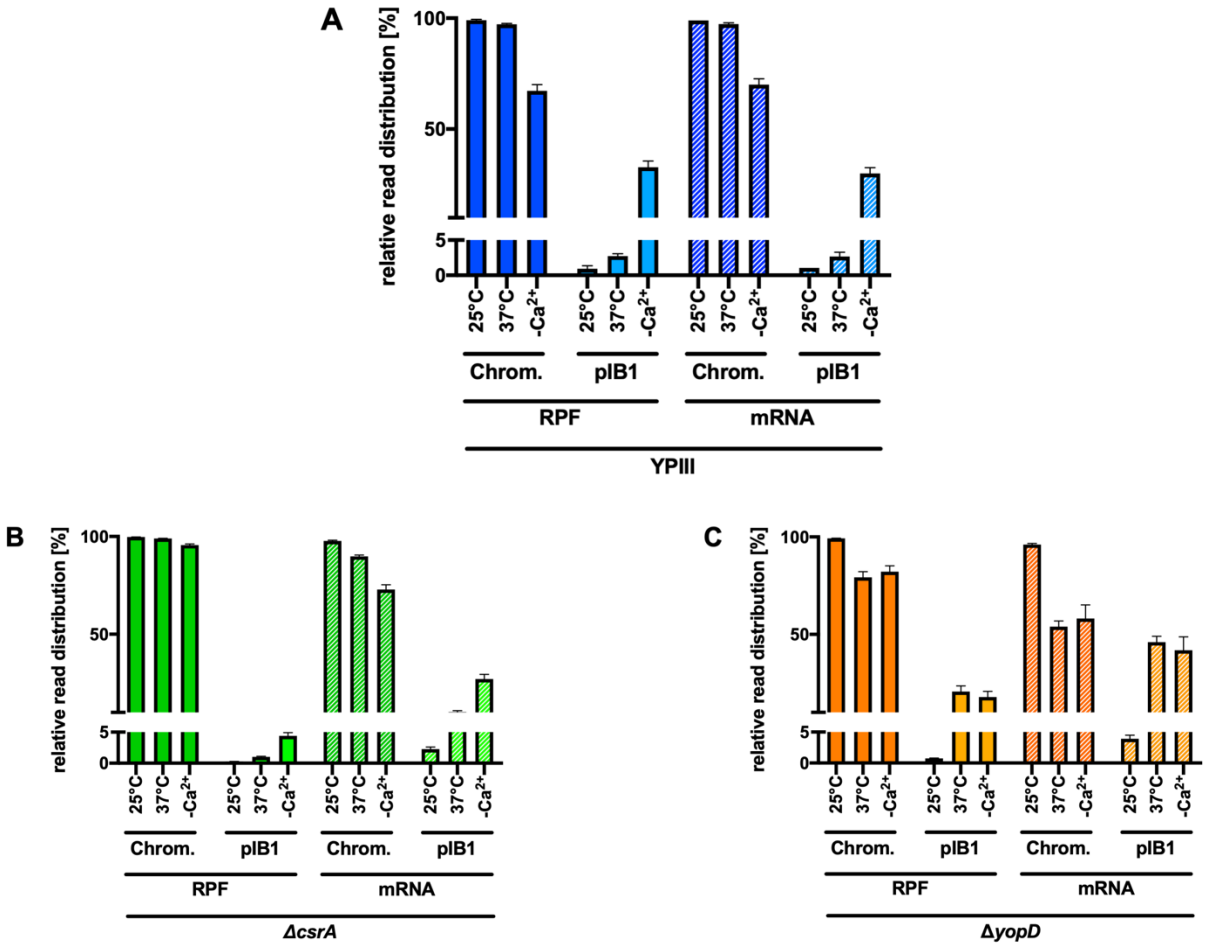

Figure 3.10) Distribution of reads between the chromosome and the virulence plasmid pIB1 of *Y. pseudotuberculosis* according to the transcriptome and translatome analysis.

Read distribution of all libraries obtained by Ribo-Seq for the transcriptome (mRNA) as well as translatome (RPF) of *Y. pseudotuberculosis* and the Δ*csrA* and Δ*yopD* mutants grown at (**A**) 25°C, (**B**) T3SS-uninduced (37°C) and (**C**) T3SS-induced conditions (-Ca^{2+}) are shown in relative distribution between the chromosome and the pIB1 plasmid. The top panel shows the relative read distribution in the wildtype (YPIII). The bottom left graph shows the relative read distribution in the Δ*csrA* mutant strain and the bottom right graph shows the relative read distribution in the Δ*yopD* mutant strain. The relative distribution was calculated to adjust different library sizes to each other. Filled bares represent the translatome (RPF) and the staffed bares represent the transcriptome (mRNA).

In the next step, differential translation and gene expression were analyzed using xtail (Xiao *et al.* 2016). For this purpose, the data of the transcriptome (mRNA) and translatome (RPF) analysis were arranged by their respective $\log_2$ fold-change calculated in the bioinformatical approach. In this approach first, the

reads per kilobase million (RPKM) value was calculated for all libraries (transcriptome and translatome), which represents the total number of reads mapping to one gene normalized by the gene size (in kilobases) and the library size (per million) (Mortazavi *et al.* 2008). In the following step, these normalized RPKM values were used to analyze changes of transcript abundance for the whole genome, including chromosome and virulence plasmid pIB1, between two conditions. Due to the differences in *ysc-yop* and *yadA* gene expression, with almost no expression at 25°C, a weak expression at 37°C and a strong expression at -Ca^{2+}, the data were analyzed between 25°C and 37°C as well as 37°C and -Ca^{2+} for the wildtype and the Δ*csrA* and Δ*yopD* mutants (Böhme *et al.* 2012; Kusmierek *et al.* 2019; Straley *et al.* 1993). This analysis was done for the transcriptome results as well as for the translatome results. The changes in transcript abundance of the transcriptome and translatome were given as a log_2 fold-change. Bast on the log_2 fold-change, a threshold with a log_2 fold-change +/- 2 was set to classify regulated transcripts in the obtained results. Transcripts with a log_2 fold-change of 2 or greater represent upregulated transcripts, while transcripts with a log_2 fold-change of -2 or lower represent downregulated transcripts. Finally, the absolute number of regulated transcripts (see Table 7.2.) in these analyses were calculated relative to the total number of genes. This relative calculation was done separately for the chromosome and the virulence plasmid pIB1.

For the analysis of the chromosome, the results for the wildtype show a more or less equal distribution of up- and down-regulated genes in the comparisons of 25°C to 37°C and 37°C to -Ca^{2+} in the transcriptome (mRNA) and the translatome (RPF). However, the number of regulated genes is higher with the shift to 37°C (10% in mRNA and 12.5% in RPF) compared to the shift to -Ca^{2+} (2.5% in mRNA and 5% in RPF), indicating that the temperature-dependent regulation is more pronounced on the chromosome. The more prominent effect of the temperature can be explained by the already mentioned changes in motility and metabolism with changing temperature that remain unchanged from 37°C to secretion (-Ca^{2+}) conditions (Heroven *et al.* 2012; Kusmierek 2018; Nuss *et al.* 2015; Nuss *et al.* 2017). This observation is similar in the transcriptome (mRNA) and the translatome (RPF) with a slightly higher number of regulated genes in the translatome which indicates a translational regulation of some genes (see Figure 3.11A). A similar result can be observed for the Δ*csrA* mutant, which only differs in the total amount of regulated genes. In the transcriptome (mRNA) the total number of regulated genes is higher for both comparisons (15% with the shift to 37°C and 10% with the shift to -Ca^{2+}) compared to the wildtype, while the total number of regulated genes in the translatome (RPF) is lower (10% with the shift to 37°C and 4% with the shift to -Ca^{2+}). This shows that the temperature-dependent regulation is still present in the Δ*csrA* mutant but with a significant deregulation resulting in a more pronounced translational regulation compared to the wildtype. This deregulation can be explained by the function of CsrA as a regulatory protein affecting transcript stability and translation initiation as mentioned earlier (Heroven *et al.* 2012; Leistra *et al.* 2018). In the case of the Δ*yopD* mutant, the number of regulated genes from 25°C to 37°C is similar to the wildtype and Δ*csrA* mutant reflecting the temperature-dependent gene regulation of the chromosome in the transcriptome (mRNA) as well as in the translatome (RPF) (15% in mRNA and 12.5% in RPF) (see Figure 3.11A). In contrast to the wildtype and the Δ*csrA* mutant, the Δ*yopD* mutant also shows a high number of regulated genes with the shift from 37°C to -Ca^{2+} similar to the number of regulated genes with the shift from 25°C to 37°C again in the transcriptome (mRNA) and the translatome (RPF) (15% in mRNA and 14% in RPF). This similarity

of both comparisons is due to the activation of the T3SS already with temperature increase without a secretion signal in the Δ*yopD* mutant. (Fowler *et al.* 2009). Thereby the shift to 37°C as well as the shift to -Ca^{2+} somehow represents the same regulation in the Δ*yopD* mutant (Kusmierek *et al.* 2019). Furthermore, the similarity between the 25°C to 37°C comparison and the 37°C to -Ca^{2+} comparison represents a combination of the temperature-dependent regulation and the weaker secretion-dependent regulation, which is observable in the wildtype, due to the fact that both changes occur simultaneously in the Δ*yopD* mutant (Kusmierek *et al.* 2019) (see Figure 3.11A).

In contrast to the chromosome, the virulence plasmid pIB1 mainly represents upregulated genes due to the activation of the virulence plasmid with temperature increase and especially with secretion (-Ca^{2+}) (Böhme *et al.* 2012; Bölin *et al.* 1988; Kusmierek *et al.* 2019). These steps of plasmid activation can also be observed in the wildtype with the shift from 25°C to 37°C and later with the shift from 37°C to -Ca^{2+}. With temperature increase, 18% of the plasmid encoded genes are upregulated at the level of transcription, while 5% are upregulated at the level of translation. The differences in the transcriptome and translatome indicate a translational control in this step which might contribute to the regulation of the *ysc-yop* and *yadA* genes as well as of the main activator of the plasmid-encoded genes *lcrF* (Kusmierek *et al.* 2019; Nuss *et al.* 2015). With the shift from 37°C to -Ca^{2+}, the plasmid-encoded genes are strongly upregulated with 50% at the level of transcription and 55% at the level of translation. This represents the strong activation of the virulence genes encoded on the virulence plasmid by the activation of the T3SS under secretion (-Ca^{2+}) conditions (Böhme *et al.* 2012; Kusmierek *et al.* 2019) (see Figure 3.11B). In contrast to the wildtype, the Δ*csrA* mutant shows a deregulation on the virulence plasmid pIB1 for both comparisons in the transcriptome (mRNA) and translatome (RPF) with around 40% upregulated genes. In comparison with the wildtype, this represents on the one hand more upregulated genes with the shift to 37°C but on the other hand, less upregulated genes with the shift to -Ca^{2+}. This deregulation can be explained by the avirulent phenotype of the Δ*csrA* mutant with a reduced expression of the *ysc-yop* and *yadA* genes (Heroven *et al.* 2012; Kusmierek *et al.* 2019; Romeo and Babitzke 2019). In addition, the number of regulated genes in this analysis includes all genes encoded on the virulence plasmid pIB1 and not only the virulence-associated ones. Around one-third of the pIB1 plasmid encodes transposases or hypothetical genes which do not contribute to virulence (Cornelis *et al.* 1998; Portnoy *et al.* 1984). This leads to the point, that the changes in regulated genes mainly affect plasmid encoded non-virulence-associated genes, due to the avirulent phenotype of the Δ*csrA* mutant and the already known reduced levels of virulence-associated genes (Kusmierek *et al.* 2019) (see Figure 3.11B). The Δ*yopD* mutant shows a result different from the wildtype as well as the Δ*csrA* mutant. While around 60% of the pIB1 plasmid are upregulated with the shift to 37°C in the transcriptome (mRNA) and translatome (RPF) only 10% are upregulated with the shift to -Ca^{2+} in the transcriptome (mRNA) or 2.5% in the translatome (RPF), respectively. This upregulation with temperature represents the T3SS activation in the Δ*yopD* mutant already with temperature increase (Fowler *et al.* 2009; Kusmierek *et al.* 2019). The addition of the secretion signal in the -Ca^{2+} condition is not activating the system further, due to the already active state resulting in no further upregulation of genes as seen in the analysis (Fowler *et al.* 2009; Kusmierek *et al.* 2019). This represents a similar upregulation of genes between 37°C and -Ca^{2+} by the T3SS active state in both growth conditions (see Figure 3.11B).

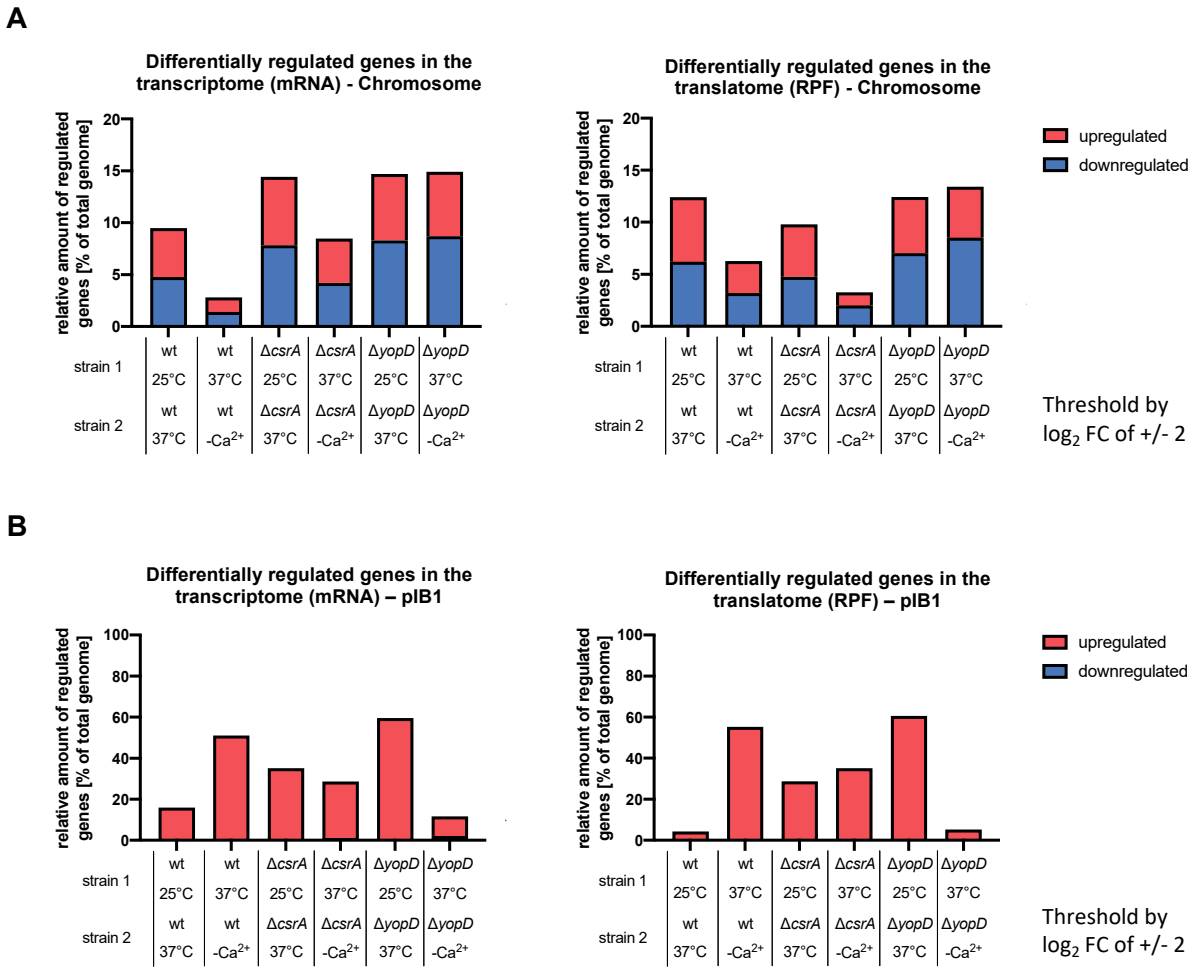

Figure 3.11) Quantitative analysis of genes differentially regulated in wildtype (YPIII), Δ*csrA* mutant, or Δ*yopD* mutant at 25°C, T3SS-uninduced (37°C) and T3SS-induced (-Ca2+) conditions.

The number of differentially regulated genes from the Ribo-Seq were calculated for the different comparisons shown on the x-axes (log2 FC of +/- 2). The amounts of upregulated genes (log_2 FC of ≦2) and downregulated genes (log_2 FC ≧ -2) were calculated relative to the representative genome. Data distinguished between the chromosome and the virulence plasmid pIB1. The data were visualized by a bar-plot with red bars representing upregulated genes and blue bars representing downregulated genes. (**A**) Differentially-regulated genes on the chromosome by the RNA-Seq (mRNA) and Ribosome profiling (RPF). (**B**) Differentially-regulated genes on the plasmid (pIB1) by mRNA and RPF.

The comparative analyses of the data obtained by Ribo-Seq confirm the effects of the temperature and secretin signal which were previously described (Heroven *et al.* 2012; Knittel *et al.* 2018; Kusmierek *et al.* 2019; Volk *et al.* 2019). For instance, the activation of the virulence-plasmid encoded *ysc-yop* and *yadA* genes in the Δ*yopD* mutant strain at 37°C and the reduced expression of these genes in the Δ*csrA* mutant background (Fowler *et al.* 2009; Kusmierek *et al.* 2019).

3.1.3 Translation of virulence-associated genes located on the virulence plasmid and the influence of CsrA and YopD on their translation

After the global transcriptome and translatome analysis, the data obtained for the virulence plasmid (pIB1) are assessed in more detail, to study the influence of translation on virulence-encoded genes. This was analyzed using the log_2-fold changes (FCs) of all plasmid-encoded genes, which passed data quality control. Most plasmid-encoded genes are slightly upregulated (log_2 FC < 2) upon a temperature shift from 25°C to 37°C. Only *yscM/lcrQ* and *lcrF* are upregulated with a log_2 FC greater than 2 (*yscM/lcrQ*: 2.8; *lcrF*: 2.21). Upon secretion (-Ca^{2+}), most genes on the plasmid are strongly upregulated,

including the T3SS structure genes (*ysc* genes) or the genes coding for regulators of the system. The most upregulated genes comprise the *yops*, *yadA,* and the operon coding for the needle tip and the translocators (operon *lcrGVH-yopBD*) with $\log_2$ FC > 5. The region for plasmid-partitioning proteins (*sopAB/parAB*) and *parDE* are not affected in the different strains and under the assessed conditions (see Figure 3.12).

In the *csrA* deletion mutant, many genes show an upregulation with increased temperature in a disorganized manner. This becomes more evident when certain genes of the T3SS structure proteins are compared such as *yscS* or *yscI* and *yscJ.* They are more strongly upregulated than other genes of the same operon. Upon Ca^{2+}-depletion (-Ca^{2+}), upregulation of the T3SS component genes is weaker than in the wildtype. The activator of the plasmid-encoded virulence genes *lcrF* also shows a deregulation. While it is somehow similarly upregulated by temperature as in the wildtype the induction remains similar under the secretion conditions where it's normally upregulated (Böhme *et al.* 2012; Steinmann and Dersch 2013). However, expression of *yops*, *yadA,* and the needle tip, and the translocator locus, is still somewhat increased, compared to the other genes (see Figure 3.12).

Strikingly, the *yopD* deletion has a strong influence on the activation of the translation upon the temperature upshift to 37°C and mimics the pattern observed for the wildtype under secretion (-Ca^{2+}) conditions (see Figure 3.12). In particular, the *yops*, *yadA,* and the operon encoding the needle tip, and the translocator loci are more strongly upregulated than the T3SS structure genes and the regulators. Upon secretion (-Ca^{2+}), most genes remain unchanged, while some are slightly downregulated. This suggests that the system is still active on a high level (see Figure 3.12). On the other hand, the slight downregulation somewhat compensates for the strong induction of the energy-consuming T3SS structure and effector secretion. The strong translation of the *yop*, *yadA,* and the *yopBD* mRNA might be connected to the stoichiometry of T3SS to Yops and YadA.

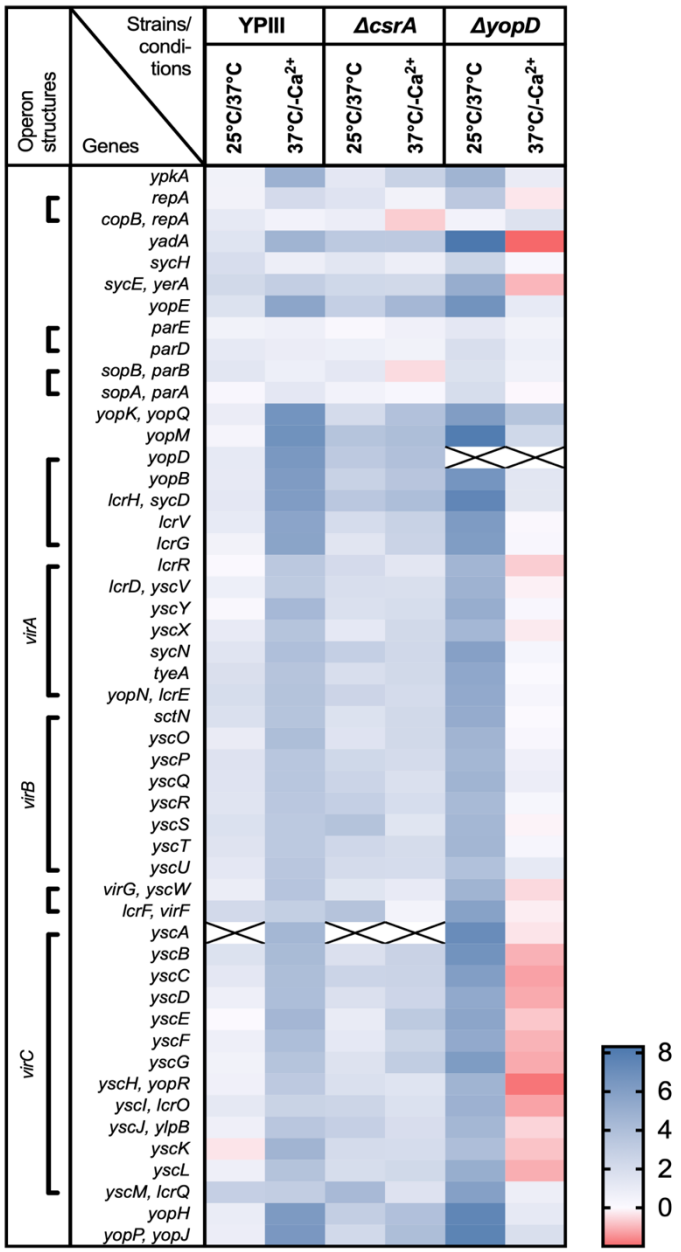

Figure 3.12) Differentially-regulated genes on the virulence plasmid pIB1 from *Y. pseudotuberculosis* by the translatome.
Log_2 fold-changes of all differentially-regulated genes (translatome data) of the pIB1 virulence plasmid of *Y. pseudotuberculosis* (YPIII) by Ribo-Seq. Comparisons were done for bacteria grown at 25°C, 37°C and under secretion (-Ca^{2+}) conditions for the wildtype and the Δ*csrA* and Δ*yopD* mutant strains. Results which did not passe the quality control, the fields are crossed.

To further address whether the genes that are upregulated in the Δ*yopD* mutant at 37°C are the same as the genes that are induced in the wildtype under secretion (-Ca^{2+}) conditions, both datasets were compared. The resulting Venn-diagram shows that 47 of the 61 genes group overlap in all datasets. Four genes are only upregulated in the translatome, while 7 are only upregulated in the Δ*yopD* mutant samples and one is only upregulated in the wildtype (see Figure 3.13). By taking a closer look at the 47 overlapping genes, it is shown that all of them belong to T3SS structure genes as well as *yops* and *yadA*. These results show that the expression of the crucial virulence factors is already strongly induced in the Δ*yopD* mutant at 37°C which are only strongly expressed under secretion (-Ca^{2+}) conditions in the wildtype.

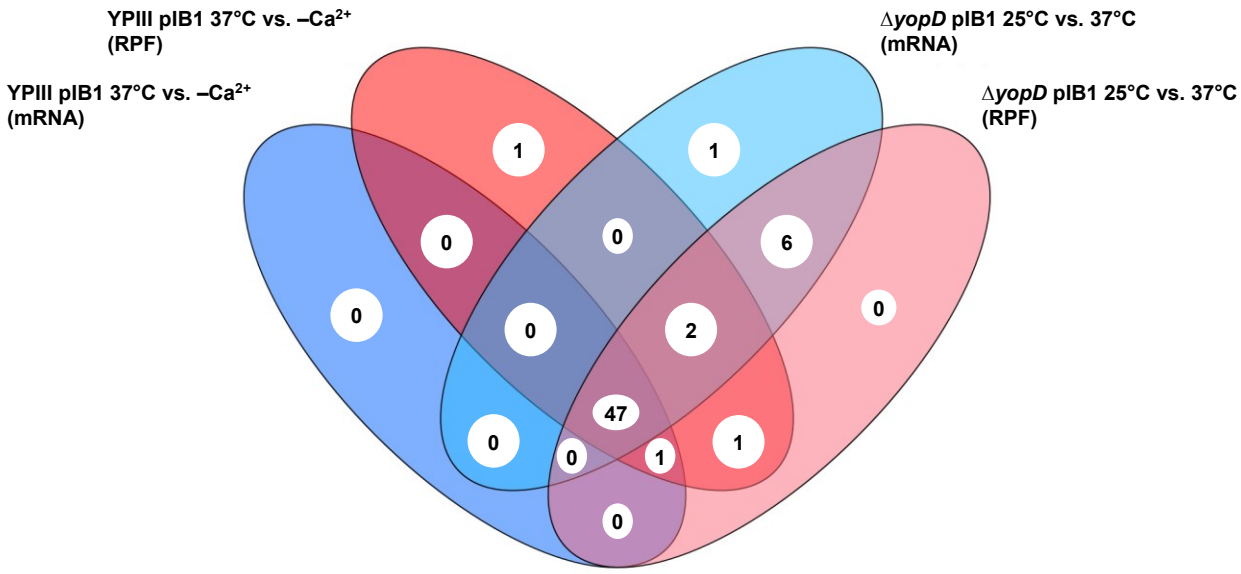

Figure 3.13) Comparison of differentially expressed genes of pIB1 under secretion conditions (-Ca^{2+}) in the wildtype with the non-secretion conditions (37°C) in the Δ*yopD* mutant strain.

Venn-diagram of differentially expressed genes of the transcriptome (mRNA) and translatome (RPF) in the wildtype (YPIII) strain at -Ca^{2+} compared to the Δ*yopD* mutant strain at 37°C.

3.1.4 The expression of Yops and YadA is translationally regulated by YopD

To determine whether genes are regulated at the translational level, the translation efficiency (TE) was calculated based on the Ribo-Seq data using xtail (Xiao *et al.* 2016). To calculate the TE, the $\log_2$ FCs of the transcriptome (mRNA) and translatome (RPF) were calculated based on the RPKM values (see section 3.1.2). The calculated $\log_2$ FCs represent the changes in read coverage of a gene on the transcriptional and translational levels. In the following step, their ratio was calculated also with a $\log_2$ FC. A $\log_2$ FC of ≧ 1 represents genes that are more affected on the translational level, while genes with a $\log_2$ FC of ≦ -1 are more transcriptionally affected. Genes with a $\log_2$ FC between 1 and -1 are not preferentially affected on the transcriptional or translational level (Brar and Weissman 2015).

In the case of the virulence plasmid-encoded genes, most genes show no significant difference in their translation efficiency under secretion conditions, indicating that these genes are not translationally regulated (see Figure 7.5 and Table 7.3). The only exceptions were the *yops* and *yadA* genes in the wildtype and the Δ*yopD* mutant strain. In the case of the wildtype a shift from 25°C to 37°C results in translational repression of the *yops*, indicated by negative $\log_2$ FCs (Francis *et al.* 2001). Upon secretion, this repression is revealed. In contrast, the Δ*yopD* mutant strain shows a translational upregulation of the *yops* and *yadA*, when shifted from 25°C to 37°C. Similar to the wildtype, this influence is not observed under secretion (-Ca^{2+}) conditions (see Figure 3.14). The genes that are mostly affected on the translational level in the wildtype and the Δ*yopD* mutant are identical. They encoding *yops*, *yadA,* and the operon coding for *yopBD* (operon *lcrGVH-yopBD*) on the virulence plasmid (see Figure 3.12 and Figure 3.14).

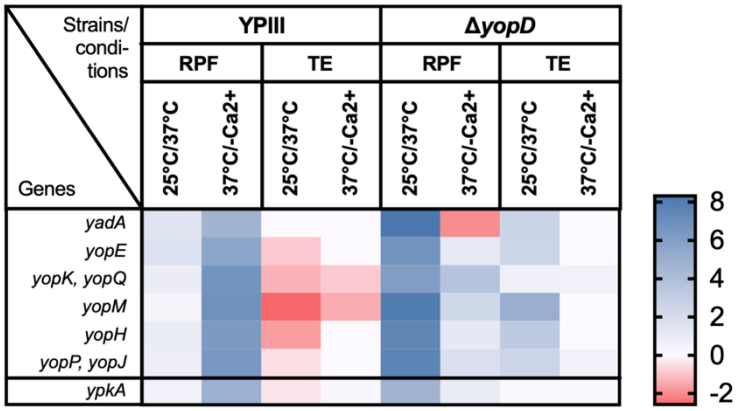

Figure 3.14) Translational activation of Yops- and YadA-expression in the Δ*yopD* mutant background.
Heatmap of the translatome data (RPF) illustrating the calculated translational efficiency (TE) for *yadA* and the known *yop* effector proteins. Translatome data and translational efficiency data are compared between 25°C and 37°C as well as 37°C and -Ca^{2+} for the wildtype and the Δ*yopD* mutant grown at 25°C, 37°C, and secretion (-Ca^{2+})

These results show translational regulation of the *yops* and *yadA* but not the T3SS structure components or regulators. This effect seems to be YopD- but not CsrA-dependent, due to the observation that the regulation is only visible in wildtype and Δ*yopD* mutant. Furthermore, it shows the opposite effect in both strains. While the TE of these genes are repressed in the wildtype where YopD is present, the TE is upregulated for the same genes in the mutant strain.

3.1.5 Validation of the translational control of virulence plasmid-encoded virulence genes in wildtype and Δ*yopD* mutant strain

To confirm the observed translational regulation of plasmid pIB1-encoded genes, the data were validated for the *Y. pseudotuberculosis* wildtype and the isogenic Δ*yopD* mutant strain. Here, the bacteria were cultivated under the conditions used for the Ribo-Seq. From these bacteria cultures, total RNA and whole-cell protein extracts were prepared. The amount of transcript was afterward analyzed by northern blot, while the protein abundance was analyzed using western blot. For the validation, *yadA* and *yopE* mRNA and proteins were detected to verify the translational effect observed by the Ribo-Seq analysis.

The mRNAs of *yadA* and *yopE* are undetectable at 25°C and only very weakly detectable at 37°C in the wildtype. Under secretion conditions, the *yopE* mRNA signal is strongly increased, while the *yadA* mRNA is also increased but not that prominent. The protein signal of YadA and YopE represent the same changes between 25°C, 37°C and secretion (-Ca^{2+}) as the mRNA signals (see Figure 3.15A). In the *yopD* deletion strain, the mRNAs for *yadA* and *yopE* are strongly upregulated at 37°C. The mRNA signal for *yopE* remains similar under secretion conditions, while the mRNA signal for *yadA* is reduced but still detectable. For the YadA protein level in the Δ*yopD* mutant, the pattern is similar to the mRNA pattern. In contrast, the YopE protein is very weakly detectable at 37°C but shows a strong increase under secretion conditions (see Figure 3.15A). Afterwards, the northern- and western-blots are quantified and the log_2 FC is calculated for the mRNA and protein levels comparing data of the conditions 25°C and 37°C as well as 37°C and -Ca^{2+} (see Figure 3.15BC). The calculated log_2 FC for the mRNA and protein levels are used subsequently for the calculation of the protein/mRNA ratio also as a log_2 FC, representing the TE (see Figure 3.15D).

The results confirm previous data about the translational regulation of *yadA* in the Δ*yopD* mutant strain from 25°C to 37°C (see Figure 3.15DE). In contrast, no translational regulation can be observed for *yopE* with the shift from 25°C to 37°C due to the absence of signals in the northern- and wester-blot, while the Ribo-Seq show an increase in read coverage upon shift to 37°C (see Figure 3.15F). This indicates that *yopE* is additionally regulated at the post-translational level. Under secretion conditions, there is a slight translational upregulation in both strains for *yadA* and *yopE*, which is not observable in the Ribo-Seq data (see Figure 3.15DEF). This difference might be due to the settings of both experiments. In the Ribo-Seq the mRNA is correlated to the ribosome occupied mRNA, while in this experiment mRNA is correlated to the protein.

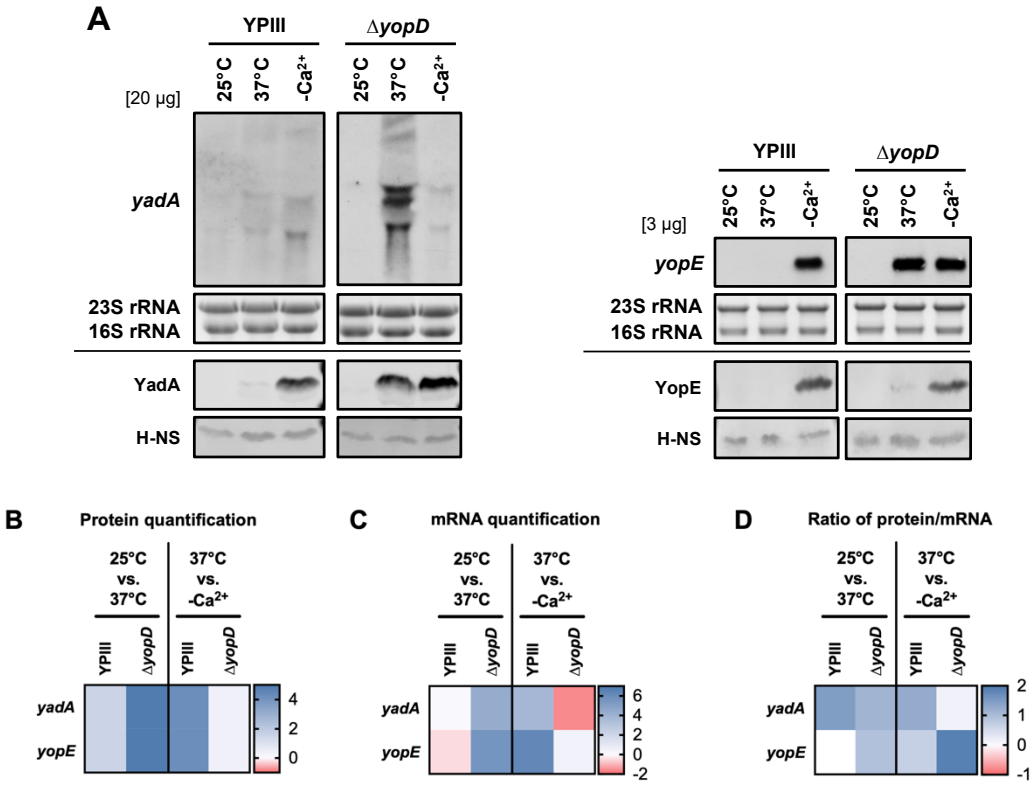

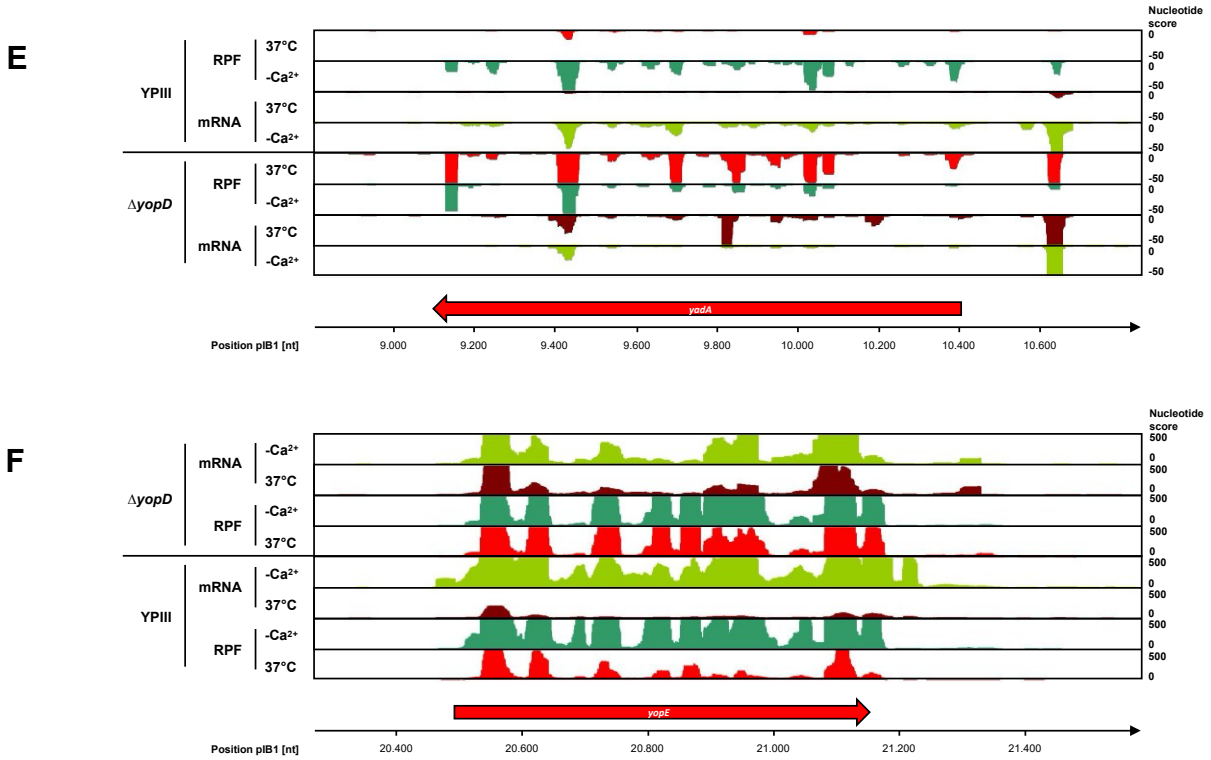

Figure 3.15) Validation of the translational regulation of *yadA* and *yopE* mRNA and proteins.

(**A**)The mRNA and protein levels of *yadA* and *yopE* were analyzed by Northern blot and Western blot, of the wildtype (YPIII) or Δ*yopD* mutant grown at 25°C, 37°C, and -Ca^{2+} conditions. For Western blots, whole-cell extracts were generated. In the Western blot H-NS (Histone-like nucleoid structuring protein) was used as loading control. YopE and YadA were detected using the all Yops antibody or YadA antibody, respectively. For Northern blots, total RNA of every sample was generated and 16S rRNA and 23S rRNA were used. The figure shows a representative set out of biological triplicates. (**B**) Heatmap of changes of the Yop protein level in the wildtype or Δ*yopD* mutant strain between different conditions displayed as log_2 fold-change. (**C**) Heatmap of the mRNA level in the mentioned strains compared in the different conditions, displayed as log_2 fold-change. (**D**) Heatmap of the calculated protein/mRNA ratio for the protein and mRNA of yopE and yadA displayed respectively as log_2 fold-change. The read coverage for *yadA* (**E**) and *yopE* (**F**) obtained by Ribo-Seq under 25°C, 37°C and -Ca^{2+} conditions in the wildtype and Δ*yopD* mutant is shown for the transcriptome (mRNA) and translatome (RPF). The graphs for read coverage represents the combination of the three biological replicates. Coding sequences of the respective genes are indicated by an arrow. Underneath every graph, the location on the virulence plasmid pIB1 is indicated by the nucleotide position.

The results confirm that expression of *yadA* and *yopE* is translationally regulated. An upregulation is observed upon a temperature shift from 25°C to 37°C in the Δ*yopD* mutant background but not in the wildtype. This confirms the results obtained by the Ribo-seq analysis. Furthermore, the data indicate a slight upregulation in TE of *yopE* and *yadA* in wildtype and Δ*yopD* mutant under secretion conditions. Therefore, the translational benefit of the *yops* and *yadA* will be characterized in more detail in the next chapter.

3.2 Strong translation of *yop* and *yadA* mRNAs is due to a unique 5' UTR structure

To find the underlying mechanism of translational control, the mRNA sequences of the *yops* and *yadA* genes were analyzed, due to their effect on translation initiation. To do so, different features of the mRNAs were predicted and analyzed for special abilities. Based on the Ribo-Seq mRNA data, the transcriptional start sites (TSS) of the different *yops* and *yadA* mRNAs were predicted. Afterwards, the 5' untranslated region (UTR) was further analyzed as well as the ribosomal binding site (RBS). After prediction and analysis, the findings were tested experimentally to identify if these features contribute to the strong translation of these genes.

3.2.1 Unique short 5’ UTRs are present in *yops*

The obtained Ribo-Seq transcriptome (mRNA) data were used for a prediction of the start of the 5’ UTR which is next to the TSS. To predict the 5’ UTR ends, every read that mapped to the genome (chromosome and pIB1) of *Y. pseudotuberculosis* was further processed bioinformatically. Every read obtained by a sequencing contains a 5’ end and 3’ end, due to the nomenclature of nucleic acids. For the standard analysis, the whole read is mapped to the genome and is further analyzed for differential gene expression (Gelhausen *et al.* 2020). For the prediction of 5’ ends, the mapped reads obtained by the transcriptome (mRNA) of the Ribo-Seq were further processed. The reads were trimmed bioinformatically to only retain the first nucleotide at the 5’ end of a read. The processed 5’ end reads were afterwards scored for every position in the genome similar to the normal scoring of nucleotides per position (nucleotide score), done in the mapping of the sequencing reads. Finally, the results were provided as coverage tracks for a genome browser (Gelhausen *et al.* 2020). To prediction the 5’ UTRs of the *yops* and *yadA* transcripts, the obtained data were visualized in a genome viewer and the positions of possible 5’ ends were compared toward the read coverage of the transcriptome. Coverage in the 5’ end enriched data was assumed as a possible 5’ UTR end when it was upstream of the CDS with a continuous read coverage between this position and the CDS in the normal coverage data of the transcriptome (mRNA) (see Figure 3.16AB for *yopE*). In addition, it was analyzed whether a RBS is located within the potential 5’ UTR in a position closely upstream of the start codon. This comparison was done for the wildtype as well as the Δ*yopD* mutant strain under 37°C and secretion (-Ca^{2+}) conditions. These conditions were chosen because only then the *yops* and *yadA* genes were expressed in the bacteria.

By comparing the data, the *yop* transcripts mostly show strong predictions of relatively short 5’ UTRs (< 50 nucleotides). In contrast, *yadA* was predicted to have a very long 5’ UTR of about 250 nucleotides. The best predictions were obtained in the wildtype under secretion conditions based on the high transcript levels. At 37°C the data allow more or less no 5’ UTR predictions for the wildtype, due to the very low expression of these genes under this condition. The 5’ UTR ends obtained for the Δ*yopD* mutant strain are very similar under both conditions and are comparable with the wildtype under secretion (-Ca^{2+}) conditions. This indicates that YopD does not affect the start of transcription of the *yop* and *yadA* transcripts. Most *yop* genes only show one 5’ UTR e. g. *yopE*, *yopM*, *yopH,* and *yadA*. In the case of *yopJ/yopP* and *yopK/yopQ,* alternative 5’ UTR ends are predicted, with the most probable ones located close to the CDS. The TSS sites predicted further upstream are less likely and thereby, they might not or very little contribute to the transcription as the others closer to the CDS. The second possible TSS of *yopK/yopQ* might promote transcription of a small open reading frame (sORF) identified upstream of *yopK/yopQ* by the Ribo-Seq analysis. The *yopK/yopQ* and sORF transcripts may be transcribed from the same promoter, while *yopK/yopQ* also harbors a second promotor downstream of the sORF (see Figure 3.16B).

A

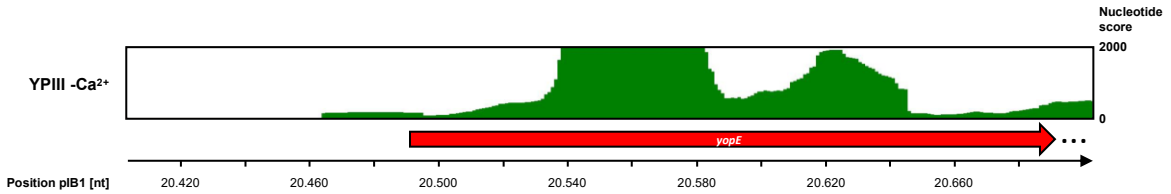
Nucleotide score
2000
0
YPIII -Ca²⁺
yopE
Position pIB1 [nt]
20.420
20.460
20.500
20.540
20.580
20.620
20.660

B

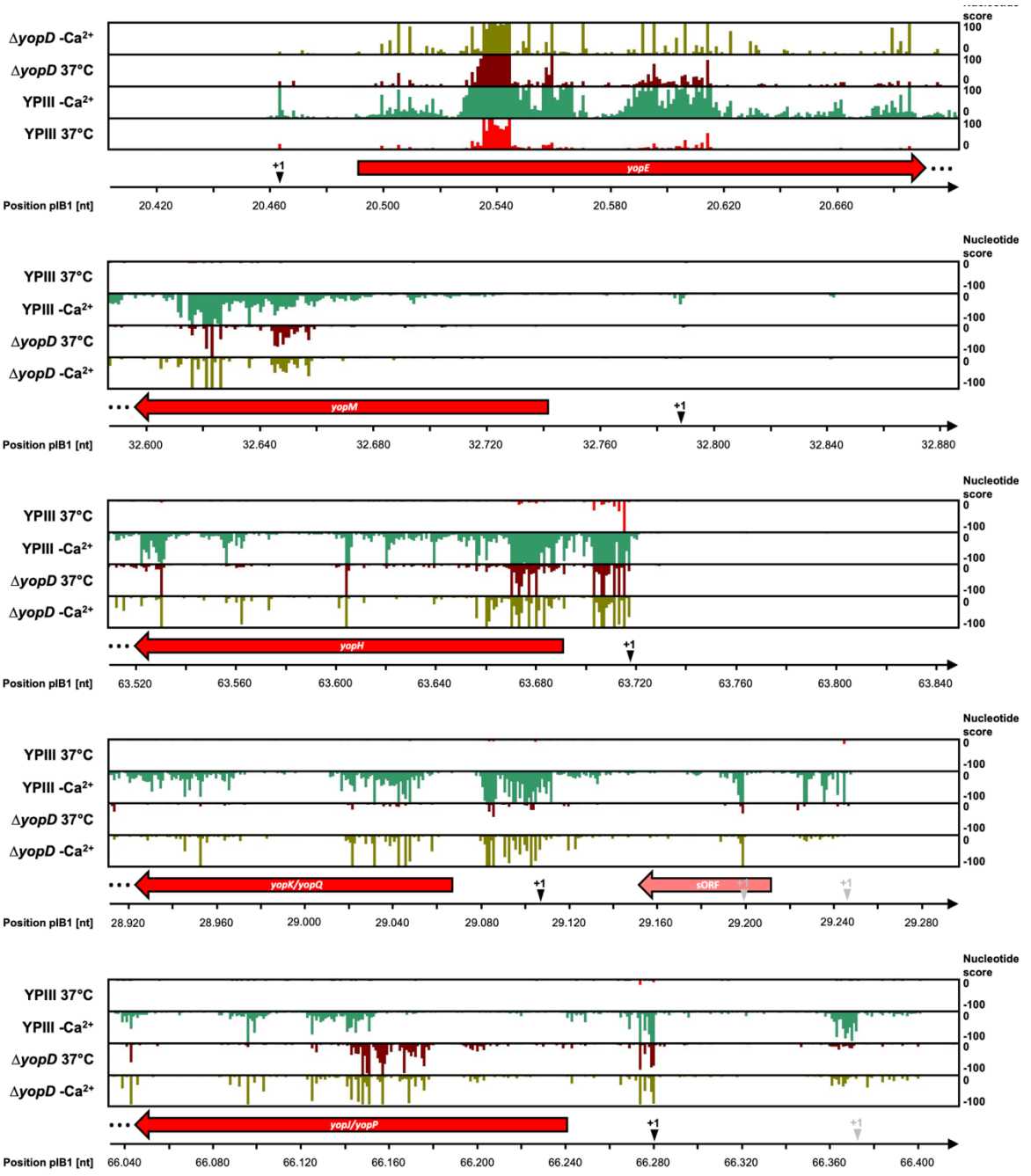
ΔyopD -Ca²⁺
ΔyopD 37°C
YPIII -Ca²⁺
YPIII 37°C
Nucleotide score
100
0
+1
yopE
Position pIB1 [nt]
20.420
20.460
20.500
20.540
20.580
20.620
20.660
YPIII 37°C
YPIII -Ca²⁺
ΔyopD 37°C
ΔyopD -Ca²⁺
-100
yopM
32.600
32.640
32.680
32.720
32.760
32.800
32.840
32.880
yopH
63.520
63.560
63.600
63.640
63.680
63.720
63.760
63.800
63.840
yopK/yopQ
sORF
28.920
28.960
29.000
29.040
29.080
29.120
29.160
29.200
29.240
29.280
yopI/yopP
66.040
66.080
66.120
66.160
66.200
66.240
66.280
66.320
66.360
66.400

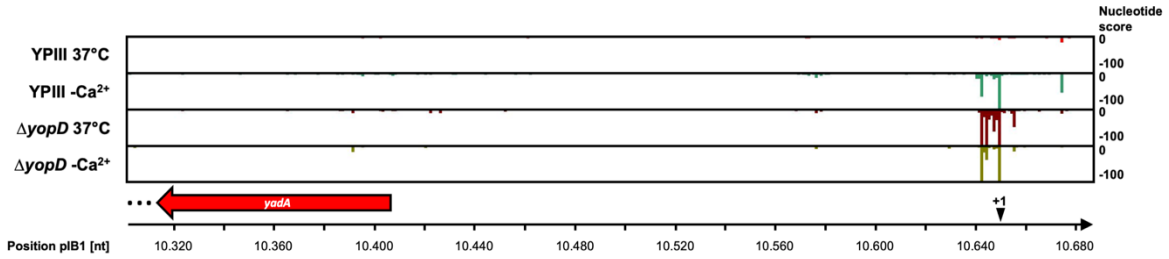

Figure 3.16) Prediction of the 5' end of the *yop* and *yadA* transcripts by the transcriptome data of the Ribo-Seq.

The transcriptional start sites (TSSs) were predicted based on the bioinformatical enrichment of 5' end reads or the transcriptome results of the Ribo-Seq. The possible 5' ends (**B**) were compared to the unchanged transcriptome reads (**A**) and the 5' end reads with a continuous coverage towards the CDS in the transcriptome were taken as possible TSSs. Afterwards, it was analyzed whether a RBS is located within the potential 5' UTR in a position closely upstream of the start codon. Graphic read coverage represents the combination of the three biological replicates for the *Y. pseudotuberculosis* wildtype and Δ*yopD* mutant at 37°C and under secretion (-Ca^{2+}) conditions. The predicted TSS positions are indicated by a triangle with the +1 marker. Coding sequences of the respective genes are indicated by an arrow. The three points at the end of every CDS indicate that the CDS continues outside of the observation area. Below every graph, the location on the virulence plasmid is indicated by the nucleotide position.

The sequences of the predicted 5' UTRs were aligned to each other according to their start codons followed by the first six codons of every CDS (see Figure 3.17A). The aligned sequences were analyzed for AU content and the length of AU rich regions. Furthermore, the potential RBS was predicted.

The alignment shows that the predicted 5' UTRs of the *yop* genes are very AU rich, ranging from 60% up to 77% in AU content (see Figure 3.17B), while the whole genome only represents an AT content of 52.5% for the chromosome and 55.2% for the pIB1 plasmid (NCBI database). In addition, this AU rich content often forms long AU-rich regions flanked by short GC interruptions. Notably, the RBS is often surrounded by long AU rich regions. The RBS itself indicates many interactions with the anti-Shine-Dalgarno sequence of the 16S rRNA with around 6 to 8 nucleotides possible to bind to the 16S rRNA (see Figure 3.17A).

A

```
Position upstream from AUG                50        40        30        20        10        1
                                          |         |         |         |         |         |
DN756_RS21690_yopE (28 nt)                                    GUUUUAAUAGCCAAGGUAAUAAAUAGUC AUG AAA AUA UCA UCA UUU
                                                                                           Met Lys Ile Sec Sec Phe

DN756_RS21785_yopM (45 nt)          AGUGAAAAACUCGAUAAUAAAAAUAUUUUCAGAAAGGCAUUCAAU AUG UUC AUA AAU CCA AGA
                                                                                           Met Phe Ile Asn Pro Arg

DN756_RS21990_yopH (25 nt)                                    CGUGUAUUUAAUUAAGGAGGGAAGC AUG AAC UUA UCA UUA AGC
                                                                                           Met Asn Leu Sec Leu Ser

DN756_RS21750_yopK/Q (44 nt)                UAUUAAAAUAGUGUAGUUUAUAAAGUAAAUUUGGGAGUAGUAACU AUG UUU AUU AAA GAU ACU
                                                                                           Met Phe Ile Lys Asp Thr

DN756_RS22005_yopJ/P (38 nt)                          UUCAUACCGCUGUUAAUUCCCUGAAUAAGGAUAAAUAA AUG AUC GGA CCA AUA UCA
                                                                                           Met Ile Gly Pro Ile Sec

DN756_RS21625_yadA (242 nt)         ...AACUGAGCUUUUAUUCACGGGAAAUUAAAGAAAUAUAAAAGGUGCUUACA AUG ACU AAA GAU UUU AAG
displayed only first 50 nt                                                                 Met Thr Lys Asp Phe Lys
```

ATG → Start Codon
AAGG → Predicted RBS interactions to 16S rRNA
GGA → GGA motive for putative CsrA binding
TTTTAATTA → AU stretches (only highlighted when at least 4 in a row)

B

Gene	AU content (5‘ UTR)
yopE	71%
yopM	76%
yopH	60%
yopK/yopQ	77%
yopJ/yopP	68%
yadA	67%
Average	69.8%
Chromosomal AT content	52,5%

Figure 3.17) Alignment of the 5’ untranslated region (UTR) of the *yop* and *yadA* genes identified under secretion conditions.

Transcription start sites (TSS) were predicted based on the transcriptome of the Ribo-Seq analysis. (**A**) Sequences were aligned based on the start codon of every transcript. Special features are highlighted in the different sequences. (**B**) AU-content, calculated for the predicted 5’ UTRs.

The predictions and further analyses show that the *yop* genes contain a rather short 5’ UTR with a high AU content. Furthermore, all genes harbor a strong RBS with often a higher conservation to the RBS consensus sequence AGGAGG (Starmer *et al.* 2006). The observations hint at the fact that the RBS can strongly attract the small subunit of the ribosome for the initiation, while the high AU content allows for easier binding, due to the no or weak formation of secondary structures within the 5’ UTRs.

3.2.2 High protein levels are the result of strong translation and not transcription

To identify if the unique structure of the 5’ UTRs affects the translation of the *yop* transcripts, expression plasmids were constructed which contain the short 5’ UTR, the whole CDS, a two amino acid linker, and a single FLAG-tag under the control of an arabinose-inducible promoter (see Figure 3.18A). This construct was used to exclude a transcriptional effect and to only assess the translational effect. The plasmids were introduced into the respective single or double mutant backgrounds to avoid interference of the plasmid-encoded gene with the native gene. The expression of all combinations was tested and the results show that all *yop* transcripts except that of *yopE* are strongly expressed in this setting. For *yopE,* a product could only be observed under secretion (-Ca^{2+}) but not under non-secretion (37°C) conditions (see Figure 7.7). To address whether efficient translation of the *yop* genes is based on the unique structure of the 5’ UTR, the *yopJ/yopP* construct was chosen as a representative example. It shows good detectability of the protein as well as of the mRNA.

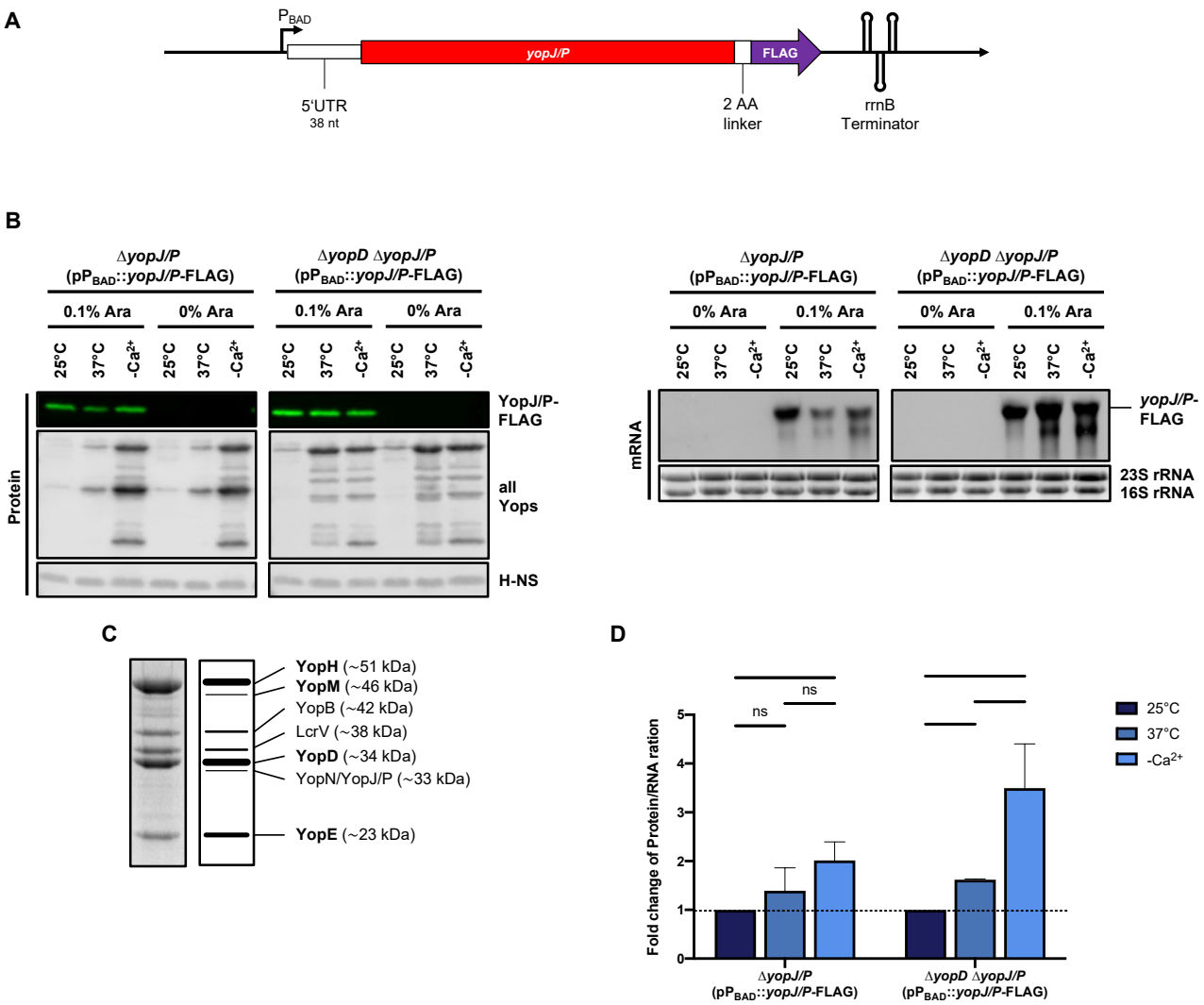

Figure 3.18) Increased translation of the 5' UTR under secretion conditions.

(**A**) Graphic overview of the construct pP_{BAD}::*yopJ/P*-Flag (pMV35), encoding a single C-terminal FLAG-tag, used for the experiment. (**B**) Representative Western blot and Northern blot detecting the protein and mRNA levels of *Y. pseudotuberculosis* Δ*yopJ/P* and the Δ*yopD*, Δ*yopJ/P* double mutant at 25°C, 37°C and secretion (-Ca^{2+}) conditions. For the preparation of Western blot samples, the direct culture method was used (see chapter 2.7.2). In the Western blot analysis, H-NS was used as loading controls, while the 16S rRNA and 23S rRNA were used as loading controls for the Northern blot. The FLAG-tagged YopJ/P was visualized using a FLAG-antibody and the Yops were visualized using an all Yops antibody. The experiment was done in biological triplicates. (**C**) Western blot analysis as example for the migration of Yops with the designation of the signals to certain Yops and their size in kDa. (**D**) Bar diagram of the calculated protein/mRNA ratio fold-change. Data were analyzed using a Student's t-test. Significance is shown above the analyzed bars (ns = >0.05; * = ≦0.05; ** = ≦0.01; *** = ≦0.001; **** = ≦0.0001).

When expression of the *yopJ/yopP*-FLAG gene is induced with 0,1% arabinose under the different conditions, both the protein and the mRNA are detectable in all samples. The controls show that the signals are specific. For protein detection, a certain culture volume was directly used (direct culture method see chapter 2.7.2) for the western blotting to include the intracellular Yops as well as the secreted ones. To further confirm, that the three conditions (25°C, 37°C and -Ca^{2+}) result in the expected *ysc-yop* gene expression and synthesis pattern, the Yops were detected in parallel. The Δ*yopD*/Δ*yopJ/P* double mutant shows a significantly higher YopJ/P-FLAG protein and transcript level compared to the $YopD^+$ counterpart (Δ*yopJ/P*). The $YopD^+$ counterpart shows a reduced YopJ/P-FLAG protein and transcript level at 37°C compared to the Δ*yopD*/Δ*yopJ/P* double mutant (see Figure 3.18B). Based on the protein and transcript quantities of the *yopJ/yopP*-FLAG gene, the protein/mRNA ratio was calculated to see if there is a translational effect. In the $YopD^+$ strain, there is only a very weak and non-

significant increase of *yopJ/P-FLAG* translation when shifted from 25°C to 37°C similar to the Ribo-Seq analysis. Under secretion (-Ca^{2+}) conditions, *yopJ/P-FLAG* translation is significantly increased in agreement with the validation (see Figure 3.18D). In the *yopD* deficient mutant, there is a weak but significant positive effect on *yopJ/yopP*-FLAG translation at 37°C and an even stronger one under secretion (-Ca^{2+}) conditions (see Figure 3.18D). Both results are in agreement with the Ribo-Seq analysis and show that the strong translation is based on the presence of the short 5' UTRs, at least for *yopJ/P*. Due to the similarity of the *yop* 5' UTRs, it can be assumed, that this result is also valid for the other *yop* genes except *yopE,* which shows a post-translational regulation (see chapter 3.1.5). Furthermore, the data also show that the protein level is somehow connected to the level of mRNA because the changes on the mRNA level are also visible on the protein level.

3.2.3 Yop expression is also controlled by LcrQ/YscM

After determining, that the translation is increased based on the short 5' UTR, especially in the absence of YopD, it needs to be tested, if the second important regulator LcrQ/YscM does not influence the results. LcrQ/YscM was expected to affect the transcripts levels of the *yops* in a YopD/LcrH-dependent manner post-transcriptionally or post-translationally by proteolytic degradation facilitated by the chaperons (Cambronne and Schneewind 2002; Francis *et al.* 2001).

To test the effect of LcrQ/YscM on the proteins in our strain background, the wildtype strain of *Y. pseudotuberculosis* YPIII and the Δ*lcrQ* mutant strain were grown at 37°C and secretion (-Ca^{2+}) conditions. Cell extracts, as well as direct culture samples including also the supernatant with secreted Yops, were generated and used for western blot analysis. This confirms that the expression of all Yops is strongly upregulated at 37°C in the Δ*lcrQ* mutant compared to the wildtype, and no difference can be observed between non-secretion (37°C) and secretion (-Ca^{2+}) conditions (see Figure 3.19A). Interestingly, this is not the case in the direct culture samples. Although most Yops are also strongly expressed at 37°C, YopE is less abundant at 37°C compared to secretion (-Ca^{2+}). This observation indicates that YopE is less secreted or more rapidly degraded in the supernatant (see Figure 3.19B).

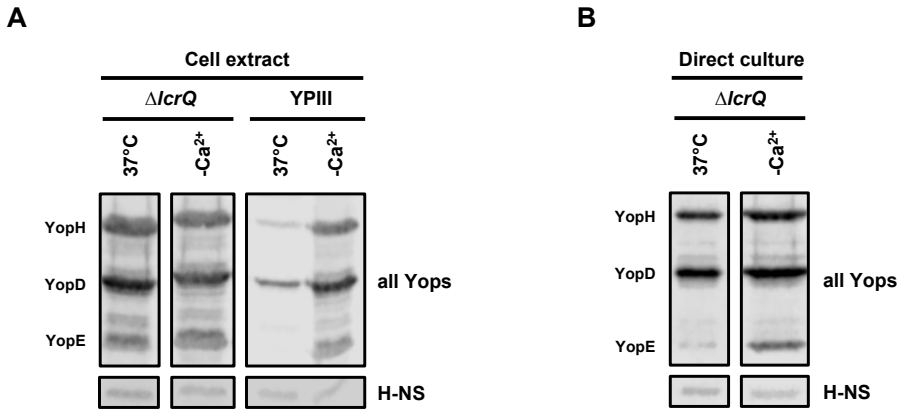

Figure 3.19) Yop expression is also regulated by LcrQ/YscM.

(**A**) Western blot against all Yops of whole-cell extract, generated from the Δ*lcrQ* mutant at 37°C and secretion (-Ca^{2+}) conditions. The graphic shows a representative example of biological triplicates. Samples for the wildtype (YPIII) were only generated once as a control sample. (**B**) Western blot against all Yops of direct culture containing intracellular and secreted proteins from the Δ*lcrQ* mutant grown at 37°C and -Ca^{2+}. In both figures, Yop expression was visualized by an all Yops antibody, while H-NS was used as the loading control.

As shown in Figure 3.19 it could be demonstrated that LcrQ/YscM also influences Yop synthesis and/or secretion in *Y. pseudotuberculosis* strain YPIII under the tested conditions. In a following approach, it was tested whether the observed protein levels of YopJ/YopP-FLAG are due to the effect of YopD or LcrQ/YscM. Therefore, cells were grown in the same manner as described before and direct culture samples were taken after induction with and without arabinose to induce the *yopJ/yopP*-FLAG expression.

The results indicate, that the level of YopJ/YopP-FLAG is affected by YopD, but not by LcrQ/YscM. Only in the *yopD* deletion strain, the level of YopJ/YopP-FLAG is increased compared to the wildtype at secretion (-Ca^{2+}) conditions, while it is similar between the wildtype and the Δ*lcrQ/yscM* mutant strain under all analyzed conditions. In contrast, a comparison of the total amount of Yops revealed no significant difference between the Δ*yopD* and Δ*lcrQ/yscM* mutant strains, when they are expressed from their native promoters (see Figure 3.20).

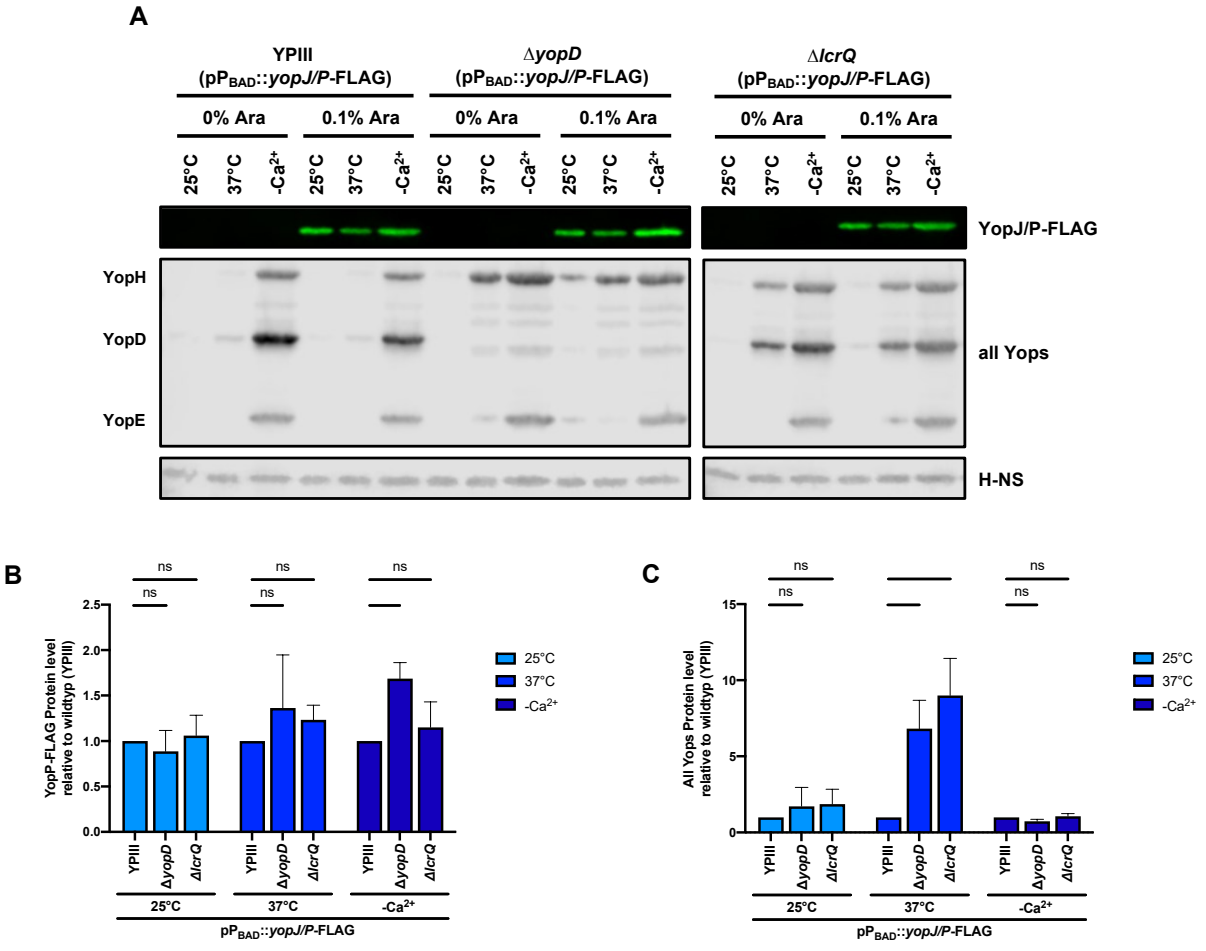

Figure 3.20) YopJ/P synthesis is regulated by YopD on a post-transcriptional level, but not LcrQ/YscM, whereas the overall Yop expression is regulated by both.

(**A**) Protein expression of YopJ/P-FLAG and all Yops in the wildtype (YPIII), Δ*yopD,* and Δ*lcrQ* mutant strains detected by western blot from direct cultures. All cells harbor the arabinose-inducible *yopJ/P*-FLAG fusion with a single FLAG-tag encoded on the plasmid pMV35. H-NS was used as the loading control. The experiment was done in biological triplicates. (**B**) Quantification of YopJ/P-FLAG fusion protein in the Δ*yopD* and Δ*lcrQ* mutant strains relative to the wildtype (YPIII) sample. (**C**) Quantification of the all-Yops protein level in the Δ*yopD* and Δ*lcrQ* mutant strains relative to the wildtype (YPIII) sample. Data were analyzed using a Student's t-test. Significance is shown above the analyzed bars (ns = >0.05; * = ≦0.05; ** = ≦0.01; *** = ≦0.001; **** = ≦0.0001).

These results, together with the previously presented data, confirm that the strong activation of translation of YopJ/P at 37°C is dependent on YopD but not LcrQ/YscM. Furthermore, these results indicate that the regulation of translation occurs at the transcript level based on the fact that YopD has

RNA-binding abilities while LcrQ/YscM binds to proteins (Anderson *et al.* 2002; Cambronne and Schneewind 2002; Francis *et al.* 2001; Kusmierek *et al.* 2019).

3.2.4 The expression of YopE is underlying a special regulation

Based on the observation, that a FLAG-tagged version of YopE is only expressed under secretion conditions, it was tested whether this effect is caused by a negative effect of LcrQ/YscM reported in several publications (Cambronne and Schneewind 2002; Wulff-Strobel *et al.* 2002). Therefore, the plasmid encoding YopE-FLAG (single FLAG-tag) expressed from the P_{BAD} promoter with the short 5' UTR was introduced into the Δ*lcrQ/yscM* mutant strain. The bacteria were cultivated at 25°C, 37°C, and secretion (-Ca^{2+}) conditions, and the expression was induced by 0.1% arabinose. Whole-cell-extracts were generated to detect the YopE-FLAG protein.

Surprisingly, the results show that the YopE-FLAG protein is only expressed under secretion conditions, but not at 37°C. In contrast, the native YopE is expressed at 37°C and -Ca^{2+}, as shown when detecting all Yops (see Figure 3.21B).

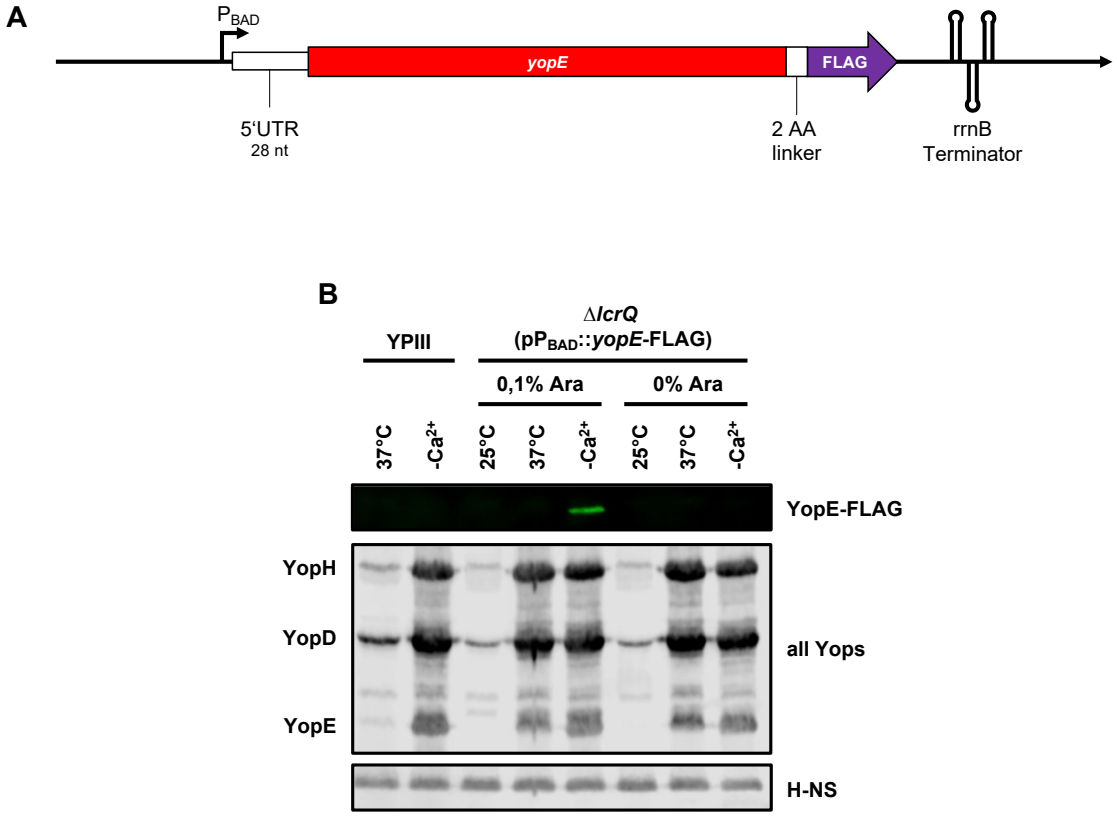

Figure 3.21) LcrQ/YscM does not affect YopE-FLAG synthesis when expressed from an inducible promoter.
(**A**) Graphic scheme of the P_{BAD}-*yopE*-FLAG expression plasmid pMV31 used for the experiment. (**B**) Western blot of whole-cell extracts from Δ*lcrQ* mutants harboring plasmid pMV31 encoding the YopE-FLAG fusion protein under the control of an arabinose-inducible promoter. H-NS was used as the loading control. The shown experiment is a representative of triplicates.

These results indicate that the expression of YopE is regulated by LcrQ/YscM but only when expressed in the native background. In the case of ectopic expression under the control of a different promoter, LcrQ/YscM shows no effect on YopE-FLAG synthesis. Furthermore, it was shown, that the translation of Yops is highly efficient due to the unique 5' UTR. This high efficiency is regulated in a YopD-dependent manner but is not affected by LcrQ/YscM.

3.3 Transcription of Yops upon virulence-associated conditions is not only activated by the virulence regulator LcrF

The identification of the fast and strong induction of Yop protein synthesis upon secretion (-Ca^{2+}) leads to the question, what benefit arises from this complex regulatory network. One hypothesis is that the expression of Yops is activated in two steps with a fast response followed by an ongoing response. This fast response could be LcrF-independent, which is predominantly expressed under secretion conditions and needs an efficient translation of the few present *yop* transcripts to ensure high levels of Yop proteins to counter the first attacks by phagocytic cells during infection. After cell-contact, when LcrF is strongly induced, it further activates transcription of the T3SS, Yops, and YadA to increase the levels of all components for additional antiphagocytic events. To prove whether this hypothesis is true, the expression of Yops must occur in the Δ*lcrF* mutant background. Moreover, this would indicate that additional factors are involved in the transcriptional activation of the *yops* in an LcrF-independent manner. Possible candidates for this activation are alternative sigma factors, which are present in the cell in an inactive form and can directly activate *yop* transcription upon activation.

3.3.1 Yop expression is LcrF independent but is significantly enhanced by LcrF under secretion (-Ca^{2+}) conditions

In order to identify, whether Yops are also synthesized in an LcrF-independent manner, *Y. pseudotuberculosis* (YPIII) wildtype and the isogenic Δ*lcrF* mutant were grown for 1 or 4 hours at 37°C or under secretion (-Ca^{2+}) conditions, respectively. Whole-cell-extracts were generated and the synthesis of Yops was analyzed by Western blotting using an all Yops antibody.

The results show that expression of certain Yops can be detected in the Δ*lcrF* mutant strain. Compared to the wildtype, this expression is considerably lower especially after 4 hours under secretion conditions (see Figure 3.22A). It was further analyzed, whether the level of Yops in the Δ*lcrF* mutant background remains equal or whether there is an increase detectable from 1 hour to 4 hours after secretion (-Ca^{2+}) induction. The level of Yops approximately increased about 2-fold between 1 hour and 4 hours after the shift to secretion (-Ca^{2+}) conditions but do not show as strong an induction as seen in the wildtype (see Figure 3.22B).

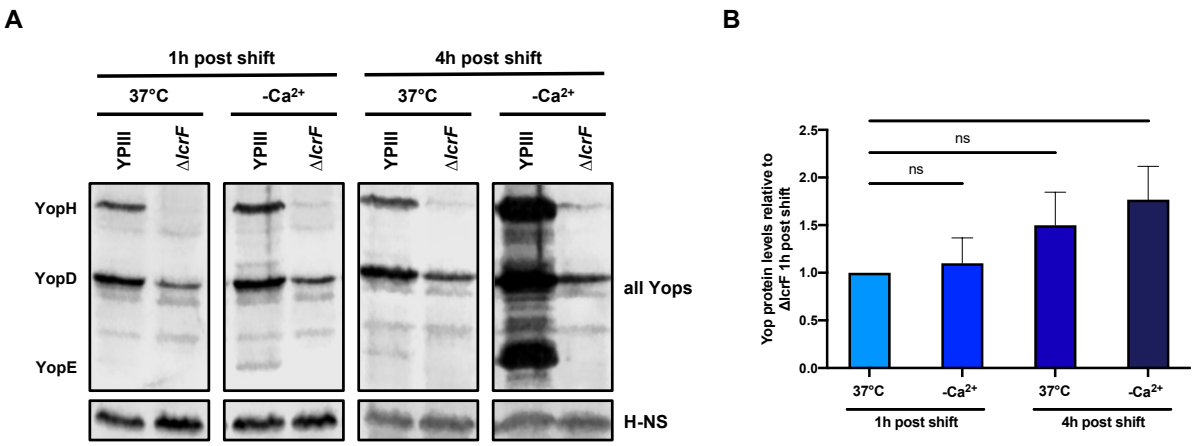

Figure 3.22) Expression of Yops in an *lcrF* deletion strain.

(**A**) The protein level of all Yop effector proteins in the wildtype (YPIII) and Δ*lcrF* strain were determined by western blot from whole-cell extracts. H-NS was used as the loading control, while the Yops were detected using an all Yops antibody. The experiment was done in biological triplicates. (**B**) Quantification of all Yops in the Δ*lcrF* mutant strains compared to the Δ*lcrF* mutant shifted to 37°C after 1 hour. Data were analyzed using a Student's t-test. Significance is shown above the analyzed bars (ns = >0.05; * = ≦0.05; ** = ≦0.01; *** = ≦0.001; **** = ≦0.0001).

From these results, it is likely that the expression of the Yops is not LcrF-dependent, a basal level and small induction is obtained even in the absence of the crucial regulator. However, for the strong induction observed under secretion (-Ca^{2+}) conditions the presence of LcrF is mandatory. These observations lead to the hypothesis that an additional factor might play a role in initial Yop expression.

3.3.2 Yop expression is activated in two steps

To further identify, how the Yop levels change under different conditions, a kinetic analysis of the *yop* transcript expression and protein synthesis was performed in the wildtype and the Δ*yopD* mutant strain.

Samples were taken 0, 1, 2, and 4 hours after the cultures were shifted from 25°C to 37°C or secretion (-Ca^{2+}) conditions. The collected samples were analyzed for their Yop and LcrF protein levels, as well as for the level of the respective mRNAs. The level of *yopE*, *yopH*, *yopM,* and *lcrF* mRNA was analyzed using qRT-PCR.

The Yop levels strongly increase one hour after the shift of all strains and under all conditions, compared to the starting condition (0 hours). Afterwards, the Yop levels in the wildtype at 37°C remain constant, while they increase continuously under secretion conditions. In the *yopD* deletion mutant, the Yop levels increase continuously over time with a first strong increase after one hour. Contrarily, LcrF is only detectable at later timepoints that correlate with the continuous increase in Yop levels at later time points (see Figure 3.23A). A similar effect can be observed when the transcript levels of the *yops* are analyzed. At 37°C in the wildtype, there is no increase at the mRNA levels of the *yops* and *lcrF.* Under secretion conditions, a first strong increase of the transcript amount is detectable one hour after the shift compared to time point zero. Subsequently, the level of all *yop* transcripts increase continuously. Again, the increase is different for the *lcrF* transcript. Quantification of the qRT-PCR reviles only a significant increase of the *lcrF* transcripts one hour after the shift (see Figure 3.23B). At later time points, the transcript level remains constant. While there is a strong increase in *yop* transcript levels over the first hour, the increase is less between two and four hours after the shift (see Figure 3.23B).

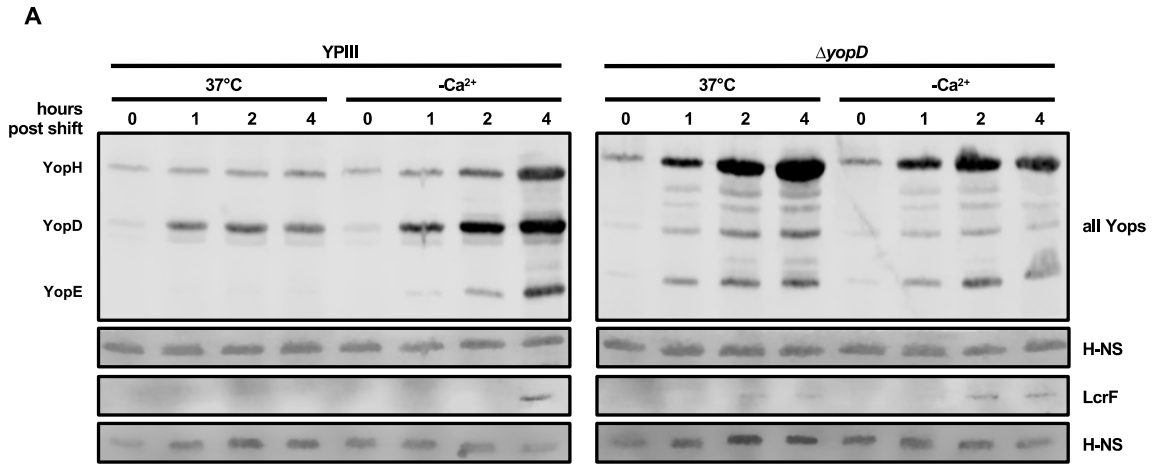

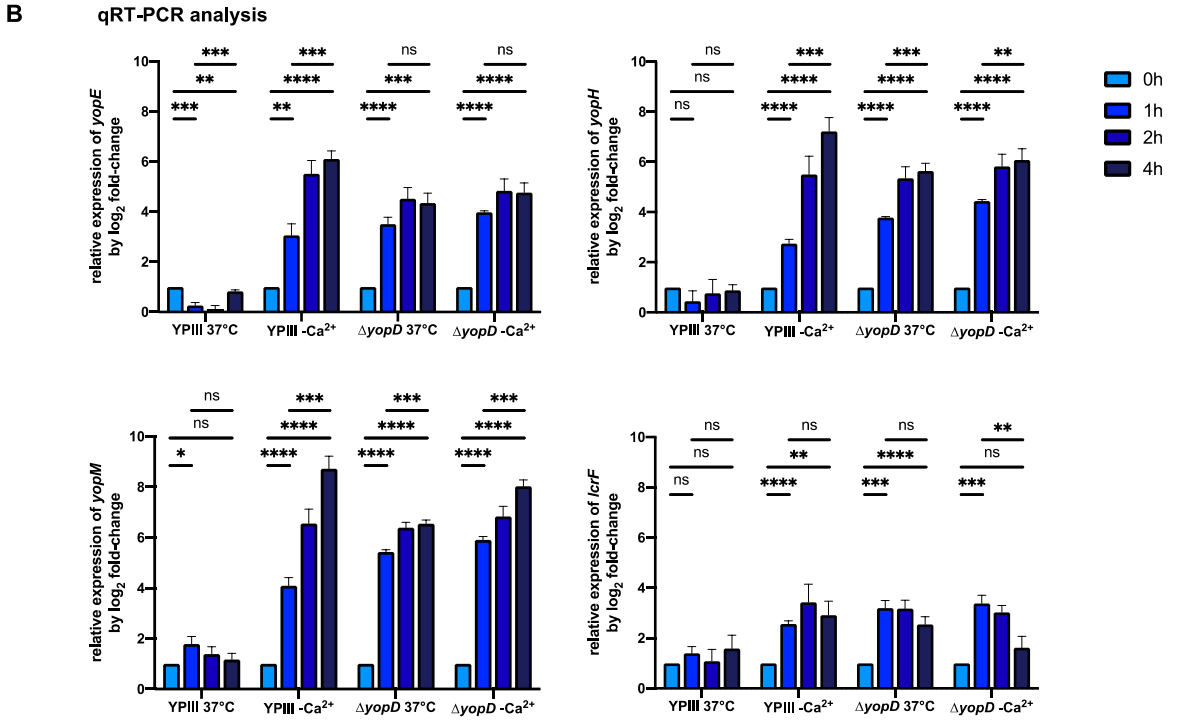

Figure 3.23) Kinetic of *yop* expression upon temperature shift and Ca^{2+} depletion in *Y. pseudotuberculosis* wildtype and Δ*yopD* mutant.

(**A**) Western blot of whole-cell extracts from wildtype (YPIII) and Δ*yopD* mutant taken at the indicated time points after the temperature shift and Ca^{2+} depletion. In the Western blot, all Yops and LcrF were detected, while H-NS was used as a loading control. The figure shows a representative example out of biological triplicates. (**B**) Quantification of the changes on transcript level of *yopE*, *yopH*, *yopM*, and *lcrF* by qRT-PCR. Samples were collected at the same time points as the Western blot samples from the same cultures. Data were normalized to the *sopB* gene and compared to time point 0 hours (before the shift) of every strain. A Student's t-test was used for data analysis. Significance is shown above the analyzed bars (ns = >0.05; * = ≦0.05; ** = ≦0.01; *** = ≦0.001; **** = ≦0.0001).

The basic expression of Yops in the Δ*lcrF* mutant strain together with the observation of a two-step induction kinetics of Yop protein synthesis and transcript expression suggests that an additional factor might play a role in early Yop expression. Furthermore, the results show that this possible factor can only be important in the initial phase of *yop* gene induction because the strong upregulation at later time points can only be achieved in the presence of LcrF.

3.3.2.1 Identification of activated alternative sigma factors under virulence-associated conditions

Potential candidates for the initial induction of *yop* gene expression are alternative sigma factors, due to their role in transcription initiation. In contrast to transcriptional activators, alternative sigma factors can bind an RNA-polymerase and recruit it to the promotor region, where transcription is directly initiated. Some alternative sigma factors are present in the cell in an inactive form bound to their anti-sigma factor. Upon sensing an activation signal, the anti-sigma factor is degraded and the released sigma factor is directly active. This response can immediately activate the transcription of target genes in contrast to a transcriptional activator which commonly must first be expressed.

To identify known alternative sigma factors that are activated under secretion (-Ca^{2+}) conditions when the *ysc-yop* genes are induced, the Ribo-Seq analysis was used to detect expression changes of known alternative sigma factors at the transcriptional or translational level.

Besides the housekeeping sigma factor RpoD (σ^{70}), the alternative sigma factors RpoE (membrane/extracytoplasmatic stress), RpoS (stationary growth), RpoN (nitrogen utilization), and RpoH (heat stress) were part of this analysis (Kazmierczak *et al.* 2005) (see Figure 3.24). The housekeeping sigma factor RpoD is found to be mainly unaffected by the different tested growth conditions or regulators CsrA and YopD. The alternative sigma factor RpoH is not activated under any conditions except under secretion (-Ca^{2+}) conditions in the Δ*yopD* mutant strain. These results exclude RpoH from a role in yop gene induction because it would be required for the activation in all Yop expressing conditions and strains. Only the alternative sigma factors RpoE, RpoS, and RpoN are activated in a temperature-dependent manner. In particular, expression of RpoS is induced on the transcriptional level and RpoE on translational level, whether RpoN shows a reduction under secretion conditions. Therefore, RpoE and RpoS are alternative sigma factors that might be active under the non-secretion (37°C) and secretion (-Ca^{2+}) conditions. The comparison of wildtype and the *yopD* mutant further revealed, that RpoE expression is considerably less induced in the Δ*yopD* strain, while RpoS is activated on the transcriptional but blocked on the translational level (see Figure 3.24).

The results support that RpoE expression is activated by an increase of temperature and remains induced under secretion conditions. This makes RpoE a good candidate for the early induction of Yop expression.

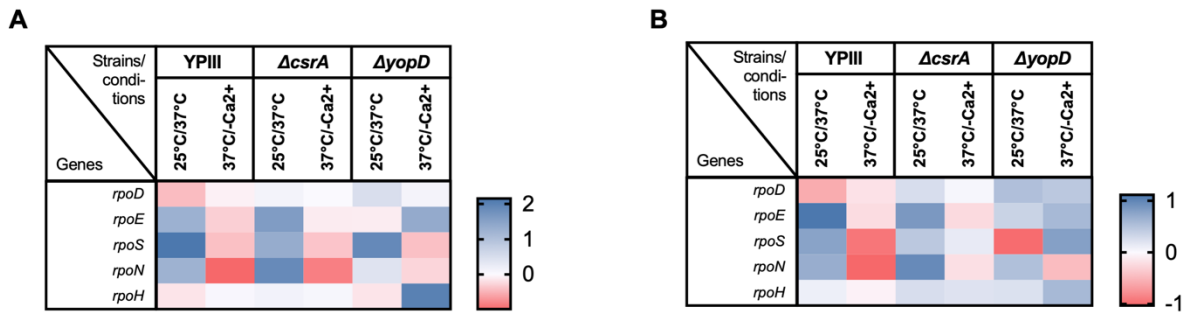

Figure 3.24) Expression of sigma factors under non-secretion and secretion conditions.

Heatmap of the housekeeping sigma factor *rpoD* (σ^{70}) and the alternative sigma factors *rpoE*, *rpoS*, *rpoN,* and *rpoH* genes. (**A**) Expression of the mentioned sigma factors on the transcript level. Comparisons were done for the wildtype (YPIII), Δ*csrA,* and Δ*yopD* mutant grown at 25°C and 37°C as well as secretion (-Ca^{2+}) conditions. (**B**) Expression of the mentioned sigma factors at the transcriptional level with the same comparisons as before.

In the next step, the signals that activate the RpoE protein were compared to those of the transcriptional activators regulating *yscW-lcrF* expression. It is published that *yscW-lcrF* expression is activated by RcsB and IscR as well as by OmpR (Kusmierek 2018; Miller *et al.* 2014; Schwiesow *et al.* 2015). The activation of the RpoE protein, by the release from its anti-sigma factor, is often attributed to different types of extracytoplasmatic stress, especially misfolded outer membrane proteins but also other stresses that affect cell envelope integrity such as heat stress, cold stress, general membrane stress, stationary growth, defects in LPS or antibacterial peptides as well as membrane perturbation (Hayden and Ades 2008; Hews *et al.* 2019; Kazmierczak *et al.* 2005). A comparison of the stimulating influences of the transcriptional activators with RpoE revealed several activating signals that are shared between the transcriptional activators and RpoE including general membrane stress, osmotic stress, or oxidative stress (see Figure 3.25). Assuming that the transcriptional activators are active under the conditions where the Yops are expressed, it is possible that the same signals trigger activation of the RpoE protein.

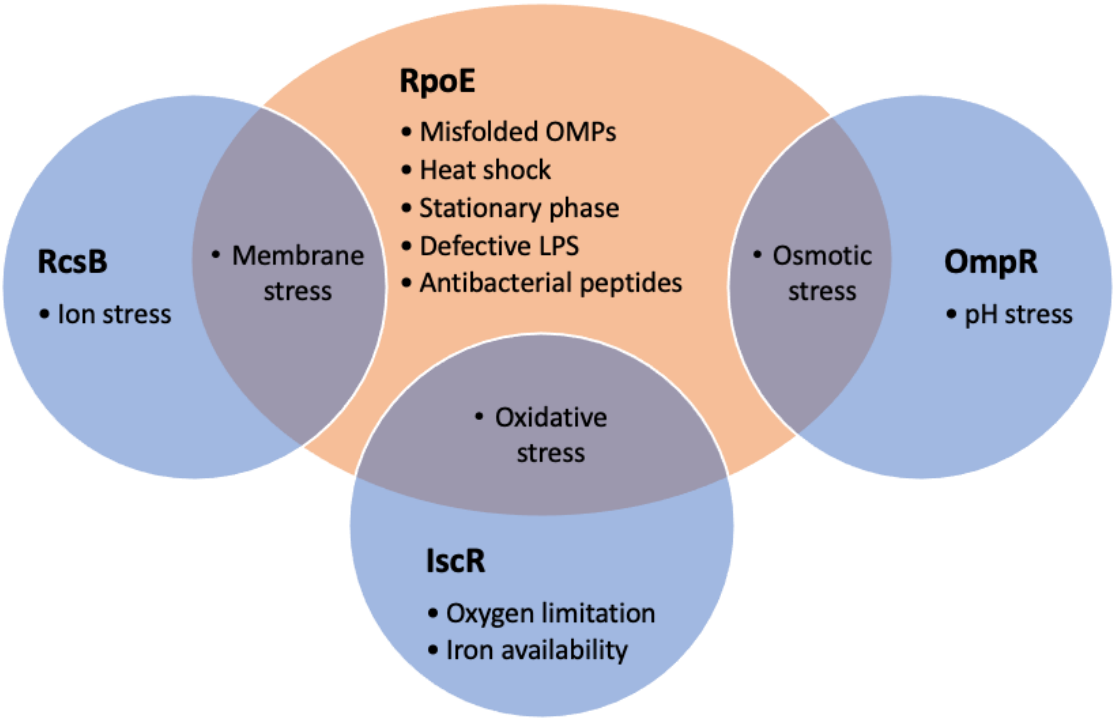

Figure 3.25) Comparison of the stimulating signals of known *lcrF* activating transcriptional regulators and the alternative sigma factor RpoE.

Venn-diagram-like overlap of signals that are known to activate RcsB, OmpR, and IscR, three known transcriptional activators of the *lcrF* gene, and the alternative sigma factor RpoE (σ^E).

A comparison of the signals that activate expression/activation of sigma factors based on the Ribo-Seq analysis with the signals activating transcriptional activators that are known to control *yscW-lcrF* expression induction, RpoE is a good candidate for the activation of yop gene expression. To confirm that RpoE is active and contributes to the *ysc-yop* gene expression, expression of other genes of the *rpoE* regulon was analyzed.

3.3.2.2 Activation of the alternative sigma factor RpoE (σ^E) is confirmed by induction of the *rpoE* regulon

To evaluate RpoE activation, it is helpful to determine the expression of *rseABC*, the genes downstream of *rpoE,* which act as regulators of the alternative sigma factor. The four genes are organized in a small operon with two annotated promoters in *E. coli.* The whole operon is expressed by a RpoD (σ^{70})-dependent promoter upstream of *rpoE* which is also recognized by RpoE. Besides this promoter, the operon encodes one additional RpoE- dependent promoter upstream of *rseA* inside the *rpoE* CDS (see Figure 3.26). These two RpoE-dependent promoters are important to upregulate *rpoE-rseABC* expression in a positive autoregulation, while the internal promoter in the *rpoE* gene only triggers upregulation of the *rseABC* gene expression. Upregulation of the *rseABC* gene expression establishes a downregulation after the stress is overcome and to avoid overshooting of the stress response (Konovalova *et al.* 2016). Thereby the negative feedback is established by the anti-sigma factor RseA functioning by binding free RpoE and recruits it to the membrane to inactive it (Campbell *et al.* 2003). Furthermore, the RseB protein functions as a transcriptional inhibitor to block the expression of genes harboring an RpoE-dependent promoter (Konovalova *et al.* 2016). The same gene organization is seen in *Y. enterocolitica* where it is assumed that the regulation is similar to *E. coli* (Heusipp *et al.* 2003). In

addition, the gene locus is also highly similar in *Y. pseudotuberculosis* YPIII. However, the promoter located within the *rpoE* gene is not described so far and only the one upstream of the *rpoE* gene is detectable in the Ribo-Seq analysis (data not shown).

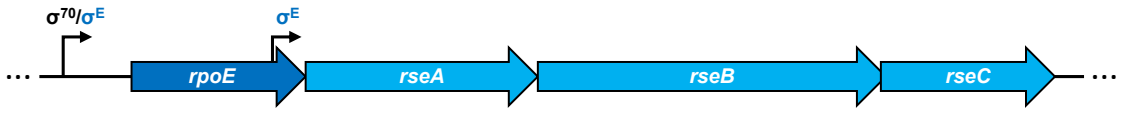

Figure 3.26) Schematic view of the *rpoE-rseABC* operon in *Y. pseudotuberculosis*.
Representation of the *rpoE-rseABC* operon in *Y. pseudotuberculosis* YPIII including the two promoters identified in the homologous operon in *E. coli*. The sigma factors that recognize the individual promoters are indicated (Konovalova et al. 2016).

Results from the Ribo-Seq analysis show that all three *rse* genes are upregulated in all tested strains with the shift from 25°C to 37°C. Their upregulation is much stronger than for *rpoE* especially on the transcript level (see Figure 3.27A). Upon Ca^{2+} depletion (-Ca^{2+}) the *rseABC* genes are downregulated to some extent in the wildtype and the Δ*csrA* mutant whereas the genes remain induced or are even further induced in the Δ*yopD* mutant (see Figure 3.27).

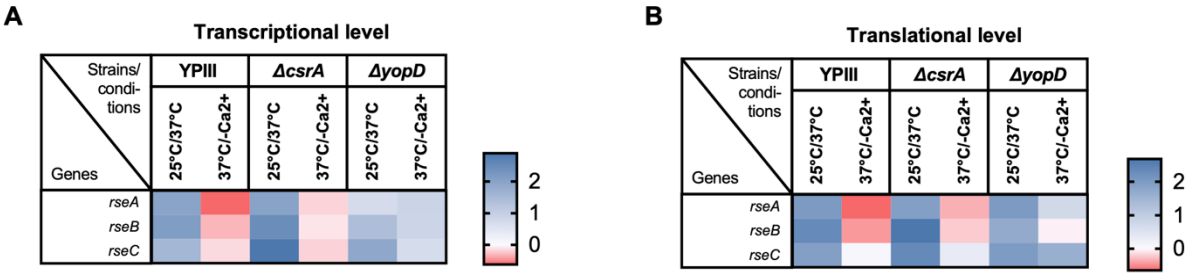

Figure 3.27) Expression of the *rseABC* genes of the *Y. pseudotuberculosis* wildtype, Δ*csrA,* and Δ*yopD* mutants under 25°C, 37°C, and secretion (-Ca^{2+}) conditions.
(**A**) Heatmap of the expression of the *rseABC* genes on the transcript level. (**B**) Heatmap of the synthesis of the *rseABC* genes on the translational level. The comparisons were done between 25°C and 37°C as well as 37°C and secretion (-Ca^{2+}) for the wildtype, Δ*csrA,* and Δ*yopD* mutants.

Upregulation of the *rpoE-rseABC* expression and translation with increased temperature which remains upregulated under secretion (-Ca^{2+}) conditions indicates that the alternative sigma factor RpoE is activated under these conditions.

3.3.3 Expression of virulence-associated genes is not controlled by the products of the *rpoE-rseABC* operon

The results described above indicate that RpoE is released from RseA and is thereby activated upon a temperature shift from 25°C to 37°C and remains in the activated state under secretion conditions.

To examine if the alternative sigma factor RpoE might contribute to the transcription of the *yop* and *yadA* genes, harboring the short 5' UTRs, the region upstream of the transcriptional start site (TSS) was investigated for RpoE binding motifs. To do so, the 50 base pairs upstream of the TSS were aligned according to this position. The potential -10 region, as well as the potential -35 region upstream of the TSS of these genes, were analyzed. In addition to the *yop* and *yadA* genes, the *lcrQ/yscM* and *yopN* genes were also included due to their regulatory function.

The comparison of the two regions with consensus sequences for RpoD (Pribnow box: -TATAAT-) and RpoE (-10 region -TCTGA-) shows that both sigma factors might be involved in promoter sequence

detection (Abril *et al.* 2020; Brosius *et al.* 1981; Rhodius *et al.* 2005). The *yopH* and *yopN* promoter regions show a strong homology to the Pribnow box and the -35 region that is detected by RpoD. The upstream region of *yopM* shows no obvious binding site attributed to RpoD or RpoE. In the case of *yopE*, *yopK/yopQ*, *yopJ/yopP*, *yadA,* and *lcrQ/yscM*, the -10 regions show high similarities to the RpoE-consensus sequence. A special feature in the -10 region of RpoE-dependent promoters is a cysteine with an upstream thymidine. Downstream of this motive, adenine, thymidine, or guanine are suitable in the predicted motive. In addition, the -35 regions of *yopJ/yopP* and *lcrQ/yscM* show strong homologies to the consensus sequence of RpoE (see Figure 3.28).

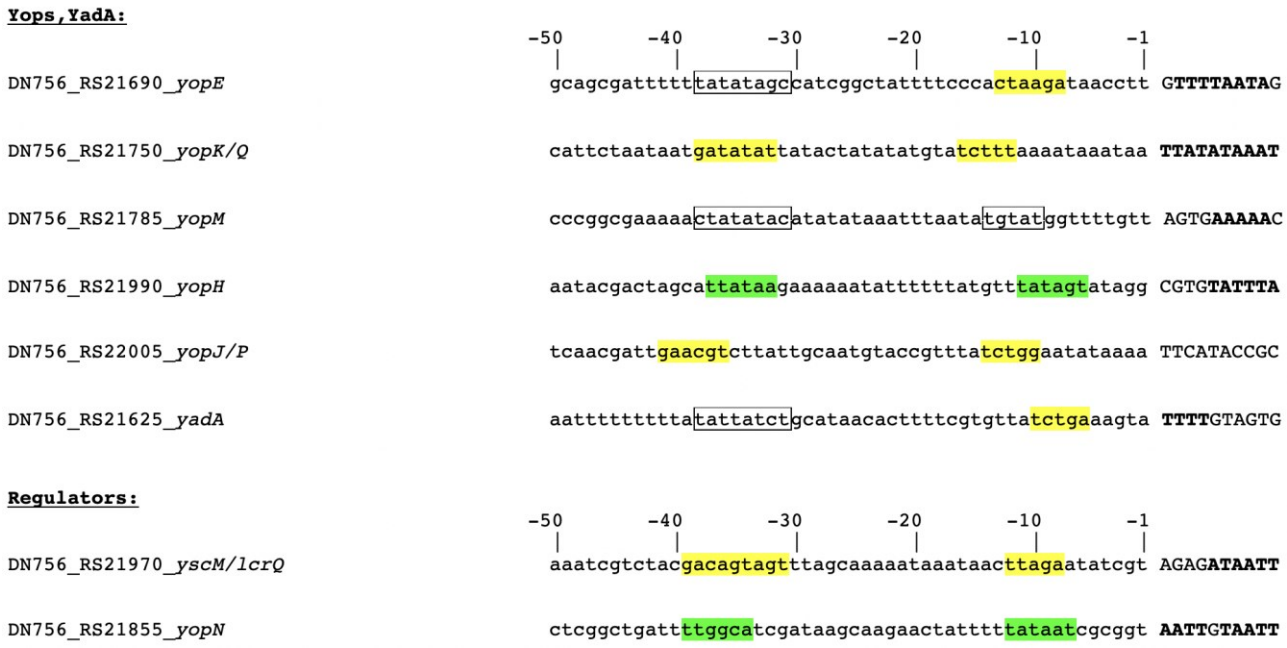

Figure 3.28) Alignment of the promoter regions and the start of the 5' UTRs of the *yop* and *yadA* genes, and two genes of regulators of the T3SS.

The -10 and -35 regions were predicted within the first 50 base pairs upstream of the predicted TSS from the transcriptome of the Ribo-Seq analysis. Sequences were aligned based on the first nucleotide of the transcribed RNA. Areas highlighted in green indicate possible binding sites for RpoD. Regions highlighted in yellow indicate possible binding sites for RpoE. The boxed region indicates potential promoter sequences with no strong homology to the sigma factor RpoD and RpoE consensus sequence.

Based on the predicted promoter region and the observation, that RpoE is active under the respective conditions, it is likely, that RpoE is involved in the transcription of several *yop* genes and their regulators.

3.3.4 Deletion of *rpoE* (σ^E) does not affect Yop expression

To test if the alternative sigma factor RpoE affects the expression of *yop* genes, a deletion mutant was constructed. Therefore, the whole *rpoE-rseABC* operon was exchanged for a kanamycin resistance cassette (see Figure 3.29). The exchange mutation was used, to test whether the whole operon is involved in yop gene expression.

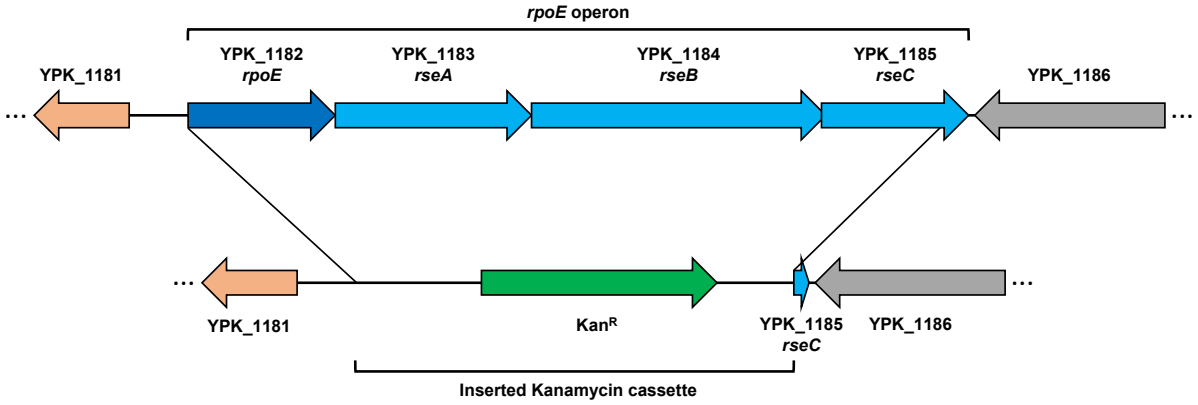

Figure 3.29) Schematic view of the constructed *rpoE-rseABC* knock-out mutant.

Visualization of the genetic organization of the *rpoE-rseABC* locus (*rpoE* operon) in *Y. pseudotuberculosis* and the resulting mutant in which the operon was exchanged by a kanamycin cassette. Genes are orientated in sense and given with gene IDs and gene names.

As in previous experiments, the wildtype, *rpoE-rseABC* deletion and *lcrF* deletion mutants as well as a double mutant of *rpoE-rseABC* and *lcrF* were grown first at 25°C and subsequently shifted to 37°C and secretion conditions (-Ca^{2+}). Samples were taken after one and four hours and whole-cell extracts were prepared. For the analysis of the 25°C conditions, samples were only collected four hours after the shift. Finally, the Yop synthesis was examined by immunoblot using an all Yops antibody.

The results show that the synthesis of Yops is equal in the wildtype and Δ(*rpoE-rseABC*) mutant strain, while the synthesis of Yops is very low in the Δ*lcrF* and Δ*lcrF*/Δ(*rpoE-rseABC*) mutant backgrounds. This pattern is detectable under all conditions and for all time points (see Figure 3.30). Yop synthesis in the Δ*lcrF* mutant strains is similar to previous experiments (see Figure 3.22).

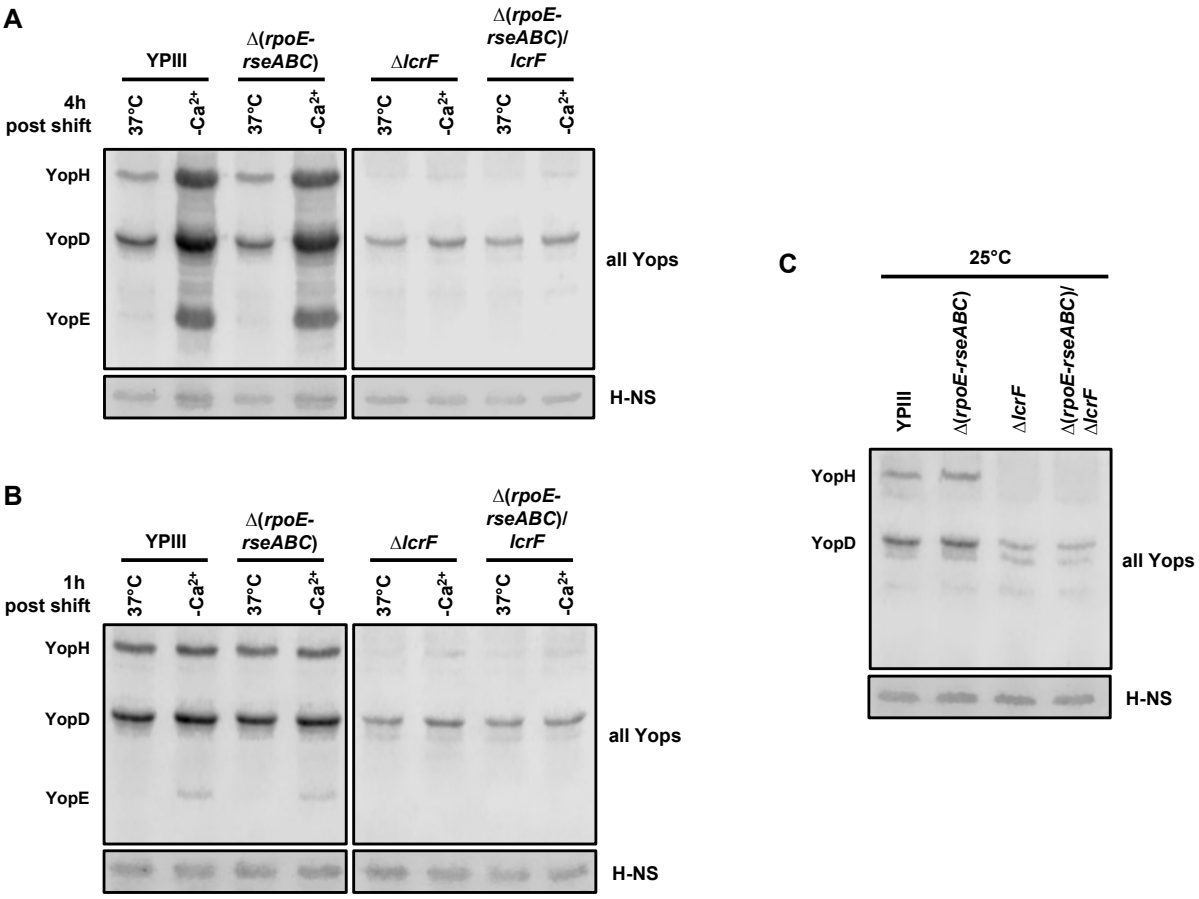

Figure 3.30) Yop synthesis in wildtype (YPIII), *rpoE-rseABC* mutant, *lcrF* mutant, and *lcrF/rpoE-rseABC* double mutant.
Western blot of whole-cell extracts from wildtype (YPIII), Δ*(rpoE-rseABC)*, Δ*lcrF,* and Δ*(rpoE-rseABC)/lcrF* mutants grown at indicated conditions for 1 hour (**A**) or 4 hours (**B**) were analyzed with an all-Yops antibody. H-NS antibody was used as loading control. The figure shows a representative example of biological triplicates. (**C**) Representative Western Blot of samples cultivated at 25°C for 6 hours.

It can be concluded from these results, that the alternative sigma factor RpoE does not affect the expression of the Yops.

3.4 Temperature-dependent changes of tRNA levels in *Y. pseudotuberculosis*

In addition to the unique 5' UTR organization that contributes to the strong overall translation of the *yop* and *yadA* transcripts, also the speed of translation could contribute strongly to the efficiency of the translation process. It was reported in previous studies, that the level of tRNAs, needed to decode a transcript, and the codon-usage play a crucial role in translation elongation speed and accuracy (Rodnina *et al.* 2017; Wohlgemuth *et al.* 2011). Based on these findings and the results from this study showing that translation of *yops* and *yadA* is highly efficient, it was investigated how the codon usage might contribute and whether the level of tRNAs changes under the different growth conditions. Finally, it was analyzed whether the codon usage of the *yops* and *yadA,* together with the detected tRNA levels could be beneficial for the translation of these transcripts.

3.4.1 Codon usage of *yop* and *yadA* genes

First, the annotation of *Y. pseudotuberculosis* YPIII (access number NC_010465.1, used for the Ribo-Seq analysis) was searched for all annotated tRNA genes. Afterwards, the codons recognized by the individual detected tRNA genes were revealed. Finally, the number of tRNA genes per codon was calculated. The data analysis shows that the genome of *Y. pseudotuberculosis* YPIII encodes 81 tRNA genes, which can be assigned to 37 codons. This results in 24 codons lacking a tRNA. Additionally, most of the codons with an associated tRNA encode one or two tRNA genes for this codon, while some encode three to four tRNA genes. The codons for methionine (AUG), as well as one of the lysine codons (AAA), encode the highest amount with seven tRNA genes (see Figure 3.31A). These results are biased in the existence as well as in the abundance of tRNA genes.

After investigation of the codons and tRNA genes, the codon usage was calculated by the codon frequency per 1000 codons. To do so, the codon frequency of the chromosome was analyzed using the CoCoPUTs-tool (Alexaki *et al.* 2019; Athey *et al.* 2017). For the virulence plasmid (pIB1) and different sets of genes, the “Sequence Manipulation Suite (SMS) - codon usage” online tool was used (Stothard 2000). The tool calculates the codon usage of single or multiple CDS. The most abundantly used codons on the chromosome are GAU (aspartic acid), GAA (glutamic acid), AUU (isoleucine), AAA (lysin), and CUA (leucine), while cysteine, serine, and arginine are in low abundance. This shows that the chromosome of *Y. pseudotuberculosis* has a preference for certain codons. For the *yop* and *yadA* transcripts as well as for the genes encoding the T3SS structure proteins, the codon frequency of highly abundant codons is similar to that of the chromosome, while there are differences in the less abundant codons. For housekeeping gene sets like ribosomal proteins, translation factors, glycolysis, or transcription, a striking pattern appears in the codon frequency. While some codons are highly abundant in these gene sets, others are more or less absent. This is especially evident for many arginines, some leucine, isoleucine, glycine, and threonine codons. Codon frequency of gene sets that encode non-housekeeping genes such as motility or DNA replication is however very similar to the codon frequency of the chromosomal genes (see Figure 3.31B).

These results demonstrate, that the codon usage/frequency is different between distinct gene sets. The results also illustrate, that those housekeeping genes seem to be more biased to a certain codon for a specific amino acid, while other gene sets such as the genes encoding virulence factors are more flexible in codon usage.

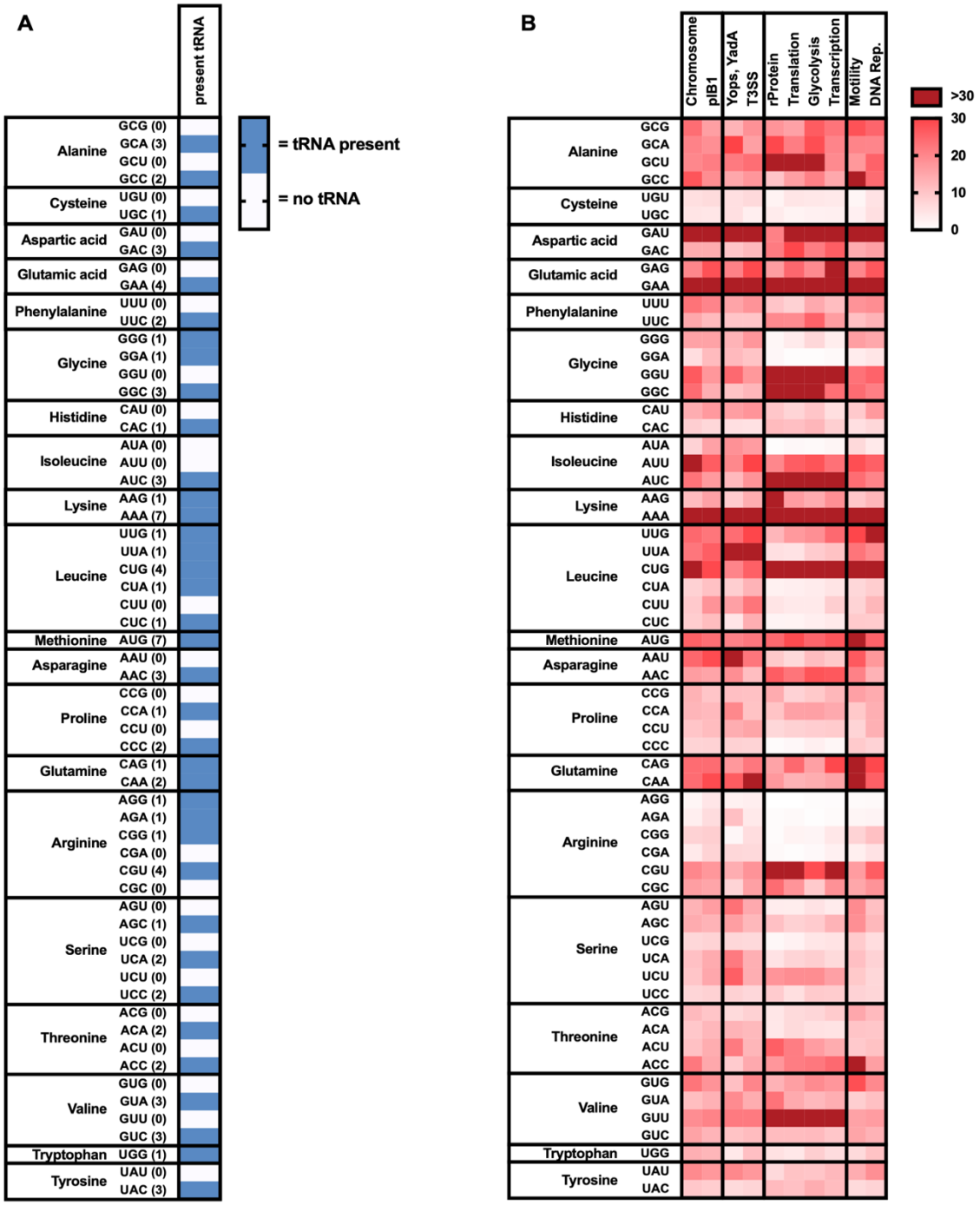

Figure 3.31) Graphic overview of tRNA codons and their frequency in the genome of *Y. pseudotuberculosis*.
(**A**) Overview of all existing mRNA codons and the presence of the tRNA detecting this codon. Numbers in brackets represent the amount of genes coding for the corresponding tRNA. (**B**) Heatmap of the codon frequency per 1000 of certain genome parts, or gene sets, of *Y. pseudotuberculosis* for every mRNA codon. Codon usage of the chromosome was calculated by the CoCoPUTs-tool (Alexaki *et al.* 2019; Athey *et al.* 2017).

To investigate the difference in more detail, the codon usage of the analyzed sets was compared to the codon usage of the chromosome. Similar codon usages between the chromosome and tested gene sets (e. g. Yops and YadA; etc.) result in a value of one. Codons that are underrepresented in the tested sets represent correlation values of zero to one, while overrepresented codons have a value of >1. For the motility and DNA replication gene sets this analysis shows that these genes are very similar to the codon frequency of the chromosome. For the housekeeping gene sets significant differences are observable, where some codons are overrepresented while others are strongly underrepresented. The genes

encoded on the virulence plasmid pIB1 including genes of *yops*, *yadA*, and the T3SS show common differences and also specific changes of individual genes compared to the chromosome. The most significant effect is that certain codons are overrepresented codons and nearly none are underrepresented. Some of the most overrepresented codons are glycine (GGA), isoleucine (AUA), and two arginines (AGG and AGA). Besides these four codons, the codons for serine (UCA and UCU) and threonine (ACU) are strongly overrepresented in the *yop* and *yadA* genes (see Figure 3.32).

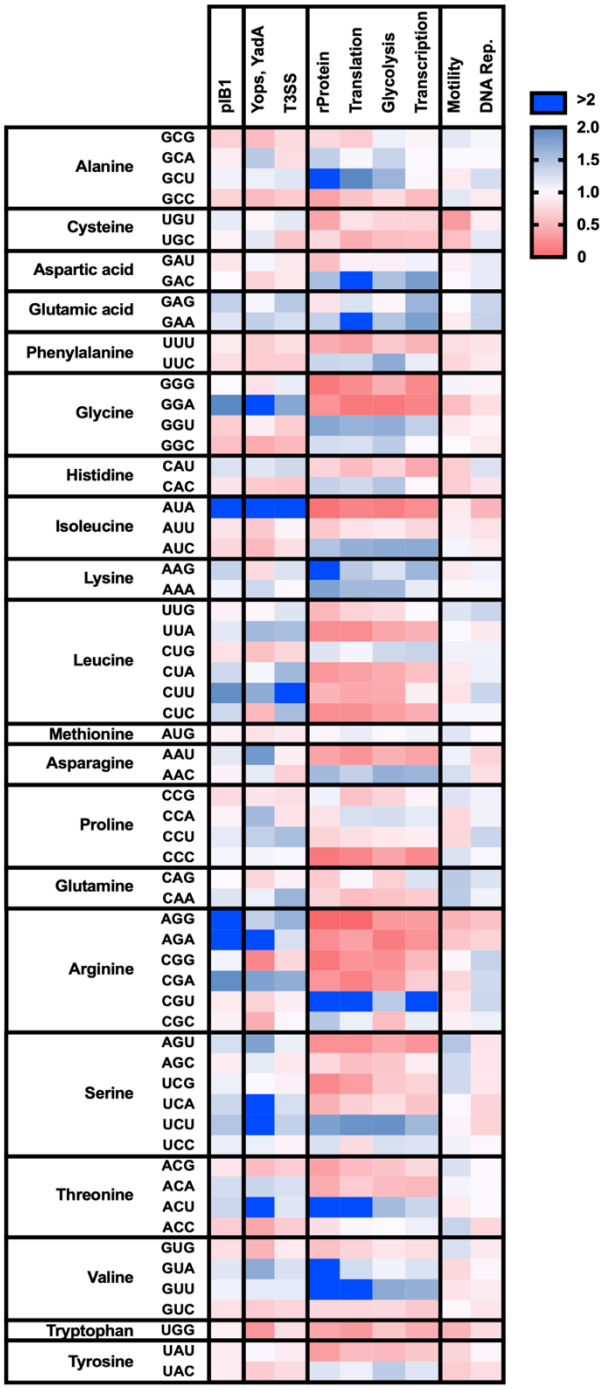

Figure 3.32) Correlation of the codon frequency between gene sets and the chromosome.
Heatmap of the codon frequency of genes encoded on the virulence plasmid pIB1 and some gene sets for protein synthesis, metabolism, RNA transcription, mobility, and DNA replication (DNA Rep.) compared to the codon frequency of the chromosome.

The analysis of the codon usage of the genes encoding the *yops* and *yadA* as well as other gene sets shows that they display different codon frequencies. In contrast to the housekeeping genes and other

chromosomally-encoded genes, the virulence plasmid and especially the genes for the *yops* and *yadA* show a preference to some codons that are underrepresented on the chromosome. Using an underrepresented codon normally results in slow translation elongation, due to the low amount of this tRNA in the cell. To see if the levels of tRNAs change under secretion conditions to support the increased translation of the *yop*, *yadA,* and also T3SS component transcripts, the tRNA levels were compared under different virulence-relevant conditions.

3.4.2 Expression changes of tRNAs frequently encoded in *yop* and *yadA* genes

To investigate the level of certain tRNAs, Northern blot analysis was performed. Therefore, different tRNAs were chosen to be analyzed based on their abundance in the genes encoding *yops* and *yadA*. When the codon was not associated with a tRNA present in the genome, the closest substitute was used. This tRNA was chosen based on the identity of the first two nucleotides of the codon. In particular, the level of the tRNAs for glutamic acid, aspartic acid, and lysine were analyzed due to the high overall abundance. In addition, the tRNAs for leucine, asparagine, and serine were chosen because of their high frequency within the *yop* genes, and the tRNA for alanine was chosen as a control since it is not highly abundant and also has no high frequency in the *yop* genes.

The results illustrate, that the level of several of the tRNAs increase in *Y. pseudotuberculosis* when cultures are shifted from 25°C to 37°C but they remain unchanged upon induction of the secretion conditions. In contrast, tRNA levels for alanine and glutamic acid are more or less unaffected by an increase in temperature or upon a shift to secretion conditions (see Figure 3.33AB). After quantification of the Northern blot results, the tRNAs for leucine, serine, and asparagine show the strongest increase in response to a temperature upshift. These three tRNAs represent overrepresented codons in the *yop* genes, while the lysine and aspartic acid tRNAs which are highly abundant overall but not strongly overrepresented in the *yop* genes show a weaker increase. As expected, the level of the tRNA for alanine which is used as control, and the overall most abundant tRNA for glutamic acid remain unchanged under the different conditions (see Figure 3.33C).

A

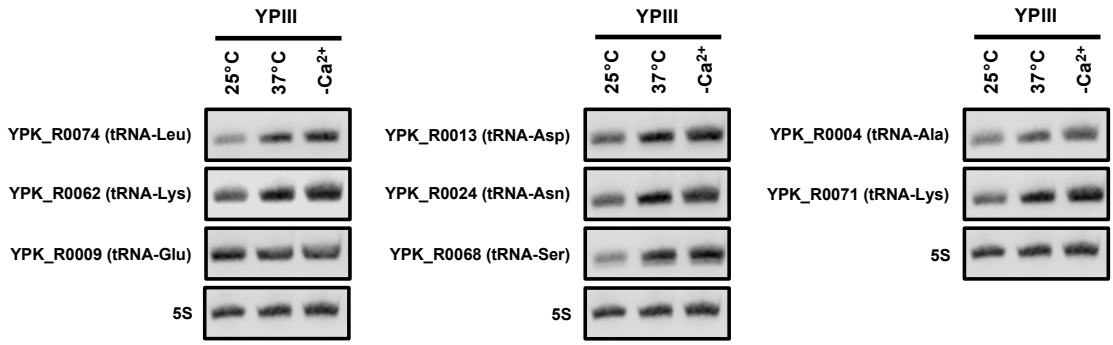

B

tRNA gene	codon	tRNA gene	codon	tRNA gene	codon
YPK_R0074 (tRNA-Leu)	UUA	YPK_R0013 (tRNA-Asp)	GAC	YPK_R0004 (tRNA-Ala)	GCA
YPK_R0062 (tRNA-Lys)	AAA	YPK_R0024 (tRNA-Asn)	AAC	YPK_R0071 (tRNA-Lys)	AAG
YPK_R0009 (tRNA-Glu)	GAA	YPK_R0068 (tRNA-Ser)	UCA		

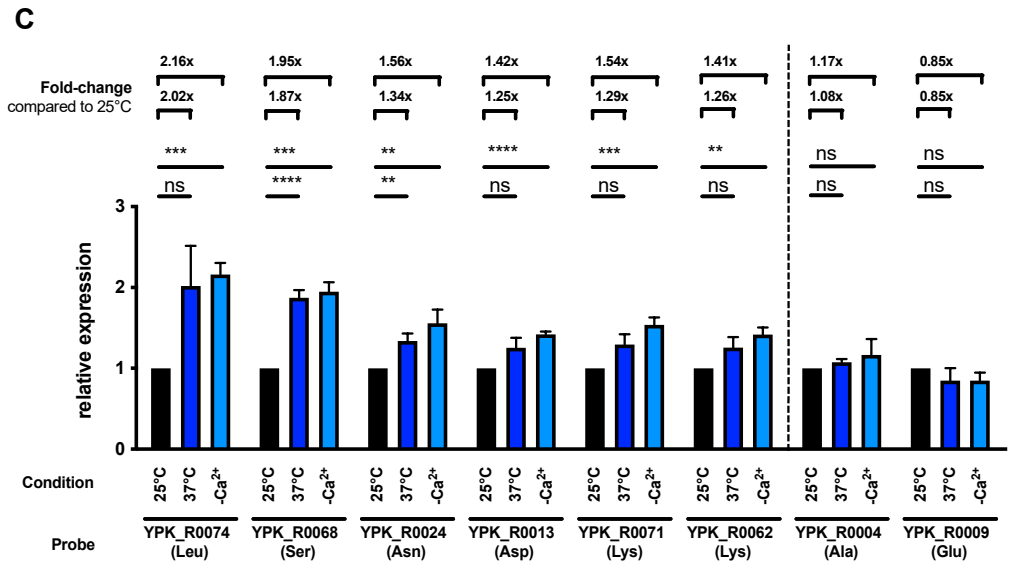

Figure 3.33) Expression changes of certain tRNAs in response to a temperature upshift.

(**A**) Northern blot detection of tRNA levels in extracts of the *Y. pseudotuberculosis* wildtype (YPIII) at 25°C, T3SS uninducing (37°C), and T3SS inducing (-Ca^{2+}) conditions. The 5S rRNA was used as a loading control. The figure represents one set out of the biological triplicates. (**B**) Table showing the codons, detected by the analyzed tRNAs. (**C**) Quantification of the Northern blot analysis showing the fold-change of the analyzed tRNA amounts in bacteria grown at indicated conditions compared to 25°C. The mean +/- SD is shown from biological triplicates. Data were analyzed using a Student's t-test. Significance is shown above the analyzed bars (ns = >0.05; * = ≦0.05; ** = ≦0.01; *** = ≦0.001; **** = ≦0.0001).

Taken together, these findings show that the investigated tRNAs for overrepresented codons in the *yop* and *yadA* genes are upregulated in response to temperature and secretion. Furthermore, highly abundant tRNAs also show an upregulation at least under secretion conditions. In contrast, no changes in the tRNA levels were detected for tRNAs that recognize codons without a difference to the overall codon usage.

To correlate the results of the overrepresented codons in the *yop* and *yadA* genes with the observed upregulation of the tRNA expression, their influence on one another under secretion conditions was analyzed. First, the number of significantly upregulated tRNAs was correlated with the number of corresponding codons, which is six in this analysis (see Figure 3.33C). Next, the proportion of the six codons of the total 61 present codons was calculated, resulting in around 10%. Second, the number of codons recognized by the tRNAs that were significantly upregulated (see Figure 3.33A) were counted relative to the whole CDS of the *yop* and *yadA* genes. For the substitute tRNAs, two codons were counted, with one codon perfectly matching the tRNA anti-codon (see Figure 3.34 "codons with direct ↑ tRNAs") and the second one representing the imperfect matching codon (see Figure 3.34 "codons with indirect ↑ tRNAs"). Finally, the 10% codons with upregulated tRNAs were compared to the number of codons for the *yop* or *yadA* transcript recognized by these tRNAs.

In case of the *yopE* and *yopH* genes, this overall 10% codons with upregulated tRNAs contribute to approximately 17% of their CDS in translation. For *yopM*, *yopK/yopQ*, *yopJ/yopP,* and *yadA* the codons of upregulated tRNAs affect more than 25% of the codons of these genes (see Figure 3.34). This demonstrates, that a small difference in the number of tRNAs might affect the translation elongation of *yop* and *yadA* transcripts on a bigger scale.

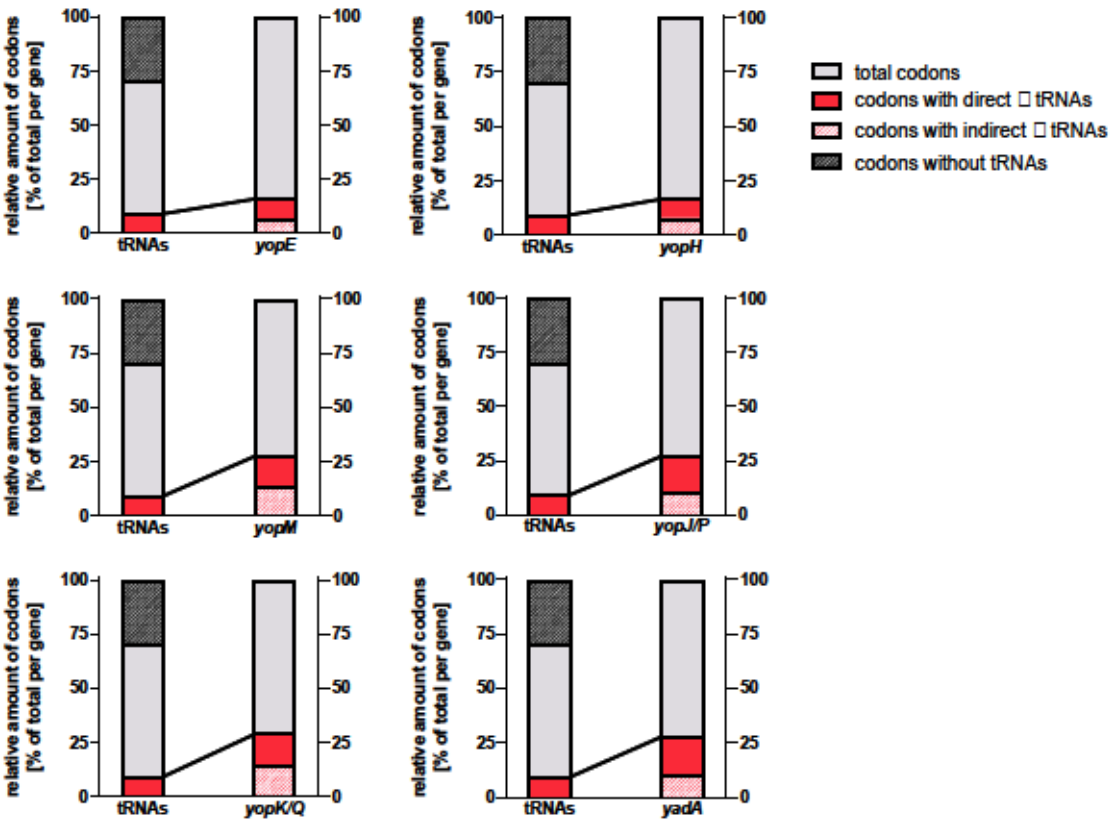

Figure 3.34) Correlation of the analyzed upregulated tRNAs and there influence on the codon usage by the *yop* and *yadA* genes.

Stacked-bar diagram for the correlation of the amount of upregulated tRNAs (fold-change of >1.4 with a significant p-value, see Figure 3.33C) to the number of affected codons by these tRNAs of the *yop* and *yadA* transcripts. Numbers are calculated relative to the total amount of codons (tRNAs) or the total amount of codons per gene (*yop* and *yadA* genes).

In summary, the analysis showed that the genes of the Yops, YadA, and the T3SS structure components are highly upregulated at the transcriptional and translational level under secretion conditions. For the *yop* and *yadA* transcripts, the translation is more efficient in relation to the transcription, which is especially evident in the *yopD* deletion mutant. This increased translation rate of the *yop* and *yadA* transcripts is promoted by the relatively short and AU-rich 5' UTRs and an efficient RBS region. This results in a fast increase of Yop and YadA synthesis shortly after induction of the system and might contribute to a very rapid response. Basal transcription to allow this response in the initial stage of the infection, when none or only a few molecules of the LcrF activator are present, is not facilitated by the alternative sigma factor RpoE but occurs in an LcrF-independent manner. Finally, it was revealed that all T3SS virulence-associated genes show a special codon usage, with distinct differences to the codon usage of genes encoded on the chromosome. Furthermore, it was demonstrated that the tRNAs that decode these codons are upregulated in response to temperature and secretion. A change of the tRNA levels affects between 17% and more than 25% of the codons of the *yop* and *yadA* genes and this could increase the speed of translation elongation.

4 Discussion

Pathogenic *Yersinia* use a T3SS to translocate the Yop effector proteins into the host immune cells to interfere with cell signaling pathways to prevent phagocytosis and trigger apoptosis (Grosdent *et al.* 2002; Rosqvist *et al.* 1988; Visser *et al.* 1995). For this purpose, T3SS expression needs to be activated and the required Yop proteins together with the adhesin YadA must be expressed and synthesized in huge amounts to promote these functions (Bölin *et al.* 1985). The main factor for the activation of the system is the transcriptional activator LcrF which activates transcription of the T3SS structure genes (*ysc* genes), the *yop* genes, and the gene encoding the adhesin *yadA* (Schwiesow *et al.* 2015). To prevent overshooting and expression of the system when it is not required (e. g. in the absence of immune cells such as macrophages and neutrophils) the system, as well as the transcriptional activator LcrF, are regulated by several factors. One is the CsrA protein, the regulatory protein of the *Csr* system. CsrA is an RNA-binding protein that affects the stability of a transcript and on the other hand is able to interfere with the translation initiation by binding to the RBS sequence in the mRNA (Heroven *et al.* 2012; Nuss *et al.* 2017; Romeo and Babitzke 2019). CsrA represses the expression of the *lcrF* gene indirectly by repressing the response regulator RcsB, which acts as a transcriptional activator, on the post-transcriptional level (Fei *et al.* 2021; Kusmierek 2018; Li *et al.* 2015). Another one is the translocon pore protein YopD. Besides the translocon pore function, YopD is harboring an RNA-binding ability that allows YopD binding to virulence-associated transcripts and the transcript of the regulator *lcrF* and to repress their synthesis (Anderson *et al.* 2002; Chen and Anderson 2011; Francis *et al.* 2001; Kusmierek *et al.* 2019). Furthermore, YopD facilitates a positive effect on the transcripts of RNase E and PNPase leading to increased levels of both RNases. The increase of these RNases leads to increased degradation of the *lcrF* transcript and thereby repressing the whole system including the T3SS, Yops, and YadA (Kusmierek *et al.* 2019).

However, the synthesis of the T3SS and the Yop effector proteins is very strongly and rapidly induced upon host cell contact, promoting the hypothesis, that they are regulated on the translational level in addition. Due to the many factors that contribute to translation, several factors and the ribosome itself might be part of the translational control of bacterial virulence factors. For instance, it was reported that bacteria can manipulate the function of the ribosome, during persistence (Byrgazov *et al.* 2013; Cho *et al.* 2015).

This study, therefore, focused on the analysis of the translational control of the T3SS-associated virulence factors of *Y. pseudotuberculosis*. It was shown in the study, that the expression of the T3SS structure components is uncontrolled on the translational level, while the mRNAs of the *yop* effector proteins and the adhesin *yadA* show an increased translation which was dependent on the translocon pore protein YopD. Furthermore, the tRNA pool of *Y. pseudotuberculosis* was found to change upon a shift from 25°C to 37°C, representing the host body temperature, which was found to support the strong translation of the *yop* and *yadA* mRNAs.

4.1 The Ribo-Seq analysis demonstrates high expression and synthesis of the *ysc*, *yop,* and *yadA* genes under secretion conditions

As reported for all human pathogenic *Yersinia* species, the expression of the T3SS and the Yops increases strongly upon cell-contact and under secretion conditions. This increase is achieved by the transcriptional activator LcrF, which triggers transcription of the *ysc-yop* and *yadA* genes (Böhme *et al.* 2012; Bölin *et al.* 1988, 1985; Hoe and Goguen 1993; Milne-Davies *et al.* 2019; Schwiesow *et al.* 2015; Steinmann and Dersch 2013; Straley and Bowmer 1986). LcrF encoded on the virulence plasmid, is itself strongly upregulated upon cell-contact and under secretion conditions, while it is repressed in the absence of cell-contact and under non-secretion conditions (Hoe and Goguen 1993; Kusmierek *et al.* 2019; Li *et al.* 2015; Miller *et al.* 2014; Schwiesow *et al*. 2015; Steinmann and Dersch 2013). The LcrF-dependent activation of the *ysc, yop,* and *yadA* gene transcripts was observed in several transcriptomic (RNA-Seq) approaches *in vivo* and *in vitro* (Kusmierek 2018; Nuss *et al.* 2015, 2017; Vollmer 2020). However, influence on translation was never analyzed, due to the lack of suitable high-throughput methods. Based on the development of new sequencing methods called Ribo-Seq, the influence of translation can nowadays be addressed (Ingolia *et al.* 2009). According to Ingolia *et. al.* (2009), this method allowed the analysis of the transcriptome and the translatome in one sample and allowed a correlation of both to each other. To analyze the translatome and possible translational regulations of *Y. pseudotuberculosis*, the method of Ribo-Seq was established in this work. Therefore, the *Y. pseudotuberculosis* (YPIII) wildtype, as well as the *csrA* and *yopD* mutant strains, grown under three different *in vitro* conditions, were analyzed. The first growth condition was 25°C which represents "*environmental*" growth under which the T3SS is not expressed. The second one was growth at 37°C under which the *ysc*, *yop,* and *yadA* are genes are express on a low level while the third condition was 37°C with calcium depletion (-Ca^{2+}) which triggers Yop secretion into the growth medium and on the other hand leads to *ysc, yop* and *yadA* expression on a high level. The Ribo-Seq analysis of this work is the first reported analysis in which the overall translation of *Y. pseudotuberculosis* is compared with the transcriptome under T3SS-active conditions in a pathogenic bacterium including mutants affecting the T3SS regulation. Overall, this analysis support published transcriptome data of *Yersinia* virulence genes (Nuss *et al.* 2015, 2017). Moreover, the data revealed significant differences between analyzed regulator-deficient mutants compared to the wildtype.

The results obtained for the wildtype grown at 25°C showed that the virulence plasmid-encoded genes nearly unexpressed, while an increase of the temperature to 37°C triggers a low activation of the genes which was strongly increased under Yop secretion conditions. This observation is supported by earlier studies of different researchers which showed that the virulence plasmid-encoded genes are only low expressed when the bacteria are grown at 37°C but show a strong expression under Yop secretion conditions or cell-contact conditions (Böhme *et al.* 2012; Bölin *et al.* 1988, 1985; Kusmierek 2018; Kusmierek *et al.* 2019; Nuss *et al.* 2015, 2017; Plano and Schesser 2013; Straley and Bowmer 1986; Vollmer 2020). A similar pattern was observed for the synthesis (translation) of the virulence plasmid-encoded genes, especially for the T3SS and Yop proteins. The deletion of *csrA* results in a similar transcription pattern of the virulence plasmid-encoded genes, while most of the transcribed virulence

genes are not translated which leads to an avirulent phenotype. In fact, a *csrA* mutant was found to be avirulent in a mouse infection model (Nuss *et al.* 2017). Also in other pathogens, it was shown that CsrA is crucial for virulence, e. g. in *Vibrio cholera* in which a mutation in *csrA* leads to attenuation in an infant mouse model (Mey *et al.* 2015). Similar observations were made for the CsrA analogon RsmA from *Pseudomonas*. Loss of RsmA in *Pseudomonas aeruginosa* leads to reduced colonization during the initial stages of an acute infection (Mulcahy *et al.* 2008).

In contrast, the *yopD* mutant shows the secretion-blind phenotype, with increased expression of the T3SS and the Yop proteins and secretion of the Yop proteins already visible at increased temperature without a secretion signal. This observation is in full agreement with previous reports analyzing the expression of individual *yop* and T3SS genes and their effect on secretion (Chen and Anderson 2011; Fowler *et al.* 2009; Jessen *et al.* 2014; Kusmierek 2018; Kusmierek *et al.* 2019; Williams and Straley 1998).

4.1.1 The mRNAs of the *yop* and *yadA* genes are controlled on the translational level when cultivated at 37°C

To analyze whether the virulence-plasmid encoded virulence factors are more efficiently translated under secretion conditions, the translation efficiency (TE) was determined. The more detailed analysis of the translation efficiency (TE) of the *ysc*, *yop*, and *yadA* transcripts revealed, that all of the genes of these virulence factors are highly transcribed under secretion conditions which is in agreement with former studies (Bölin *et al.* 1982; Straley and Bowmer 1986). The TE is the rate of transcript translation in cells and is used to identify if a gene is regulated on the transcriptional level or the translational level (Chothani *et al.* 2019; Ingolia *et al.* 2009; Xiao *et al.* 2016). High expression of effector proteins and T3SS components was also observable in *Yersinia* and other pathogenic bacteria under T3SS-active conditions previously without the use of high-throughput sequencing (Yerushalmi *et al.* 2014). However, the TE calculation in this study represents the first comparison of the transcriptome and the translatome of a pathogen by a combined sequencing approach. The expression of most T3SS components in *Yersinia* is equally upregulated on the transcriptional and translational level resulting in a TE of one under secretion conditions. This demonstrated that the strong upregulation of the T3SS and Yop and YadA proteins was mainly achieved by upregulation of the transcription and a general high translation efficiency of the *ysc*, *yop,* and *yadA* transcripts. Strong upregulation on the transcriptional level, is consistent with previous analysis by Kusmierek (2018) and Vollmer (2020) (Kusmierek 2018; Vollmer 2020). The transcription process is generally faster than translation when comparing the RNAP elongation speed of 5 to 60 nucleotides per second in the rRNA genes and between 250 to 400 nucleotides per second in intergenic regions to 22 codons per second in translation (Chen *et al.* 2015; Dennis *et al.* 2009; Großmann *et al.* 2017; Sørensen and Pedersen 1991). This shows that RNAP can polymerase nucleotides at a much faster speed than the ribosome can synthesize peptide-bonds. To reach the same level of reading coverage in the translatome of the Ribo-Seq approach, the ribosome needs to interact with the mRNA with a very high binding affinity (Evfratov *et al.* 2017; Ma *et al.* 2002; Park *et al.* 2007). The fact that the translation efficiency of the virulence plasmid-encoded genes is about 1 under secretion conditions indicates that translation initiation and elongation is highly efficient and allows the synthesis of high levels of T3SS, Yop, and YadA proteins.

At 37°C under non-secretion conditions, the *ysc-yop* and *yadA* genes are only slightly activated on the transcriptional level but the translation is less efficient, especially for the *yop* and *yadA* transcripts, suggesting repression of translation. A multi-omic approach (transcriptome and proteome) in *Y. pestis* and *Y. pseudotuberculosis* also showed increased transcript levels of the *ysc* and *yop* genes with the shift from 28°C to 37°C while an increase on protein level was not observed for *Y. pseudotuberculosis* while a slight increase was observed for *Y. pestis* which also leads to the suggestion of translational repression (Ansong *et al.* 2013). In the absence of the translocator YopD, this repression was removed. The absence of YopD mimics secretion even without a secretion signal (Fowler *et al.* 2009; Williams and Straley 1998). The *yop* and *yadA* transcripts showed a stronger upregulation of translational compared to transcription. This is consistent with previous studies showing a strong expression and secretion of Yop proteins in a *yopD* deletion mutant (Francis *et al.* 2001; Kusmierek *et al.* 2019; Williams and Straley 1998). Moreover, a strong upregulation and secretion of the T3SS system can also be observed is also present in other pathogenic bacteria such as *Salmonella enterica* and *Shigella flexneri* when their translocator protein *sipD* of *ipaD* are deleted (Glasgow *et al.* 2017; Roehrich *et al.* 2013). This indicates that translational repression by T3SS translocators is conserved among gram-negative bacterial pathogens. YopD is a known to have the ability to interact with RNA and control expression of the *ysc-yop* genes (Chen and Anderson 2011; Kusmierek *et al.* 2019). This and the results of this study support that YopD contributes to the regulation of the system by interfering with translation. This interference could be achieved by the binding of YopD to the 5'UTR of the *ysc* and *yop* transcripts which would block translation initiation.

The stronger differences in the upregulation of translational compared to transcription for the *yop* and *yadA* transcripts in contrast to the *ysc* transcripts might be important for the stoichiometry between the T3SS and the Yop proteins. This is important because one T3SS is capable of secreting or translocating many effector proteins. On the other hand, the T3SS can only transport Yop proteins if a pool of Yop proteins is present in the bacterial cell which is faster refilled than secreted or translocated by the T3SS. Significant higher synthesis of the Yop proteins is required so that a high amount can be translocated into innate immune cells to inhibit phagocytosis (Viboud and Bliska 2001). It was shown for the T3SS itself that the stichometry is important to build a functional T3SS that is able to translocate Yop proteins (Zilkenat *et al.* 2016). A significantly higher amount of Yop proteins compared to other T3SS components with a similar increase in transcript levels in the *yopD* mutant could be achieved by a translational advantage of the *yop* transcripts. Stronger upregulation of the translation of *yop* transcripts under secretion conditions is less pronounced in the presence of YopD. This could be explained by the fact that YopD although secreted is still produced in the bacteria and is never completely absent as in the Δ*yopD* mutant strain.

4.2 The mRNA of the *yop* transcripts is optimized for a rapid translational response

The fact, that the *yop* mRNAs are efficiently translated was further investigated. It was found, that this high efficient translation is supported by the nature of the 5' UTR of the *yop* transcripts. It is known that two phases of translation can contribute to the high translational efficiency: (i) regulation of the

translation initiation, and/or (ii) translation elongation (Goyal *et al.* 2015; Gualerzi and Pon 2015; Milón and Rodnina 2012).

To analyze the effect on the translation initiation, the 5' UTR of the *yop* transcripts were determined based on the transcriptome of the Ribo-Seq and a special 5' end read counting. It was reported in different studies, that different regions in the 5' UTR of mRNAs contribute to the translation initiation and to the switch to elongation. The important regions include the RBS (Shine-Dalgarno sequence), the start codon, and an AU-rich content of the 5' UTR (Ma *et al.* 2002; Ringquist *et al.* 1992; Shine and Dalgarno 1975). The first observation showed, that all analyzed 5' UTRs of the *yop* transcripts contain an extended RBS and a canonical AUG start codon. This structure represents the most abundant group of mRNAs with an RBS-carrying 5' UTR in prokaryotes (Srivastava *et al.* 2016), including the 5' UTRs of known highly translated genes such as the ribosomal proteins. The combination of an extended RBS together with AUG as the first codon further increases translation efficiency (Ma *et al.* 2002).

Additional components responsible for an increased translational efficiency are the RBS itself, as well as the AU-content of the 5' UTR and possible enhancer sequences upstream of the RBS (Evfratov *et al.* 2017; Ma *et al.* 2002; Takahashi *et al.* 2013). All *yop* transcripts contain extended highly conserved RBS sequences that can interact with 4 to 8 nucleotides with the anti-Shine-Dalgarno sequence in the 16S rRNA. Typical interaction sites for an RBS harbor 4 to 5 interacting nucleotides. It was reported that longer RBS regions increase the translational efficiency in bacteria, due to a better recruitment of ribosomes, based on a more stable interaction between the RBS and the anti-Shine-Dalgarno sequence (Evfratov *et al.* 2017; Ma *et al.* 2002; Park *et al.* 2007). However, an *in vitro* kinetic approach, also revealed that the ribosome is recruited better but can also show a slow dissociation from the initiation site (Takahashi *et al.* 2013). Although no statements can be made for the dissociation of the ribosome from the initiation site, large amounts of ribosomes were found to cover and promote the translation of virulence-associated genes on the virulence plasmid. In particular, the *yop* transcripts show this observation in the Ribo-Seq analysis, indicating that the dissociation from the initiation site is not affected in this context.

In addition to the extended RBS, the 5' UTRs of the *yop* transcripts are very AU-rich (>60%), in comparison to the AU-content of the chromosome. This can contribute to the high translational efficiency in two ways. First, it can act as an enhancer element for translation initiation by facilitating the interaction with the S1 protein, present in *Yersinia* spp. (Park *et al.* 2007). The S1 protein binds the transcripts and assists in the unfolding of secondary structures. Furthermore, it can support binding of S1 to the initiation complex (Duval *et al.* 2013; Takahashi *et al.* 2013). Through its function, S1 can assist in the translational initiation but also in recruiting the transcripts to the ribosome and forming the translational initiation complex. Moreover, short AU-rich 5' UTRs of *yop* and *yadA* transcripts are unlikely to form strong secondary structures. Unstructured and weakly-structured transcripts allow a more efficient docking of the 30S subunit of the ribosome to form the translation initiation complex which can increase translational efficiency (Duval *et al.* 2013; Evfratov *et al.* 2017; Takahashi *et al.* 2013). For this function, the S1 protein is not important, due to the unfolded structure of the mRNA. Hence, it can be said that the *yop* and *yadA* transcripts encode typical features that allow highly efficient translation initiation.

Notably, a short 5' UTR with around 50 nucleotides and their effect on translation was also shown for IpaH 9.8 from *Shigella flexneri*, indicating that this feature might be conserved in other T3SS expressing pathogens. However, this was not reported for IpaH 7.8 or other effector proteins in *Shigella flexneri* (Bongrand *et al.* 2012).

4.3 Synthesis of YopE is additionally regulated at the post-translational level

In the case of the *yopE* transcript, which contains a short AU-rich 5' UTR structure as all *yop* transcripts, the synthesis of YopE induced from the arabinose promoter only results in YopE production under secretion conditions. In contrast, the synthesis of all other Yop proteins from the inducible arabinose promoter was achieved under all tested conditions. This suggested that YopE is, apart from the increased translation efficiency, also regulated additionally on the post-translational level. In other studies, it was shown, that free YopE protein inside of the bacterial cell needs its cognate chaperon SycE to be stabile (Bliska *et al.* 1993; Woestyn *et al.* 1996). Furthermore, the chaperon is needed to secret YopE by the T3SS (Lee *et al.* 1998; Wattiau and Cornells 1993). Free YopE is rapidly degraded in the bacterial cell (Cheng *et al.* 1997). Therefore, it is only possible to express YopE with SycE present in the cell. Besides this, it was shown that the level of YopE in the cell is strongly regulated by LcrQ (YscM), because loss of *lcrQ* leads to increased levels of YopE (Sorg *et al.* 2005; Wulff-Strobel *et al.* 2002). Based on this fact, it should be possible to express YopE in an *lcrQ* deletion mutant or when the chaperon *sycE* is overexpressed. Surprisingly, a FLAG-tagged version of *yopE* was only detectable under secretion conditions. An explanation could be that native YopE is still present in an Δ*lcrQ* mutant. This could reduce the amount of SycE available for the artificially expressed YopE-FLAG. On the other hand, this could also explain, why it is only detectable under secretion conditions, due to the fact that it is secreted from the bacterial cells and no longer affected by cellular degradation.

4.4 The strong translation might contribute to a rapid induction of the T3SS in an LcrF-independent manner

To further analyze the role of the observed highly efficient translation of the *yop* transcripts during the process of T3SS induction, their expression kinetics were determined. For the *yop*-activator encoding gene *lcrF*, it was already shown that the expression is upregulated in two steps, with a first weak increase upon temperature shift and/or cell-contact, respectively. A second, strong upregulation occurs at a later timepoint (70 minutes) after temperature shift and/or cell-contact while the Yops are already synthesized (Cornelis 1993; Kusmierek *et al.* 2019). A similar two-step upregulation can be observed for the *yop* genes with a fast upregulation and a further continuous upregulation later on, on the transcript but especially on protein level when Yop secretion is highly induced. Interestingly, the second continuously high upregulation of *yop* genes was only observed, when the LcrF activator protein was produced while the first upregulation was observed when LcrF was still undetectable. When the *yopD* gene, encoding the translocator, was deleted, the continuously high upregulation starts earlier, directly following the first fast upregulation. Furthermore, a low amount of Yops was still observable in an *lcrF* deletion mutant. These results contradict previous data showing that the *ysc-yop* and *yadA* genes are controlled by LcrF

and should, therefore, only be expressed in an LcrF-dependent manner (Böhme *et al.* 2012; Hoe and Goguen 1993; Kusmierek *et al.* 2019; Skurnik and Toivanen 1992; Yother *et al.* 1986). It should be mentioned, that most of the published studies did not assess the effect of LcrF on the kinetics of Yop expression. They only focused on secreted but not intracellular Yops and studied Yop expression only two to four hours after secretion induction. The later strong induction of the Yop synthesis is clearly LcrF-dependent and in full agreement with the published data. However, the initial weaker induction of *yop* gene expression is likely to be driven by another factor than LcrF. This could lead to a fast response that is characterized by a weak transcription but could benefit from the general high efficient translation identified in this study. This would ensure a first anti-phagocytotic response to overcome the initial attack of the first immune cells reaching the bacteria. On the other hand, the LcrF-driven strong expression would provide the armory for encountering the high number of recruited macrophages and neutrophils at later time points of the infection.

Based on the results obtained in this study, the alternative sigma factors RpoE and RpoS were identified as possible candidates prone to activate the transcription of the *yop* genes for the first fast response. Both alternative sigma factors were upregulated upon a temperature shift from 25°C to 37°C. However, RpoS was directly excluded from the candidates because it showed no effect on the virulence of *Y. pseudotuberculosis* (Nuss *et al.* 2017) (Nuss, unpublished data). RpoE seemed a very likely candidate, because it is present in the cell at the inner membrane in an inactive form at all times and can be activated by different external stress signals (Campbell *et al.* 2003; Missiakas *et al.* 1997; Rowley *et al.* 2006). Upon activation, RpoE activates transcription of its own gene located in an operon with *rseABC* which in their part regulate RpoE activation. RseA and RseB function as negative regulators of RpoE activation, whereby RseA works as an anti-sigma factor for RpoE, while RseB binds to RseA and supports the negative effect of RseA (Missiakas *et al.* 1997). In contrast, RseC facilitates a positive effect on the activation of RpoE and is thought to act as an anti-anti sigma factor for RseA (Missiakas *et al.* 1997). Moreover, in a mouse infection study, expression of the *rpoE-rseABC* operon was shown to be activated during *Y. pseudotuberculosis* colonization of the Peyer's patches (Nuss *et al.* 2017). Some of the activating signals for RpoE release are heat stress, oxidative stress, or osmolarity stress, all of which are stresses encountered during an infection (Amar *et al.* 2018; Nuss *et al.* 2013; Palonen *et al.* 2013). In *Salmonella enterica,* it was reported that RpoE activation affects effector genes of the T3SS encoded on the pathogenicity island SPI-2. This includes the effector gene *sseB* which is also regulated by SsrB which is important for virulence and survival in phagosomes (Osborne and Coombes 2009). In addition to human pathogens, it was also shown that AlgU, the RpoE homolog from *Pseudomonas spp*., is important in the virulence of the plant-pathogen *Pseudomonas syringae* by regulating T3SS-associated virulence genes such as the *hrp* genes encoding the T3SS itself (ex. *hopP1, hrpA1, hrpZ, shcA*) and effector proteins (ex. *hopY1, hrpB, hrpE, hopE1*) (Markel *et al.* 2016). Also, a positive effect of RpoE in *Y. pseudotuberculosis* was suggested based on increased levels of secreted Yop proteins in a Δ*rseA* mutant (Carlsson *et al.* 2007). In contrast to these assumptions, this study showed that a deletion of the *rpoE-rseABC* operon has no considerable effect on *yop* gene expression and secreted proteins. Concerning the differences in mutation construction, it should be mentioned that the reported *rseA* and *rpoE* knock-out mutants were in-frame deletion and thereby resulted in the disruption of a single gene (Carlsson *et al.* 2007; Palonen *et al*. 2013), leaving the surrounding genes

of the *rpoE-rseABC* operon unaffected. In this study, however, the whole operon was replaced by a kanamycin cassette. In *E. coli* it was shown, that RseB and RseC also have functions in regulating RpoE activity. RseB, like RseA, is a negative regulator of RpoE present in the periplasm, while RseC is a positive regulator of RpoE activation (Missiakas *et al.* 1997). Thus, it is possible that the deletion of the entire operon affects the function of RseC, which is still present in the mutant used by Carlsson *et al.* (2007). Furthermore, it was reported, that RseC is able to facilitate positive effects independent of RpoE but how is still unknown (Beck *et al.* 1997; Missiakas *et al.* 1997).

An independent study in *Y. enterocolitica* showed that the phage shock protein (Psp) system is required for virulence (Darwin and Miller 2001). The Psp system is also induced by membrane stress, heat, or osmolarity as reported for RpoE, hence both systems might be active at the same time (Brissette *et al.* 1990; Rowley *et al.* 2006). The Psp system possesses a transcriptional activator (PspF) that can interact with σ^{54} (RpoN) and is thought to thereby support transcription of closed promoter regions such as *nifH* of *S. meliloti* (Bordes *et al.* 2003). It was also shown that the Psp system is important for the virulence of *Salmonella enterica* by supporting the uptake of ions like Zn^{2+} through the activation of the Zn^{2+} transporter ZupT. This activation is important for *S. enterica* to survive in macrophages (Karlinsey *et al.* 2010). Furthermore, the Psp system was strongly upregulated in *Shigella flexneri* during infection of macrophages (Lucchini *et al.* 2005). The Psp genes were also upregulated at 37°C and secretion as seen in the transcriptome and translatome analysis. Thus, is possible that expression of the *ysc-yop* and *yadA* genes is facilitated by the Psp system.

4.5 Changes in the tRNA pool allow an optimized translation elongation, enhancing Yop expression

As mentioned previously (see chapter 4.1), translation elongation is a second important component in determining the translation efficiency. This is especially evident when the assumed time required for translation initiation is compared with the time for elongation. While the former can be assumed to be one second per initiation, the elongation can only proceed with 6 to 22 amino acids per second (Mitarai *et al.* 2008; Sørensen and Pedersen 1991; Wohlgemuth *et al.* 2011). The one second per translation initiation is a general assumption of different studies that determine the times for the different steps in translation in *E. coli* (Mitarai *et al.* 2008; Wohlgemuth *et al.* 2011) For YopJ/YopP, which was analyzed exemplarily in this study, this suggests, that translation elongation would require between 13 seconds and 48 seconds while initiation would only need around one second. This illustrates the strong effect of translation elongation on translation efficiency, due to the time-limiting quality of this step (Mitarai *et al.* 2008; Wohlgemuth *et al.* 2011). Furthermore, it is important to enable a fast translation of all codons to reduce the number of ribosome collisions on one mRNA. Ribosome collision can strongly reduce the efficiency of translation. After the collision, ribosomes would stay on the mRNA without further function and would block the transcript for translation. Additionally, this would lead to unorganized dissociation of the ribosome from the mRNA (Mitarai *et al.* 2008; Zhang *et al.* 2010). To determine whether elongation of *yop* gene transcripts is optimized, the codons usage, as well as the tRNA levels, were analyzed. The impact of the codon usage in combination with an increase of certain tRNAs for the synthesis of *yop* and *yadA* transcripts was never before analyzed in pathogenic bacteria.

During codon usage and tRNA analysis, it was observed that not all codons in *Y. pseudotuberculosis* encode a cognate tRNA gene. The observation that not all codons encode a cognate tRNA was also made for other enterobacteria like *Salmonella enterica*. It is thought that this lack of tRNAs is overcome by the codon bias and the wobble theory of the base interaction, such as recognition of multiple codons by certain tRNAs (Rojas *et al.* 2018). Moreover, it was shown that most of the frequently used codons encode a tRNA while less used codons are more likely to lack one (Rojas *et al.* 2018). In most cases, this is in full agreement with the observations made in this study. However, one striking difference is that one of the most abundant codons detecting aspartic acid (GAU) lacks a tRNA and is thought to be recognized by the alternative tRNA detecting the codon GAC. This recognition by alternative tRNAs is further supported by the wobble hypothesis where uracil (U) can also interact with a U (U-U) as well as with cytosine (C) (U-C) (Crick 1966). The wobble hypothesis agrees with the observation that most of the missing tRNAs would recognize a U at the third position of the codon, while the tRNA recognizing a C at the third position are present in the genome. Furthermore, a *superwobbling*, which allows the identification of even more codons by less cognate tRNAs is shown in the plant organism *Nicotiana tabacum* (Rogalski *et al.* 2008). Due to the similarity in translation elongation between bacteria and eukaryotes (e. g. plants), it can be assumed that *superwobbling* is also possible in bacteria. Overall, the data show that the tRNA genes encoded in the genome represent the most abundantly used codons with small differences between different bacteria.

Besides the tRNA genes, also the codon usage is important for translation efficiency. The housekeeping genes of *E. coli* generally exhibit a strong bias towards certain codons, which normally correlate with the most abundant codons (Frumkin *et al.* 2018). In the case of the *Y. pseudotuberculosis* virulence plasmid pIB1, the genes are more unbiased which includes also rare codons. Furthermore, these most abundant codons often encode a cognate tRNA (Frumkin *et al.* 2018). In the study of Frumkin *et al.* (2018), it was shown that the translation efficiency of highly expressed genes in *E. coli* is reduced when the codon usage is changed from abundant codons to rare codons, while the other way around translation efficiency is increased. Here, we confirm these observations that the highly expressed genes (e. g. ribosomal proteins, translation, glycolysis, transcription) show a biased codon usage which represents the most abundant codons in *Y. pseudotuberculosis*. On the other hand, the *yop* genes show a more unbiased codon usage without such a strong bias towards highly abundant codons. This would normally result in low translation efficiency since the needed tRNAs are rare (Frumkin *et al.* 2018; Zhong *et al.* 2015). In fact, the *yop* genes are not always highly expressed such as the genes encoding translation, glycolysis, or transcription components. They are only strongly induced in a virulence-relevant situation (e. g. secretion). To allow high efficient translation of the *yop* transcripts, a change in the tRNAs under this conditions is an easy way to overcome this limitation (Wohlgemuth *et al.* 2013; Zhong *et al.* 2015). So far, changes in the tRNA pool under different environmental conditions are often neglected and it is often generally assumed that it remains constant under any condition (Wohlgemuth *et al.* 2013). However, an adjustment of tRNA levels would improve the translation efficiency of the *yop* transcripts without altering the availability of tRNAs for other transcripts. This fits observations from *E. coli* for which it was shown that increased tRNA levels for codons encoded in oxidative stress genes improve the adaptation to oxidative stress (Zhong *et al.* 2015). Based on this observation, an increase of tRNA levels important for the decoding of the *yops* transcripts would greatly increase the translation

efficiency by reducing (i) the time required for elongation and (ii) the stalling and collision of ribosomes on the transcripts. In fact, the strongest upregulated tRNAs in *Yersinia* under secretion conditions represents rarely used codons on a genomic scale, while they are more frequently used in *yop* genes (e. g. serine [UCA and UCU], arginine [AGA], or isoleucine [AUA]).

When *Y. pseudotuberculosis* is cultivated *in vitro* under secretion conditions (37°C with Ca^{2+} depletion), the strains are arrested in growth while they use the T3SS to secret the effector Yops into the growth media (Perry *et al.* 1986; Sample *et al.* 1987; Schwiesow *et al.* 2015). A study by Hooker-Romero *et. al.* (2019) already showed that the oxygen level and iron availability have a strong effect on the growth arrest of *Yersinia* under T3SS active conditions (Hooker-Romero *et al.* 2019). Besides, changes in the pH were also reported to affect the growth of *Yersinia* and can lead to growth arrest (Keto-Timonen *et al.* 2018). Interestingly, similar to the growth arrest *Yersinia* encounters under secretion conditions, *E. coli* challenged with oxidative stress start degrading tRNAs, which leads to reduced growth, while cell viability and protein production are mostly unaffected (Zhong *et al.* 2015). It was shown that this was due to a reduced speed of translation elongation. This was beneficial for the bacteria to overcome the stress and prevent misfolding of proteins (Wohlgemuth *et al.* 2013; Zhong *et al.* 2015). In the case of *Yersinia*, the expression of the T3SS components and the Yop effectors consume high amounts of tRNAs, based on the strong increase of pIB1 encoded gene translation from around < 1% of total gene translation (chromosome and plasmid) at 25°C to 2,5 % at 37°C and > 30% under secretion conditions. This may cause a reduction of the translation of other gene transcripts resulting in the growth arrest of the bacteria under secretion conditions. The increase of tRNAs supporting the translation of *yop* and the T3SS gene transcripts might, therefore, also be a method to overcome the translational arrest.

To summarize, it was shown that the increase of tRNAs decoding rarely used codons in *yop* transcripts provides a benefit for the translation of these genes under secretion conditions. Furthermore, it was shown that a lack of tRNAs for certain codons can be balanced by another tRNA recognizing a similar codon. Besides the effect on *yop* translation itself, changes of the tRNA pool might explain why *Yersinia* encounter a growth arrest under secretion condition.

4.6 Conclusion

This is the first study in which Ribo-Seq was used in pathogenic bacteria to analyze the activation of the T3SS can be analyzed. The results showed, that the effector proteins (Yops) of *Yersinia* are not only regulated at the transcriptional but also at the translational level. Different translational control mechanisms were identified which allowed a very high efficiency of *yop* transcript translation leading to strongly elevated levels of Yop proteins under secretion conditions. To inhibit over synthesis of Yop proteins under non-secretion conditions, the RNA-binding protein YopD inhibits the translation of transcripts of the *ysc-yop*, *yadA*, and *lcrF* genes. The YopD effect could be promoted through a direct interaction of YopD with the 5' UTR of the *ysc*, *yop,* and *lcrF* transcripts. Protein-RNA binding assays, performed with purified YopD protein of *Y. pestis* and *Y. pseudotuberculosis*, have shown that YopD has the capacity to interact with sequences within the 5' UTR of the *ysc*, *yop*, and *lcrF* transcripts (Chen and Anderson 2011; Kusmierek et al. 2019). However, YopD also shows the ability to bind unspecifically to many transcripts *in vitro*. So it remains to be shown whether this interaction is responsible for the

translational repression *in vivo*. Furthermore, YopD also influences RNases such as RNase E or PNPase which have an effect on transcript stability and were shown to affect the *ysc*, *yop*, and *lcrF* transcripts negatively (Kusmierek *et al.* 2019; Steinmann 2013). In this study, it was further shown that this increased translational efficiency of the *yop* transcripts is also supported by the short length of the 5' UTRs as well as a shift in the tRNA pool supporting the *yop* transcript codon usage under secretion conditions. The 5' UTRs of the *yop* transcripts were found to be AU-rich with strong, extended RBS that could contribute to the observed high translational efficiency. Furthermore, the present study showed a change of the tRNA pool under virulence-relevant conditions which favors rare codons and thus the expression of virulence-associated genes of the *Yersinia* virulence plasmid. Besides these effects on virulence, observed changes in the tRNA pool could also be responsible for a translational arrest of other genes leading to a growth arrest under secretion conditions. This growth arrest could be the result of a shift of translation towards virulence genes, which is associated with a reduction of tRNAs required for translation of housekeeping genes.

At 25°C (environmental conditions) the virulence plasmid-encoded genes are not expressed. This is due to the absence of LcrF, the master regulator of virulence. LcrF expression is blocked by the *Yersinia* modulator protein A (YmoA) at the transcriptional level and a closed RNA thermometer element that prevents translation initiation of the *lcrF* transcript located in the 5'UTR of the *lcrF* transcript (Kusmierek 2018; Kusmierek et al. 2019). Under these conditions, the majority of ribosomes occupy chromosomally-encoded transcripts and *Yersinia* expresses a tRNA pool which is optimal for the translation of chromosomally encoded transcripts (see Figure 4.1).

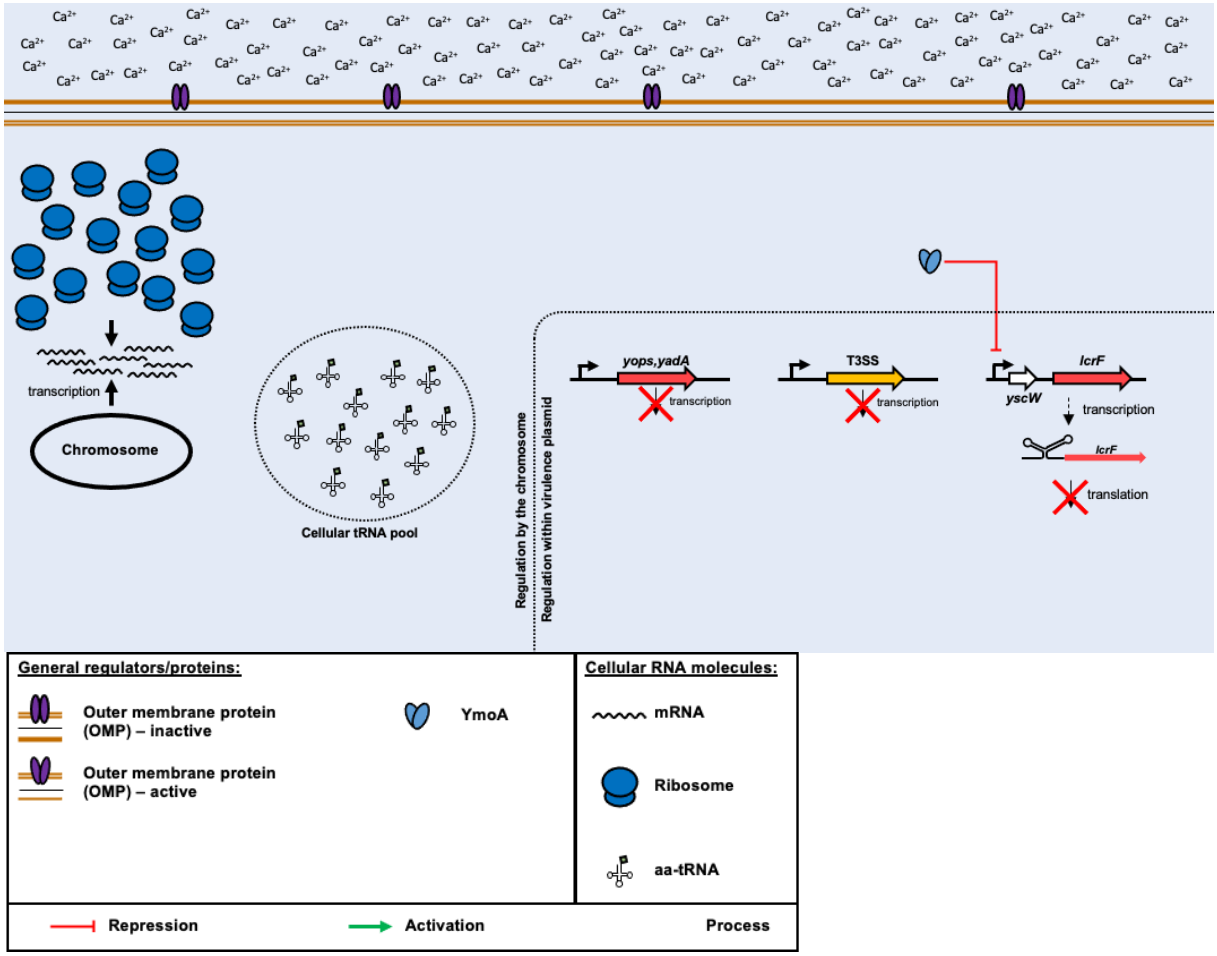

Figure 4.1) Proposed regulation scheme of the T3SS, Yop, YadA, and LcrF expression at 25°C (environmental conditions).

The figure displays repression of the virulence plasmid-encoded genes and illustrates the recruitment of ribosomes to the chromosomally encoded transcripts. Furthermore, it shows the tRNA pool of the bacterial cell which supports the translation of chromosomally-encoded transcripts. Underneath the figure, the legend explains the different components in the figure.

With an increase from environmental conditions (25°C) to 37°C, the expression of the T3SS, Yops, YadA, and LcrF is only slightly induced but maintained on a very low level. This low induction is supported by proteolytic degradation of the transcriptional repressor YmoA by ClpXP and Lon proteases (Jackson *et al.* 2004). In addition, the thermometer element in the 5' UTR of the *lcrF* transcript opens to allow translation of *lcrF* (Böhme *et al.* 2012). With the synthesis of LcrF, the plasmid-encoded *ysc*, *yop,* and *yadA* genes are transcribed and a small proportion of ribosomes start translating these plasmid-encoded transcripts, while the majority of ribosomes still translates chromosomally-encoded transcripts. YopD which is present in the bacterial cell under non-secretion conditions is implicated in the reduced translation of the plasmid-encoded transcripts, although its exact role remains unclear. This might be achieved by the interaction of YopD with the 5' UTRs of the *ysc*, *yop*, *yadA,* and *lcrF* transcripts blocking translation initiation or YopD influence on RNases degrading the *lcrF* transcript (Chen and Anderson 2011; Kusmierek *et al.* 2019). In addition, *lcrF* expression is also repressed by CsrA, the RNA-binding protein of the carbon storage regulator (Csr) system. CsrA represses the transcriptional activator RcsB which would induce transcription of the *yscW-lcrF* operon (Kusmierek 2018; Li *et al.* 2015). Upon temperature upshift, also the upregulation of certain rare tRNAs is induced which encode codons that are found in several *yop* genes and this contributes to an efficient translation of these important virulence

genes. All these regulatory components result in an improved translation, especially of the *yop* transcripts (see Figure 4.2).

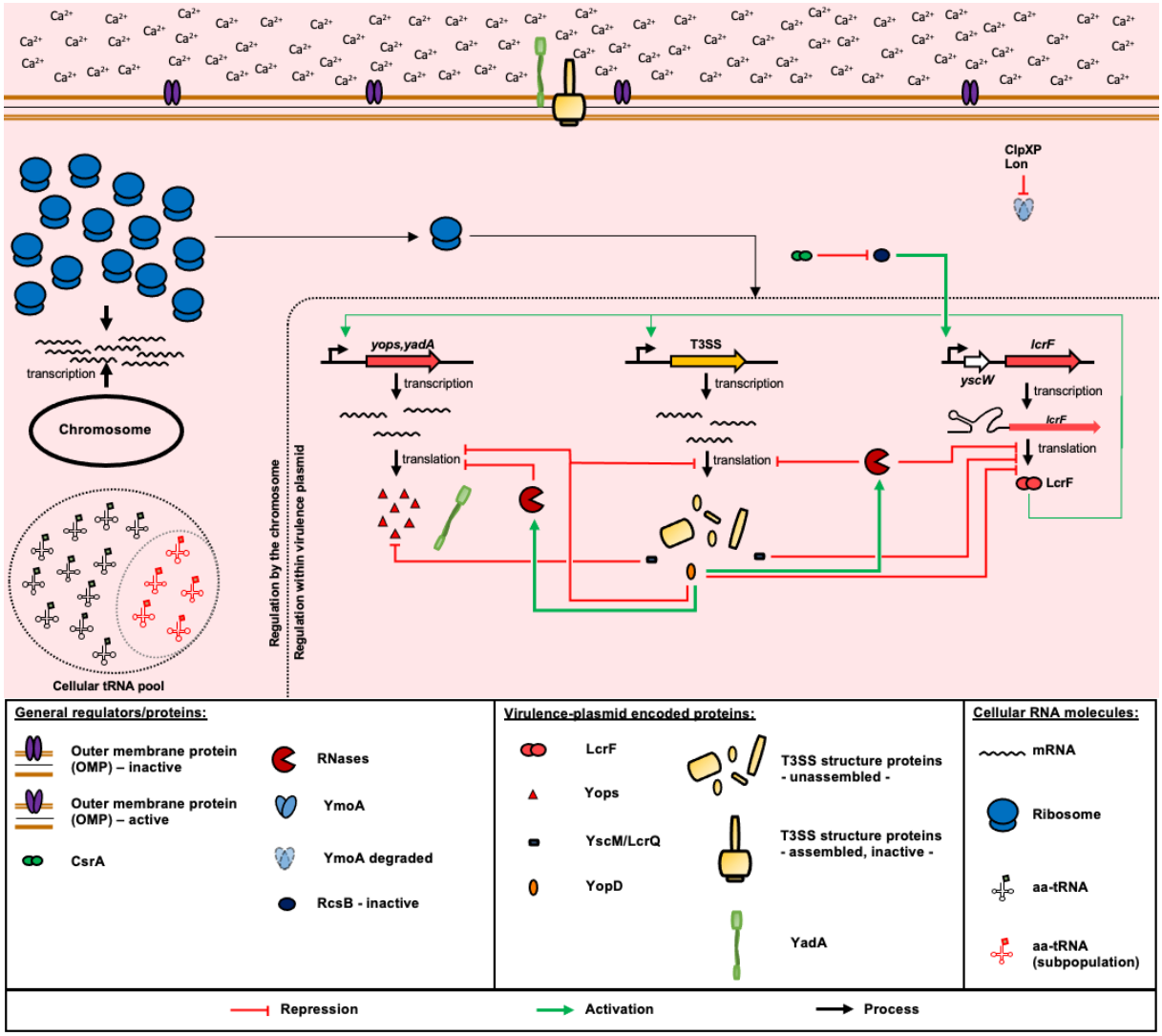

Figure 4.2) Proposed regulation scheme at 37°C under non-secretion conditions.

The figure shows regulatory changes that occur upon a temperature upshift from 25°C to 37°C. While the expression of the *ysc*, *yop*, *yadA,* and *lcrF* genes is slightly induced due to the proteolytic degradation of YmoA all components are repressed by several factors. The *ysc*, *yop*, *yadA,* and *lcrF* transcripts are repressed by YopD by direct interaction and by RNases which are positively affected by YopD. In addition, Yop proteins are negatively regulated proteolytic degradation supported by YscM/LcrQ. Expression of *yscW-lcrF* is further repressed by CsrA which represses the transcriptional activator RcsB. This results in a shift of a small proportion of ribosomes starting to translate appearing transcripts of the plasmid-encoded genes. This is supported by tRNA pool changes leading to higher levels of tRNAs (red tRNAs) that are required to decode rare codons found in *ysc* and *yop* genes. Underneath the figure, the legend explains the different components in the figure.

When in addition *Yersinia* receives a secretion signal, e. g. artificially via calcium-depletion or upon contact to innate immune cells, expression of the T3SS, Yops, YadA, and LcrF is strongly induced (Kusmierek 2018; Kusmierek *et al.* 2019). The induced response can be separated into a fast, initial response and a later or ongoing response. In the initial response, the repression of *ysc*, *yop*, *yadA,* and *lcrF* translation by YopD is released. In accordance with previous studies, this is achieved by the secretion of YopD via the T3SS. The depletion of YopD leads to an activation of *lcrF* transcription and translation together with CsrA (Kusmierek 2018; Kusmierek *et al.* 2019). This is enhanced through downregulation of *lcrF* transcript degradation by RNases such as PNPase, RNase E, and RNase III (Kusmierek 2018; Kusmierek *et al.* 2019; Vollmer 2020). Their expression is also under YopD control. Rapid accumulation of the LcrF promotes transcription of all *ysc*, *yop*, and *yadA* genes. As a

consequence, the translation machinery is efficiently recruited to plasmid-encoded transcripts, especially the *yop* transcripts. Short AU-rich 5' UTRs and the adjusted tRNA pool allow a highly efficient translation of the plasmid-encoded transcripts and a rapid increase of T3SSand Yop synthesis. Under these conditions, the level of LcrF remains relatively low in the cell and the overall increase of plasmid-encoded transcripts is moderate. In this context, the high efficiency in translation might compensate for the lower transcript amounts during the initial phase of secretion (see Figure 4.3). Transferring the data to the *in vivo* situation, this might reflect the situation in which the enteropathogenic *Yersinia* encounters the few residual macrophages after entering the Payer's patches. By the displayed initial response, the bacteria might overcome the first immune cells they encounter in this tissue.

After the fast initial response, the system changes to the later or ongoing response. In this stage, high efficiency of the translation process of the *ysc*, *yop,* and *yadA* transcripts is less important, due to the fact that LcrF reached a significantly higher level that promotes transcription of the plasmid-encoded virulence genes. As levels of the transcripts of the T3SS apparatus and Yop effector proteins increase the overall high translation rate of the plasmid-encoded virulence gene transcripts, promoted by efficient recruitment of ribosomes to the 5' UTRs and the increased tRNA pool leads to high amounts of T3SSs, Yops, and YadA (see Figure 4.4). Transferred to the *in vivo* situation, this might be in particular beneficial for the bacteria when they colonize the Payer's patches which is accompanied by massive recruitment of neutrophils to the infection sites (Nuss *et al.* 2017).

In summary, this study analyzing the influence of translational control on *ysc* and *yop* gene expression is the first under virulence-relevant conditions. The results show that translation is regulated to ensure a strong and rapid expression of virulence-associated genes only under appropriate conditions. This enables *Yersinia* to fastly counteract the immune system while the energy burden is caped as low as possible to allow survival.

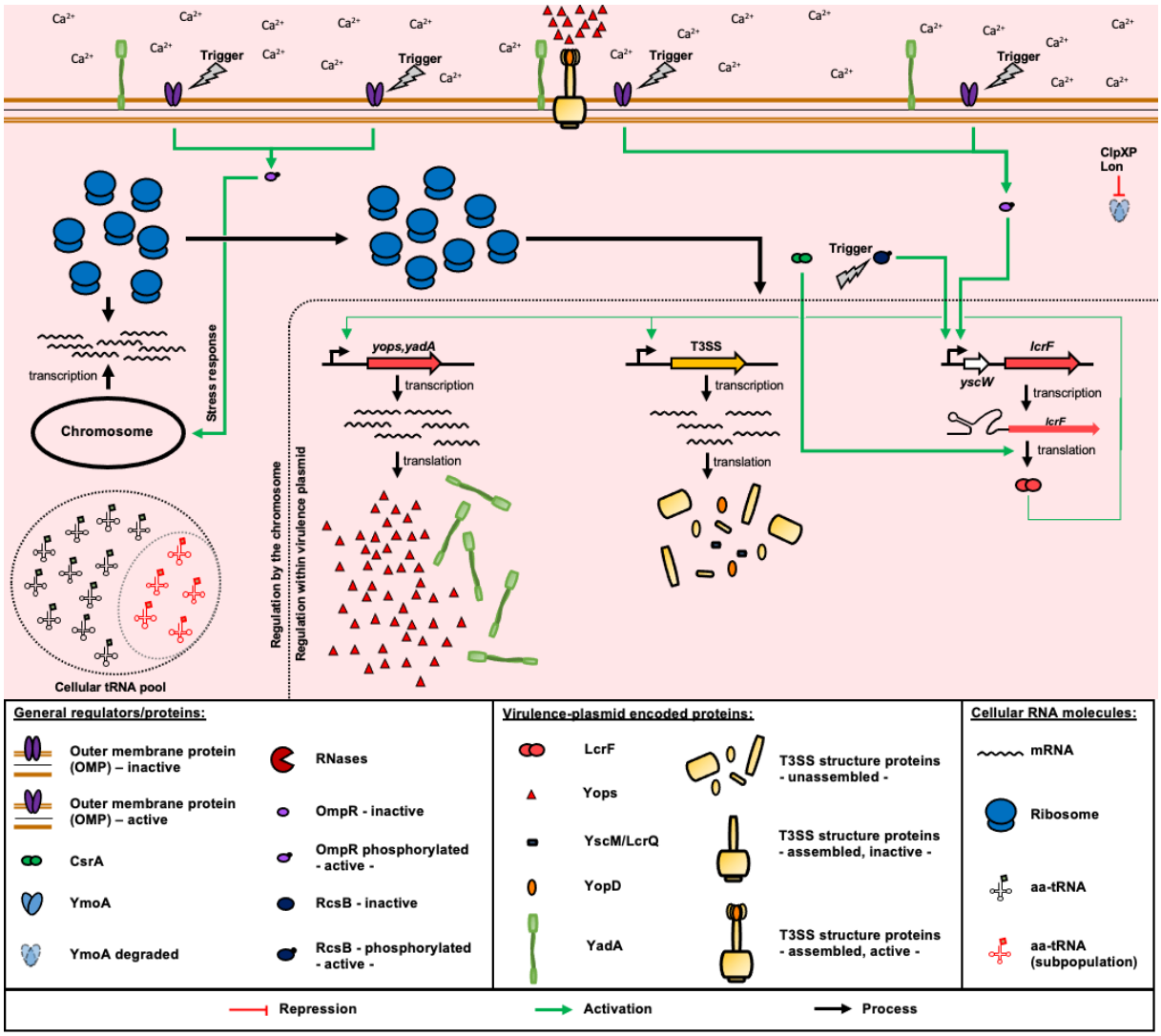

Figure 4.3) Proposed regulation schema at 37°C under secretion conditions with a fast initial response.

The figure shows changes in the regulatory network upon secretion in the initial state after receiving the secretion signal. The repressive function of YopD and YscM/LcrQ at 37°C is realized due to the secretion of both proteins into the culture medium. In addition, the positive YopD effect on RNases is also released, leading to reduced degradation of the *ysc*, *yop*, *yadA,* and *lcrF* transcripts. Furthermore, RcsB is activated and triggers transcription of the *yscW-lcrF* operon leading to increased LcrF protein level which further activates expression of the *ysc*, *yop,* and *yadA* genes. Translation of the *lcrF* transcript is additionally supported by CsrA which contributes in opening the thermometer element in the 5' UTR of the *lcrF* transcript allowing translational initiation. This results in a shift of a big proportion of ribosomes to strongly translate plasmid-encoded genes. This is supported by the already changed tRNA pool (red tRNAs) that are required to decode rare codons found in *ysc* and *yop* genes. Underneath the figure, the legend explains the different components in the figure.

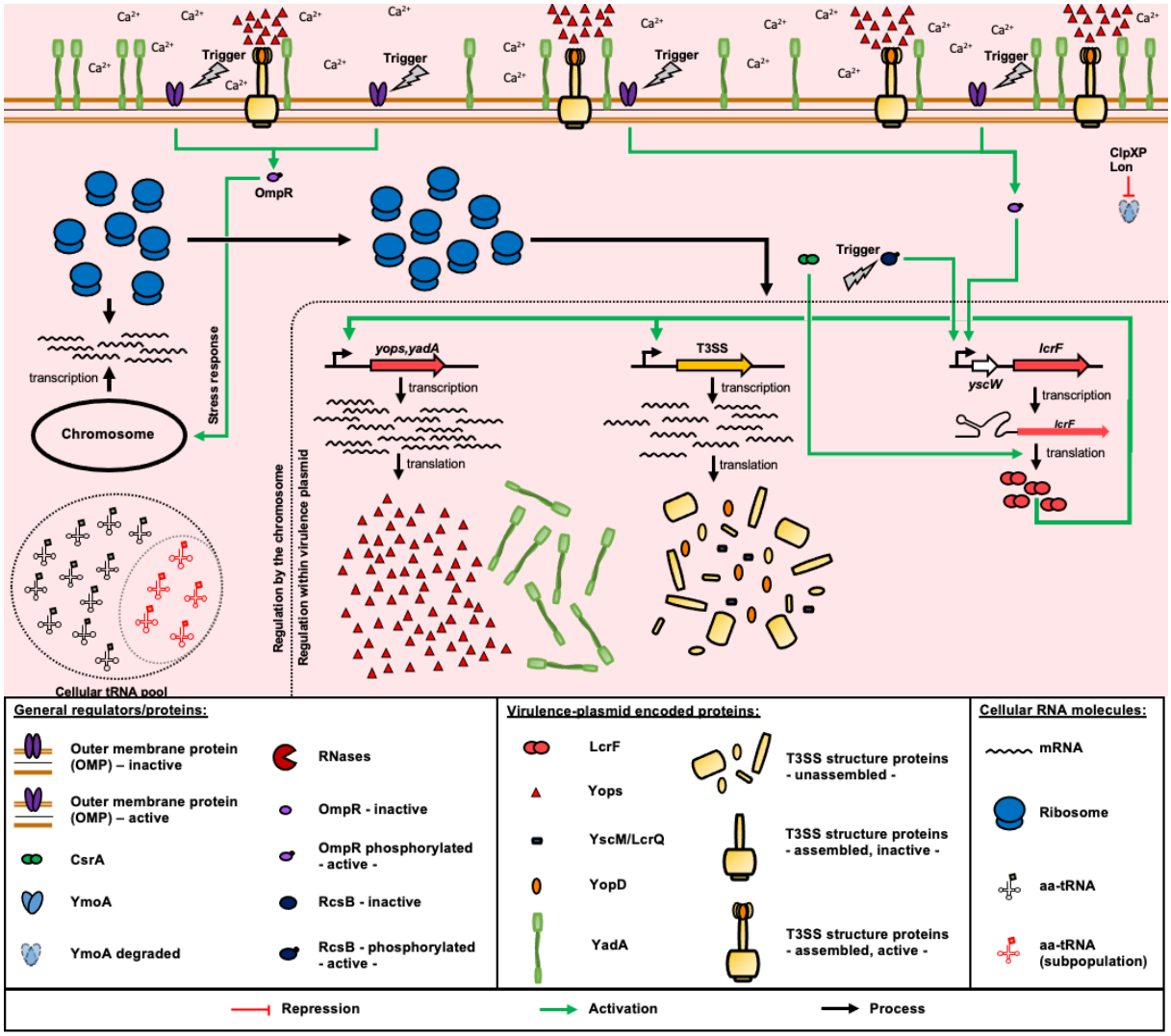

Figure 4.4) Proposed regulation schema under secretion conditions (37°C) with the later response.

After the initial secretion state, the system further increases expression of the *ysc*, *yop*, *yadA,* and *lcrF* transcripts which represents the ongoing secretion state. As in the initial secretion state, the repressive effects of YopD, YscM/lcrQ, and CsrA are released, while the activating effect of RcsB on *yscW-lcrF* transcription is still present, together with the positive effect of CsrA on *lcrF* translation. This leads to strongly increased levels of LcrF. The high levels of LcrF strongly induce the transcription of the *ysc*, *yop,* and *yadA* genes. The high amounts of virulence plasmid-encoded transcripts result in strengthen the shift of a big proportion of ribosomes to strongly translate plasmid-encoded genes. This is still supported by the already changed tRNA pool (red tRNAs) that are required to decode rare codons found in *ysc* and *yop* genes. Underneath the figure, the legend explains the different components in the figure.

5 Outlook

In the present study, the method of Ribo-Seq was established to analyze the translation of *Y. pseudotuberculosis* under T3SS active and inactive conditions at host temperature as well as under "environmental" conditions. It was shown, that the expression of virulence-associated genes coding for T3SS effector proteins is not only regulated on the transcriptional level, it is also regulated at the translational level, e. g. by an increase of the translation efficiency. This is mediated by several factors, including RNA regulators such as YopD and the adjustment of the tRNA pool of the cells to support the synthesis of these virulence factors.

Since the Ribo-Seq is a high throughput sequencing technique covering the entire translatome, a deeper look should be taken at translational control mechanism affecting genes encoded on the chromosome. Interesting candidates would be housekeeping genes, which are translationally repressed under secretion conditions without a strong reduction of their transcription. These regulations could contribute to the growth arrest during secretion conditions. Special attention should be taken to metabolic genes and pathways to see if there are changes in response to temperature and/or secretion to further understand the behavior of the bacteria under these conditions. To further improve the results obtained by the Ribo-Seq analysis, a new set of samples should be generated for deeper sequencing to generate a sufficient per codon read coverage. In addition, a Ribo-Seq approach in which translational initiation complexes are enriched by the addition of retapamulin (referred to as Ribo-RET (Meydan *et al.* 2019)) would help to identify the effect of the short AU-rich 5' UTRs of the *yop* transcripts on translation initiation and the translation efficiency. Besides this sequencing approach, the function of the 5' UTRs should be analyzed in more detail. Therefore, a library of point mutations should be introduced into the 5' UTRs to analyze their effect on translation efficiency and YopD interaction. These point mutations should affect the AU-rich region upstream of the RBS, the RBS itself, and the first codons which might also affect the translation efficiency. However, it needs to be mentioned that certain effects on translation only appear when all features are present (Evfratov *et al.* 2017; Osterman *et al.* 2013; Park *et al.* 2007). Finally, it would be of interest to test whether high translation efficiency associated with the 5' UTR regions of the *yop* genes can be transferred to other genes or if it is a special feature only functional in the context of these virulence-associated genes.

Another interesting observation which requires further analysis is the influence of tRNA pool and tRNA expression on virulence gene translation. As shown in this study, the expression of rare tRNAs that supports the synthesis of Yop proteins is upregulated. To investigate this on a genomic scale, a tRNA sequencing or microarray analysis should be performed to study tRNA expression on a global scale under the same conditions used for the Ribo-Seq. In this context, it should be tested how certain codons affect the expression of genes under different conditions by using a reporter system with exchangeable codons. Moreover, it should be analyzed if the expression of certain tRNA genes from an inducible plasmid would affect the growth of the bacteria under secretion conditions. This would also address the hypothesis that the growth arrest observed upon T3SS secretion of Yops might result from the consumption of most tRNAs used for translation of virulence-associated gene transcripts. As most experiments in this study have been performed with growth conditions that induce Yop secretion *in vitro*

it should be confirmed whether observed changes in tRNA levels are also present and affect the expression of the Yops and the T3SS when the bacteria are in contact with immune cells.

In addition to the translation efficiency, the effect of the *rpoE-rseABC* operon in the context of virulence should be analyzed in more detail. Therefore a defined inframe deletion mutant of *rpoE* should be generated to confirm the observed effect of RpoE on the expression of the T3SS components and secretion. Moreover, a *rseA* inframe deletion mutant should be generated, due to the regulatory effect of the anti-sigma factor RseA on RpoE activity. Furthermore, it should be analyzed if the (*rpoE-rseABC)*::Kan^R exchange mutant, generated in this study, shows similar characteristics as the inframe deletion mutants of Δ*rpoE* and Δ*rseA* in the publications of Palonen *et. al.* (2013) and Carlsson *et al.* (2007). Besides the analysis of the RpoE and RseA function on virulence gene expression in *Y. pseudotuberculosis,* other potential factors should be analyzed that might contribute to the expression of these genes. A potential candidate would be the Psp system which was reported to affect the expression of the *ysc* and *yop* genes somehow (Darwin and Miller 2001; Flores-Kim and Darwin 2012).

6 References

Abril, Ana G., Jose Luis R. Rama, A. Sánchez-Pérez, and Tomás G. Villa. **2020**. "Prokaryotic Sigma Factors and Their Transcriptional Counterparts in Archaea and Eukarya." *Applied Microbiology and Biotechnology* 104(10):4289–4302.

Acharya, A. S., P. B. Moore, and F. M. Richards. **1973**. "Cross-Linking of Elongation Factor EF-G to the 50S Ribosomal Subunit of *Escherichia Coli*." *Biochemistry* 12(16):3108–14.

Achtman, M., K. Zurth, G. Morelli, G. Torrea, A. Guiyoule, and E. Carniel. **1999**. "*Yersinia Pestis*, the Cause of Plague, Is a Recently Emerged Clone of *Yersinia Pseudotuberculosis*." *Proceedings of the National Academy of Sciences of the United States of America* 96(24):14043–48.

Ackermann, Nikolaus, Maximilian Tiller, Gisela Anding, Andreas Roggenkamp, and Jürgen Heesemann. **2008**. "Contribution of Trimeric Autotransporter C-Terminal Domains of Oligomeric Coiled-Coil Adhesin (Oca) Family Members YadA, UspA1, EibA, and Hia to Translocation of the YadA Passenger Domain and Virulence of *Yersinia Enterocolitica*." *Journal of Bacteriology* 190(14):5031–43.

Aepfelbacher, Martin, Claudia Trasak, Gottfried Wilharm, Agnès Wiedemann, Konrad Trülzsch, Kristina Krauss, Peter Gierschik, and Jürgen Heesemann. **2003**. "Characterization of YopT Effects on Rho GTPases in *Yersinia Enterocolitica* -Infected Cells." *Journal of Biological Chemistry* 278(35):33217–23.

Agirrezabala, Xabier and Joachim Frank. **2010**. "From DNA to Proteins via the Ribosome: Structural Insights into the Workings of the Translation Machinery." *Human Genomics* 4(4):226.

Agrain, Céline, Isabel Sorg, Cécile Paroz, and Guy R. Cornelis. **2005**. "Secretion of YscP from *Yersinia Enterocolitica* Is Essential to Control the Length of the Injectisome Needle but Not to Change the Type III Secretion Substrate Specificity." *Molecular Microbiology* 57(5):1415–27.

Aili, Margareta, Elin L. Isaksson, Sara E. Carlsson, Hans Wolf-Watz, Roland Rosqvist, and Matthew S. Francis. **2008**. "Regulation of *Yersinia* Yop-Effector Delivery by Translocated YopE." *International Journal of Medical Microbiology* 298(3–4):183–92.

Aili, Margareta, Maxim Telepnev, Bengt Hallberg, Hans Wolf-Watz, and Roland Rosqvist. **2003**. "In Vitro GAP Activity towards RhoA, Rac1 and Cdc42 Is Not a Prerequisite for YopE Induced HeLa Cell Cytotoxicity." *Microbial Pathogenesis* 34(6):297–308.

Alexaki, Aikaterini, Jacob Kames, David D. Holcomb, John Athey, Luis V. Santana-Quintero, Phuc Vihn Nguyen Lam, Nobuko Hamasaki-Katagiri, Ekaterina Osipova, Vahan Simonyan, Haim Bar, Anton A. Komar, and Chava Kimchi-Sarfaty. **2019**. "Codon and Codon-Pair Usage Tables (CoCoPUTs): Facilitating Genetic Variation Analyses and Recombinant Gene Design." *Journal of Molecular Biology* 431(13):2434–41.

Amar, Agustina, Magdalena Pezzoni, Ramón A. Pizarro, and Cristina S. Costa. **2018**. "New Envelope Stress Factors Involved in σE Activation and Conditional Lethality of RpoE Mutations in *Salmonella Enterica*." *Microbiology* 164(10):1293–1307.

Amer, Ayad A. A., Jyoti M. Gurung, Tiago R. D. Costa, Kristina Ruuth, Anton V. Zavialov, Åke Forsberg, and Matthew S. Francis. **2016**. "YopN and TyeA Hydrophobic Contacts Required for Regulating Ysc-Yop Type III Secretion Activity by *Yersinia Pseudotuberculosis*." *Frontiers in Cellular and Infection Microbiology* 6(JUN):1–17.

Anderson, Deborah M., Kumaran S. Ramamurthi, Christina Tam, and Olaf Schneewind. **2002**. "YopD and LcrH Regulate Expression of *Yersinia Enterocolitica* YopQ by a Posttranscriptional Mechanism and Bind to YopQ RNA." *Journal of Bacteriology* 184(5):1287–95.

Andersson, Kerstin, Karl-Eric Magnusson, Meytham Majeed, Olle Stendahl, and Maria Fällman. **1999**. "*Yersinia Pseudotuberculosis*-Induced Calcium Signaling in Neutrophils Is Blocked by the Virulence Effector YopH" edited by E. I. Tuomanen. *Infection and Immunity* 67(5):2567–74.

Ansong, Charles, Alexandra C. Schrimpe-Rutledge, Hugh D. Mitchell, Sadhana Chauhan, Marcus B. Jones, Young-Mo Kim, Kathleen McAteer, Brooke L. Deatherage Kaiser, Jennifer L. Dubois, Heather M. Brewer, Bryan C. Frank, Jason E. McDermott, Thomas O. Metz, Scott N. Peterson, Richard D. Smith, Vladimir L. Motin, and Joshua N. Adkins. **2013**. "A Multi-Omic Systems Approach to Elucidating *Yersinia* Virulence Mechanisms." *Mol. BioSyst.* 9(1):44–54.

Athey, John, Aikaterini Alexaki, Ekaterina Osipova, Alexandre Rostovtsev, Luis V. Santana-Quintero, Upendra Katneni, Vahan Simonyan, and Chava Kimchi-Sarfaty. **2017**. "A New and Updated Resource for Codon Usage Tables." *BMC Bioinformatics* 18(1):391.

Autenrieth, I. B. and R. Firsching. **1996**. "Penetration of M Cells and Destruction of Peyer's Patches by *Yersinia Enterocolitica*: An Ultrastructural and Histological Study." *Journal of Medical Microbiology* 44(4):285–94.

Bamyaci, Sarp, Sofie Ekestubbe, Roland Nordfelth, Saskia F. Erttmann, Tomas Edgren, and Åke Forsberg. **2018**. "YopN Is Required for Efficient Effector Translocation and Virulence in *Yersinia Pseudotuberculosis*" edited by S. M. Payne. *Infection and Immunity* 86(8).

Beck, B. J., L. E. Connolly, A. De Las Peñas, and D. M. Downs. **1997**. "Evidence That RseC, a Gene in the RpoE Cluster, Has a Role in Thiamine Synthesis in *Salmonella Typhimurium*." *Journal of Bacteriology* 179(20):6504–8.

Becker, Annemarie H., Eugene Oh, Jonathan S. Weissman, Günter Kramer, and Bernd Bukau. **2013**. "Selective Ribosome Profiling as a Tool for Studying the Interaction of Chaperones and Targeting Factors with Nascent Polypeptide Chains and Ribosomes." *Nature Protocols* 8(11):2212–39.

Bertherat, Eric. **2019**. "Plague around the World in 2019." *Weekly Epidemiological Record* 94(25):289–92.

Black, D. S. **1997**. "Identification of P130Cas as a Substrate of *Yersinia* YopH (Yop51), a Bacterial Protein Tyrosine Phosphatase That Translocates into Mammalian Cells and Targets Focal Adhesions." *The EMBO Journal* 16(10):2730–44.

Blaylock, Bill, Kelly E. Riordan, Dominique M. Missiakas, and Olaf Schneewind. **2006**. "Characterization of the *Yersinia Enterocolitica* Type III Secretion ATPase YscN and Its Regulator, YscL." *Journal of Bacteriology* 188(10):3525–34.

Bliska, J. B., M. C. Copass, and S. Falkow. **1993**. "The *Yersinia Pseudotuberculosis* Adhesin YadA Mediates Intimate Bacterial Attachment to and Entry into HEp-2 Cells." *Infection and Immunity* 61(9):3914–21.

Bliska, J. B., K. L. Guan, J. E. Dixon, and S. Falkow. **1991**. "Tyrosine Phosphate Hydrolysis of Host Proteins by an Essential *Yersinia* Virulence Determinant." *Proceedings of the National Academy of Sciences* 88(4):1187–91.

Bliska, James B. **2006**. "*Yersinia* Inhibits Host Signaling by Acetylating MAPK Kinases." *ACS Chemical Biology* 1(6):349–51.

Böhme, Katja, Rebekka Steinmann, Jens Kortmann, Stephanie Seekircher, Ann Kathrin Heroven, Evelin Berger, Fabio Pisano, Tanja Thiermann, Hans Wolf-Watz, Franz Narberhaus, and Petra Dersch. **2012**. "Concerted Actions of a Thermo-Labile Regulator and a Unique Intergenic RNA Thermosensor Control *Yersinia* Virulence." *PLoS Pathogens* 8(2).

Boland, Anne, Sophie Havaux, and Guy R. Cornelis. **1998**. "Heterogeneity of The *Yersinia* YopM Protein." *Microbial Pathogenesis* 25(6):343–48.

Bölin, I., A. Forsberg, L. Norlander, M. Skurnik, and H. Wolf-Watz. **1988**. "Identification and Mapping of the Temperature-Inducible, Plasmid-Encoded Proteins of *Yersinia* Spp." *Infection and Immunity* 56(2):343–48.

Bölin, I., L. Norlander, and H. Wolf-Watz. **1982**. "Temperature-Inducible Outer Membrane Protein of *Yersinia Pseudotuberculosis* and *Yersinia Enterocolitica* Is Associated with the Virulence Plasmid." *Infection and Immunity* 37(2):506–12.

Bölin, I., D. A. Portnoy, and H. Wolf-Watz. **1985**. “Expression of the Temperature-Inducible Outer Membrane Proteins of *Yersiniae*.” *Infection and Immunity* 48(1):234–40.

Bölin, I. and H. Wolf-Watz. **1988**. “The Plasmid-Encoded Yop2b Protein of *Yersinia Pseudotuberculosis* Is a Virulence Determinant Regulated by Calcium and Temperature at the Level of Transcription.” *Molecular Microbiology* 2(2):237–45.

Bongrand, Clotilde, Philippe J. Sansonetti, and Claude Parsot. **2012**. “Characterization of the Promoter, MxiE Box and 5′ UTR of Genes Controlled by the Activity of the Type III Secretion Apparatus in *Shigella Flexneri*” edited by N. J. Mantis. *PLoS ONE* 7(3):e32862.

Bordes, P., S. R. Wigneshweraraj, J. Schumacher, X. Zhang, M. Chaney, and M. Buck. **2003**. “The ATP Hydrolyzing Transcription Activator Phage Shock Protein F of *Escherichia Coli*: Identifying a Surface That Binds 54.” *Proceedings of the National Academy of Sciences* 100(5):2278–83.

Brar, Gloria A. and Jonathan S. Weissman. **2015**. “Ribosome Profiling Reveals the What, When, Where and How of Protein Synthesis.” *Nature Reviews Molecular Cell Biology* 16(11):651–64.

Brissette, J. L., M. Russel, L. Weiner, and P. Model. **1990**. “Phage Shock Protein, a Stress Protein of *Escherichia Coli*.” *Proceedings of the National Academy of Sciences* 87(3):862–66.

Brosius, Jurgen, Thomas J. Dull, Doxald D. Sleeter Amii, and Harry F. Noller. **1981**. “Gene Organization and Primary Structure of a Ribosomal RNA Operon from Escherichia Coli.” *J. Mol. Riol* 148:107–27.

Broz, Petr, Catherine A. Mueller, Shirley A. Müller, Ansgar Philippsen, Isabel Sorg, Andreas Engel, and Guy R. Cornelis. **2007**. “Function and Molecular Architecture of the *Yersinia* Injectisome Tip Complex.” *Molecular Microbiology* 65(5):1311–20.

Burgess, R. R. **1969**. “Separation and Characterization of the Subunits of Ribonucleic Acid Polymerase.” *The Journal of Biological Chemistry* 244(22):6168–76.

Burgess, R. R., A. A. Travers, J. J. Dunn, and E. K. Bautz. **1969**. “Factor Stimulating Transcription by RNA Polymerase.” *Nature* 221(5175):43–46.

Byrgazov, Konstantin, Oliver Vesper, and Isabella Moll. **2013**. “Ribosome Heterogeneity: Another Level of Complexity in Bacterial Translation Regulation.” *Current Opinion in Microbiology* 16(2):133–39.

Bzymek, Krzysztof P., Brent Y. Hamaoka, and Partho Ghosh. **2012**. “Two Translation Products of *Yersinia* YscQ Assemble To Form a Complex Essential to Type III Secretion.” *Biochemistry* 51(8):1669–77.

Cambronne, Eric D., Luisa W. Cheng, and Olaf Schneewind. **2000**. “LcrQ/YscM1, Regulators of the *Yersinia* Yop Virulon, Are Injected into Host Cells by a Chaperone-Dependent Mechanism.” *Molecular Microbiology* 37(2):263–73.

Cambronne, Eric D. and Olaf Schneewind. **2002**. “*Yersinia Enterocolitica* Type III Secretion: YscM1 and YscM2 Regulate Yop Gene Expression by a Posttranscriptional Mechanism That Targets the 5′ Untranslated Region of Yop MRNA.” *Journal of Bacteriology* 184(21):5880–93.

Campbell, Elizabeth A., Jonathan L. Tupy, Tanja M. Gruber, Sheng Wang, Meghan M. Sharp, Carol A. Gross, and Seth A. Darst. **2003**. “Crystal Structure of *Escherichia Coli* σE with the Cytoplasmic Domain of Its Anti-σ RseA.” *Molecular Cell* 11(4):1067–78.

Cao, Shi-Yang, Wan-Bin Liu, Ya-Fang Tan, Hui-Ying Yang, Ting-Ting Zhang, Tong Wang, Xiao-Yi Wang, Ya-Jun Song, Rui-Fu Yang, and Zong-Min Du. **2017**. “An Interaction between the Inner Rod Protein YscI and the Needle Protein YscF Is Required to Assemble the Needle Structure of the *Yersinia* Type Three Secretion System.” *Journal of Biological Chemistry* 292(13):5488–98.

Carlsson, Katrin E., Junfa Liu, Petra J. Edqvist, and Matthew S. Francis. **2007**. “Extracytoplasmic-Stress-Responsive Pathways Modulate Type III Secretion in *Yersinia Pseudotuberculosis*.” *Infection and Immunity* 75(8):3913–24.

Chakravarty, Shubham and Eric Massé. **2019**. “RNA-Dependent Regulation of Virulence in Pathogenic Bacteria.” *Frontiers in Cellular and Infection Microbiology* 9.

Chaplin, David D. **2010**. “Overview of the Immune Response.” *Journal of Allergy and Clinical Immunology* 125(2):S3–23.

Chaudhury, Sukanya, Kevin P. Battaile, Scott Lovell, Gregory V. Plano, and Roberto N. De Guzman. **2013**. “Structure of the *Yersinia Pestis* Tip Protein LcrV Refined to 1.65 Å Resolution.” *Acta Crystallographica Section F Structural Biology and Crystallization Communications* 69(5):477–81.

Chen, Huiyi, Katsuyuki Shiroguchi, Hao Ge, and Xiaoliang Sunney Xie. **2015**. “Genome-wide Study of MRNA Degradation and Transcript Elongation in *Escherichia Coli*.” *Molecular Systems Biology* 11(1):781.

Chen, Peter E., Christopher Cook, Andrew C. Stewart, Niranjan Nagarajan, Dan D. Sommer, Mihai Pop, Brendan Thomason, Maureen P. Kiley Thomason, Shannon Lentz, Nichole Nolan, Shanmuga Sozhamannan, Alexander Sulakvelidze, Alfred Mateczun, Lei Du, Michael E. Zwick, and Timothy D. Read. **2010**. “Genomic Characterization of the *Yersinia* Genus.” *Genome Biology* 11(1):R1.

Chen, Shiyun, Karl M. Thompson, and Matthew S. Francis. **2016**. “Environmental Regulation of *Yersinia* Pathophysiology.” *Frontiers in Cellular and Infection Microbiology* 6(March).

Chen, Yuqing and Deborah M. Anderson. **2011**. “Expression Hierarchy in the *Yersinia* Type III Secretion System Established through YopD Recognition of RNA.” *Molecular Microbiology* 80(4):966–80.

Cheng, L. W., O. Kay, and O. Schneewind. **2001**. “Regulated Secretion of YopN by the Type III Machinery of *Yersinia Enterocolitica*.” *Journal of Bacteriology* 183(18):5293–5301.

Cheng, Luisa W., Deborah M. Anderson, and Olaf Schneewind. **1997**. “Two Independent Type III Secretion Mechanisms for YopE in *Yersinia Enterocolitica*.” *Molecular Microbiology* 24(4):757–65.

Chlebicz, Agnieszka and Katarzyna Śliżewska. **2018**. “Campylobacteriosis, Salmonellosis, Yersiniosis, and Listeriosis as Zoonotic Foodborne Diseases: A Review.” *International Journal of Environmental Research and Public Health* 15(5):863.

Cho, Junho, Janet Rogers, Mark Kearns, Macall Leslie, Steven D. Hartson, and Kevin S. Wilson. **2015**. “*Escherichia Coli* Persister Cells Suppress Translation by Selectively Disassembling and Degrading Their Ribosomes.” *Molecular Microbiology* 95(2):352–64.

Chothani, Sonia, Eleonora Adami, John F. Ouyang, Sivakumar Viswanathan, Norbert Hubner, Stuart A. Cook, Sebastian Schafer, and Owen J. L. Rackham. **2019**. “DeltaTE: Detection of Translationally Regulated Genes by Integrative Analysis of Ribo-seq and RNA-seq Data.” *Current Protocols in Molecular Biology* 129(1).

Chung, Lawton K., Yong Hwan Park, Yueting Zheng, Igor E. Brodsky, Patrick Hearing, Daniel L. Kastner, Jae Jin Chae, and James B. Bliska. **2016**. “The *Yersinia* Virulence Factor YopM Hijacks Host Kinases to Inhibit Type III Effector-Triggered Activation of the Pyrin Inflammasome.” *Cell Host & Microbe* 20(3):296–306.

Clemons, William M., Joanna L. C. May, Brian T. Wimberly, John P. McCutcheon, Malcolm S. Capel, and V. Ramakrishnan. **1999**. “Structure of a Bacterial 30S Ribosomal Subunit at 5.5 Å Resolution.” *Nature* 400(6747):833–40.

Cleri, D. J., J. R. Vernaleo, L. J. Lombardi, M. S. Rabbat, A. Mathew, R. Marton, and M. C. Reyelt. **1997**. “Plague Pneumonia Disease Caused by *Yersinia Pestis*.” *Seminars in Respiratory Infections* 12(1):12–23.

Cornelis, G. R. **2000**. “Type III Secretion: A Bacterial Device for Close Combat with Cells of Their Eukaryotic Host.” *Philosophical Transactions of the Royal Society of London. Series B, Biological Sciences* 355(1397):681–93.

Cornelis, G. R., T. Biot, C. Lambert Rouvroit, T. Michiels, B. Mulder, C. Sluiters, M. P. Sory, M. Bouchaute, and J. C. Vanooteghem. **1989**. “The *Yersinia* Yop Regulon.” *Molecular Microbiology* 3(10):1455–59.

Cornelis, G., C. Sluiters, C. L. de Rouvroit, and T. Michiels. **1989**. “Homology between VirF, the Transcriptional Activator of the *Yersinia* Virulence Regulon, and AraC, the *Escherichia Coli* Arabinose Operon Regulator.” *Journal of Bacteriology* 171(1):254–62.

Cornelis, Guy R. **1993**. “Role of the Transcription Activator VirF and the Histone-like Protein YmoA in the Thermoregulation of Virulence Functions in *Yersiniae*.” *Zentralblatt Für Bakteriologie* 278(2–3):149–64.

Cornelis, Guy R. **2002**. “*Yersinia* Type III Secretion.” *Journal of Cell Biology* 158(3):401–8.

Cornelis, Guy R., Anne Boland, Aoife P. Boyd, Cecile Geuijen, Maite Iriarte, Cécile Neyt, Marie-Paule Sory, and Isabelle Stainier. **1998**. “The Virulence Plasmid of *Yersinia*, an Antihost Genome.” *Microbiology and Molecular Biology Reviews* 62(4):1315–52.

Cossart, Pascale and Philippe J. Sansonetti. **2004**. “Bacterial Invasion: The Paradigm of Enteroinvasive Pathogens.” *Science* 304(12):242–48.

Costa, Tiago R. D., Petra J. Edqvist, Jeanette E. Bröms, Monika K. Åhlund, Åke Forsberg, and Matthew S. Francis. **2010**. “YopD Self-Assembly and Binding to LcrV Facilitate Type III Secretion Activity by *Yersinia Pseudotuberculosis*.” *Journal of Biological Chemistry* 285(33):25269–84.

Craigen, W. J. and C. T. Caskey. **1987**. “The Function, Structure and Regulation of *E. Coli* Peptide Chain Release Factors.” *Biochimie* 69(10):1031–41.

Craigen, W. J., R. G. Cook, W. P. Tate, and C. T. Caskey. **1985**. “Bacterial Peptide Chain Release Factors: Conserved Primary Structure and Possible Frameshift Regulation of Release Factor 2.” *Proceedings of the National Academy of Sciences of the United States of America* 82(11):3616–20.

Crick, F. H. C. **1966**. “Codon—Anticodon Pairing: The Wobble Hypothesis.” *Journal of Molecular Biology* 19(2):548–55.

Crick, Francis. **1970**. “Central Dogma of Molecular Biology.” *Nature* 227(5258):561–63.

Crowell, B. C. .. et. all. **1919**. “Pathologic Anatomy of Bubonic Plague.” *Philippine Journal of Science, Sect. B. Trop. Med.* 10(4).

Cuatrecasas, P., S. Fuchs, and C. B. Anfinsen. **1967**. “Catalytic Properties and Specificity of the Extracellular Nuclease of *Staphylococcus Aureus*.” *The Journal of Biological Chemistry* 242(7):1541–47.

Cukier-Kahn, R., M. Jacquet, and F. Gros. **1972**. “Two Heat-Resistant, Low Molecular Weight Proteins from *Escherichia Coli* That Stimulate DNA-Directed RNA Synthesis.” *Proceedings of the National Academy of Sciences* 69(12):3643–47.

Darwin, Andrew J. and Virginia L. Miller. **2001**. “The Psp Locus of *Yersinia Enterocolitica* Is Required for Virulence and for Growth in Vitro When the Ysc Type III Secretion System Is Produced.” *Molecular Microbiology* 39(2):429–45.

Datsenko, K. A. and B. L. Wanner. **2000**. “One-Step Inactivation of Chromosomal Genes in *Escherichia Coli* K-12 Using PCR Products.” *Proceedings of the National Academy of Sciences* 97(12):6640–45.

Day, James B. and Gregory V. Plano. **1998**. “A Complex Composed of SycN and YscB Functions as a Specific Chaperone for YopN in *Yersinia Pestis*.” *Molecular Microbiology* 30(4):777–88.

Demeure, Christian, Olivier Dussurget, Guillem Mas Fiol, Anne Sophie Le Guern, Cyril Savin, and Javier Pizarro-Cerdá. **2019**. “*Yersinia Pestis* and Plague: An Updated View on Evolution, Virulence Determinants, Immune Subversion, Vaccination and Diagnostics.” *Microbes and Infection* 21(5–6):202–12.

Deng, Wanyin, Natalie C. Marshall, Jennifer L. Rowland, James M. McCoy, Liam J. Worrall, Andrew S. Santos, Natalie C. J. Strynadka, and B. Brett Finlay. **2017**. “Assembly, Structure, Function and Regulation of Type III Secretion Systems.” *Nature Reviews Microbiology* 15(6):323–37.

Dennis, P. P., M. Ehrenberg, D. Fange, and H. Bremer. **2009**. “Varying Rate of RNA Chain Elongation during Rrn Transcription in *Escherichia Coli*.” *Journal of Bacteriology* 191(11):3740–46.

Dewoody, Rebecca, Peter M. Merritt, Andrew S. Houppert, and Melanie M. Marketon. **2011**. “YopK Regulates the *Yersinia Pestis* Type III Secretion System from within Host Cells.” *Molecular Microbiology* 79(6):1445–61.

Dewoody, Rebecca, Peter M. Merritt, and Melanie M. Marketon. **2013**. “YopK Controls Both Rate and Fidelity of Yop Translocation.” *Molecular Microbiology* 87(2):301–17.

Dewoody, Rebecca S., Peter M. Merritt, and Melanie M. Marketon. **2013**. “Regulation of the Yersinia Type III Secretion System: Traffic Control.” *Frontiers in Cellular and Infection Microbiology* 3(February):1–13.

Diepold, Andreas, Marlise Amstutz, Sören Abel, Isabel Sorg, Urs Jenal, and Guy R. Cornelis. **2010**. “Deciphering the Assembly of the *Yersinia* Type III Secretion Injectisome.” *EMBO Journal* 29(11):1928–40.

Diepold, Andreas, Mikhail Kudryashev, Nicolas J. Delalez, Richard M. Berry, and Judith P. Armitage. **2015**. “Composition, Formation, and Regulation of the Cytosolic C-Ring, a Dynamic Component of the Type III Secretion Injectisome” edited by A. M. Stock. *PLOS Biology* 13(1):e1002039.

Diepold, Andreas and Samuel Wagner. **2014**. “Assembly of the Bacterial Type III Secretion Machinery.” *FEMS Microbiology Reviews* 38(4):802–22.

Diepold, Andreas, Ulrich Wiesand, and Guy R. Cornelis. **2011**. “The Assembly of the Export Apparatus (YscR,S,T,U,V) of the *Yersinia* Type III Secretion Apparatus Occurs Independently of Other Structural Components and Involves the Formation of an YscV Oligomer.” *Molecular Microbiology* 82(2):502–14.

Dole, Sudhanshu, V. Nagarajavel, and Karin Schnetz. **2004**. “The Histone-like Nucleoid Structuring Protein H-NS Represses the *Escherichia Coli* Bgl Operon Downstream of the Promoter.” *Molecular Microbiology* 52(2):589–600.

Dubey, Ashok K., Carol S. Baker, Tony Romeo, and Paul Babitzke. **2005**. “CsrA − RNA Interaction RNA Sequence and Secondary Structure Participate in High-Affinity CsrA – RNA Interaction.” *Rna* (11):1579–87.

Duval, Mélodie, Alexey Korepanov, Olivier Fuchsbauer, Pierre Fechter, Andrea Haller, Attilio Fabbretti, Laurence Choulier, Ronald Micura, Bruno P. Klaholz, Pascale Romby, Mathias Springer, and Stefano Marzi. **2013**. “*Escherichia Coli* Ribosomal Protein S1 Unfolds Structured MRNAs Onto the Ribosome for Active Translation Initiation” edited by J. Hershey. *PLoS Biology* 11(12):e1001731.

Ebright, R. H. and S. Busby. **1995**. “The Escherichia Coli RNA Polymerase Alpha Subunit: Structure and Function.” *Current Opinion in Genetics & Development* 5(2):197–203.

Edqvist, Petra J., Margareta Aili, Junfa Liu, and Matthew S. Francis. **2007**. “Minimal YopB and YopD Translocator Secretion by *Yersinia* Is Sufficient for Yop-Effector Delivery into Target Cells.” *Microbes and Infection* 9(2):224–33.

Eitel, Julia, Julia Eitel, Petra Dersch, and Petra Dersch. **2002**. “The YadA Protein Of *Yersinia Pseudotuberculosis* Mediates High-efficiency Uptake Into Human Cells Under Environmental Conditions In Which Invasin Is Repressed” *Society* 70(9):4880–91.

Emetz, D. and G. Klug. **1998**. “Cloning and Characterization of the RpoH Gene of *Rhodobacter Capsulatus*.” *Molecular and General Genetics MGG* 260(2–3):212–17.

Erfurth, Stella E., Sabine Gröbner, Uwe Kramer, Dani S. J. Gunst, Irena Soldanova, Martin Schaller, Ingo B. Autenrieth, and Stefan Borgmann. **2004**. “*Yersinia Enterocolitica* Induces Apoptosis and Inhibits Surface Molecule Expression and Cytokine Production in Murine Dendritic Cells.” *Infection and Immunity* 72(12):7045–54.

Erhardt, Marc and Petra Dersch. **2015**. “Regulatory Principles Governing *Salmonella* and *Yersinia* Virulence.” *Frontiers in Microbiology* 6(SEP):1–20.

Erickson, J. W. and C. A. Gross. **1989**. “Identification of the Sigma E Subunit of *Escherichia Coli* RNA Polymerase: A Second Alternate Sigma Factor Involved in High-Temperature Gene Expression.” *Genes & Development* 3(9):1462–71.

Estrem, S. T., T. Gaal, W. Ross, and R. L. Gourse. **1998**. “Identification of an UP Element Consensus Sequence for Bacterial Promoters.” *Proceedings of the National Academy of Sciences of the United States of America* 95(17):9761–66.

Estrem, S. T., W. Ross, T. Gaal, Z. W. Chen, W. Niu, R. H. Ebright, and R. L. Gourse. **1999**. “Bacterial Promoter Architecture: Subsite Structure of UP Elements and Interactions with the Carboxy-Terminal Domain of the RNA Polymerase Alpha Subunit.” *Genes & Development* 13(16):2134–47.

Evfratov, Sergey A., Ilya A. Osterman, Ekaterina S. Komarova, Alexandra M. Pogorelskaya, Maria P. Rubtsova, Timofei S. Zatsepin, Tatiana A. Semashko, Elena S. Kostryukova, Andrey A. Mironov, Evgeny Burnaev, Ekaterina Krymova, Mikhail S. Gelfand, Vadim M. Govorun, Alexey A. Bogdanov, Petr V. Sergiev, and Olga A. Dontsova. **2017**. “Application of Sorting and next Generation Sequencing to Study 5´-UTR Influence on Translation Efficiency in *Escherichia Coli*.” *Nucleic Acids Research* 45(6):3487–3502.

Ewels, Philip, Måns Magnusson, Sverker Lundin, and Max Käller. **2016**. “MultiQC: Summarize Analysis Results for Multiple Tools and Samples in a Single Report.” *Bioinformatics* 32(19):3047–48.

Fahlgren, Anna, Linda Westermark, Karen Akopyan, and Maria Fällman. **2009**. “Cell Type-Specific Effects of *Yersinia Pseudotuberculosis* Virulence Effectors.” *Cellular Microbiology* 11(12):1750–67.

Fällman, Maria, Fabienne Deleuil, and Karen McGee. **2002**. “Resistance to Phagocytosis by *Yersinia*.” *International Journal of Medical Microbiology : IJMM* 291(6–7):501–9.

Fei, Keke, Hong-Jun Chao, Yangbo Hu, Matthew S. Francis, and Shiyun Chen. **2021**. “CpxR Regulates the Rcs Phosphorelay System in Controlling the Ysc-Yop Type III Secretion System in *Yersinia Pseudotuberculosis*.” *Microbiology* 167(1).

Feklístov, Andrey, Brian D. Sharon, Seth A. Darst, and Carol A. Gross. **2014**. “Bacterial Sigma Factors: A Historical, Structural, and Genomic Perspective.” *Annual Review of Microbiology* 68(1):357–76.

Ferracci, Franco, Florian D. Schubot, David S. Waugh, and Gregory V Plano. **2005**. “Selection and Characterization of *Yersinia Pestis* YopN Mutants That Constitutively Block Yop Secretion.” *Molecular Microbiology* 57(4):970–87.

Flores-Kim, Josué and Andrew J. Darwin. **2012**. “Links between Type III Secretion and Extracytoplasmic Stress Responses in *Yersinia*.” *Frontiers in Cellular and Infection Microbiology* 2(October):125.

Forsberg, A. and H. Wolf-Watz. **1990**. “Genetic Analysis of the YopE Region of *Yersinia* Spp.: Identification of a Novel Conserved Locus, YerA, Regulating YopE Expression.” *Journal of Bacteriology* 172(3):1547–55.

Forsberg, Åke, Roland Rosqvist, and Hans Wolf-Watt. **1994**. “Regulation and Polarized Transfer of the *Yersinia* Outer Proteins (Yops) Involved in Antiphagocytosis.” *Trends in Microbiology* 2(1):14–19.

Fowler, Janet M., Christine R. Wulff, Susan C. Straley, and Robert R. Brubaker. **2009**. “Growth of Calcium-Blind Mutants of *Yersinia Pestis* at 37 °C in Permissive Ca2+-Deficient Environments.” *Microbiology* 155(8):2509–21.

Francis, Matthew S., Scott A. Lloyd, and Hans Wolf-Watz. **2001**. “The Type III Secretion Chaperone LcrH Co-Operates with YopD to Establish a Negative, Regulatory Loop for Control of Yop Synthesis in *Yersinia Pseudotuberculosis*.” *Molecular Microbiology* 42(4):1075–93.

Freese, Nowlan H., David C. Norris, and Ann E. Loraine. **2016**. “Integrated Genome Browser: Visual Analytics Platform for Genomics.” *Bioinformatics* 32(14):2089–95.

Frumkin, Idan, Marc J. Lajoie, Christopher J. Gregg, Gil Hornung, George M. Church, and Yitzhak Pilpel. **2018**. "Codon Usage of Highly Expressed Genes Affects Proteome-Wide Translation Efficiency." *Proceedings of the National Academy of Sciences of the United States of America* 115(21):E4940–49.

Gamez, A., R. Mukerjea, M. Alayyoubi, M. Ghassemian, and P. Ghosh. **2012**. "Structure and Interactions of the Cytoplasmic Domain of the *Yersinia* Type III Secretion Protein YscD." *Journal of Bacteriology* 194(21):5949–58.

Gay, P., D. Le Coq, M. Steinmetz, T. Berkelman, and C. I. Kado. **1985**. "Positive Selection Procedure for Entrapment of Insertion Sequence Elements in Gram-Negative Bacteria." *Journal of Bacteriology* 164(2):918–21.

Gelhausen, Rick, Sarah L. Svensson, Kathrin Froschauer, Florian Heyl, Lydia Hadjeras, Cynthia M. Sharma, Florian Eggenhofer, and Rolf Backofen. **2020**. "HRIBO: High-Throughput Analysis of Bacterial Ribosome Profiling Data" edited by V. Alfonso. *Bioinformatics*.

Gentry, Daniel R. and Richard R. Burgess. **1993**. "Cross-Linking of *Escherichia Coli* RNA Polymerase Subunits: Identification of .Beta.' as the Binding Site of .Omega." *Biochemistry* 32(41):11224–27.

Geyer, Rebecca. **2014**. "Analysis of the Molecular Function of Invasin-like Proteins of *Yersinia Pseudotuberculosis* and Their Role in Pathogenesis." MHH Hannover.

Ghosh, Pallavi, Akira Ishihama, and Dipankar Chatterji. **2001**. "*Escherichia Coli* RNA Polymerase Subunit ω and Its N-Terminal Domain Bind Full-Length B′ to Facilitate Incorporation into the α 2 β Subassembly." *European Journal of Biochemistry* 268(17):4621–27.

Glasgow, Anum Azam, Han Teng Wong, and Danielle Tullman-Ercek. **2017**. "A Secretion-Amplification Role for *Salmonella Enterica* Translocon Protein SipD." *ACS Synthetic Biology* 6(6):1006–15.

Goguen, J. D., J. Yother, and S. C. Straley. **1984**. "Genetic Analysis of the Low Calcium Response in *Yersinia Pestis* Mu D1(Ap Lac) Insertion Mutants." *Journal of Bacteriology* 160(3):842–48.

Goodin, Jeremy L., Ronald W. Raab, Robert L. McKown, George L. Coffman, Bradford S. Powell, Jeff T. Enama, John A. Ligon, and Gerard P. Andrews. **2005**. "*Yersinia Pestis* Outer Membrane Type III Secretion Protein YscC: Expression, Purification, Characterization, and Induction of Specific Antiserum." *Protein Expression and Purification* 40(1):152–63.

Goyal, Akanksha, Riccardo Belardinelli, Cristina Maracci, Pohl Milón, and Marina V. Rodnina. **2015**. "Directional Transition from Initiation to Elongation in Bacterial Translation." *Nucleic Acids Research* 43(22):10700–712.

Grainger, David C. **2016**. "Structure and Function of Bacterial H-NS Protein." *Biochemical Society Transactions* 44(6):1561–69.

Grentzmann, G., D. Brechemier-Baey, V. Heurgue, L. Mora, and R. H. Buckingham. **1994**. "Localization and Characterization of the Gene Encoding Release Factor RF3 in *Escherichia Coli*." *Proceedings of the National Academy of Sciences of the United States of America* 91(13):5848–52.

Grosdent, Nadine, Isabelle Maridonneau-Parini, Marie-Paule Sory, and Guy R. Cornelis. **2002**. "Role of Yops and Adhesins in Resistance of *Yersinia Enterocolitica* to Phagocytosis." *Infection and Immunity* 70(8):4165–76.

Gross, C. A., C. Chan, A. Dombroski, T. Gruber, M. Sharp, J. Tupy, and B. Young. **1998**. "The Functional and Regulatory Roles of Sigma Factors in Transcription." *Cold Spring Harbor Symposia on Quantitative Biology* 63:141–55.

Grossman, A. D., D. B. Straus, W. A. Walter, and C. A. Gross. **1987**. "Sigma 32 Synthesis Can Regulate the Synthesis of Heat Shock Proteins in *Escherichia Coli*." *Genes & Development* 1(2):179–84.

Großmann, Peter, Anja Lück, and Christoph Kaleta. **2017**. "Model-Based Genome-Wide Determination of RNA Chain Elongation Rates in *Escherichia Coli*." *Scientific Reports* 7(1):17213.

Gruber, Tanja M. and Carol A. Gross. **2003**. “Multiple Sigma Subunits and the Partitioning of Bacterial Transcription Space.” *Annual Review of Microbiology* 57(1):441–66.

Gualerzi, Claudio O. and Cynthia L. Pon. **2015**. “Initiation of MRNA Translation in Bacteria: Structural and Dynamic Aspects.” *Cellular and Molecular Life Sciences* 72(22):4341–67.

Gualerzi, Claudio, Gianfranco Risuleo, and Cynthia L. Pon. **1977**. “Initial Rate Kinetic Analysis of the Mechanism of Initiation Complex Formation and the Role of Initiation Factor IF-3.” *Biochemistry* 16(8):1684–89.

Guinet, Françoise, Patrick Avé, Louis Jones, Michel Huerre, and Elisabeth Carniel. **2008**. “Defective Innate Cell Response and Lymph Node Infiltration Specify *Yersinia Pestis* Infection” edited by K. Nielsen. *PLoS ONE* 3(2):e1688.

Gutiérrez, Pablo, Yan Li, Michael J. Osborne, Ekaterina Pomerantseva, Qian Liu, and Kalle Gehring. **2005**. “Solution Structure of the Carbon Storage Regulator Protein CsrA from *Escherichia Coli*.” *Journal of Bacteriology* 187(10):3496–3501.

Guzman, L. M., D. Belin, M. J. Carson, and J. Beckwith. **1995**. “Tight Regulation, Modulation, and High-Level Expression by Vectors Containing the Arabinose P(BAD) Promoter.” *Journal of Bacteriology* 177(14):4121–30.

Håkansson, S., T. Bergman, J. C. Vanooteghem, G. Cornelis, and H. Wolf-Watz. **1993**. “YopB and YopD Constitute a Novel Class of *Yersinia* Yop Proteins.” *Infection and Immunity* 61(1):71–80.

Håkansson, S., K. Schesser, C. Persson, E. E. Galyov, R. Rosqvist, F. Homblé, and H. Wolf-Watz. **1996**. “The YopB Protein of *Yersinia Pseudotuberculosis* Is Essential for the Translocation of Yop Effector Proteins across the Target Cell Plasma Membrane and Displays a Contact-Dependent Membrane Disrupting Activity.” *The EMBO Journal* 15(21):5812–23.

Hamid, N., A. Gustavsson, K. Andersson, K. McGee, C. Persson, C. E. Rudd, and M. Fällman. **1999**. “YopH Dephosphorylates Cas and Fyn-Binding Protein in Macrophages.” *Microbial Pathogenesis* 27(4):231–42.

Hamzaoui, Nadim, Sophie Kernéis, Elise Caliot, and Eric Pringault. **2004**. “Expression and Distribution of B1 Integrins in in Vitro-Induced M Cells: Implications for *Yersinia* Adhesion to Peyer’s Patch Epithelium.” *Cellular Microbiology* 6(9):817–28.

Hayden, Jennifer D. and Sarah E. Ades. **2008**. “The Extracytoplasmic Stress Factor, σE, Is Required to Maintain Cell Envelope Integrity in *Escherichia Coli*” edited by S. Sandler. *PLoS ONE* 3(2):e1573.

Hayward, Richard S., Kazuhiko Igarashi, and Akira Ishihama. **1991**. “Functional Specialization within the α-Subunit of *Escherichia Coli* RNA Polymerase.” *Journal of Molecular Biology* 221(1):23–29.

Heise, Tanja and Petra Dersch. **2006**. “Identification of a Domain in *Yersinia* Virulence Factor YadA That Is Crucial for Extracellular Matrix-Specific Cell Adhesion and Uptake.” *Proceedings of the National Academy of Sciences of the United States of America* 103(9):3375–80.

Heroven, Ann Kathrin, Katja Böhme, and Petra Dersch. **2012**. “Regulation of Virulence Gene Expression by Regulatory RNA Elements in *Yersinia Pseudotuberculosis*.” Pp. 315–23 in.

Heroven, Ann Kathrin, Katja Bo̎hme, Petra Dersch, Katja Böhme, and Petra Dersch. **2012**. “The Csr/Rsm System of *Yersinia* and Related Pathogens.” *RNA Biology* 9(4):379–91.

Heroven, Ann Kathrin, Katja Böhme, Manfred Rohde, and Petra Dersch. **2008**. “A Csr-Type Regulatory System, Including Small Non-Coding RNAs, Regulates the Global Virulence Regulator RovA of *Yersinia Pseudotuberculosis* through RovM.” *Molecular Microbiology* 68(5):1179–95.

Heroven, Ann Kathrin and Petra Dersch. **2014**. “Coregulation of Host-Adapted Metabolism and Virulence by Pathogenic *Yersiniae*.” *Frontiers in Cellular and Infection Microbiology* 4(October):1–13.

Heroven, Ann Kathrin, Maike Sest, Fabio Pisano, Matthias Scheb-Wetzel, Rebekka Steinmann, Katja Böhme, Johannes Klein, Richard Münch, Dietmar Schomburg, and Petra Dersch. **2012**. "Crp Induces Switching of the CsrB and CsrC RNAs in *Yersinia Pseudotuberculosis* and Links Nutritional Status to Virulence." *Frontiers in Cellular and Infection Microbiology* 2.

Heusipp, Gerhard, M. Alexande. Schmidt, and Virginia L. Miller. **2003**. "Identification of RpoE and NadB as Host Responsive Elements of *Yersinia Enterocolitica*." *FEMS Microbiology Letters* 226(2):291–98.

Hews, Claire L., Timothy Cho, Gary Rowley, and Tracy L. Raivio. **2019**. "Maintaining Integrity Under Stress: Envelope Stress Response Regulation of Pathogenesis in Gram-Negative Bacteria." *Frontiers in Cellular and Infection Microbiology* 9.

Hirashima, A. and A. Kaji. **1970**. "Factor Dependent Breakdown of Polysomes." *Biochemical and Biophysical Research Communications* 41(4):877–83.

Hirashima, A. and A. Kaji. **1972**. "Purification and Properties of Ribosome-Releasing Factor." *Biochemistry* 11(22):4037–44.

Hoaglanf, M. B., M. L. Stephenson, J. F. Scott, L. I. Hecht, and P. C. Zamecnik. **1958**. "A Soluble Ribonucleic Acid Intermediate in Protein Synthesis." *The Journal of Biological Chemistry* 231(1):241–57.

Hoe, N. P. and J. D. Goguen. **1993**. "Temperature Sensing in *Yersinia Pestis*: Translation of the LcrF Activator Protein Is Thermally Regulated." *Journal of Bacteriology* 175(24):7901–9.

Höfling, Sabrina, Benjamin Grabowski, Stefanie Norkowski, M. Alexander Schmidt, and Christian Rüter. **2015**. "Current Activities of the *Yersinia* Effector Protein YopM." *International Journal of Medical Microbiology* 305(3):424–32.

Hooker-Romero, Diana, Erin Mettert, Leah Schwiesow, David Balderas, Pablo A. Alvarez, Anadin Kicin, Azuah L. Gonzalez, Gregory V. Plano, Patricia J. Kiley, and Victoria Auerbuch. **2019**. "Iron Availability and Oxygen Tension Regulate the *Yersinia* Ysc Type III Secretion System to Enable Disseminated Infection" edited by J. Mecsas. *PLOS Pathogens* 15(12):e1008001.

Hoßmann, Jörn. **2017**. "RNA-Based Control of the Expression of the Type III Secretion System of *Yersinia Pseudotuberculosis*." TU Braunschweig.

Hu, Ping, Jeffrey Elliott, Paula McCready, Evan Skowronski, Jeffrey Garnes, Arthur Kobayashi, Robert R. Brubaker, and Emilio Garcia. **1998**. "Structural Organization of Virulence-Associated Plasmids of *Yersinia Pestis*." *Journal of Bacteriology* 180(19):5192–5202.

Hurst, Mark R. H., S. Anette Becher, Sandra D. Young, Tracey L. Nelson, and Travis R. Glare. **2011**. "*Yersinia Entomophaga* Sp. Nov., Isolated from the New Zealand Grass Grub Costelytra Zealandica." *International Journal of Systematic and Evolutionary Microbiology* 61(Pt 4):844–49.

Ibba, Michael and Dieter Söll. **2000**. "Aminoacyl-TRNA Synthesis." *Annual Review of Biochemistry* 69(1):617–50.

Ingolia, Nicholas T., Gloria A. Brar, Silvia Rouskin, Anna M. McGeachy, and Jonathan S. Weissman. **2012**. "The Ribosome Profiling Strategy for Monitoring Translation in Vivo by Deep Sequencing of Ribosome-Protected MRNA Fragments." *Nature Protocols* 7(8):1534–50.

Ingolia, Nicholas T., Sina Ghaemmaghami, John R. S. Newman, and Jonathan S. Weissman. **2009**. "Genome-Wide Analysis in Vivo of Translation with Nucleotide Resolution Using Ribosome Profiling." *Science* 324(5924):218–23.

Isberg, R. R. **1989**. "Mammalian Cell Adhesion Functions and Cellular Penetration of Enteropathogenic *Yersinia* Species." *Molecular Microbiology* 3(10):1449–53.

Jackson, Michael W., Eugenia Silva-Herzog, and Gregory V Plano. **2004**. "The ATP-Dependent ClpXP and Lon Proteases Regulate Expression of the *Yersinia Pestis* Type III Secretion System via

Regulated Proteolysis of YmoA, a Small Histone-like Protein." *Molecular Microbiology* 54(5):1364–78.

Jalava, Katri, Marjaana Hakkinen, Miia Valkonen, Ulla-Maija Nakari, Taito Palo, Saija Hallanvuo, Jukka Ollgren, Anja Siitonen, and J. Pekka Nuorti. **2006**. "An Outbreak of Gastrointestinal Illness and Erythema Nodosum from Grated Carrots Contaminated with *Yersinia Pseudotuberculosis*." *The Journal of Infectious Diseases* 194(9):1209–16.

Janosi, L., H. Hara, S. Zhang, and A. Kaji. **1996**. "Ribosome Recycling by Ribosome Recycling Factor (RRF)-an Important but Overlooked Step of Protein Biosynthesis." *Advances in Biophysics* 32:121–201.

Jaskunas, S. Richard, Lasse Lindahl, Masayasu Nomura, and Richard R. Burgess. **1975**. "Identification of Two Copies of the Gene for the Elongation Factor EF–Tu in E. Coli." *Nature* 257(5526):458–62.

Jessen, Danielle L., David S. Bradley, and Matthew L. Nilles. **2014**. "A Type III Secretion System Inhibitor Targets YopD While Revealing Differential Regulation of Secretion in Calcium-Blind Mutants of *Yersinia Pestis*." *Antimicrobial Agents and Chemotherapy* 58(2):839–50.

Johnson, C. M. and R. F. Schleif. **1995**. "In Vivo Induction Kinetics of the Arabinose Promoters in *Escherichia Coli*." *Journal of Bacteriology* 177(12):3438–42.

Joseph, Sabrina S. and Gregory V Plano. **2013**. "The SycN/YscB Chaperone-Binding Domain of YopN Is Required for the Calcium-Dependent Regulation of Yop Secretion by *Yersinia Pestis*." *Frontiers in Cellular and Infection Microbiology* 3:1.

Kaasch, A. J., J. Dinter, T. Goeser, G. Plum, and H. Seifert. **2012**. "*Yersinia Pseudotuberculosis* Bloodstream Infection and Septic Arthritis: Case Report and Review of the Literature." *Infection* 40(2):185–90.

Kanaya, Takashi, Ifor R. Williams, and Hiroshi Ohno. **2020**. "Intestinal M Cells: Tireless Samplers of Enteric Microbiota." *Traffic* 21(1):34–44.

Kapatral, V., J. W. Olson, J. C. Pepe, V. L. Miller, and S. A. Minnich. **1996**. "Temperature-Dependent Regulation of *Yersinia Enterocolitica* Class III Flagellar Genes." *Molecular Microbiology* 19(5):1061–71.

Karlinsey, Joyce E., Michael E. Maguire, Lynne A. Becker, Marie-Laure V. Crouch, and Ferric C. Fang. **2010**. "The Phage Shock Protein PspA Facilitates Divalent Metal Transport and Is Required for Virulence of *Salmonella Enterica* Sv. Typhimurium." *Molecular Microbiology* 78(3):669–85.

Kay, Alan C. and M. Grunberg-Manago. **1972**. "The Mechanism of Action of Initiation Factor IF1: Non-Analogy with Elongation Factor EFTs." *Biochimica et Biophysica Acta (BBA) - Nucleic Acids and Protein Synthesis* 277(1):225–30.

Kazmierczak, Mark J., Martin Wiedmann, and Kathryn J. Boor. **2005**. "Alternative Sigma Factors and Their Roles in Bacterial Virulence." *Microbiology and Molecular Biology Reviews : MMBR* 69(4):527–43.

Keto-Timonen, Riikka, Anna Pöntinen, Mariella Aalto-Araneda, and Hannu Korkeala. **2018**. "Growth of *Yersinia Pseudotuberculosis* Strains at Different Temperatures, PH Values, and NaCl and Ethanol Concentrations." *Journal of Food Protection* 81(1):142–49.

Khesin, R. B., M. F. Shemyakin, A. M. Gorlenko, S. Z. Mindlin, and T. S. Ilyina. **1969**. "Studies on the RNA Polymerase in *Escherichia Coli* K12 Using the Mutation Affecting Its Activity." *Journal of Molecular Biology* 42(3):401–11.

Knittel, Vanessa, Ines Vollmer, Marcel Volk, and Petra Dersch. **2018**. "Discovering RNA-Based Regulatory Systems for *Yersinia* Virulence." *Frontiers in Cellular and Infection Microbiology* 8(October):1–15.

Kobayashi, Nobuhide, Daisuke Takahashi, Shunsuke Takano, Shunsuke Kimura, and Koji Hase. **2019**. "The Roles of Peyer's Patches and Microfold Cells in the Gut Immune System: Relevance to Autoimmune Diseases." *Frontiers in Immunology* 10.

Kobe, B. **2001**. “The Leucine-Rich Repeat as a Protein Recognition Motif.” *Current Opinion in Structural Biology* 11(6):725–32.

Konovalova, Anna, Jaclyn A. Schwalm, and Thomas J. Silhavy. **2016**. “A Suppressor Mutation That Creates a Faster and More Robust σE Envelope Stress Response” edited by R. L. Gourse. *Journal of Bacteriology* 198(17):2345–51.

Kortmann, Jens and Franz Narberhaus. **2012**. “Bacterial RNA Thermometers: Molecular Zippers and Switches.” *Nature Reviews Microbiology* 10(4):255–65.

Kowal, Julia, Mohamed Chami, Philippe Ringler, Shirley A. Müller, Mikhail Kudryashev, Daniel Castaño-Díez, Marlise Amstutz, Guy R. Cornelis, Henning Stahlberg, and Andreas Engel. **2013**. “Structure of the Dodecameric *Yersinia Enterocolitica* Secretin YscC and Its Trypsin-Resistant Core.” *Structure* 21(12):2152–61.

Kusmierek, Maria. **2018**. “Identification of Regulatory Mechanisms Important to Control the *Yersinia Pseudotuberculosis* Type III Secretion and Virulence.” TU Braunschweig.

Kusmierek, Maria, Jörn Hoßmann, Rebekka Witte, Wiebke Opitz, Ines Vollmer, Marcel Volk, Ann Kathrin Heroven, Hans Wolf-Watz, and Petra Dersch. **2019**. “A Bacterial Secreted Translocator Hijacks Riboregulators to Control Type III Secretion in Response to Host Cell Contact” edited by J. Mecsas. *PLOS Pathogens* 15(6):e1007813.

de la Puerta, María Luisa, Antonio G. Trinidad, María del Carmen Rodríguez, Jori Bogetz, Mariano Sánchez Crespo, Tomas Mustelin, Andrés Alonso, and Yolanda Bayón. **2009**. “Characterization of New Substrates Targeted By *Yersinia* Tyrosine Phosphatase YopH” edited by P. Bozza. *PLoS ONE* 4(2):e4431.

Lamond, Angus I. and Andrew A. Travers. **1983**. “Requirement for an Upstream Element for Optimal Transcription of a Bacterial TRNA Gene.” *Nature* 305(5931):248–50.

Lange, R. and R. Hengge-Aronis. **1991**. “Identification of a Central Regulator of Stationary-Phase Gene Expression in *Escherichia Coli*.” *Molecular Microbiology* 5(1):49–59.

LaRock, Christopher N. and Brad T. Cookson. **2012**. “The *Yersinia* Virulence Effector YopM Binds Caspase-1 to Arrest Inflammasome Assembly and Processing.” *Cell Host & Microbe* 12(6):799–805.

Lee, David J., Stephen D. Minchin, and Stephen J. W. Busby. **2012**. “Activating Transcription in Bacteria.” *Annual Review of Microbiology* 66(1):125–52.

Lee, N., G. Wilcox, W. Gielow, J. Arnold, P. Cleary, and E. Englesberg. **1974**. “In Vitro Activation of the Transcription of AraBAD Operon by AraC Activator.” *Proceedings of the National Academy of Sciences* 71(3):634–38.

Lee, Vincent T., Deborah M. Anderson, and Olaf Schneewind. **1998**. “Targeting of *Yersinia* Yop Proteins into the Cytosol of HeLa Cells: One-step Translocation of YopE across Bacterial and Eukaryotic Membranes Is Dependent on SycE Chaperone.” *Molecular Microbiology* 28(3):593–601.

Lee, Vincent T., Sarkis K. Mazmanian, and Olaf Schneewind. **2001**. “A Program of *Yersinia Enterocolitica* Type III Secretion Reactions Is Activated by Specific Signals.” *Journal of Bacteriology* 183(17):4970–78.

Lee, Wei Lin, Pavithra Singaravelu, Sheena Wee, Bo Xue, Khay Chun Ang, Jayantha Gunaratne, Jonathan M. Grimes, Kunchithapadam Swaminathan, and Robert C. Robinson. **2017**. “Mechanisms of *Yersinia* YopO Kinase Substrate Specificity.” *Scientific Reports* 7(1):39998.

Leistra, A. N., G. Gelderman, S. W. Sowa, A. Moon-Walker, H. M. Salis, and L. M. Contreras. **2018**. “A Canonical Biophysical Model of the CsrA Global Regulator Suggests Flexible Regulator-Target Interactions.” *Scientific Reports* 8(1):9892.

Leo, Jack C. and Mikael Skurnik. **2011**. “Adhesins of Human Pathogens from the Genus *Yersinia*.” *Advances in Experimental Medicine and Biology* 715:1–15.

Leontis, Neocles B. and Eric Westhof. **2001**. “Geometric Nomenclature and Classification of RNA Base Pairs.” *RNA* 7(4):S1355838201002515.

Li, H., B. Handsaker, A. Wysoker, T. Fennell, J. Ruan, N. Homer, G. Marth, G. Abecasis, and R. Durbin. **2009**. “The Sequence Alignment/Map Format and SAMtools.” *Bioinformatics* 25(16):2078–79.

Li, Yunlong, Yangbo Hu, Matthew S. Francis, and Shiyun Chen. **2015**. “RcsB Positively Regulates the *Yersinia* Ysc-Yop Type III Secretion System by Activating Expression of the Master Transcriptional Regulator LcrF.” *Environmental Microbiology* 17(4):1219–33.

Li, Yunlong, Lamei Li, Li Huang, Matthew S. Francis, Yangbo Hu, and Shiyun Chen. **2014**. “*Yersinia* Ysc-Yop Type III Secretion Feedback Inhibition Is Relieved through YscV-Dependent Recognition and Secretion of LcrQ.” *Molecular Microbiology* 91(3):494–507.

Lilleorg, Silva, Kaspar Reier, Arto Pulk, Aivar Liiv, Triin Tammsalu, Lauri Peil, Jamie H. D. Cate, and Jaanus Remme. **2019**. “Bacterial Ribosome Heterogeneity: Changes in Ribosomal Protein Composition during Transition into Stationary Growth Phase.” *Biochimie* 156:169–80.

Lilleorg, Silva, Kaspar Reier, Pavel Volõnkin, Jaanus Remme, and Aivar Liiv. **2020**. “Phenotypic Effects of Paralogous Ribosomal Proteins BL31A and BL31B in *E. Coli*.” *Scientific Reports* 10(1):11682.

Lilley, D. M. **2001**. “The Ribosome Functions as a Ribozyme.” *Chembiochem : A European Journal of Chemical Biology* 2(1):31–35.

Lindler, L. E., G. V Plano, V. Burland, G. F. Mayhew, and F. R. Blattner. **1998**. “Complete DNA Sequence and Detailed Analysis of the *Yersinia Pestis* KIM5 Plasmid Encoding Murine Toxin and Capsular Antigen.” *Infection and Immunity* 66(12):5731–42.

Liu, M. Y. and T. Romeo. **1997**. “The Global Regulator CsrA of *Escherichia Coli* Is a Specific mRNA-Binding Protein.” *Journal of Bacteriology* 179(14):4639–42.

Liu, Mu Ya, Gaojun Gui, Bangdong Wei, James F. Preston, Lawrence Oakford, Ümit Yüksel, David P. Giedroc, and Tony Romeo. **1997**. “The RNA Molecule CsrB Binds to the Global Regulatory Protein CsrA and Antagonizes Its Activity in *Escherichia Coli*.” *Journal of Biological Chemistry* 272(28):17502–10.

Liu, Xiaoxiang, Lei Ji, Xu Wang, Jianrong Li, Junli Zhu, and Aihua Sun. **2018**. “Role of RpoS in Stress Resistance, Quorum Sensing and Spoilage Potential of *Pseudomonas Fluorescens*.” *International Journal of Food Microbiology* 270:31–38.

Loh, Edmund, Francesco Righetti, Hannes Eichner, Christian Twittenhoff, and Franz Narberhaus. **2019**. “RNA Thermometers in Bacterial Pathogens.” Pp. 57–73 in *Regulating with RNA in Bacteria and Archaea*. Vol. 6. American Society of Microbiology.

Lonetto, Michael A., Timothy J. Donohue, Carol A. Gross, and Mark J. Buttner. **2019**. “Discovery of the Extracytoplasmic Function σ Factors.” *Molecular Microbiology* 112(2):348–55.

Lucchini, Sacha, Hong Liu, Qi Jin, Jay C. D. Hinton, and Jun Yu. **2005**. “Transcriptional Adaptation of *Shigella Flexneri* during Infection of Macrophages and Epithelial Cells: Insights into the Strategies of a Cytosolic Bacterial Pathogen.” *Infection and Immunity* 73(1):88–102.

Ma, Jiong, Allan Campbell, and Samuel Karlin. **2002**. “Correlations between Shine-Dalgarno Sequences and Gene Features Such as Predicted Expression Levels and Operon Structures.” *Journal of Bacteriology* 184(20):5733–45.

Malik, Haleema S. and James B. Bliska. **2020**. “The Pyrin Inflammasome and the *Yersinia* Effector Interaction.” *Immunological Reviews* 297(1):96–107.

Manoil, C. and J. Beckwith. **1986**. “A Genetic Approach to Analyzing Membrane Protein Topology.” *Science* 233(4771):1403–8.

Markel, Eric, Paul Stodghill, Zhongmeng Bao, Christopher R. Myers, and Bryan Swingle. **2016**. “AlgU Controls Expression of Virulence Genes in *Pseudomonas Syringae* Pv. Tomato DC3000” edited by A. Becker. *Journal of Bacteriology* 198(17):2330–44.

Martin, Marcel. **2011**. “Cutadapt Removes Adapter Sequences from High-Throughput Sequencing Reads.” *EMBnet.Journal* 17(1):10.

McNally, Alan, Nicholas R. Thomson, Sandra Reuter, and Brendan W. Wren. **2016**. “‘Add, Stir and Reduce’: *Yersinia* Spp. as Model Bacteria for Pathogen Evolution.” *Nature Reviews Microbiology* 14(3):177–90.

Mecsas, Joan. **1996**. “Molecular Mechanisms of Bacterial Virulence: Type III Secretion and Pathogenicity Islands.” *Emerging Infectious Diseases* 2(4):271–88.

Melnikov, Sergey, Adam Ben-Shem, Nicolas Garreau De Loubresse, Lasse Jenner, Gulnara Yusupova, and Marat Yusupov. **2012**. “One Core, Two Shells: Bacterial and Eukaryotic Ribosomes.” *Nature Structural and Molecular Biology* 19(6):560–67.

Mey, Alexandra R., Heidi A. Butz, and Shelley M. Payne. **2015**. “*Vibrio Cholerae* CsrA Regulates ToxR Levels in Response to Amino Acids and Is Essential for Virulence” edited by R. K. Taylor. *MBio* 6(4).

Meydan, Sezen, James Marks, Dorota Klepacki, Virag Sharma, Pavel V. Baranov, Andrew E. Firth, Tõnu Margus, Amira Kefi, Nora Vázquez-Laslop, and Alexander S. Mankin. **2019**. “Retapamulin-Assisted Ribosome Profiling Reveals the Alternative Bacterial Proteome.” *Molecular Cell* 74(3):481-493.e6.

Mikula, Kornelia M., Robert Kolodziejczyk, and Adrian Goldman. **2013**. “*Yersinia* Infection Tools—Characterization of Structure and Function of Adhesins.” *Frontiers in Cellular and Infection Microbiology* 2:169.

Mikuni, O., K. Ito, J. Moffat, K. Matsumura, K. McCaughan, T. Nobukuni, W. Tate, and Y. Nakamura. **1994**. “Identification of the PrfC Gene, Which Encodes Peptide-Chain-Release Factor 3 of *Escherichia Coli*.” *Proceedings of the National Academy of Sciences of the United States of America* 91(13):5798–5802.

Miller, D. L. **1972**. “Elongation Factors EF Tu and EF G Interact at Related Sites on Ribosomes.” *Proceedings of the National Academy of Sciences* 69(3):752–55.

Miller, Halie K., Laura Kwuan, Leah Schwiesow, David L. Bernick, Erin Mettert, Hector A. Ramirez, James M. Ragle, Patricia P. Chan, Patricia J. Kiley, Todd M. Lowe, and Victoria Auerbuch. **2014**. “IscR Is Essential for *Yersinia Pseudotuberculosis* Type III Secretion and Virulence” edited by P. Ghosh. *PLoS Pathogens* 10(6):e1004194.

Milne-Davies, Bailey, Carlos Helbig, Stephan Wimmi, Dorothy W. C. Cheng, Nicole Paczia, and Andreas Diepold. **2019**. “Life After Secretion—*Yersinia Enterocolitica* Rapidly Toggles Effector Secretion and Can Resume Cell Division in Response to Changing External Conditions.” *Frontiers in Microbiology* 10.

Milon, Pohl, Marcello Carotti, Andrey L. Konevega, Wolfgang Wintermeyer, Marina V Rodnina, and Claudio O. Gualerzi. **2010**. “The Ribosome-Bound Initiation Factor 2 Recruits Initiator tRNA to the 30S Initiation Complex.” *EMBO Reports* 11(4):312–16.

Milón, Pohl and Marina V. Rodnina. **2012**. “Kinetic Control of Translation Initiation in Bacteria.” *Critical Reviews in Biochemistry and Molecular Biology* 47(4):334–48.

Missiakas, Dominique, Matthias P. Mayer, Marc Lemaire, Costa Georgopoulos, and Satish Raina. **1997**. “Modulation of the *Escherichia Coli* σ E (RpoE) Heat-shock Transcription-factor Activity by the RseA, RseB and RseC Proteins.” *Molecular Microbiology* 24(2):355–71.

Mitarai, Namiko, Kim Sneppen, and Steen Pedersen. **2008**. “Ribosome Collisions and Translation Efficiency: Optimization by Codon Usage and mRNA Destabilization.” *Journal of Molecular Biology* 382(1):236–45.

Monack, D. M., J. Mecsas, N. Ghori, and S. Falkow. **1997**. “*Yersinia* Signals Macrophages to Undergo Apoptosis and YopJ Is Necessary for This Cell Death.” *Proceedings of the National Academy of Sciences* 94(19):10385–90.

Montagner, C., C. Arquint, and G. R. Cornelis. **2011**. “Translocators YopB and YopD from *Yersinia Enterocolitica* Form a Multimeric Integral Membrane Complex in Eukaryotic Cell Membranes.” *Journal of Bacteriology* 193(24):6923–28.

Moran, Charles P., Naomi Lang, S. F. LeGrice, Gloria Lee, Michael Stephens, A. L. Sonenshein, Janice Pero, and Richard Losick. **1982**. “Nucleotide Sequences That Signal the Initiation of Transcription and Translation in *Bacillus Subtilis*.” *Molecular & General Genetics : MGG* 186(3):339–46.

Morrissey, David V. and Mark L. Collins. **1989**. “Nucleic Acid Hybridization Assays Employing DA-Tailed Capture Probes. Single Capture Methods.” *Molecular and Cellular Probes* 3(2):189–207.

Mortazavi, Ali, Brian A. Williams, Kenneth McCue, Lorian Schaeffer, and Barbara Wold. **2008**. “Mapping and Quantifying Mammalian Transcriptomes by RNA-Seq.” *Nature Methods* 5(7):621–28.

Mühlenkamp, Melanie, Philipp Oberhettinger, Jack C. Leo, Dirk Linke, and Monika S. Schütz. **2015**. “*Yersinia* Adhesin A (YadA)--Beauty & Beast.” *International Journal of Medical Microbiology : IJMM* 305(2):252–58.

Mulcahy, Heidi, Julie O’Callaghan, Eoin P. O’Grady, María D. Maciá, Nuria Borrell, Cristina Gómez, Pat G. Casey, Colin Hill, Claire Adams, Cormac G. M. Gahan, Antonio Oliver, and Fergal O’Gara. **2008**. “*Pseudomonas Aeruginosa* RsmA Plays an Important Role during Murine Infection by Influencing Colonization, Virulence, Persistence, and Pulmonary Inflammation.” *Infection and Immunity* 76(2):632–38.

Murakami, K. S. **2002**. “Structural Basis of Transcription Initiation: RNA Polymerase Holoenzyme at 4 A Resolution.” *Science* 296(5571):1280–84.

Nanninga, N. **1967**. “Fine Structure Observed In 50S Ribosomal Subunit Of *Bacillus Subtiles*.” *Journal of Cell Biology* 33(2):C1-6.

Ndah, Elvis, Veronique Jonckheere, Adam Giess, Eivind Valen, Gerben Menschaert, and Petra Van Damme. **2017**. “REPARATION: Ribosome Profiling Assisted (Re-)Annotation of Bacterial Genomes.” *Nucleic Acids Research* 45(20):e168–e168.

Nitzan, Mor, Rotem Rehani, and Hanah Margalit. **2017**. “Integration of Bacterial Small RNAs in Regulatory Networks.” *Annual Review of Biophysics* 46(1):131–48.

Nuss, Aaron M., Fazal Adnan, Lennart Weber, Bork A. Berghoff, Jens Glaeser, and Gabriele Klug. **2013**. “DegS and RseP Homologous Proteases Are Involved in Singlet Oxygen Dependent Activation of RpoE in *Rhodobacter Sphaeroides*” edited by R. Misra. *PLoS ONE* 8(11):e79520.

Nuss, Aaron M., Michael Beckstette, Maria Pimenova, Carina Schmühl, Wiebke Opitz, Fabio Pisano, Ann Kathrin Heroven, and Petra Dersch. **2017**. “Tissue Dual RNA-Seq Allows Fast Discovery of Infection-Specific Functions and Riboregulators Shaping Host–Pathogen Transcriptomes.” *Proceedings of the National Academy of Sciences* 114(5):E791–800.

Nuss, Aaron M., Ann Kathrin Heroven, and Petra Dersch. **2017**. “RNA Regulators: Formidable Modulators of *Yersinia* Virulence.” *Trends in Microbiology* 25(1):19–34.

Nuss, Aaron M., Ann Kathrin Heroven, Barbara Waldmann, Jan Reinkensmeier, Michael Jarek, Michael Beckstette, and Petra Dersch. **2015**. “Transcriptomic Profiling of *Yersinia Pseudotuberculosis* Reveals Reprogramming of the Crp Regulon by Temperature and Uncovers Crp as a Master Regulator of Small RNAs.” *PLoS Genetics* 11(3):1–26.

Oh, Eugene, Annemarie H. Becker, Arzu Sandikci, Damon Huber, Rachna Chaba, Felix Gloge, Robert J. Nichols, Athanasios Typas, Carol A. Gross, Günter Kramer, Jonathan S. Weissman, and Bernd Bukau. **2011**. “Selective Ribosome Profiling Reveals the Cotranslational Chaperone Action of Trigger Factor in Vivo.” *Cell* 147(6):1295–1308.

Ohnishi, K., K. Kutsukake, H. Suzuki, and T. Iino. **1990**. “Gene FliA Encodes an Alternative Sigma Factor Specific for Flagellar Operons in *Salmonella Typhimurium*.” *Molecular & General Genetics : MGG* 221(2):139–47.

Olsson, Jan, Petra J. Edqvist, Jeanette E. Bröms, Åke Forsberg, Hans Wolf-Watz, and Matthew S.

Francis. **2004**. “The YopD Translocator of *Yersinia Pseudotuberculosis* Is a Multifunctional Protein Comprised of Discrete Domains.” *Journal of Bacteriology* 186(13):4110–23.

Orth, Kim. **2002**. “Function of the *Yersinia* Effector YopJ.” *Current Opinion in Microbiology* 5(1):38–43.

Osborne, Suzanne E. and Brian K. Coombes. **2009**. “RpoE Fine Tunes Expression of a Subset of SsrB-Regulated Virulence Factors in *Salmonella Enterica* Serovar Typhimurium.” *BMC Microbiology* 9(1):45.

Osterman, Ilya A., Sergey A. Evfratov, Petr V. Sergiev, and Olga A. Dontsova. **2013**. “Comparison of mRNA Features Affecting Translation Initiation and Reinitiation.” *Nucleic Acids Research* 41(1):474–86.

Otto, Christian, Peter F. Stadler, and Steve Hoffmann. **2014**. “Lacking Alignments? The next-Generation Sequencing Mapper Segemehl Revisited.” *Bioinformatics* 30(13):1837–43.

Paget, Mark S. B. and John D. Helmann. **2003**. “The Sigma70 Family of Sigma Factors.” *Genome Biology* 4(1):203.

Palmer, Lance E., Alessandra R. Pancetti, Steven Greenberg, and James B. Bliska. **1999**. “YopJ of *Yersinia* Spp. Is Sufficient To Cause Downregulation of Multiple Mitogen-Activated Protein Kinases in Eukaryotic Cells” edited by P. J. Sansonetti. *Infection and Immunity* 67(2):708–16.

Palonen, Eveliina, Miia Lindström, Panu Somervuo, and Hannu Korkeala. **2013**. “Alternative Sigma Factor σE Has an Important Role in Stress Tolerance of *Yersinia Pseudotuberculosis* IP32953.” *Applied and Environmental Microbiology* 79(19):5970–77.

Park, Young Seoub, Sang Woo Seo, Seungha Hwang, Hun Su Chu, Jin-Ho Ahn, Tae-Wan Kim, Dong-Myung Kim, and Gyoo Yeol Jung. **2007**. “Design of 5′-Untranslated Region Variants for Tunable Expression in *Escherichia Coli*.” *Biochemical and Biophysical Research Communications* 356(1):136–41.

Pasternak, Cécile, Weizhen Chen, Claudia Heck, and Gabriele Klug. **1996**. “Cloning, Nucleotide Sequence and Characterization of the RpoD Gene Encoding the Primary Sigma Factor of *Rhodobacter Capsulatus*.” *Gene* 176(1–2):177–84.

Von Pawel-Rammingen, Ulrich, Maxim V. Telepnev, Gudula Schmidt, Klaus Aktories, Hans Wolf-Watz, and Roland Rosqvist. **2002**. “GAP Activity of the *Yersinia* YopE Cytotoxin Specifically Targets the Rho Pathway: A Mechanism for Disruption of Actin Microfilament Structure.” *Molecular Microbiology* 36(3):737–48.

Payne, Patricia L. and Susan C. Straley. **1999**. “YscP of *Yersinia Pestis* Is a Secreted Component of the Yop Secretion System.” *Journal of Bacteriology* 181(9):2852–62.

Pechous, Roger D., Vijay Sivaraman, Nikolas M. Stasulli, and William E. Goldman. **2016**. “Pneumonic Plague: The Darker Side of *Yersinia Pestis*.” *Trends in Microbiology* 24(3):190–97.

Perry, R. D. and J. D. Fetherston. **1997**. “*Yersinia Pestis*--Etiologic Agent of Plague.” *Clinical Microbiology Reviews* 10(1):35–66.

Perry, R. D., P. A. Harmon, W. S. Bowmer, and S. C. Straley. **1986**. “A Low-Ca2+ Response Operon Encodes the V Antigen of *Yersinia Pestis*.” *Infection and Immunity* 54(2):428–34.

Pha, Khavong and Lorena Navarro. **2016**. “*Yersinia* Type III Effectors Perturb Host Innate Immune Responses.” *World Journal of Biological Chemistry* 7(1):1.

Pha, Khavong, Matthew E. Wright, Tasha M. Barr, Richard A. Eigenheer, and Lorena Navarro. **2014**. “Regulation of *Yersinia* Protein Kinase A (YpkA) Kinase Activity by Multisite Autophosphorylation and Identification of an N-Terminal Substrate-Binding Domain in YpkA.” *Journal of Biological Chemistry* 289(38):26167–77.

Pilsl, H., H. Killmann, K. Hantke, and V. Braun. **1996**. “Periplasmic Location of the Pesticin Immunity Protein Suggests Inactivation of Pesticin in the Periplasm.” *Journal of Bacteriology* 178(8):2431–

35.

Pilz, D., T. Vocke, J. Heesemann, and V. Brade. **1992**. “Mechanism of YadA-Mediated Serum Resistance of *Yersinia Enterocolitica* Serotype O3.” *Infection and Immunity* 60(1):189–95.

Pinto, Daniela, Qiang Liu, and Thorsten Mascher. **2019**. “ECF σ Factors with Regulatory Extensions: The One-component Systems of the σ Universe.” *Molecular Microbiology* 112(2):399–409.

Plano, Gregory V. and Kurt Schesser. **2013**. “The *Yersinia Pestis* Type III Secretion System: Expression, Assembly and Role in the Evasion of Host Defenses.” *Immunologic Research* 57(1–3):237–45.

Portnoy, D. A., H. Wolf-Watz, I. Bolin, A. B. Beeder, and S. Falkow. **1984**. “Characterization of Common Virulence Plasmids in *Yersinia* Species and Their Role in the Expression of Outer Membrane Proteins.” *Infection and Immunity* 43(1):108–14.

Pribnow, D. **1975**. “Nucleotide Sequence of an RNA Polymerase Binding Site at an Early T7 Promoter.” *Proceedings of the National Academy of Sciences* 72(3):784–88.

R, Simon, Prieffer U, and Puhler A. **1983**. “A Broad Host Range Mobilization System for in Vivo Genetic Engineering: Transposon Mutagenesis in Gram Negative Bacteria.” *Biotechnology* (1):784–90.

Ramakrishnan, V. **2002**. “Ribosome Structure and the Mechanism of Translation.” *Cell* 108(4):557–72.

Reuter, S., T. R. Connor, L. Barquist, D. Walker, T. Feltwell, S. R. Harris, M. Fookes, M. E. Hall, N. K. Petty, T. M. Fuchs, J. Corander, M. Dufour, T. Ringwood, C. Savin, C. Bouchier, L. Martin, M. Miettinen, M. Shubin, J. M. Riehm, R. Laukkanen-Ninios, L. M. Sihvonen, A. Siitonen, M. Skurnik, J. P. Falcao, H. Fukushima, H. C. Scholz, M. B. Prentice, B. W. Wren, J. Parkhill, E. Carniel, M. Achtman, A. McNally, and N. R. Thomson. **2014**. “Parallel Independent Evolution of Pathogenicity within the Genus *Yersinia*.” *Proceedings of the National Academy of Sciences* 111(18):6768–73.

Rhodius, Virgil A., Won Chul Suh, Gen Nonaka, Joyce West, and Carol A. Gross. **2005**. “Conserved and Variable Functions of the σE Stress Response in Related Genomes” edited by J. A. Eisen. *PLoS Biology* 4(1):e2.

Richman, N. and J. W. Bodley. **1972**. “Ribosomes Cannot Interact Simultaneously with Elongation Factors EF Tu and EF G.” *Proceedings of the National Academy of Sciences* 69(3):686–89.

Righetti, Francesco, Aaron M. Nuss, Christian Twittenhoff, Sascha Beele, Kristina Urban, Sebastian Will, Stephan H. Bernhart, Peter F. Stadler, Petra Dersch, and Franz Narberhaus. **2016**. “Temperature-Responsive in Vitro RNA Structurome of *Yersinia Pseudotuberculosis*.” *Proceedings of the National Academy of Sciences* 113(26):7237–42.

Rimpiläinen, M., A. Forsberg, and H. Wolf-Watz. **1992**. “A Novel Protein, LcrQ, Involved in the Low-Calcium Response of *Yersinia Pseudotuberculosis* Shows Extensive Homology to YopH.” *Journal of Bacteriology* 174(10):3355–63.

Ringquist, Steven, Sidney Shinedling, Doug Barrick, Louis Green, Jonathan Binkley, Gary D. Stormo, and Larry Gold. **1992**. “Translation Initiation in *Escherichia Coli*: Sequences within the Ribosome-Binding Site.” *Molecular Microbiology* 6(9):1219–29.

Rodnina, Marina V. **2018**. “Translation in Prokaryotes.” *Cold Spring Harbor Perspectives in Biology* 10(9):1–22.

Rodnina, Marina V., Niels Fischer, Cristina Maracci, and Holger Stark. **2017**. “Ribosome Dynamics during Decoding.” *Philosophical Transactions of the Royal Society B: Biological Sciences* 372(1716):20160182.

Roehrich, A. Dorothea, Enora Guillossou, Ariel J. Blocker, and Isabel Martinez-Argudo. **2013**. “*Shigella* IpaD Has a Dual Role: Signal Transduction from the Type III Secretion System Needle Tip and Intracellular Secretion Regulation.” *Molecular Microbiology* 87(3):690–706.

Rogalski, Marcelo, Daniel Karcher, and Ralph Bock. **2008**. “Superwobbling Facilitates Translation with Reduced tRNA Sets.” *Nature Structural and Molecular Biology* 15(2):192–98.

Rojas, Joaquín, Gabriel Castillo, Lorenzo Eugenio Leiva, Sara Elgamal, Omar Orellana, Michael Ibba, and Assaf Katz. **2018**. "Codon Usage Revisited: Lack of Correlation between Codon Usage and the Number of TRNA Genes in Enterobacteria." *Biochemical and Biophysical Research Communications* 502(4):450–55.

Rolán, Hortensia G., Enrique A. Durand, and Joan Mecsas. **2013**. "Identifying *Yersinia* YopH-Targeted Signal Transduction Pathways That Impair Neutrophil Responses during In Vivo Murine Infection." *Cell Host & Microbe* 14(3):306–17.

Romeo, T., M. Gong, M. Y. Liu, and A. M. Brun-Zinkernagel. **1993**. "Identification and Molecular Characterization of CsrA, a Pleiotropic Gene from *Escherichia Coli* That Affects Glycogen Biosynthesis, Gluconeogenesis, Cell Size, and Surface Properties." *Journal of Bacteriology* 175(15):4744–55.

Romeo, Tony and Paul Babitzke. **2019**. "Global Regulation by CsrA and Its RNA Antagonists." Pp. 341–54 in *Regulating with RNA in Bacteria and Archaea*. Vol. 6. American Society of Microbiology.

Romeo, Tony, Christopher A. Vakulskas, and Paul Babitzke. **2013**. "Post-Transcriptional Regulation on a Global Scale: Form and Function of Csr/Rsm Systems." *Environmental Microbiology* 15(2):313–24.

Rosqvist, R., I. Bölin, and H. Wolf-Watz. **1988**. "Inhibition of Phagocytosis in *Yersinia Pseudotuberculosis*: A Virulence Plasmid-Encoded Ability Involving the Yop2b Protein." *Infection and Immunity* 56(8):2139–43.

Ross, A. J., R. R. Rucker, and W. H. Ewing. **1966**. "Description of a Bacterium Associated with Redmouth Disease of Rainbow Trout (*Salmo Gairdneri*)." *Canadian Journal of Microbiology* 12(4):763–70.

Ross, W., K. Gosink, J. Salomon, K. Igarashi, C. Zou, A. Ishihama, K. Severinov, and R. Gourse. **1993**. "A Third Recognition Element in Bacterial Promoters: DNA Binding by the Alpha Subunit of RNA Polymerase." *Science* 262(5138):1407–13.

Rowley, Gary, Michael Spector, Jan Kormanec, and Mark Roberts. **2006**. "Pushing the Envelope: Extracytoplasmic Stress Responses in Bacterial Pathogens." *Nature Reviews Microbiology* 4(5):383–94.

Ruckdeschel, K., A. Roggenkamp, V. Lafont, P. Mangeat, J. Heesemann, and B. Rouot. **1997**. "Interaction of *Yersinia Enterocolitica* with Macrophages Leads to Macrophage Cell Death through Apoptosis." *Infection and Immunity* 65(11):4813–21.

Rüter, Christian, Mariana Ruiz Silva, Benjamin Grabowski, Marie-Luise Lubos, Julia Scharnert, Marija Poceva, Dominik von Tils, Antje Flieger, Jürgen Heesemann, James B. Bliska, and M. Alexander Schmidt. **2014**. "Rabbit Monoclonal Antibodies Directed at the T3SS Effector Protein YopM Identify Human Pathogenic *Yersinia* Isolates." *International Journal of Medical Microbiology* 304(3–4):444–51.

Sadana, Pooja, Rebecca Geyer, Joern Pezoldt, Saskia Helmsing, Jochen Huehn, Michael Hust, Petra Dersch, and Andrea Scrima. **2018**. "The Invasin D Protein from *Yersinia Pseudotuberculosis* Selectively Binds the Fab Region of Host Antibodies and Affects Colonization of the Intestine." *The Journal of Biological Chemistry* 293(22):8672–90.

Sadana, Pooja, Manuel Mönnich, Carlo Unverzagt, and Andrea Scrima. **2017**. "Structure of the *Y. Pseudotuberculosis* Adhesin InvasinE." *Protein Science : A Publication of the Protein Society* 26(6):1182–95.

Saiki, R., D. Gelfand, S. Stoffel, S. Scharf, R. Higuchi, G. Horn, K. Mullis, and H. Erlich. **1988**. "Primer-Directed Enzymatic Amplification of DNA with a Thermostable DNA Polymerase." *Science* 239(4839):487–91.

Sample, Allen K., Janet M. Fowler, and Robert R. Brubaker. **1987**. "Modulation of the Low-Calcium Response in *Yersinia Pestis* via Plasmid-Plasmid Interaction." *Microbial Pathogenesis* 2(6):443–53.

Sana, Thibault G., Aurélie Laubier, and Sophie Bleves. **2014**. “Gene Transfer: Conjugation.” Pp. 17–22 in.

Sander, G., R. C. Marsh, J. Voigt, and A. Parmeggiani. **1975**. “A Comparative Study of the 50S Ribosomal Subunit and Several 50S Subparticles in EF-T-and EF-G-Dependent Activities.” *Biochemistry* 14(9):1805–14.

Sansonetti, Philippe J. **2004**. “War and Peace at Mucosal Surfaces.” *Nature Reviews Immunology* 4(12):953–64.

Sarker, Mahfuzur R., Cécile Neyt, Isabelle Stainier, and Guy R. Cornelis. **1998**. “The *Yersinia* Yop Virulon: LcrV Is Required for Extrusion of the Translocators YopB and YopD.” *Journal of Bacteriology* 180(5):1207–14.

Sauert, Martina, Michael T. Wolfinger, Oliver Vesper, Christian Müller, Konstantin Byrgazov, and Isabella Moll. **2016**. “The MazF-Regulon: A Toolbox for the Post-Transcriptional Stress Response in *Escherichia Coli*.” *Nucleic Acids Research* 44(14):6660–75.

Savin, Cyril, Alexis Criscuolo, Julien Guglielmini, Anne-Sophie Le Guern, Elisabeth Carniel, Javier Pizarro-Cerdá, and Sylvain Brisse. **2019**. “Genus-Wide *Yersinia* Core-Genome Multilocus Sequence Typing for Species Identification and Strain Characterization.” *Microbial Genomics* 5(10).

Scherer, Günther F. E., Malcolm D. Walkinshaw, Struther Arnott, and D. Jame. Morré. **1980**. “The Ribosome Binding Sites Recognized by *E. Coli* Ribosomes Have Regions with Signal Character in Both the Leader and Protein Coding Segments.” *Nucleic Acids Research* 8(17):3895–3908.

Schiano, C. A., J. T. Koo, M. J. Schipma, A. J. Caulfield, N. Jafari, and W. W. Lathem. **2014**. “Genome-Wide Analysis of Small RNAs Expressed by *Yersinia Pestis* Identifies a Regulator of the Yop-Ysc Type III Secretion System.” *Journal of Bacteriology* 196(9):1659–70.

Schiano, Chelsea A., Jovanka T. Koo, Matthew J. Schipma, Adam J. Caulfield, Nadereh Jafari, and Wyndham W. Lathem. **2014**. “Genome-Wide Analysis of Small RNAs Expressed by *Yersinia Pestis* Identifies a Regulator of the Yop-Ysc Type III Secretion System.” *Journal of Bacteriology* 196(9):1659–70.

Schiemann, D. A. **1987**. “*Yersinia Enterocolitica* in Milk and Dairy Products.” *Journal of Dairy Science* 70(2):383–91.

Schindler, Magnus K. H., Monika S. Schütz, Melanie C. Mühlenkamp, Suzan H. M. Rooijakkers, Teresia Hallström, Peter F. Zipfel, and Ingo B. Autenrieth. **2012**. “*Yersinia Enterocolitica* YadA Mediates Complement Evasion by Recruitment and Inactivation of C3 Products.” *The Journal of Immunology* 189(10):4900–4908.

Schleif, Robert. **2010**. “AraC Protein, Regulation of the l-Arabinose Operon in *Escherichia Coli*, and the Light Switch Mechanism of AraC Action.” *FEMS Microbiology Reviews* 34(5):779–96.

Schmeing, T. Martin and V. Ramakrishnan. **2009**. “What Recent Ribosome Structures Have Revealed about the Mechanism of Translation.” *Nature* 461(7268):1234–42.

Schoberle, Taylor J., Lawton K. Chung, Joseph B. McPhee, Ben Bogin, and James B. Bliska. **2016**. “Uncovering an Important Role for YopJ in the Inhibition of Caspase-1 in Activated Macrophages and Promoting *Yersinia Pseudotuberculosis* Virulence” edited by C. R. Roy. *Infection and Immunity* 84(4):1062–72.

Schütz, M., E. M. Weiss, M. Schindler, T. Hallström, P. F. Zipfel, D. Linke, and I. B. Autenrieth. **2010**. “Trimer Stability of YadA Is Critical for Virulence of *Yersinia Enterocolitica*.” *Infection and Immunity* 78(6):2677–90.

Schweer, Janina, Devesha Kulkarni, Annika Kochut, Joern Pezoldt, Fabio Pisano, Marina C. Pils, Harald Genth, Jochen Huehn, and Petra Dersch. **2013**. “The Cytotoxic Necrotizing Factor of *Yersinia Pseudotuberculosis* (CNFY) Enhances Inflammation and Yop Delivery during Infection by

Activation of Rho GTPases" edited by J. B. Bliska. *PLoS Pathogens* 9(11):e1003746.

Schwiesow, Leah, Hanh Lam, Petra Dersch, and Victoria Auerbuch. **2015**. "*Yersinia* Type III Secretion System Master Regulator LcrF." *Journal of Bacteriology* 198(4):604–14.

Sebbane, F., C. O. Jarrett, D. Gardner, D. Long, and B. J. Hinnebusch. **2006**. "Role of the *Yersinia Pestis* Plasminogen Activator in the Incidence of Distinct Septicemic and Bubonic Forms of Flea-Borne Plague." *Proceedings of the National Academy of Sciences* 103(14):5526–30.

Sette, M., P. van Tilborg, R. Spurio, R. Kaptein, M. Paci, C. O. Gualerzi, and R. Boelens. **1997**. "The Structure of the Translational Initiation Factor IF1 from *E.Coli* Contains an Oligomer-Binding Motif." *The EMBO Journal* 16(6):1436–43.

Severinov, Konstantin, Rachel Mooney, Seth A. Darst, and Robert Landick. **1997**. "Tethering of the Large Subunits of *Escherichia Coli* RNA Polymerase." *Journal of Biological Chemistry* 272(39):24137–40.

Shaban, Lamyaa, Giang T. Nguyen, Benjamin D. Mecsas-Faxon, Kenneth D. Swanson, Shumin Tan, and Joan Mecsas. **2020**. "*Yersinia Pseudotuberculosis* YopH Targets SKAP2-Dependent and Independent Signaling Pathways to Block Neutrophil Antimicrobial Mechanisms during Infection" edited by E. Oswald. *PLOS Pathogens* 16(5):e1008576.

Shi, Zhen, Kotaro Fujii, Kyle M. Kovary, Naomi R. Genuth, Hannes L. Röst, Mary N. Teruel, and Maria Barna. **2017**. "Heterogeneous Ribosomes Preferentially Translate Distinct Subpools of mRNAs Genome-Wide." *Molecular Cell* 67(1):71-83.e7.

Shimada, Tomohiro, Kan Tanaka, and Akira Ishihama. **2017**. "The Whole Set of the Constitutive Promoters Recognized by Four Minor Sigma Subunits of *Escherichia Coli* RNA Polymerase." *PloS One* 12(6):e0179181.

Shine, John and Lynn Dalgarno. **1975**. "Terminal-Sequence Analysis of Bacterial Ribosomal RNA. Correlation between the 3'-Terminal-Polypyrimidine Sequence of 16-S RNA and Translational Specificity of the Ribosome." *European Journal of Biochemistry* 57(1):221–30.

Silva-Herzog, Eugenia, Franco Ferracci, Michael W. Jackson, Sabrina S. Joseph, and Gregory V. Plano. **2008**. "Membrane Localization and Topology of the *Yersinia Pestis* YscJ Lipoprotein." *Microbiology* 154(2):593–607.

Silva, Francisco J., Eugeni Belda, and Santiago E. Talens. **2006**. "Differential Annotation of TRNA Genes with Anticodon CAT in Bacterial Genomes." *Nucleic Acids Research* 34(20):6015–22.

Simonet, M. and S. Falkow. **1992**. "Invasin Expression in *Yersinia Pseudotuberculosis*." *Infection and Immunity* 60(10):4414–17.

Simonetti, Angelita, Stefano Marzi, Alexander G. Myasnikov, Attilio Fabbretti, Marat Yusupov, Claudio O. Gualerzi, and Bruno P. Klaholz. **2008**. "Structure of the 30S Translation Initiation Complex." *Nature* 455(7211):416–20.

Skurnik, M. and P. Toivanen. **1992**. "LcrF Is the Temperature-Regulated Activator of the YadA Gene of *Yersinia Enterocolitica* and *Yersinia Pseudotuberculosis*." *Journal of Bacteriology* 174(6):2047–51.

Skurnik, M. and H. Wolf-Watz. **1989**. "Analysis of the YopA Gene Encoding the Yop1 Virulence Determinants of *Yersinia* Spp." *Molecular Microbiology* 3(4):517–29.

Snellings, Norma J., Michael Popek, and Luther E. Lindler. **2001**. "Complete DNA Sequence Of." *Plasmid* 69(7):4627–38.

Sørensen, Michael A. and Steen Pedersen. **1991**. "Absolute in Vivo Translation Rates of Individual Codons in *Escherichia Coli*." *Journal of Molecular Biology* 222(2):265–80.

Sorg, Joseph A., Nathan C. Miller, Melanie M. Marketon, and Olaf Schneewind. **2005**. "Rejection of Impassable Substrates by *Yersinia* Type III Secretion Machines." *Journal of Bacteriology* 187(20):7090–7102.

Souza, Clarice de Azevedo, Kristian L. Richards, YoSon Park, Michael Schwartz, Julie Torruellas Garcia, Sara Schesser Bartra, and Gregory V. Plano. **2018**. “The YscE/YscG Chaperone and YscF N-Terminal Sequences Target YscF to the *Yersinia Pestis* Type III Secretion Apparatus.” *Microbiology* 164(3):338–48.

Srivastava, Ambuj, Prerana Gogoi, Bhagyashree Deka, Shrayanti Goswami, and Shankar Prasad Kanaujia. **2016**. “In Silico Analysis of 5′-UTRs Highlights the Prevalence of Shine–Dalgarno and Leaderless-Dependent Mechanisms of Translation Initiation in Bacteria and Archaea, Respectively.” *Journal of Theoretical Biology* 402:54–61.

Stainier, Isabelle, Maite Iriarte, and Guy R. Cornelis. **1997**. “YscM1 and YscM2, Two *Yersinia Enterocolitica* Proteins Causing Downregulation of Yop Transcription.” *Molecular Microbiology* 26(4):833–43.

Starmer, J., A. Stomp, M. Vouk, and D. Bitzer. **2006**. “Predicting Shine-Dalgarno Sequence Locations Exposes Genome Annotation Errors.” *PLoS Computational Biology* 2(5):454–66.

Starnbach, M. N. and S. Lory. **1992**. “The FliA (RpoF) Gene of *Pseudomonas Aeruginosa* Encodes an Alternative Sigma Factor Required for Flagellin Synthesis.” *Molecular Microbiology* 6(4):459–69.

Steinmann, Rebekka. **2013**. “Characterization of Temperature Dependent and Feedback Controlled Expression of the Virulence Activator LcrF in *Yersinia Pseudotuberculosis*.” TU Braunschweig.

Steinmann, Rebekka and Petra Dersch. **2013**. “Thermosensing to Adjust Bacterial Virulence in a Fluctuating Environment.” *Future Microbiology* 8(1):85–105.

Steitz, Thomas A. **2008**. “A Structural Understanding of the Dynamic Ribosome Machine.” *Nature Reviews Molecular Cell Biology* 9(3):242–53.

Stephanie Christine Seekircher. **2014**. “Identification of Regulatory Factors That Control the Synthesis of the Small Regulatory RNA CsrC in *Yersinia Pseudotuberculosis*.” TU Braunschweig.

Stothard, Paul. **2000**. “The Sequence Manipulation Suite: JavaScript Programs for Analyzing and Formatting Protein and DNA Sequences.” *BioTechniques* 28(6):1102–4.

Straley, S. C. and W. S. Bowmer. **1986**. “Virulence Genes Regulated at the Transcriptional Level by Ca2+ in *Yersinia Pestis* Include Structural Genes for Outer Membrane Proteins.” *Infection and Immunity* 51(2):445–54.

Straley, Susan C., Gregory V Plano, Elźbieta Skrzypek, Pryce L. Haddix, and Kenneth A. Fields. **1993**. “Regulation by Ca 2+ in the *Yersinia* Low-Ca 2+ Response.” *Molecular Microbiology* 8(6):1005–10.

Sun, D., P. Fajardo-Cavazos, M. D. Sussman, F. Tovar-Rojo, R. M. Cabrera-Martinez, and P. Setlow. **1991**. “Effect of Chromosome Location of *Bacillus Subtilis* Forespore Genes on Their Spo Gene Dependence and Transcription by E Sigma F: Identification of Features of Good E Sigma F-Dependent Promoters.” *Journal of Bacteriology* 173(24):7867–74.

Suzuki, Kazushi. **2006**. “Identification of a Novel Regulatory Protein (CsrD) That Targets the Global Regulatory RNAs CsrB and CsrC for Degradation by RNase E.” *Genes & Development* 20(18):2605–17.

Sweet, Charles R., Joseph Conlon, Douglas T. Golenbock, Jon Goguen, and Neal Silverman. **2007**. “YopJ Targets TRAF Proteins to Inhibit TLR-Mediated NF-κB, MAPK and IRF3 Signal Transduction.” *Cellular Microbiology* 9(11):2700–2715.

El Tahir, Y; Skurnik M. **2001**. “YadA, the Multifaceted Adhesin.” *International Journal of Medical Microbiology* 291(3):209–18.

Takahashi, Shuntaro, Hiroyuki Furusawa, Takuya Ueda, and Yoshio Okahata. **2013**. “Translation Enhancer Improves the Ribosome Liberation from Translation Initiation.” *Journal of the American Chemical Society* 135(35):13096–106.

Taylor, F. J. R. and D. Coates. **1989**. “The Code within the Codons.” *Biosystems* 22(3):177–87.

Temmel, Hannes, Christian Müller, Martina Sauert, Oliver Vesper, Ariela Reiss, Johannes Popow, Javier Martinez, and Isabella Moll. **2017**. “The RNA Ligase RtcB Reverses MazF-Induced Ribosome Heterogeneity in *Escherichia Coli*.” *Nucleic Acids Research* 45(8):4708–21.

Thaiss, Christoph A., Niv Zmora, Maayan Levy, and Eran Elinav. **2016**. “The Microbiome and Innate Immunity.” *Nature* 535(7610):65–74.

Thinwa, Josephine, Jesus A. Segovia, Santanu Bose, and Peter H. Dube. **2014**. “Integrin-Mediated First Signal for Inflammasome Activation in Intestinal Epithelial Cells.” *The Journal of Immunology* 193(3):1373–82.

Thomas, Mark S. and Sivaramesh Wigneshweraraj. **2014**. “Regulation of Virulence Gene Expression.” *Virulence* 5(8):832–34.

Thomas, Nikhil A. and B. Brett Finlay. **2003**. “Establishing Order for Type III Secretion Substrates – a Hierarchical Process.” *Trends in Microbiology* 11(8):398–403.

Thorslund, Sara E., David Ermert, Anna Fahlgren, Saskia F. Erttmann, Kristina Nilsson, Ava Hosseinzadeh, Constantin F. Urban, and Maria Fällman. **2013**. “Role of YopK in *Yersinia Pseudotuberculosis* Resistance against Polymorphonuclear Leukocyte Defense” edited by J. B. Bliska. *Infection and Immunity* 81(1):11–22.

Timmermans, Johan and Laurence Van Melderen. **2010**. “Post-Transcriptional Global Regulation by CsrA in Bacteria.” *Cellular and Molecular Life Sciences* 67(17):2897–2908.

Tony Romeo, Christopher A. Vakulskas, and Paul Babitzke. **2012**. “Posttranscriptional Regulation on a Global Scale: Form and Function of Csr/Rsm Systems.” *Environ Microbiol.* 15(2):313–24.

Trosky, Jennifer E., Amy D. B. Liverman, and Kim Orth. **2008**. “*Yersinia* Outer Proteins: Yops.” *Cellular Microbiology* 10(3):557–65.

Vasala, M., S. Hallanvuo, P. Ruuska, R. Suokas, A. Siitonen, and M. Hakala. **2014**. “High Frequency of Reactive Arthritis in Adults after *Yersinia Pseudotuberculosis* O:1 Outbreak Caused by Contaminated Grated Carrots: Table 1.” *Annals of the Rheumatic Diseases* 73(10):1793–96.

Vesper, Oliver, Shahar Amitai, Maria Belitsky, Konstantin Byrgazov, Anna Chao Kaberdina, Hanna Engelberg-Kulka, and Isabella Moll. **2011**. “Selective Translation of Leaderless mRNAs by Specialized Ribosomes Generated by MazF in *Escherichia Coli*.” *Cell* 147(1):147–57.

Viboud, G. I. and J. B. Bliska. **2001**. “A Bacterial Type III Secretion System Inhibits Actin Polymerization to Prevent Pore Formation in Host Cell Membranes.” *The EMBO Journal* 20(19):5373–82.

Viboud, Gloria I. and James B. Bliska. **2005**. “*YERSINIA* OUTER PROTEINS: Role in Modulation of Host Cell Signaling Responses and Pathogenesis.” *Annual Review of Microbiology* 59(1):69–89.

Viboud, Gloria I., Edison Mejia, and James B. Bliska. **2006**. “Comparison of YopE and YopT Activities in Counteracting Host Signalling Responses to *Yersinia Pseudotuberculosis* Infection.” *Cellular Microbiology* 8(9):1504–15.

Vieux, Ellen F. and Doug Barrick. **2011**. “Deletion of Internal Structured Repeats Increases the Stability of a Leucine-Rich Repeat Protein, YopM.” *Biophysical Chemistry* 159(1):152–61.

Visser, L. G., A. Annema, and R. van Furth. **1995**. “Role of Yops in Inhibition of Phagocytosis and Killing of Opsonized *Yersinia Enterocolitica* by Human Granulocytes.” *Infection and Immunity* 63(7):2570–75.

Volk, Marcel, Ines Vollmer, Ann Kathrin Heroven, and Petra Dersch. **2019**. “Transcriptional and Post-Transcriptional Regulatory Mechanisms Controlling Type III Secretion.” in *Current Topics in Microbiology and Immunology*.

Vollmer, Ines. **2020**. “Analysis of the RNA-Based Mechanisms Controlling Virulence in *Yersinia Pseudotuberculosis*.” TU Braunschweig.

Wang, He, Kemal Avican, Anna Fahlgren, Saskia F. Erttmann, Aaron M. Nuss, Petra Dersch, Maria Fallman, Tomas Edgren, and Hans Wolf-Watz. **2016**. “Increased Plasmid Copy Number Is Essential for *Yersinia* T3SS Function and Virulence.” *Science (New York, N.Y.)* 353(6298):492–95.

Wang, Miao, Zeqian Gao, Zhongwang Zhang, Li Pan, and Yongguang Zhang. **2014**. “Roles of M Cells in Infection and Mucosal Vaccines.” *Human Vaccines & Immunotherapeutics* 10(12):3544–51.

Watson, J. D. and F. H. C. Crick. **1953**. “Molecular Structure of Nucleic Acids: A Structure for Deoxyribose Nucleic Acid.” *Nature* 171(4356):737–38.

Wattiau, P., B. Bernier, P. Deslee, T. Michiels, and G. R. Cornelis. **1994**. “Individual Chaperones Required for Yop Secretion by *Yersinia*.” *Proceedings of the National Academy of Sciences* 91(22):10493–97.

Wattiau, Pierre and Guy R. Cornells. **1993**. “SycE, a Chaperone-like Protein of *Yersinia Enterocolitica* Involved in the Secretion of YopE.” *Molecular Microbiology* 8(1):123–31.

Wattiau, Pierre, Sophie Woestyn, and Guy R. Cornelis. **1996**. “Customized Secretion Chaperones in Pathogenic Bacteria.” *Molecular Microbiology* 20(2):255–62.

Weilbacher, Thomas, Kazushi Suzuki, Ashok K. Dubey, Xin Wang, Seshigirao Gudapaty, Igor Morozov, Carol S. Baker, Dimitris Georgellis, Paul Babitzke, and Tony Romeo. **2003**. “A Novel sRNA Component of the Carbon Storage Regulatory System of *Escherichia Coli*.” *Molecular Microbiology* 48(3):657–70.

Weiss, Andy, Brittney D. Moore, Miguel H. J. Tremblay, Dale Chaput, Astrid Kremer, and Lindsey N. Shaw. **2017**. “The ω Subunit Governs RNA Polymerase Stability and Transcriptional Specificity in *Staphylococcus Aureus*” edited by V. J. DiRita. *Journal of Bacteriology* 199(2).

Wiley, David J., Roland Rosqvist, and Kurt Schesser. **2007**. “Induction of the *Yersinia* Type 3 Secretion System as an All-or-None Phenomenon.” *Journal of Molecular Biology* 373(1):27–37.

Williams, Andrew W. and Susan C. Straley. **1998**. “YopD of *Yersinia Pestis* Plays a Role in Negative Regulation of the Low-Calcium Response in Addition to Its Role in Translocation of Yops.” *Journal of Bacteriology* 180(2):350–58.

Wimberly, B. T., D. E. Brodersen, W. M. Clemons, R. J. Morgan-Warren, A. P. Carter, C. Vonrhein, T. Hartsch, and V. Ramakrishnan. **2000**. “Structure of the 30S Ribosomal Subunit.” *Nature* 407(6802):327–39.

Winardhi, Ricksen S., Jie Yan, and Linda J. Kenney. **2015**. “H-NS Regulates Gene Expression and Compacts the Nucleoid: Insights from Single-Molecule Experiments.” *Biophysical Journal* 109(7):1321–29.

Woestyn, S., A. Allaoui, P. Wattiau, and G. R. Cornelis. **1994**. “YscN, the Putative Energizer of the *Yersinia* Yop Secretion Machinery.” *Journal of Bacteriology* 176(6):1561–69.

Woestyn, Sophie, Marie-Paule Sory, Anne Boland, Olivier Lequenne, and Guy R. Cornelis. **1996**. “The Cytosolic SycE and SycH Chaperones of *Yersinia* Protect the Region of YopE and YopH Involved in Translocation across Eukaryotic Cell Membranes.” *Molecular Microbiology* 20(6):1261–71.

Wohlgemuth, Ingo, Corinna Pohl, Joerg Mittelstaet, Andrey L. Konevega, and Marina V. Rodnina. **2011**. “Evolutionary Optimization of Speed and Accuracy of Decoding on the Ribosome.” *Philosophical Transactions of the Royal Society B: Biological Sciences* 366(1580):2979–86.

Wohlgemuth, Sibylle E., Thomas E. Gorochowski, and Johannes A. Roubos. **2013**. “Translational Sensitivity of the *Escherichia Coli* Genome to Fluctuating TRNA Availability.” *Nucleic Acids Research* 41(17):8021–33.

Wong, J. T. F. **1975**. “A Co-Evolution Theory of the Genetic Code.” *Proceedings of the National Academy of Sciences* 72(5):1909–12.

Wood, Sarah E., Jin Jin, and Scott A. Lloyd. **2008**. “YscP and YscU Switch the Substrate Specificity of

the *Yersinia* Type III Secretion System by Regulating Export of the Inner Rod Protein YscI." *Journal of Bacteriology* 190(12):4252–62.

Wösten, M. M. 1998. "Eubacterial Sigma-Factors." *FEMS Microbiology Reviews* 22(3):127–50.

Wren, Brendan W. **2003**. "The *Yersiniae* — a Model Genus to Study the Rapid Evolution of Bacterial Pathogens." *Nature Reviews Microbiology* 1(1):55–64.

Wulff-Strobel, Christine R., Andrew W. Williams, and Susan C. Straley. **2002**. "LcrQ and SycH Function Together at the Ysc Type III Secretion System in *Yersinia Pestis* to Impose a Hierarchy of Secretion." *Molecular Microbiology* 43(2):411–23.

Xiao, Zhengtao, Qin Zou, Yu Liu, and Xuerui Yang. **2016**. "Genome-Wide Assessment of Differential Translations with Ribosome Profiling Data." *Nature Communications* 7(1):11194.

Yang, Ji, Marija Tauschek, and Roy M. Robins-Browne. **2011**. "Control of Bacterial Virulence by AraC-like Regulators That Respond to Chemical Signals." *Trends in Microbiology* 19(3):128–35.

Yerushalmi, G., Y. Litvak, L. Gur-Arie, and I. Rosenshine. **2014**. "Dynamics of Expression and Maturation of the Type III Secretion System of Enteropathogenic *Escherichia Coli*." *Journal of Bacteriology* 196(15):2798–2806.

Yother, J., T. W. Chamness, and J. D. Goguen. **1986**. "Temperature-Controlled Plasmid Regulon Associated with Low Calcium Response in *Yersinia Pestis*." *Journal of Bacteriology* 165(2):443–47.

Yusupov, Marat M., Gulnara Zh Yusupova, Albion Baucom, Kate Lieberman, Thomas N. Earnest, J. H. D. Cate, and Harry F. Noller. **2001**. "Crystal Structure of the Ribosome at 5 . 5 Å Resolution." *Science* 292(May):883–96.

Zamecnik, Paul. **2005**. "From Protein Synthesis to Genetic Insertion." *Annual Review of Biochemistry* 74(1):1–28.

Zhang, Gong, Ivan Fedyunin, Oskar Miekley, Angelo Valleriani, Alessandro Moura, and Zoya Ignatova. **2010**. "Global and Local Depletion of Ternary Complex Limits Translational Elongation." *Nucleic Acids Research* 38(14):4778–87.

Zhang, Peng, Dandan He, Yi Xu, Jiakai Hou, Bih-Fang Pan, Yunfei Wang, Tao Liu, Christel M. Davis, Erik A. Ehli, Lin Tan, Feng Zhou, Jian Hu, Yonghao Yu, Xi Chen, Tuan M. Nguyen, Jeffrey M. Rosen, David H. Hawke, Zhe Ji, and Yiwen Chen. **2017**. "Genome-Wide Identification and Differential Analysis of Translational Initiation." *Nature Communications* 8(1):1749.

Zhong, Jiayong, Chuanle Xiao, Wei Gu, Gaofei Du, Xuesong Sun, Qing Yu He, and Gong Zhang. **2015**. "Transfer RNAs Mediate the Rapid Adaptation of *Escherichia Coli* to Oxidative Stress." *PLoS Genetics* 11(6):1–24.

Zilkenat, Susann, Mirita Franz-Wachtel, York-Dieter Stierhof, Jorge E. Galán, Boris Macek, and Samuel Wagner. **2016**. "Determination of the Stoichiometry of the Complete Bacterial Type III Secretion Needle Complex Using a Combined Quantitative Proteomic Approach." *Molecular & Cellular Proteomics* 15(5):1598–1609.

7 Supplements

7.1 Footprint preparation for Ribo-Seq

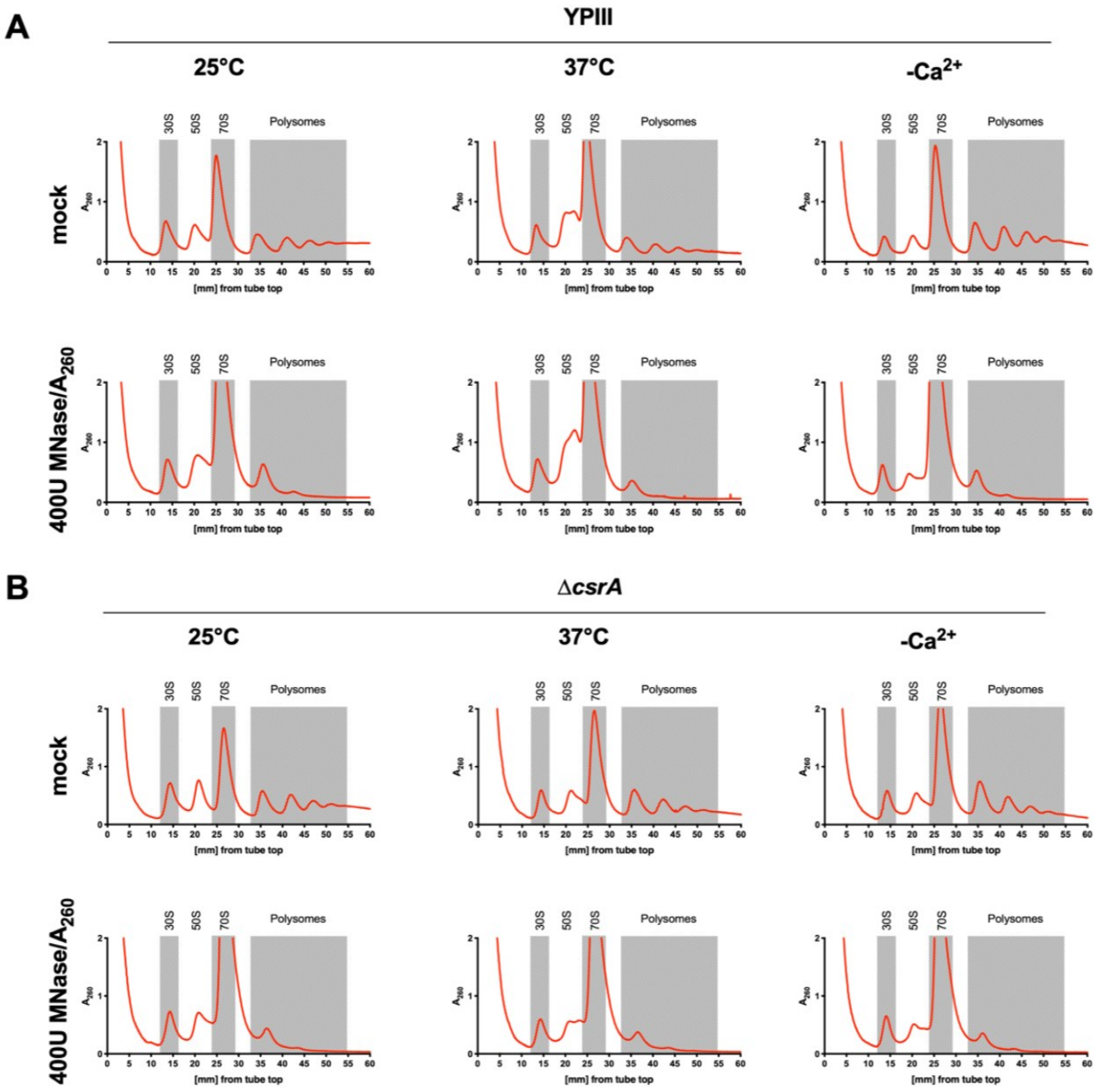

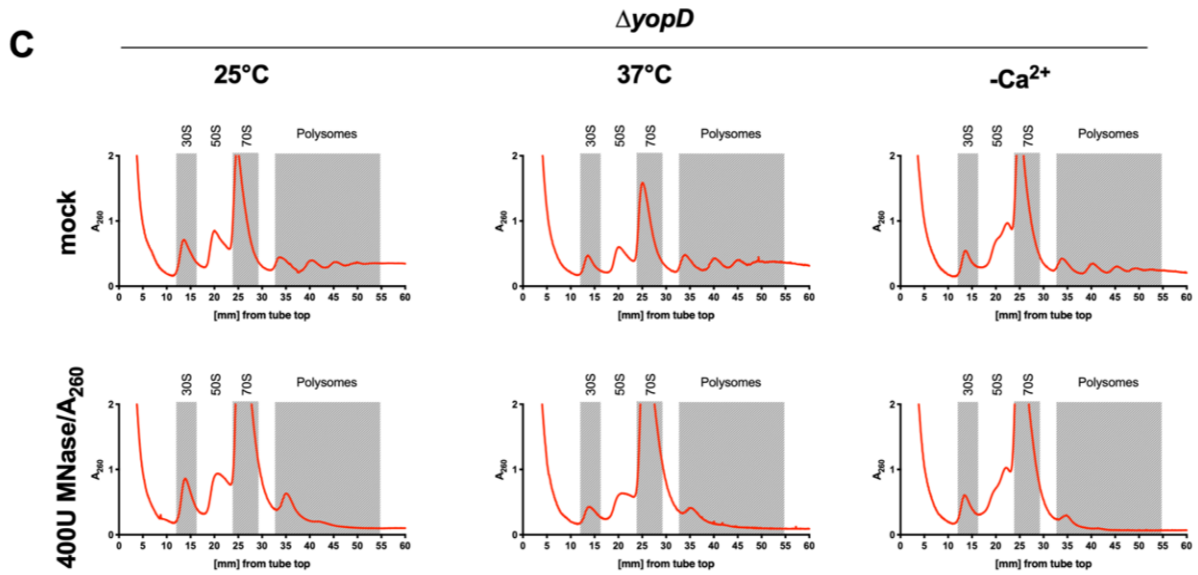

Figure 7.1) Ribosome fragmentation profile of *Y. pseudotuberculosis* and the Δ*csrA* and Δ*yopD* mutant grown at 25°C, 37°C and under secretion (-Ca^{2+}) conditions.

Ribosome profile obtained by sucrose-based gradient ultracentrifugation and detection of the absorption at 260 nm throughout the whole gradient from top to bottom as indicated by the x-axis. The representing samples were generated from *Y. pseudotuberculosis* (**A**) wildtype, (**B**) Δ*csrA*, and (**C**) Δ*yopD* mutant grown at 25°C, 37°C, and under secretion (-Ca^{2+}) conditions. The different ribosome fractions are indicated on top of every graphic, while the top graphic shows an undigested sample (mock) and the bottom graph shows an MNase treated sample (400U MNase/A_{260}).

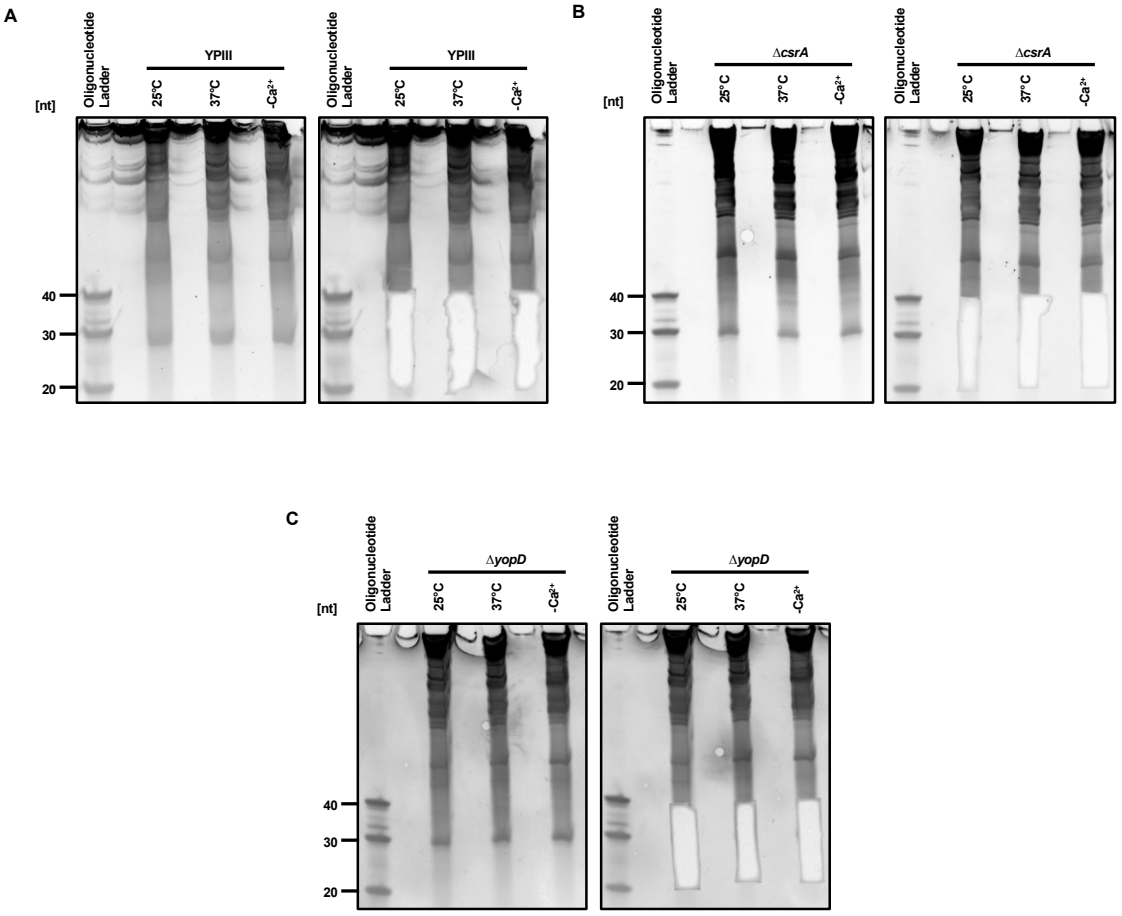

Figure 7.2) Footprint isolation from purified samples of the fractionated 70S ribosomal particles from *Y. pseudotuberculosis* and the Δ*csrA* and Δ*yopD* mutant.

Representative gel for ribosome footprint isolation from *Y. pseudotuberculosis* (**A**) wildtype, (**B**) Δ*csrA*, and (**C**) Δ*yopD* mutants grown at 25°C, 37°C and under secretion (-Ca^{2+}) conditions. Marker was prepared from three oligonucleotides with the size of 20, 30, and 40 nucleotides. On the left side, the gel is shown before cutting, and on the right side, the extracted area is shown.

7.2 RNAseq results

Strain	Read type	Class	RPF 25°C_1	RPF 25°C_2	RPF 25°C_3	RPF 37°C_1	RPF 37°C_2	RPF 37°C_3	RPF -Ca2+_1	RPF -Ca2+_2	RPF -Ca2+_3	mRNA 25°C_1	mRNA 25°C_2	mRNA 25°C_3	mRNA 37°C_1	mRNA 37°C_2	mRNA 37°C_3	mRNA -Ca2+_1	mRNA -Ca2+_2	mRNA -Ca2+_3
wildtype (YPIII)	total reads	total	7736837,25	9472380,55	19646466,6	10038938,7	7064574,62	19084157,26	11754480,34	12048246,12	20281249,25	47888626,25	37234403	41847129	46907174	29556076,6	64061781	3630222,92	4594443,84	5673140,77
		CDS	5316138,2	5328077,4	12972099	3590381,81	3272499,39	8427059,5	2455583,28	3078645,35	5725078,3	6634327,4	8094563,3	8202526	5854853,9	4038012,2	7606156	462716,41	644456,05	5403627,4
		rRNA	7197176,39	8930529,58	18330109,2	9671241,36	6728437,14	18212485,65	11499952,17	11727727,45	19679798,86	25579019,95	21067781,78	22777833,28	25259164,5	18142124,24	40509740,6	2287633,18	2824265,19	3582283,32
		tRNA	8047,04	9043,23	19148,4	8665,53	8888,09	27165,66	8944,89	12654,32	28942,86	15674915,6	10786772,02	10866677,02	15791115,86	7376682,2	15945888,65	879873,33	1125722,4	1550494,71
	unique reads	total	674466	795853	1806865	533646	624138	1388653	416252	567590	1074088	1080894	970065	1084641	982410	603261	1204249	679534	924878	928218
		CDS	525991	530001	1285742	356377	323536	830854	243627	304500	566593	611374	751546	789640	556077	391375	741223	439610	611812	514085
		rRNA	147169	264327	518247	175821	298617	553258	171024	260977	502385	70878	25898	39427	42651	30641	54967	24135	43005	47161
		tRNA	1306	1525	2876	1448	1985	4541	1601	2113	5110	398642	192621	255574	383682	181245	408059	215789	270061	366972
ΔcsrA	total reads	total	12869202,56	18407822,93	12285848,23	9898902,91	13021515,73	12184741,77	9101501,51	18356436,5	10945397,24	79798859,43	68571893,37	47385537,91	63259004,06	51880067,86	44525344,46	8113688,81	6250104,38	4657993,02
		CDS	769947,23	1973118,69	1008722,89	641411,38	933721,8	687744,76	482304,33	596043,87	3719303,28	2493028,9	2464474,29	1289254,31	1863036,65	1681449,71	1444325,45	1937219,31	1556117,46	1175660,18
		rRNA	12090412,51	16414917,97	11264796,34	9246149,78	12073342,09	11485945,12	8608480,81	17745296,94	10563935,79	47288837,45	39698859,16	30542816,66	39473032,98	32926637	23343822,22	5681654,15	4166955,31	3126619,77
		tRNA	9142,82	19786,27	12329	11041,75	14451,84	11051,89	10716,37	15095,69	9558,17	7579930,8	4228559,2	3950019,4	5158334,43	2119811,5	6738267,9	494815,35	527031,61	3567130,7
	unique reads	total	2433828	3801745	2357344	1942071	2693774	2274341	1526412	2866206	1851981	2771958	2632367	1446727	2026364	1771724	1694676	2148718	1755330	1321663
		CDS	766514	1966833	1006097	639060	929589	684978	480437	593638	370443	2458792	2443252	1254230	1850109	1668178	1420323	1913775	1527630	1158107
		rRNA	1665182	1829920	1349006	1300850	1760172	1567029	1043803	2268889	1479389	29479	16749	13914	18940	5749	20505	10083	13667	11193
		tRNA	2132	5192	2241	2161	4013	2334	2172	3679	2159	283687	172366	178583	157315	97797	243848	224860	214033	152363
ΔcsrA	total reads	total	182459324,84	97637371,01	102415702,23	117985104,45	102372116,26	102822941,39	122975054,34	85838695,64	202505544,76	58379299,01	56231311,7	58014428,44	56957385,35	46581771,41	64733502,28	76150982,74	42451070,04	85568978,49
		CDS	46116837,87	16112039,98	31350661,45	9908003,69	6955935,96	12986191,91	5726549,48	3508387,88	11322582,72	15049997,63	13959387,28	17155564,15	14019941,42	12171136,5	15939771,61	13006856,78	4399240,27	11635395,75
		rRNA	136068813,63	81412517,7	70895513,12	107898893,71	95267745,51	94980130,22	117080187,53	82221128,37	190857755,09	40252588,67	39572777,67	36653350	38051765,52	30453571,51	43518894,62	50900112,8	35806602,08	58384552,12
		tRNA	27281,34	11335,33	16995,66	17813,05	14534,79	26291,26	17168,33	10729,39	32206,95	307642,71	269916,75	420522,29	488620,41	395683,4	527484,05	1224417,16	225264,69	155493,62
	unique reads	total	5986698	2381227	3835861	2009853	1699003	2330213	1642929	1204953	3193242	1617038	1468286	1818779	1546709	1319221	1723528	1633865	503685	1554869
		CDS	4591731	1605850	3127647	987459	693011	1294637	570069	349704	1128517	1488557	1383254	1697821	1392835	1207969	1581812	1290744	434125	1154929
		rRNA	1388146	773052	704583	1018591	1002840	1029830	1069416	852797	2055868	40583	10013	17820	25433	11197	15821	35234	5514	48398
		tRNA	7111	2325	3631	3803	3152	5746	3444	2452	8857	87898	75019	103138	128441	100055	125895	307887	64046	351542

Table 7.1) Mapping statistics of the Ribo-Seq analysis for the *Y. pseudotuberculosis* wildtype and Δ*csrA* and Δ *yopD* mutants.

Table 7.2) Number of regulated genes by Ribo-Seq analysis for the chromosoe and the virulence plasmid pIB1.

		YPIII 25°C vs 37°C		YPIII 37°C vs -Ca^{2+}		Δ*csrA* 25°C vs 37°C		Δ*csrA* 37°C vs -Ca^{2+}		Δ*yopD* 25°C vs 37°C		Δ*yopD* 37°C vs -Ca^{2+}	
		RPF	mRNA	RPF	mRNA	RPF	mRNA	RPF	mRNA	RPF	mRNA	RPF	mRNA
Chromosome (4250 genes)	upregulated $log_2FC \geqq 2$	263	200	131	59	215	280	54	182	229	272	208	263
	downregulated $log_2FC \leqq -2$	264	203	136	60	202	333	85	179	299	353	362	370
	upregulated $log_2FC \geqq 2$	6.19	4.71	3.08	1.39	5.06	6.59	1.27	4.28	5.39	6.40	4.89	6.19
	downregulated $log_2FC \leqq -2$	6.21	4.78	3.20	1.41	4.75	7.84	2.00	4.21	7.04	8.31	8.52	8.71
pIB1 (95 genes)	upregulated $log_2FC \geqq 2$	4	15	52	48	27	33	33	26	57	56	5	9
	downregulated $log_2FC \leqq -2$	0	0	0	0	0	0	0	1	0	0	0	2
	upregulated $log_2FC \geqq 2$	4.26	15.96	55.32	51.06	28.72	35.11	35.11	27.66	60.64	59.57	5.32	9.57
	downregulated $log_2FC \leqq -2$	0	0	0	0	0	0	0	1.06	0	0	0	2.13

Table 7.3) Genes with affected translational efficacy (TE) by Ribo-Seq (cut off: log^2FC +2/-2, p-value ≤ 0.05)

GenebankAcc	GeneSymbols	Definition	YPIII 25°C vs. 37°C TE_log_2FC	p value
YPK_2267	*ripB, ich-Y*	dehydratase	4.35	0.038
YPK_2404	*fliR-2*	flagellar biosynthesis protein FliR	3.87	4.87E-04
YPK_2423	*flgD-2*	flagellar basal body rod modification	2.99	0.008
YPK_1611	*rbsB-3*	monosaccharide-transporting ATPase	2.51	4.40E-06
YPK_2399	*fliM-2*	flagellar motor switch protein	-2.30	0.022
YPK_2567	*yeiB*	hypothetical protein	-2.49	2.97E-04
YPK_3240		hypothetical protein	-2.90	1.04E-04
YPK_0079		hypothetical protein	-3.25	0.010
YPK_3143		hypothetical protein	-3.28	0.005
YPK_2101		hypothetical protein	-3.31	0.003
YPK_1501	*ccmF*	cytochrome c-type biogenesis protein CcmF	-3.65	3.75E-04
YPK_2326		hypothetical protein	-4.20	5.98E-05
YPK_0401		ImpA family type VI secretion-associated protein	-4.30	0.001
YPK_3462	*fhuC*	iron-hydroxamate transporter ATP-binding subunit	-5.20	0.005
YPK_1031	*tas*	putative aldo-keto reductase	-5.21	2.46E-07
YPK_4044	*fimD-4, fimC-4, mrkC-4, htrE-4, cssD-4*	fimbrial biogenesis outer membrane usher protein	-5.26	0.001
GenebankAcc	**GeneSymbols**	**Definition**	**Δ*csrA* 25°C vs. 37°C TE_log_2FC**	**p value**
YPK_1892	*sapA, dppA*	extracellular solute-binding protein	3.92	0.014
YPK_3634	*rimI*	ribosomal-protein-alanine N-acetyltransferase	3.88	0.023
YPK_1156	*kdpD*	sensor protein KdpD	3.71	0.024
YPK_0752		amino acid adenylation domain-containing protein	2.56	0.010
DN756_ RS21970	*yscM, lcrQ*	yscM, lcrQ; type III secretion regulatory;protein-tyrosine phosphatase YopH	2.56	0.007
YPK_0446		beta-lactamase domain-containing protein	2.53	0.038
YPK_4061	*ilvG*	acetolactate synthase 2 catalytic subunit	2.10	0.030
YPK_1694	*ptsG-2*	PTS system glucose-specific transporter subunit IIBC	2.09	0.003

YPK_2744		2OG-Fe(II) oxygenase	-2.00	0.009
YPK_3590	*rpsT*	30S ribosomal protein S20	-2.00	4.48E-06
YPK_2501		hypothetical protein	-2.12	0.015
YPK_1769		hypothetical protein	-2.15	0.014
YPK_1798	*togB*	extracellular solute-binding protein	-2.20	0.001
YPK_0273	*tusC*	sulfur relay protein TusC	-2.21	0.018
YPK_3350	*yfiH*	hypothetical protein	-2.23	0.019
YPK_2724	*artJ*	cationic amino acid ABC transporter periplasmic binding protein	-2.24	0.042
YPK_2388	*doc*	death-on-curing family protein	-2.24	0.002
YPK_1114	*proW*	glycine betaine transporter membrane protein	-2.24	0.016
YPK_3019	*ybeB*	hypothetical protein	-2.26	1.81E-06
YPK_0269	*slyX*	hypothetical protein	-2.32	0.022
YPK_2737	*deoC-2*	deoxyribose-phosphate aldolase	-2.33	0.001
YPK_1070	*dxr*	1-deoxy-D-xylulose 5-phosphate reductoisomerase	-2.44	5.19E-07
YPK_0517		BolA family protein	-2.50	7.11E-07
YPK_1345	*pstC-1*	binding-protein-dependent transport system inner membrane protein	-2.53	0.018
YPK_2868		hypothetical protein	-2.54	0.036
YPK_0244	*pabA*	para-aminobenzoate synthase component II	-2.61	0.040
YPK_2801		hypothetical protein	-2.63	5.79E-05
YPK_3172	*rosA-1, fsr-1*	putative membrane efflux protein	-2.67	0.001
YPK_1615	*dmlR*	LysR family transcriptional regulator	-2.79	0.018
YPK_0780		hypothetical protein	-2.84	0.003
YPK_1057	*queF*	7-cyano-7-deazaguanine reductase	-2.90	0.027
YPK_0044		hypothetical protein	-2.97	0.027
YPK_1541	*hisP*	histidine/lysine/arginine/ornithine transporter subunit	-3.02	0.010
YPK_2178	*hemK, prmC*	N5-glutamine S-adenosyl-L-methionine-dependent methyltransferase	-3.03	0.018
YPK_3780		hypothetical protein	-3.14	0.035
YPK_3136		hypothetical protein	-3.21	0.042
YPK_4005		hypothetical protein	-3.26	7.55E-10
YPK_4116	*yiiR*	hypothetical protein	-3.27	0.006
YPK_2141	*znuC*	high-affinity zinc transporter ATPase	-3.29	4.28E-04
YPK_0232	*cysG-1*	siroheme synthase	-3.61	0.041
YPK_3203		hypothetical protein	-3.63	3.55E-05
YPK_2925		hypothetical protein	-3.65	2.68E-05
YPK_3989	*glpC*	sn-glycerol-3-phosphate dehydrogenase subunit C	-3.87	0.031
YPK_2527	*hisC*	histidinol-phosphate aminotransferase	-3.92	0.003
YPK_1516	*yfcA*	hypothetical protein	-4.13	0.034
YPK_3168		hypothetical protein	-4.13	0.008
YPK_4097		YiaAB two helix domain-containing protein	-4.16	0.001
YPK_0089	*dppB*	dipeptide transporter permease DppB	-4.38	0.049
YPK_3763	*yhcN*	hypothetical protein	-4.50	2.87E-18
YPK_0261	*tauD*	taurine dioxygenase	-4.66	2.29E-04
YPK_3055	*ner-1, nlp-1, sfsB-1*	putative transcriptional regulator Nlp	-4.77	0.001
YPK_2450	*yeaB*	hypothetical protein	-5.07	0.021
YPK_0716	*flgN-1*	hypothetical protein	-5.35	0.003

YPK_1452		4Fe-4S ferredoxin	-5.35	0.041
YPK_0741		ShET2 enterotoxin domain-containing protein	-5.40	3.61E-04
YPK_1487		hypothetical protein	-5.45	0.025
DN756_ RS21985		transposase incomplete	-5.57	0.036
YPK_1483	*impJ-3, vasE-3*	type VI secretion protein	-5.82	1.65E-05
YPK_1241		hypothetical protein	-6.13	0.008
YPK_2172		glycerophosphoryl diester phosphodiesterase	-6.38	0.002
YPK_0930		tail fiber repeat 2-containing protein	-6.42	1.15E-05
YPK_0625		hypothetical protein	-6.68	1.68E-10
YPK_0980		hypothetical protein	-6.68	9.11E-05
YPK_0895		transcriptional activator Ogr/delta	-6.95	2.04E-05
YPK_2441		hypothetical protein	-7.11	1.85E-07
YPK_2251		hypothetical protein	-7.37	0.020
YPK_1146	*celC*	PTS system N,N'-diacetylchitobiose-specific transporter subunit IIA	-7.44	0.015
YPK_0960		hypothetical protein	-7.47	7.55E-10
YPK_2057	*yciI*	hypothetical protein	-7.94	6.51E-06
YPK_2511		putative thiol-disulfide oxidoreductase DCC	-8.10	0.023
YPK_1657		hypothetical protein	-8.39	0.022
YPK_2490	*mtfA*	hypothetical protein	-8.83	9.65E-15

GenebankAcc	**GeneSymbols**	**Definition**	**Δ*csrA* 37°C vs. -Ca^{2+}**	
			TE_log_2FC	**p value**
YPK_1492	*phnA*	alkylphosphonate utilization operon protein PhnA	2.31	0.017
YPK_2156	*shlA, hhdA, hpmA, hlyA*	filamentous hemagglutinin domain-containing protein	2.25	0.024
YPK_0162	*malQ*	4-alpha-glucanotransferase	2.17	0.018
YPK_3877	*terZ*	stress protein	2.02	1.51E-04
YPK_0218		hypothetical protein	-2.10	0.043
YPK_2375	*yecS*	polar amino acid ABC transporter inner membrane subunit	-2.39	0.002
YPK_1214		hypothetical protein	-2.63	0.017
YPK_3959	*ugpC*	glycerol-3-phosphate transporter ATP-binding subunit	-2.82	0.049
YPK_2079		hypothetical protein	-2.85	0.017
YPK_1887		hypothetical protein	-3.02	0.048
YPK_0930		tail fiber repeat 2-containing protein	-3.40	0.043
YPK_1892	*sapA, dppA*	extracellular solute-binding protein	-3.47	0.018
YPK_3612	*trpR*	Trp operon repressor	-3.50	0.045
YPK_1378	*ydeN*	sulfatase	-3.54	0.005
YPK_3869		putative periplasmic chaperone protein	-4.29	0.006
YPK_4068	*yphF-6, ytfQ-6*	periplasmic binding protein/LacI transcriptional regulator	-4.47	0.010
YPK_1025	*galR-1*	DNA-binding transcriptional regulator GalR	-4.97	0.026
YPK_0372	*lysC*	aspartate kinase III	-5.01	6.99E-06
YPK_2916	*betB*	betaine aldehyde dehydrogenase	-5.34	1.58E-06
YPK_2247	*ybbP-1*	hypothetical protein	-5.34	0.020
YPK_2185	*ychH*	hypothetical protein	-5.42	0.006
YPK_3997	*rhtC*	threonine efflux system	-5.62	0.001
YPK_0445	*pcp-1*	17 kDa surface antigen	-5.66	0.001
YPK_0640	*bacA*	undecaprenyl pyrophosphate phosphatase	-5.78	1.67E-04

YPK_2903	*yadH-2, ybhR-2, ybhS-2, yhhJ-2*	ABC-2 type transporter	-5.81	0.018
YPK_3537	*leuC*	isopropylmalate isomerase large subunit	-5.94	0.018
YPK_3374	*recX*	recombination regulator RecX	-6.23	2.11E-04
YPK_0870		hypothetical protein	-6.49	0.001
YPK_1465		LuxR family transcriptional regulator	-6.77	4.65E-04
YPK_3331		hypothetical protein	-7.24	0.007
YPK_3834		peptidase M60 viral enhancin protein	-7.24	1.03E-04
YPK_2267	*ripB, ich-Y*	dehydratase	-7.30	0.018
YPK_1624	*trp14A-1*	transposase IS3/IS911 family protein	-7.30	4.89E-05
YPK_3591	*nhaR*	transcriptional activator NhaR	-7.35	2.87E-05
YPK_1870	*sepC*	Rhs family protein-like protein	-7.42	2.33E-08
YPK_0805	*vgrG-2*	ImpA family type VI secretion-associated protein	-7.65	0.035
YPK_1963	*rbsB-4*	periplasmic binding protein/LacI transcriptional regulator	-7.65	6.32E-11
YPK_0097		coagulation factor 5/8 type domain-containing protein	-7.65	0.020
YPK_0131		two component transcriptional regulator	-7.78	1.35E-05
YPK_2400	*fliN-2*	flagellar motor switch protein FliN	-7.81	0.017
YPK_0017	*ghrB*	NAD-binding D-isomer specific 2-hydroxyacid dehydrogenase	-8.10	3.79E-14
YPK_1830	*btuD*	vitamin B12-transporter ATPase	-8.23	0.005
YPK_0146	*yehU, ypdA*	signal transduction histidine kinase LytS	-8.31	0.026
YPK_2807		RpiR family transcriptional regulator	-8.34	1.72E-15
YPK_0033		hypothetical protein	-8.47	3.14E-04
YPK_0650		hypothetical protein	-8.98	0.007

GenebankAcc	**GeneSymbols**	**Definition**	**Δ*yopD* 25°C vs. 37°C**	
			TE_log$_2$FC	**p value**
YPK_0794		lipoprotein	4.52	0.001
YPK_3172	*rosA-1, fsr-1*	putative membrane efflux protein	4.47	4.48E-04
YPK_3738	*yhbY*	hypothetical protein	4.09	0.049
YPK_1534	*cvpA*	colicin V production protein	3.70	0.002
YPK_2428	*flgN-2*	FlgN family protein	3.28	0.034
YPK_3826	*dcuA*	anaerobic C4-dicarboxylate transporter	3.19	0.035
YPK_1151	*seqA*	replication initiation regulator SeqA	2.98	3.29E-07
YPK_2831	*pla2*	outer membrane protease	2.84	0.047
YPK_2693	*clpS*	ATP-dependent Clp protease adaptor protein ClpS	2.80	6.42E-05
YPK_2940	*modF*	putative molybdenum transport ATP-binding protein ModF	2.59	0.045
DN756_RS21625	*yadA*	hypothetical protein;YadA domain-containing protein	2.57	3.17E-10
YPK_2140	*znuA*	high-affinity zinc transporter periplasmic protein	2.33	0.004
YPK_2182	*ipk, ispE*	4-diphosphocytidyl-2-C-methyl-D-erythritol kinase	2.20	0.006
YPK_2841		major facilitator transporter	2.18	0.017
YPK_1956	*tauB-2*	ABC transporter-like protein	2.04	0.021
YPK_3433	*ygbE*	hypothetical protein	2.01	0.001
YPK_1710	*nagK*	N-acetyl-D-glucosamine kinase	-2.09	0.016
DN756_RS21575	*tap*	RepA leader peptide Tap	-2.10	0.033
YPK_1974	*aldB*	aldehyde dehydrogenase	-2.12	0.001

YPK_1496	*ccmA*	cytochrome c biogenesis protein CcmA	-2.13	0.025
YPK_2141	*znuC*	high-affinity zinc transporter ATPase	-2.16	0.002
YPK_2952	*pnuC*	nicotinamide mononucleotide transporter PnuC	-2.16	0.047
YPK_2416	*flgK*	flagellar hook-associated protein FlgK	-2.20	0.024
YPK_3771	*msrA*	methionine sulfoxide reductase A	-2.23	0.033
YPK_0593	*bglX*	glycoside hydrolase family 3	-2.23	0.047
YPK_1747	*motA-2*	flagellar motor protein MotA	-2.26	0.035
YPK_0159	*glpE*	thiosulfate sulfurtransferase	-2.29	0.047
YPK_2011	*rnfG, rsxG*	electron transport complex protein RnfG	-2.47	0.040
YPK_3951	*ysgA*	carboxymethylenebutenolidase	-2.48	0.005
YPK_2763	*fruK*	1-phosphofructokinase	-2.67	0.033
YPK_3878		hypothetical protein	-2.89	0.016
YPK_3051		RpiR family transcriptional regulator	-2.90	2.63E-06
YPK_1515	*mepA*	penicillin-insensitive murein endopeptidase	-2.91	0.018
YPK_0855	*lysE, argO*	arginine exporter protein	-3.30	0.004
YPK_4182	*xanP*	uracil-xanthine permease	-3.31	0.007
YPK_2378	*fliZ*	flagella biosynthesis protein FliZ	-3.34	0.041
YPK_4107		hypothetical protein	-3.46	0.008
YPK_2130	*mdtI*	multidrug efflux system protein MdtI	-3.48	0.019
YPK_2399	*fliM-2*	flagellar motor switch protein FliM	-3.72	2.45E-07
YPK_3462	*fhuC*	iron-hydroxamate transporter ATP-binding subunit	-3.89	0.042
YPK_3947		hypothetical protein	-3.98	0.036
YPK_4053		hypothetical protein	-4.04	0.047
YPK_4130		hypothetical protein	-4.63	0.030
YPK_2498	*dctM, ygiK*	TRAP dicarboxylate transporter subunit DctM	-5.27	0.001
YPK_3665		type I restriction-modification system, M subunit	-5.29	0.048
YPK_1523	*flk*	flagella biosynthesis regulator	-5.41	0.045
YPK_1837	*arnF, yfbJ*	hypothetical protein	-5.58	0.004
YPK_1234		hypothetical protein	-5.62	0.001
DN756_ RS21595		hypothetical protein	-6.04	2.57E-04
YPK_2452	*hpaC*	4-hydroxyphenylacetate 3-monooxygenase, reductase subunit	-6.25	1.03E-06
YPK_1639		hypothetical protein	-6.39	3.93E-06
YPK_1778		spore coat U domain-containing protein	-6.53	0.006
YPK_1612	*rbsA-3*	ABC transporter-like protein	-7.06	2.95E-09
YPK_3692	*nrdG*	anaerobic ribonucleoside-triphosphate reductase activating protein	-7.10	0.002
YPK_4165		hypothetical protein	-8.00	3.77E-06
YPK_3919	*ssrB*	two component LuxR family transcriptional regulator	-8.07	4.29E-06
YPK_2473		hypothetical protein	-8.13	4.55E-06

GenebankAcc	**GeneSymbols**	**Definition**	**Δ*yopD* 37°C vs. -Ca^{2+} TE_log_2FC**	**p value**
YPK_0908		hypothetical protein	4.80	0.023
YPK_3193	*hemH*	ferrochelatase	3.94	0.020
YPK_0454	*prmA*	50S ribosomal protein L11 methyltransferase	3.38	0.006
YPK_1740	*cspC-1*	cold-shock DNA-binding domain-containing protein	2.89	0.017
YPK_2802		colicin D	2.65	0.034
YPK_0635	*dnaG*	DNA primase	2.64	0.020

YPK_3353	*yfiA, raiA*	sigma 54 modulation protein/30S ribosomal protein S30EA	2.55	0.002
YPK_2508	*fucD*	mandelate racemase/muconate lactonizing protein	2.45	6.68E-05
YPK_4098	*rpmE*	50S ribosomal protein L31	2.02	3.42E-05
YPK_1322		hypothetical protein	-2.30	0.002
YPK_2994	*glnS*	glutaminyl-tRNA synthetase	-2.35	3.95E-05
YPK_4179	*trmH*	tRNA guanosine-2'-O-methyltransferase	-2.92	0.002
YPK_3178	*manB-2*	phosphomannomutase	-2.93	0.016
YPK_0175	*hslO*	Hsp33-like chaperonin	-2.95	0.041
YPK_1897	*pspD*	peripheral inner membrane phage-shock protein	-2.98	0.046
YPK_2554	*metG*	methionyl-tRNA synthetase	-3.02	6.75E-05
YPK_4073	*btuB*	vitamin B12/cobalamin outer membrane transporter	-3.25	0.015
YPK_2620	*rlmI, yccW*	PUA domain-containing protein	-3.43	0.045
YPK_2837		hypothetical protein	-3.79	0.011
YPK_3765	*mpl*	UDP-N-acetylmuramate--L-alanyl-gamma-D-glutamyl-meso-diaminopimelate ligase	-3.92	0.001
YPK_1263	*yhfZ*	hypothetical protein	-3.97	0.007
YPK_0671	*metC-1*	cystathionine beta-lyase	-4.03	0.045
YPK_2028	*pgpB*	phosphatidylglycerophosphatase B	-4.06	4.25E-05
YPK_3350	*yfiH*	hypothetical protein	-4.08	0.001
YPK_1358		hypothetical protein	-4.11	0.038
YPK_3816	*frdD*	fumarate reductase subunit D	-4.66	0.002
YPK_2415	*flgL*	flagellar hook-associated protein FlgL	-4.82	0.003
YPK_3322	*ybdL*	putative aminotransferase	-5.28	0.030
YPK_0820	*mutY*	adenine DNA glycosylase	-5.38	2.12E-04
YPK_4122	*ybhI*	anion transporter	-5.46	0.030
YPK_3576		hypothetical protein	-5.57	0.041
YPK_2507		hypothetical protein	-5.70	0.003
YPK_1481	*hcp-3*	Hcp1 family type VI secretion system effector	-5.90	2.12E-04
YPK_0416	*yphD-1, ytfT-1, yjfF-1*	RbsD or FucU transporter	-5.99	3.58E-05
YPK_0404		hypothetical protein	-6.13	1.71E-04
YPK_1024	*lysA*	diaminopimelate decarboxylase	-6.19	0.028
YPK_0512	*mlaF*	putative ABC transporter ATP-binding protein YrbF	-6.44	0.001
YPK_1058	*syd*	SecY interacting protein Syd	-6.50	0.001
YPK_0814	*rbsC-2*	monosaccharide-transporting ATPase	-6.71	0.001
DN756_ RS21660		hypothetical protein	-6.77	0.005
YPK_1978		hypothetical protein	-6.93	0.020
YPK_3685	*yjgK*	hypothetical protein	-7.54	0.007
YPK_2764	*fruB*	bifunctional PTS system fructose-specific transporter subunit IIA/HPr protein	-7.74	2.12E-04
YPK_3826	*dcuA*	anaerobic C4-dicarboxylate transporter	-8.06	4.47E-08
YPK_1106	*gloB*	hydroxyacylglutathione hydrolase	-8.12	8.61E-05
YPK_3481	*yacC*	hypothetical protein	-8.22	0.016
YPK_1526		AraC family transcriptional regulator	-8.72	3.58E-05
YPK_1630		hypothetical protein	-8.87	0.001
YPK_3841	*rhaR*	transcriptional activator RhaR	-8.88	2.24E-05
YPK_1154		hypothetical protein	-8.91	0.007

YPK_0451		hypothetical protein	-9.07	1.05E-05
YPK_1534	*cvpA*	colicin V production protein	-9.11	1.15E-04

A YPIII 25°C vs. 37°C

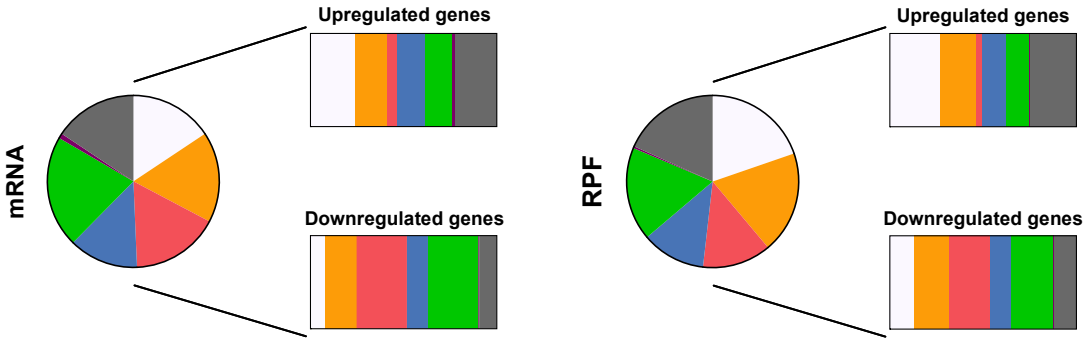

YPIII 37°C vs. –Ca^{2+}

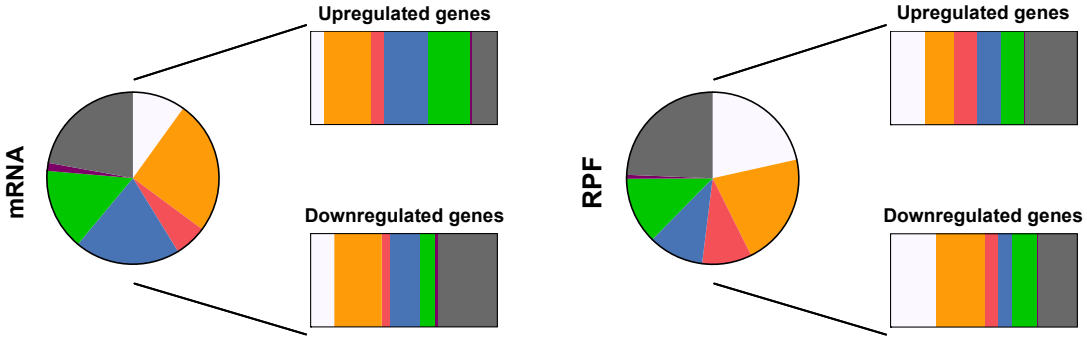

B Δ*csrA* 25°C vs 37°C

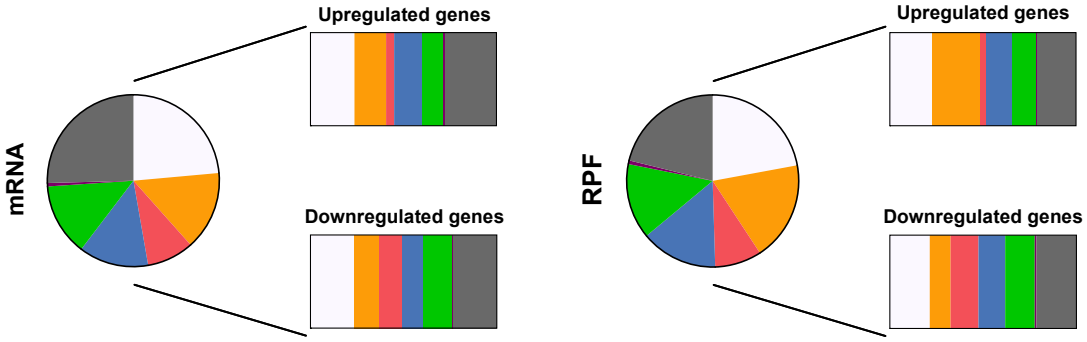

Δ*csrA* 37°C vs –Ca^{2+}

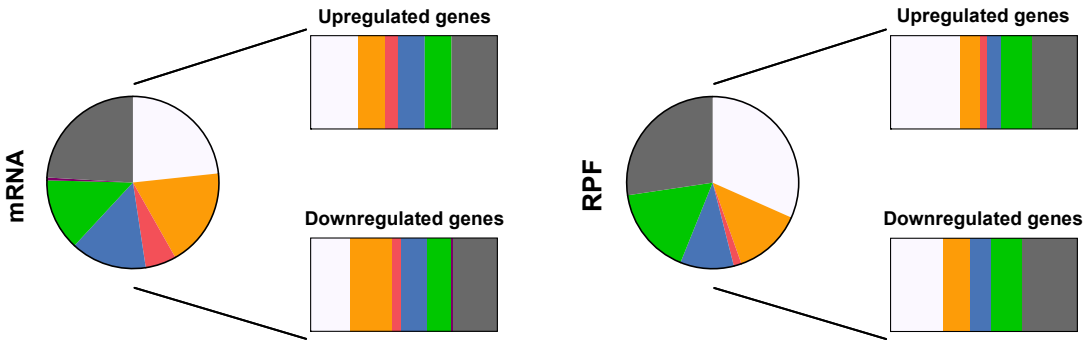

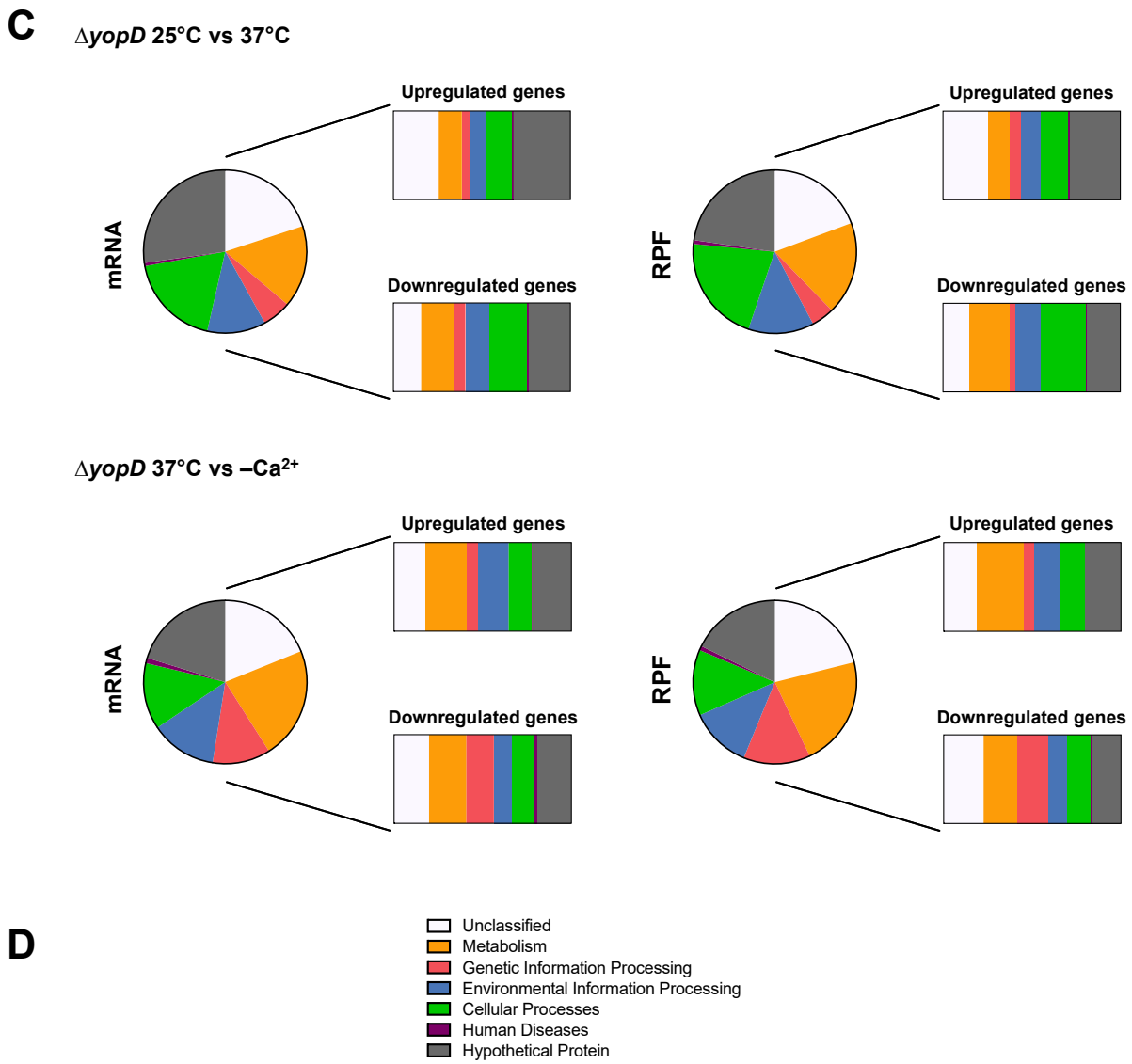

Figure 7.3) Up- and down-regulated genes on transcriptional (mRNA) and translational (RPF) level in the *Y. pseudotuberculosis* wildtype, Δ*csrA*, and Δ*yopD* mutants sorted by pathway.

Based on the Ribo-Seq results for the *Y. pseudotuberculosis* (**A**) wildtype, (**B**) Δ*csrA*, and (**C**) Δ*yopD* mutant, all up- and down-regulated genes (cut off: log^2FC +2/-2) on the transcription (mRNA) and translation (RPF) level from 25°C to 37°C and 37°C to secretion (-Ca^{2+}) conditions were assigned to a pathway. Afterward, the results were visualized in total by a pie chart. In addition, the results only for up- or down-regulated genes are also visualized next to the pie chart. (**D**) The legend for the different pathways visualizes in the pie charts is located at the end of the figure.

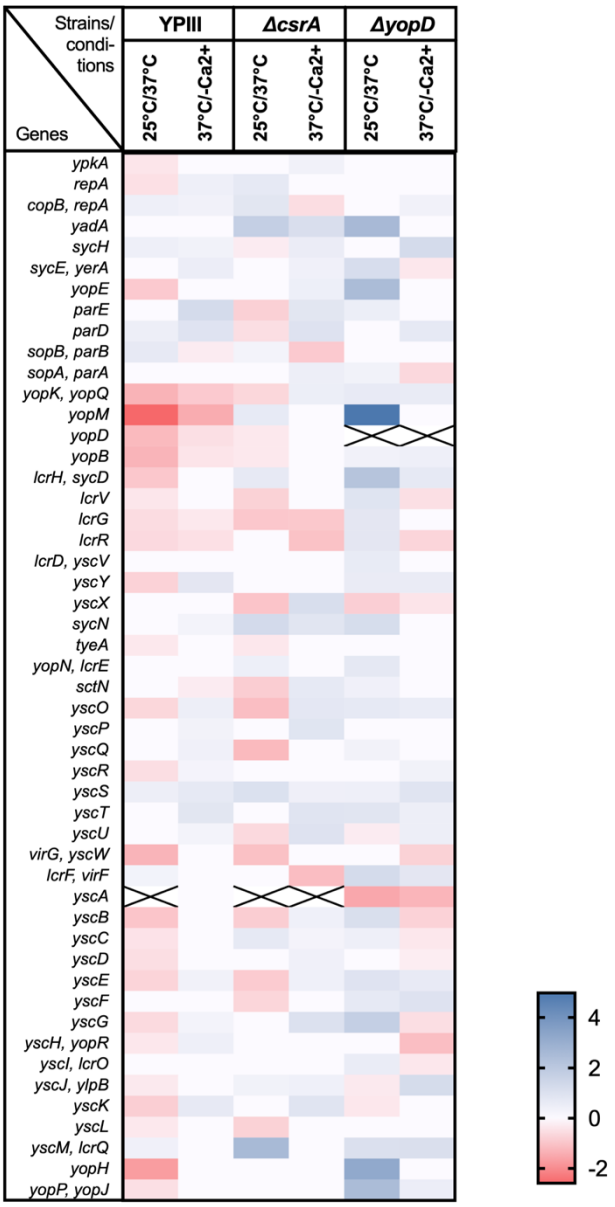

Figure 7.4) Differentially-regulated genes on the virulence plasmid pIB1 from *Y. pseudotuberculosis* by the translation efficiency (TE).

Log^2 fold-changes of the translation efficiency of the pIB1 virulence plasmid of Y. pseudotuberculosis (YPIII) by Ribo-Seq. Comparisons were done for bacteria grown at 25°C, 37°C and under secretion ($-Ca^{2+}$) conditions for the wildtype and the Δ*csrA* and Δ*yopD* mutant strains. Results which did not passe the quality control, the fields are crossed.

Table 7.4) Calculated log^2 fold-changes of the TEs with p-value for the virulence plasmid-encoded genes:

		YPIII 25°C vs. 37°C		YPIII 37°C vs. -Ca2+		*ΔcsrA* 25°C vs. 37°C		*ΔcsrA* 37°C vs. -Ca2+		*ΔyopD* 25°C vs. 37°C		*ΔyopD* 37°C vs. -Ca2+	
GenebankAcc	GeneSymbols	log2FC_TE	p-value	log2FC_TE	p-value	log2FC_TE	p-value	log2FC_TE	p-value	log2FC_TE	p-value	log2FC_TE	p-value
DN756_RS21540	*ypkA*	-0,407	0,229	0,149	0,601	-0,092	0,716	0,339	0,189	0,034	0,900	0,084	0,792
DN756_RS21545		-0,155	0,690	-0,380	0,205	-1,021	0,012	0,652	0,094	0,621	0,031	-0,366	0,253
DN756_RS21560		-0,499	0,550	0,047	0,964	-3,521	0,010	2,671	0,168	0,244	0,892	-1,635	0,278
DN756_RS21570	*repA*	-0,498	0,313	0,426	0,334	0,680	0,219	0,064	0,913	-0,124	0,753	0,030	0,952
DN756_RS21575	*tap*	0,600	0,255	0,959	0,054	-1,745	0,107	0,389	0,843	-2,096	0,001	1,592	0,101
DN756_RS21580	*copB, repA*	0,439	0,254	0,337	0,362	0,828	0,150	-0,560	0,349	-0,038	0,917	0,338	0,543
DN756_RS21595		-0,967	0,559	No Data	No Data	-3,105	0,065	-0,521	0,549	-6,044	0,000	-0,548	0,652
DN756_RS21610		No Data	No Data	No Data	No Data	No Data	No Data	No Data	No Data	-0,231	0,920	No Data	No Data
DN756_RS21615		No Data	No Data	No Data	No Data	No Data	No Data	No Data	No Data	No Data	No Data	-2,961	0,013
DN756_RS21620		No Data	No Data	No Data	No Data	No Data	No Data	No Data	No Data	0,420	0,809	1,357	0,695
DN756_RS21625	*yadA*	-0,104	0,999	-0,034	0,922	1,729	0,053	1,109	0,030	2,574	0,000	0,044	0,937
DN756_RS21635	*tnpA*	-0,500	0,457	-0,316	0,713	-0,004	0,995	-0,107	0,880	-0,361	0,680	0,629	0,642
DN756_RS21640		-0,605	0,073	0,360	0,373	0,051	0,885	1,334	0,000	0,407	0,216	-0,350	0,489
DN756_RS21645		0,363	0,494	0,846	0,043	0,030	0,997	-0,072	0,865	0,574	0,642	-1,343	0,050
DN756_RS21650		No Data	No Data	No Data	No Data	No Data	No Data	No Data	No Data	0,000	0,990	1,635	0,468
DN756_RS21660		-1,067	0,305	0,964	0,282	0,217	0,855	1,860	0,414	No Data	No Data	-6,770	0,000
DN756_RS21665	*sycH*	0,417	0,178	0,320	0,253	-0,277	0,470	0,543	0,196	-0,049	0,871	1,262	0,041
DN756_RS21675		-1,173	0,024	0,134	0,783	-0,797	0,405	-1,669	0,070	-0,731	0,210	-1,345	0,030
DN756_RS21685	*sycE*	-0,158	0,650	0,509	0,039	-0,243	0,485	0,370	0,203	1,171	0,000	-0,372	0,240
DN756_RS21690	*yopE*	-0,920	0,342	-0,113	0,746	-0,020	0,923	0,450	0,060	2,490	0,006	-0,168	0,604
DN756_RS21695	*parE*	-0,249	0,390	1,251	0,000	-0,810	0,022	0,818	0,025	0,496	0,082	0,127	0,816
DN756_RS21700	*parD*	0,466	0,122	0,922	0,005	-0,546	0,085	0,943	0,007	0,226	0,418	0,677	0,102
DN756_RS21710		No Data	No Data	No Data	No Data	No Data	No Data	No Data	No Data	-0,016	0,998	No Data	No Data
DN756_RS21715	*sopB, parB*	0,669	0,047	-0,289	0,421	0,268	0,517	-0,925	0,007	-0,152	0,625	0,245	0,603
DN756_RS21720	*sopA, parA*	-0,111	0,709	-0,117	0,667	-0,130	0,633	0,483	0,106	0,316	0,254	-0,648	0,065
DN756_RS21735	*traT*	-0,919	0,134	1,380	0,000	-0,271	0,680	1,279	0,000	1,475	0,000	0,353	0,383
DN756_RS21740		-1,753	0,232	-0,986	0,016	1,408	0,238	0,767	0,235	2,634	0,256	1,064	0,003
DN756_RS21750	*yopK, yopQ*	-1,330	0,356	-0,915	0,022	-0,679	0,028	0,497	0,060	0,620	0,471	0,577	0,092
DN756_RS21765		-0,712	0,156	1,034	0,010	0,546	0,588	0,109	0,902	1,749	0,000	0,834	0,046
DN756_RS21775		No Data	No Data	No Data	No Data	No Data	No Data	No Data	No Data	No Data	No Data	-0,120	0,953
DN756_RS21785	*yopM*	-2,586	0,178	-1,448	0,001	0,663	0,152	-0,046	0,846	4,972	0,034	-0,117	0,743
DN756_RS21800	*yopD*	-1,213	0,351	-0,520	0,189	-0,361	0,184	0,086	0,778	7,592	0,021	0,358	0,615
DN756_RS21805	*yopB*	-1,306	0,319	-0,429	0,250	-0,349	0,281	-0,135	0,623	0,337	0,722	0,426	0,244
DN756_RS21810	*lcrH, sycD*	-0,966	0,292	-0,106	0,728	0,667	0,077	0,149	0,660	2,174	0,014	0,679	0,023
DN756_RS21815	*lcrV*	-0,394	0,377	-0,184	0,557	-0,783	0,025	0,054	0,877	0,886	0,028	-0,530	0,122
DN756_RS21820	*lcrG*	-0,585	0,220	-0,353	0,276	-0,973	0,037	-0,955	0,005	0,777	0,038	0,173	0,682
DN756_RS21825	*lcrR*	-0,627	0,173	-0,499	0,155	0,220	0,769	-1,074	0,007	0,774	0,029	-0,708	0,078
DN756_RS21830	*lcrD, yscV*	0,205	0,480	-0,178	0,480	-0,186	0,497	0,025	0,931	0,612	0,018	0,202	0,550
DN756_RS21835	*yscY*	-0,771	0,123	0,780	0,040	0,178	0,786	-0,241	0,520	0,570	0,092	0,567	0,117
DN756_RS21840	*yscX*	-0,164	0,677	-0,065	0,835	-1,028	0,028	1,118	0,003	-0,834	0,031	-0,424	0,231
DN756_RS21845	*sycN*	-0,062	0,873	0,281	0,358	1,281	0,009	0,852	0,019	1,189	0,001	-0,065	0,848
DN756_RS21850	*tyeA*	-0,358	0,329	0,091	0,730	-0,368	0,233	-0,178	0,500	0,196	0,501	-0,015	0,958
DN756_RS21855	*yopN, lcrE*	-0,173	0,617	-0,003	0,995	0,457	0,100	0,009	0,978	0,720	0,018	-0,061	0,846
DN756_RS21860	*sctN*	0,021	0,951	-0,283	0,384	-0,847	0,004	0,696	0,013	0,390	0,153	-0,082	0,781
DN756_RS21865	*yscO*	-0,685	0,037	0,471	0,111	-1,125	0,001	0,746	0,016	0,682	0,009	0,555	0,110
DN756_RS21870	*yscP*	0,212	0,568	0,311	0,359	0,086	0,792	0,863	0,001	0,248	0,434	0,198	0,568
DN756_RS21875	*yscQ*	-0,044	0,908	0,394	0,181	-1,212	0,004	0,011	0,976	0,308	0,266	0,248	0,476
DN756_RS21880	*yscR*	-0,541	0,147	0,251	0,425	-0,014	0,962	0,012	0,983	-0,111	0,691	0,316	0,369
DN756_RS21885	*yscS*	0,467	0,483	0,676	0,163	1,017	0,307	0,412	0,482	0,425	0,366	0,865	0,086
DN756_RS21890	*yscT*	0,025	0,941	0,833	0,043	0,142	0,804	0,866	0,039	0,836	0,018	0,471	0,268
DN756_RS21895	*yscU*	0,126	0,750	0,276	0,368	-0,641	0,031	0,964	0,006	-0,279	0,451	0,488	0,291
DN756_RS21900	*virG, yscW*	-1,313	0,117	-0,097	0,883	-1,079	0,206	0,145	0,839	-0,176	0,773	-0,783	0,196
DN756_RS21905	*lcrF, virF*	0,304	0,599	0,132	0,731	0,175	0,899	-1,154	0,022	1,250	0,004	0,781	0,121
DN756_RS21910	*yscA*	No Data	No Data	-0,013	0,939	No Data	No Data	No Data	No Data	-1,542	0,104	-1,287	0,210
DN756_RS21915	*yscB*	-1,012	0,024	-0,048	0,911	-0,847	0,082	0,398	0,250	1,096	0,000	-0,771	0,092
DN756_RS21920	*yscC*	-0,465	0,200	0,074	0,833	0,678	0,025	0,264	0,301	0,420	0,172	-0,366	0,355
DN756_RS21925	*yscD*	-0,537	0,144	0,099	0,788	0,152	0,690	0,382	0,144	-0,118	0,687	-0,251	0,522
DN756_RS21930	*yscE*	-0,727	0,093	0,350	0,293	-0,892	0,038	0,398	0,199	0,922	0,015	0,635	0,105
DN756_RS21935	*yscF*	0,049	0,877	0,085	0,777	-0,699	0,061	0,154	0,660	0,704	0,052	0,953	0,013
DN756_RS21940	*yscG*	-0,616	0,068	0,279	0,342	-0,130	0,687	1,014	0,001	1,728	0,000	-0,551	0,099
DN756_RS21945	*yscH, yopR*	-0,366	0,256	0,438	0,170	-0,016	0,969	-0,028	0,920	0,243	0,427	-1,133	0,002
DN756_RS21950	*yscI*	-0,095	0,770	0,053	0,854	-0,012	0,965	0,195	0,504	0,547	0,048	-0,370	0,348
DN756_RS21955	*yscJ*	-0,328	0,321	0,201	0,486	0,334	0,364	0,402	0,563	-0,328	0,445	1,231	0,008
DN756_RS21960	*yscK*	-0,838	0,065	0,674	0,120	-0,099	0,880	0,868	0,031	-0,379	0,313	-0,159	0,685
DN756_RS21965	*yscL*	-0,336	0,398	0,108	0,766	-0,776	0,048	0,086	0,775	0,183	0,565	0,025	0,956
DN756_RS21970	*yscM, lcrQ*	0,374	0,413	0,129	0,672	2,557	0,000	0,142	0,764	1,045	0,011	1,085	0,009
DN756_RS21990	*yopH*	-1,730	0,252	-0,115	0,760	0,047	0,924	0,240	0,344	3,210	0,009	-0,245	0,478
DN756_RS22005	*yopP, yopJ*	-0,516	0,716	-0,159	0,655	-0,196	0,703	-0,164	0,615	2,493	0,079	0,511	0,115

7.3 Growth curves of mutant validation

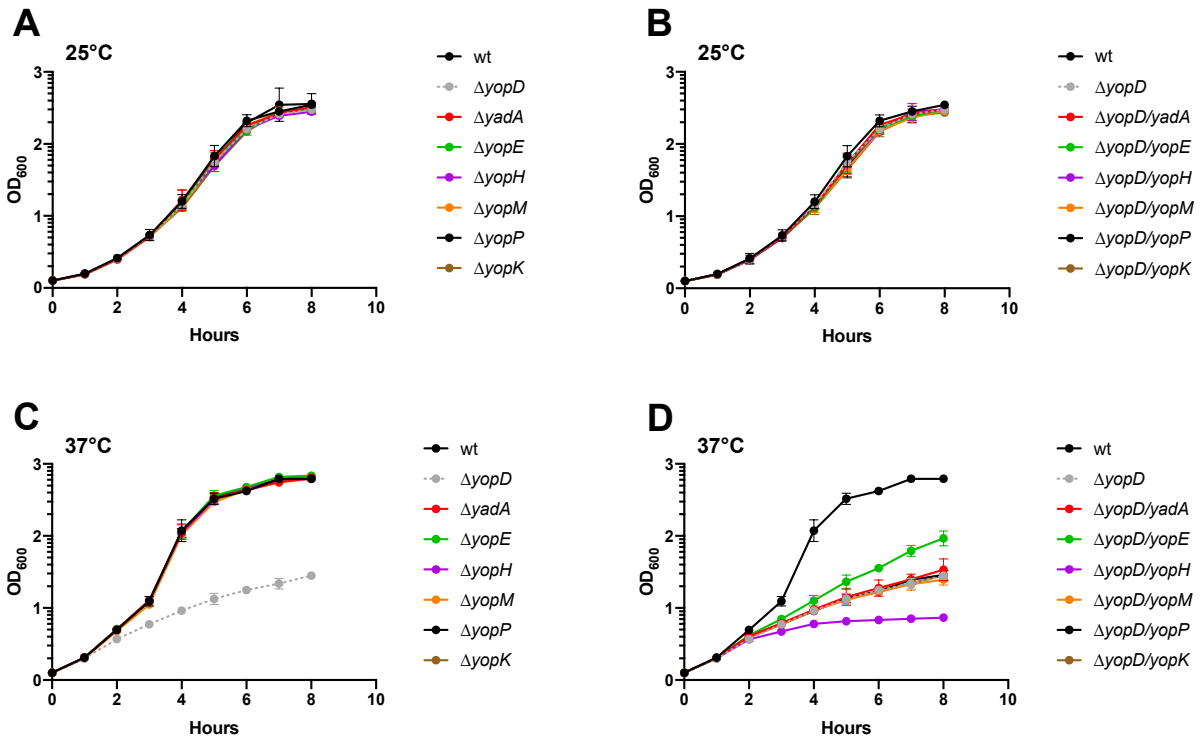

Figure 7.5) Growth analysis of the constructed *yop* deletion mutans for mutant validation.

The contracted *yop* and *yadA* single or double mutants were constructed based on the *Y. pseudotuberculosis* wildtype (single mutants) or Δ*yopD* mutant (double mutants). The different mutants were grown in LB liquid media at (A and B) 25°C or (C and D) 37°C and the optical density was measured continuously. The analysis was carried out in biological triplicates.

7.4 Test expression of inducible pBAD plasmids

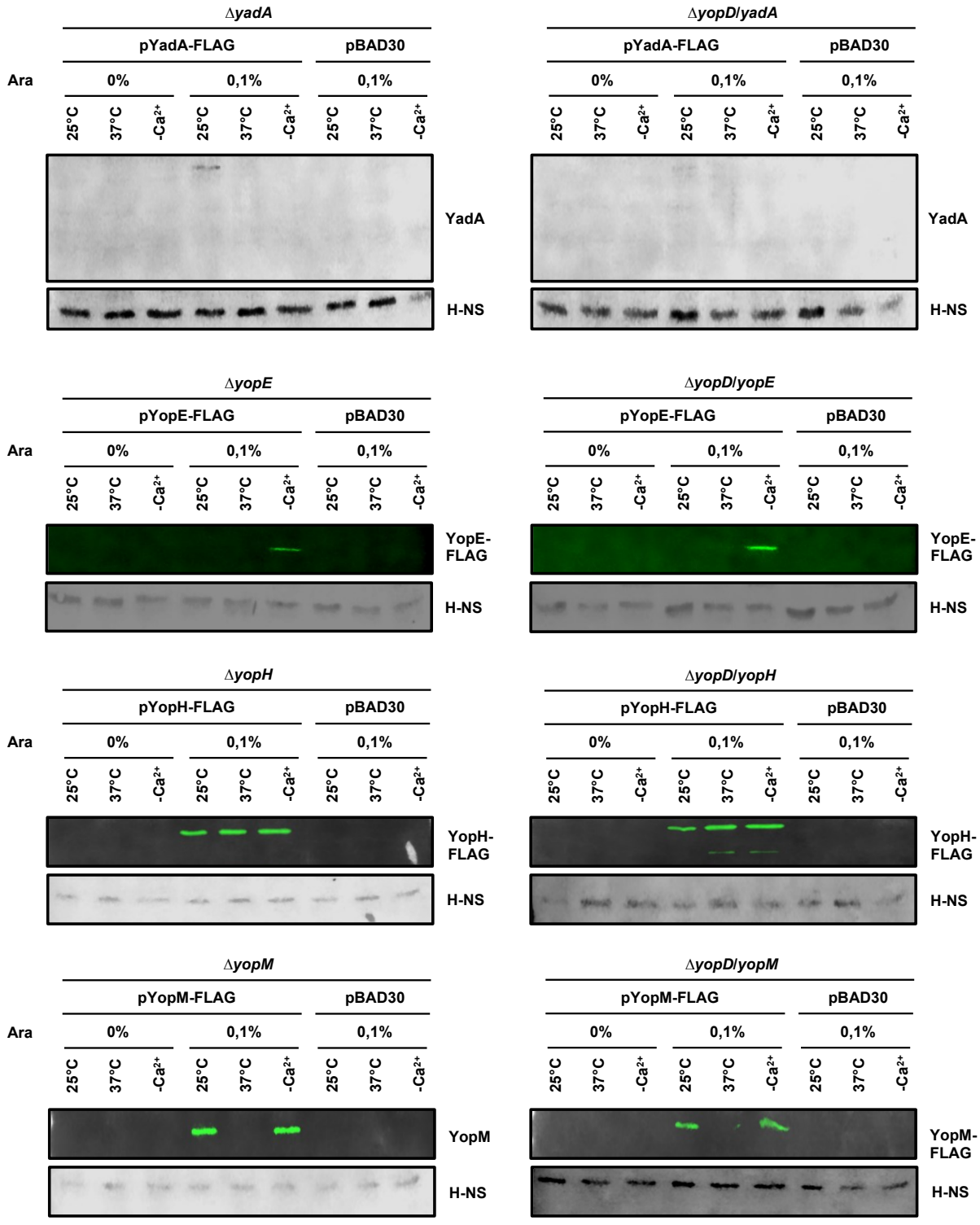

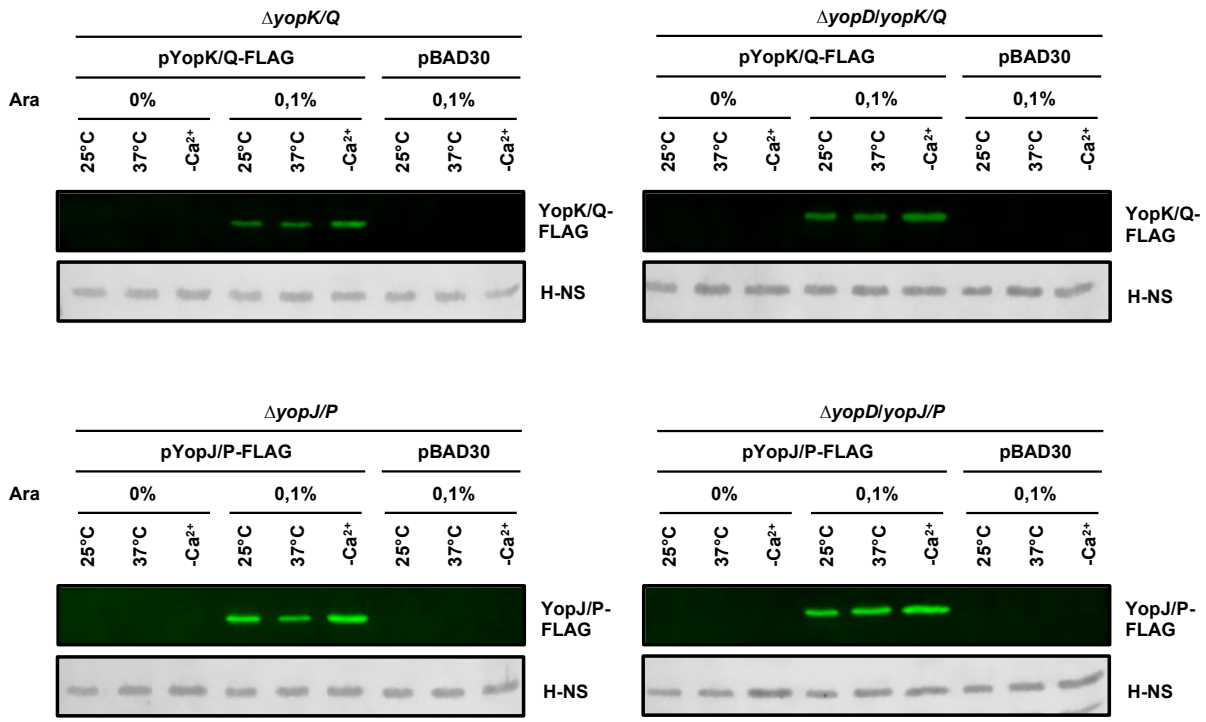

Figure 7.6) Test expression of all *yop* and *yadA* gene fusions with a FLAG-tag in the respective *yop* or *yadA* single mutants or *yop* and *yadA* plus *yopD* double mutants.

Representative Western blot detecting the Yop or YadA protein levels in the respective *Y. pseudotuberculosis* single mutants or Δ*yopD* mutant based double mutants at 25°C, 37°C and secretion (-Ca^{2+}) conditions. Expression of the fusion genes was induced by the addition of 0,1% arabinose into the LB liquid growth media. For the preparation of Western blot samples, the direct culture method was used (see chapter 2.7.2). In the Western blot analysis, H-NS was used as loading controls. The FLAG-tagged Yop proteins were visualized using a FLAG-antibody, while YadA was visualized using a YadA-antibody. The experiment was done in biological duplicates.

7.5 Codon usage/frequency as table

Table 7.5) Codon frequency and absolute number of codons for the chromosome, pIB1, Yops, T3SS, ribosomal proteins, translational components, glycolysis, transcriptional components, motility and DNA replication.

		Chromosome		Virulence Plasmid (pIB1)		Summe Yops			Summe T3SS			Summe Ribosomal Proteins			Summe Translation			Summe Glycolysis			Summe Transcription			Summe Motility			Summe DNA Replication		
		Frequency/	abs.	Frequency/	abs.	Frequency	rel. to	abs.	Frequency	rel. to	abs.	Frequency	rel. to	abs.	Frequency	rel. to	abs.	Frequency	rel. to	abs.	Frequency	rel. to	abs.	Frequency	rel. to	abs.	Frequency	rel. to	abs.
AA	Codon	1000	abundance	1000	abundance	/1000	chrom	abundance	/1000	chrom	abundance	/1000	chrom	abundance	/1000	chrom	abundance	/1000	chrom	abundance	/1000	chrom	abundance	/1000	chrom	abundance	/1000	chrom	abundance
Ala	GCG	24,0	62930	16,4	283	13,0	0,54	112	18,4	0,77	131	18,0	0,75	59	15,9	0,66	150	26,4	1,10	116	22,9	0,95	503	27,8	1,16	167	25,0	1,04	
Ala	GCA	20,8	54642	18,8	324	29,9	1,44	99	16,2	0,78	213	29,2	1,40	80	21,5	1,03	161	28,4	1,36	104	20,5	0,99	373	20,6	0,99	136	20,3	0,98	
Ala	GCT	20,0	52543	21,5	371	21,9	1,10	145	23,8	1,19	318	43,6	2,18	149	40,1	2,00	186	32,8	1,64	99	19,5	0,98	317	17,5	0,88	170	25,4	1,27	
Ala	GCC	27,5	72120	19,2	331	15,0	0,54	108	17,7	0,65	74	10,1	0,37	61	16,4	0,60	120	21,1	0,77	75	14,8	0,54	576	31,8	1,16	162	24,2	0,88	
Cys	TGT	5,7	14880	6,4	111	5,5	0,97	40	6,6	1,16	16	2,2	0,39	17	4,6	0,81	23	4,1	0,72	20	3,9	0,70	33	1,8	0,32	34	5,1	0,90	
Cys	TGC	4,7	12417	4,5	77	5,5	1,16	18	3,0	0,62	26	3,6	0,75	8	2,2	0,45	15	2,6	0,56	14	2,8	0,58	49	2,7	0,57	37	5,5	1,17	
Asp	GAT	37,3	98044	31,2	539	38,4	1,03	197	32,3	0,87	153	21,0	0,56	129	34,7	0,93	195	34,3	0,92	204	40,2	1,08	623	34,4	0,92	287	42,9	1,15	
Asp	GAC	14,2	37267	14,2	245	10,0	0,70	74	12,1	0,86	159	21,8	1,54	109	29,3	2,06	123	21,7	1,53	132	26,0	1,83	258	14,3	1,01	107	16,0	1,13	
Glu	GAG	20,1	52706	28,0	483	20,9	1,04	177	29,0	1,45	121	16,6	0,83	92	24,7	1,23	111	19,5	0,97	166	32,7	1,63	362	20,0	1,00	181	27,1	1,35	
Glu	GAA	33,9	89126	40,5	700	47,4	1,40	261	42,8	1,26	345	47,3	1,39	269	72,3	2,13	288	50,7	1,49	312	61,5	1,81	547	30,2	0,89	312	46,7	1,37	
Phe	TTT	23,1	60754	20,3	351	15,5	0,67	111	18,2	0,79	74	10,1	0,44	30	8,1	0,35	83	14,6	0,63	58	11,4	0,49	327	18,1	0,78	128	19,1	0,83	
Phe	TTC	14,8	38985	11,8	204	10,0	0,67	61	10,0	0,67	144	19,7	1,33	72	19,4	1,30	144	25,4	1,71	84	16,6	1,12	198	10,9	0,74	86	12,9	0,87	
Gly	GGG	15,8	41506	15,8	272	13,0	0,82	108	17,7	1,12	12	1,6	0,10	13	3,5	0,22	40	7,0	0,45	16	3,2	0,20	299	16,5	1,05	100	15,0	0,95	
Gly	GGA	5,9	15705	11,7	202	12,0	2,03	63	10,3	1,75	11	1,5	0,26	2	0,5	0,09	3	0,5	0,09	5	1,0	0,17	59	3,3	0,55	31	4,6	0,79	
Gly	GGT	26,7	70260	17,6	303	24,4	0,91	107	17,5	0,66	341	46,7	1,75	164	44,1	1,65	257	45,3	1,69	188	37,1	1,39	420	23,2	0,87	169	25,3	0,94	
Gly	GGC	24,1	63195	13,8	238	10,5	0,44	76	12,5	0,52	223	30,6	1,27	112	30,1	1,25	195	34,3	1,43	120	23,6	0,98	436	24,1	1,00	142	21,2	0,88	
His	CAT	14,0	36640	17,1	296	16,5	1,18	110	18,0	1,29	72	9,9	0,71	28	7,5	0,54	57	10,0	0,72	29	5,7	0,41	168	9,3	0,67	115	17,2	1,23	
His	CAC	8,4	22132	7,0	121	5,5	0,65	32	5,2	0,62	85	11,7	1,38	41	11,0	1,31	71	12,5	1,48	42	8,3	0,98	100	5,5	0,66	47	7,0	0,83	
Ile	ATA	7,8	20574	15,9	275	18,4	2,36	102	16,7	2,14	4	0,5	0,07	5	1,3	0,17	6	1,1	0,13	9	1,8	0,23	122	6,7	0,86	26	3,9	0,50	
Ile	ATT	31,6	83100	26,2	453	19,9	0,63	183	30,0	0,95	146	20,0	0,63	97	26,1	0,82	157	27,6	0,87	118	23,3	0,74	513	28,4	0,90	172	25,7	0,81	
Ile	ATC	23,0	60475	17,1	295	12,0	0,52	111	18,2	0,79	252	34,5	1,50	143	38,4	1,67	225	39,6	1,72	201	39,6	1,72	432	23,9	1,04	138	20,6	0,90	
Lys	AAG	11,6	30437	15,9	275	9,0	0,77	86	14,1	1,22	261	35,8	3,09	62	16,7	1,44	81	14,3	1,23	95	18,7	1,62	180	9,9	0,86	84	12,6	1,08	
Lys	AAA	31,8	83473	34,4	593	41,4	1,30	189	31,0	0,98	414	56,7	1,79	188	50,5	1,59	285	50,2	1,58	184	36,3	1,14	559	30,9	0,97	217	32,4	1,02	
Leu	TTG	24,6	64592	22,7	392	23,9	0,97	180	29,5	1,20	91	12,5	0,51	64	17,2	0,70	107	18,8	0,77	124	24,4	0,99	534	29,5	1,20	218	32,6	1,33	
Leu	TTA	22,6	59275	26,1	450	35,9	1,59	212	34,8	1,54	40	5,5	0,24	19	5,1	0,23	51	9,0	0,40	54	10,6	0,47	412	22,8	1,01	131	19,6	0,87	
Leu	CTG	35,3	92705	29,1	502	20,4	0,58	157	25,7	0,73	309	42,4	1,20	138	37,1	1,05	283	46,3	1,31	244	48,1	1,36	690	38,1	1,08	256	38,3	1,08	
Leu	CTA	8,1	21332	10,7	184	8,5	1,04	79	13,0	1,60	18	2,5	0,30	11	3,0	0,36	20	3,5	0,43	24	4,7	0,58	126	7,0	0,86	59	8,8	1,09	
Leu	CTT	9,3	24524	18,1	313	16,0	1,71	139	22,8	2,44	34	4,7	0,50	14	3,8	0,40	22	3,9	0,42	43	8,5	0,91	137	7,6	0,81	83	12,4	1,33	
Leu	CTC	8,8	23169	11,5	198	4,5	0,51	84	13,8	1,56	15	2,1	0,23	8	2,2	0,24	17	3,0	0,34	20	3,9	0,45	166	9,2	1,04	61	9,1	1,03	
Met	ATG	25,6	67357	23,8	410	20,9	0,82	136	22,3	0,87	179	24,5	0,96	107	28,8	1,12	142	25,0	0,98	139	27,4	1,07	551	30,5	1,19	170	25,4	0,99	
Asn	AAT	24,8	65026	28,7	496	46,4	1,87	138	22,6	0,91	69	9,5	0,38	25	6,7	0,27	66	11,6	0,47	48	9,5	0,38	485	26,8	1,08	117	17,5	0,71	
Asn	AAC	16,6	43573	15,5	267	18,9	1,14	69	11,3	0,68	191	26,2	1,58	85	22,8	1,38	157	27,6	1,67	137	27,0	1,63	378	20,9	1,26	88	13,2	0,79	
Pro	CCG	13,3	34873	10,1	174	11,0	0,83	65	10,7	0,80	105	14,4	1,08	29	7,8	0,59	54	9,5	0,72	63	12,4	0,94	291	16,1	1,21	96	14,4	1,08	
Pro	CCA	12,7	33253	12,0	207	19,9	1,58	64	10,5	0,83	75	10,3	0,81	59	15,9	1,25	91	16,0	1,27	74	14,6	1,15	171	9,5	0,75	91	13,6	1,07	
Pro	CCT	10,0	26358	11,6	200	14,0	1,39	94	15,4	1,54	51	7,0	0,70	30	8,1	0,80	49	8,6	0,86	46	9,1	0,90	135	7,5	0,74	90	13,5	1,34	
Pro	CCC	7,6	19945	7,9	136	8,0	1,05	47	7,7	1,02	5	0,7	0,09	5	1,3	0,18	16	2,8	0,37	8	1,6	0,21	167	9,2	1,22	52	7,8	1,02	
Gln	CAG	24,0	63007	24,1	416	17,4	0,73	136	22,3	0,93	114	15,6	0,65	91	24,5	1,02	92	16,2	0,68	148	29,2	1,22	626	34,6	1,44	195	29,2	1,22	
Gln	CAA	24,0	63150	28,8	498	26,4	1,10	241	39,5	1,64	126	17,3	0,72	49	13,2	0,55	80	14,1	0,59	79	15,6	0,65	624	34,5	1,43	172	25,7	1,07	
Arg	AGG	1,8	4713	4,5	78	2,5	1,39	18	3,0	1,65	0	0,0	0,00	0	0,0	0,00	3	0,5	0,30	3	0,6	0,33	16	0,9	0,49	7	1,0	0,58	
Arg	AGA	3,0	7902	6,1	105	11,0	3,64	23	3,8	1,25	5	0,7	0,23	4	1,1	0,36	2	0,4	0,12	4	0,8	0,26	33	1,8	0,61	14	2,1	0,70	
Arg	CGG	8,0	20974	8,5	146	1,5	0,19	36	5,9	0,74	5	0,7	0,09	8	2,2	0,27	11	1,9	0,24	21	4,1	0,52	140	7,7	0,97	73	10,9	1,37	
Arg	CGA	3,9	10215	7,6	131	7,0	1,79	40	6,6	1,69	8	1,1	0,28	2	0,5	0,14	7	1,2	0,32	13	2,6	0,66	52	2,9	0,74	34	5,1	1,31	
Arg	CGT	19,9	52344	17,6	304	14,0	0,70	111	18,2	0,91	437	59,9	3,01	164	44,1	2,21	162	28,5	1,43	229	45,1	2,27	304	16,8	0,84	176	26,3	1,32	
Arg	CGC	16,5	43415	15,4	265	7,5	0,45	99	16,2	0,98	176	24,1	1,46	67	18,0	1,09	52	9,2	0,55	94	18,5	1,12	274	15,1	0,92	121	18,1	1,09	
Ser	AGT	13,1	34460	16,6	286	23,4	1,79	89	14,6	1,11	24	3,3	0,25	12	3,2	0,25	29	5,1	0,39	18	3,5	0,27	351	19,4	1,48	73	10,9	0,83	
Ser	AGC	14,4	37768	13,0	224	16,5	1,14	75	12,3	0,86	79	10,8	0,75	30	8,1	0,56	51	9,0	0,62	66	13,0	0,90	341	18,8	1,31	82	12,3	0,85	
Ser	TCG	7,0	18445	7,7	132	7,0	0,99	40	6,6	0,93	10	1,4	0,20	9	2,4	0,34	25	4,4	0,63	25	4,9	0,70	164	9,1	1,29	40	6,0	0,85	
Ser	TCA	10,8	28474	14,3	247	21,9	2,02	83	13,6	1,26	37	5,1	0,47	28	7,5	0,69	48	8,5	0,78	33	6,5	0,60	199	11,0	1,01	52	7,8	0,72	
Ser	TCT	10,0	26275	14,9	257	25,9	2,59	84	13,8	1,38	131	18,0	1,80	71	19,1	1,91	109	19,2	1,92	81	16,0	1,60	171	9,5	0,95	47	7,0	0,70	
Ser	TCC	7,3	19240	8,1	140	8,0	1,09	42	6,9	0,94	66	9,0	1,24	21	5,6	0,77	52	9,2	1,25	45	8,9	1,21	142	7,8	1,07	48	7,2	0,98	
Thr	ACG	12,0	31610	10,1	174	13,0	0,54	49	8,0	0,67	32	4,4	0,36	24	6,5	0,54	41	7,2	0,60	46	9,1	0,75	269	14,9	1,24	79	11,8	0,98	
Thr	ACA	9,8	25623	12,3	213	13,0	1,33	74	12,1	1,24	31	4,2	0,44	24	6,5	0,66	30	5,3	0,54	25	4,9	0,51	185	10,2	1,05	66	9,9	1,01	
Thr	ACT	10,7	28027	14,1	243	21,9	2,06	77	12,6	1,18	189	25,9	2,43	80	21,5	2,02	95	16,7	1,57	72	14,2	1,33	169	9,3	0,88	71	10,6	0,99	
Thr	ACC	22,2	58283	14,8	256	9,0	0,40	89	14,6	0,66	129	17,7	0,80	80	21,5	0,97	126	22,2	1,00	124	24,4	1,10	547	30,2	1,36	110	16,4	0,74	
Val	GTG	22,8	59924	18,2	314	11,0	0,48	123	20,2	0,88	96	13,2	0,58	61	16,4	0,72	110	19,4	0,85	90	17,7	0,78	512	28,3	1,24	132	19,7	0,87	
Val	GTA	11,3	29781	13,4	231	19,4	1,71	86	14,1	1,24	168	23,0	2,03	54	14,5	1,28	69	12,2	1,07	70	13,8	1,22	153	8,5	0,75	73	10,9	0,96	
Val	GTT	19,1	50194	20,7	357	21,9	1,15	134	22,0	1,15	343	47,0	2,46	169	45,4	2,38	188	33,1	1,73	162	31,9	1,67	286	15,8	0,83	112	16,7	0,88	
Val	GTC	15,7	41213	12,8	221	10,5	0,67	71	11,6	0,74	84	11,5	0,73	43	11,6	0,74	67	11,8	0,75	50	9,9	0,63	279	15,4	0,98	88	13,2	0,84	
Trp	TGG	13,7	35920	12,6	217	4,0	0,29	67	11,0	0,80	39	5,3	0,39	16	4,3	0,31	48	8,5	0,62	31	6,1	0,45	118	6,5	0,48	70	10,5	0,77	
Tyr	TAT	19,6	51543	17,4	301	19,9	1,02	106	17,4	0,89	48	6,6	0,34	39	10,5	0,53	57	10,0	0,51	62	12,2	0,62	254	14,0	0,72	126	18,8	0,96	
Tyr	TAC	9,8	25658	8,8	152	6,5	0,66	46	7,5	0,77	86	11,8	1,21	40	10,8	1,10	79	13,9	1,42	59	11,6	1,19	118	6,5	0,67	51	7,6	0,78	
End	TGA	1,1	2762	2,4	41	2		15			5			1			1			2			20			3			
End	TAG	0,5	1356	0,5	9	1		1			0			0			1			1			11			3			
End	TAA	1,9	4971	2,1	36	3		9			51			9			13			6			36			10			

Danksagung

Als erstes möchte ich mich bei meiner Mentorin Prof. Dr. Petra Dersch dafür bedanken, dass sie mir die Möglichkeit dieses Projekt in ihrer Gruppe gegeben hat. Darüber hinaus möchte ich mich auch für Ihre Unterstützung und Betreuung während meiner Zeit in der Gruppe bedanken.

Ein weiterer Dank geht an die Mitglieder meines Thesis- und Prüfungs-Komitees hier in Münster, bestehend aus Frau Prof. Dr. Eva Liebau und Herrn Prof. Dr. Alexander Mellmann, für die Unterstützung meiner Thesis nach dem Umzug nach Münster, sowie für die Begutachtung meiner Arbeit und die Durchführung meiner mündliche Prüfung.

Daneben möchte ich mich auch bei meinem Thesis-Komitee aus Braunschweig bedanken. Der Dank geht an Frau Prof. Dr. Susanne Häußler und Frau PD Dr. Simone Bergmann die mich in der Anfangszeit meiner Thesis mit einigen wichtigen und interessanten Diskussionen und Ideen unterstützt haben.

Ich möchte mich besonders bei unserer In-House seqeuncing Facility (GEMK) und hier besonders bei Michael Jarek und Maren Scharfe bedanken die mich bei allen NGS Angelegenheiten immer sehr gut unterstützten. Darüber hinaus auch bei Florian Eggenhofer und Rick Gelhausen für die Bioinformatische Auswertung meiner Ribo-Seq und der Hilfe bei allen fragen die ich hatte.

Ein weiterer Dank geht an Dr. Florian Altegoer und Prof. Dr. Gert Bange die sich um die Cryo-EM Strukturen meiner Ribosomen gekümmert haben auch wenn diese leider nicht in dieser Arbeit enthalten sind.

Ein ganz besonderer Dank geht an meine Postdoc Betreuerin Dr. Ann Kathrin Heroven, die mich in Braunschweig betreut hat und mir bei vielen Problemen im Labor und Drumherum geholfen hat. Außerdem danke ich ihr das sie sich auch die Zeit genommen hat diese Thesis in teilen korrektur zu lesen. Auch Herr Dr. Christoph Cichon der diese Betreuung nach dem Umzug in Münster übernommen hat möchte ich sehr danken. Die Diskussionen über mein Projekt und auch über den Gebrauch und nicht Gebrauch von Geräten werde ich so schnell nicht vergessen.

Der größte und, persönlich gesehen wichtigste Dank geht an alle meinen ehemaligen Kollegen aus der MIBI in Braunschweig Für all die schönen und lustigen Stunden im Labor, die das Arbeiten so viel angenehmer gemacht haben. Besonders Maria, Vanessa, Carina, die sich ein Büro mit mir geteilt haben, sowie Ines, Paweena und Sabrina möchte ich hier danken für die Zeit im Labor, im Büro, auf Konferenzen oder an jedem sonstigen Ort an dem wir waren. Mit euch war es nie langweilig und es gab immer was zu lachen, auch wenn es eigentlich Garnichts der Moment dazu war. Sabrina möchte ich auch zusetzlich nochmal danken das sie mir geholfen hat meine Arbeit zu korrigieren. Auch dem ehemaligen MIBI Jörn möchte ich danken, der immer geholfen hat, wenn mal Not am Mann war. Neben den MIBIs möchte ich mich auch bei den IFIs in Münster bedanken für die angenehme Zeit hier im Labor.

Auch bei Lorena von den MOBAs möchte ich danken für Ihre Hilfe bei der Etablierung der Ribo-Seq mit Methoden aber auch für die Diskussionen über die Durchführung die uns am Ende beiden geholfen hat. Und neben Ihr natürlich auch bei den anderen Mädels aus der MOBA.

Neben allen bereits benannten Menschen aus meiner Laborzeit möchte ich einen sehr großen Dank an Dr. Lennart Weber, meinen ehemaligen Betreuer aus der Bachelor Thesis, aussprechen. Sein Engagement mir neues Wissen, Methoden, deren Anwendung und das darüber hinaus denken beizubringen kann ich erst jetzt im vollen Maße begreifen. Auch dafür, dass er im Anschluss an meine Bachelor Thesis immer noch bereit war, mich jeder Zeit mit Rat und Tat zu unterstützen, möchte ich mich bedanken. Außerdem bedanke ich mich für die Gespräche die ich auch jetzt noch mit Ihm über mein Projekt führen kann und die immer sehr produktive für mich sind, sowie das ein oder andere Feierabendbier. Dieses Mal vergesse ich dich auch nicht in meiner Danksagung.

Neben Lennart möchte ich mich aber auch bei allen anderen Freunden bedanken, die mit mir durch die Doktoranden Zeit gegangen sind. Aber auch für die Momente in denen wir das einfach alles mal hinter uns gelassen haben. Als Letztes möchte ich mich bei meinen Eltern und meiner Schwester bedanken für die Unterstützung in dieser Zeit sowie bereits lange vor der Doktorarbeit.

Curriculum vitae

Erklärungen

Ich (Marcel Volk) erkläre, dass ich nicht wegen eines Verbrechens zu dem ich meine wissenschaftliche Qualifikation missbraucht habe, verurteilt worden bin.

Hiermit versicher ich Marcel Volk, dass die von mir vorgelegte Dissertation selbst und ohne unerlaubte Hilfe angefertigt wurde. Desweiteren versiche ich, dass alle in Anspruch genommenen Quellen und Hilfsmittel in der Dissertation angegeben sind und die Dissertation nicht bereits anderweitig als Prüfungsarbeit vorgelegt wurde.

_____
Datum, Ort

_____
Marcel Volk

(Vorlage für die Erklärungen ist § 7(3) Punkt 2. und 6. der Promotionsordnung des Fachbereichs Biologie der Westfälischen Wilhelms-Universität Münster vom 30.10.2019 einschließlich der Änderungsordnung vom 04.08.2020)